

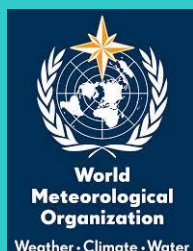
Izaña Atmospheric Research Center



Activity Report 2019-2020

**Joint publication of State Meteorological Agency (AEMET)
and World Meteorological Organization (WMO)**

WMO/GAW Report No. 276



Cover photograph: Izaña Observatory (Photo: Conchy Bayo-Pérez)

Citation:

Cuevas, E., Milford, C., Barreto, A., Bustos, J. J., García, O. E., García, R. D., Marrero, C., Prats, N., Ramos, R., Redondas, A., Reyes, E., Rivas-Soriano, P. P., Romero-Campos, P. M., Torres, C. J., Schneider, M., Yela, M., Belmonte, J., Almansa, F., López-Solano, C., Basart, S., Werner, E., Rodríguez, S., Afonso, S., Alcántara, A., Alvarez, O., Bayo, C., Berjón, A., Carreño, V., Castro, N. J., China, N., Cruz, A. M., Damas, M., Gómez-Trueba, V., González, Y., Guirado-Fuentes, C., Hernández, C., León-Luís, S. F., López-Fernández, R., López-Solano, J., Parra, F., Pérez de la Puerta, J., Rodríguez-Valido, M., Sálamo, C., Santana, D., Santo-Tomás, F., Sepúlveda, E. and Serrano, A.: Izaña Atmospheric Research Center Activity Report 2019-2020. (Eds. Cuevas, E., Milford, C. and Tarasova, O.), State Meteorological Agency (AEMET), Madrid, Spain and World Meteorological Organization, Geneva, Switzerland, NIPO: 666-22-014-0, WMO/GAW Report No. 276, <https://doi.org/10.31978/666-22-014-0>, 2022.

For more information, please contact:

Izaña Atmospheric Research Center
Headquarters: Calle La Marina, 20
Santa Cruz de Tenerife
Tenerife, 38001, Spain
Tel: +34 922 151 718
Fax: +34 922 574 475
E-mail: ciai@aemet.es
<http://izana.aemet.es>

State Meteorological Agency (AEMET)
Headquarters: Calle Leonardo Prieto Castro, 8
Ciudad Universitaria
28071, Madrid, Spain
www.aemet.es

World Meteorological Organization (WMO)
7bis, avenue de la Paix
P.O. Box 2300
CH-1211 Geneva 2, Switzerland
www.wmo.int

NIPO: 666-22-014-0
WMO/GAW Report No. 276
<https://doi.org/10.31978/666-22-014-0>

Disclaimer: The contents of this publication may be reused, citing the source and date.



Izaña Atmospheric Research Center

Activity Report 2019-2020

Prepared by:

E. Cuevas¹, C. Milford¹, A. Barreto¹, J. J. Bustos¹, O. E. García¹, R. D. García^{2,3}, C. Marrero¹, N. Prats¹, R. Ramos¹, A. Redondas¹, E. Reyes¹, P. P. Rivas-Soriano¹, P. M. Romero-Campos¹, C. J. Torres¹, M. Schneider⁴, M. Yela⁵, J. Belmonte⁶, F. Almansa^{1,7}, C. López-Solano⁸, S. Basart⁹, E. Werner¹⁰, S. Rodríguez¹¹, S. Afonso^{1*}, A. Alcántara¹, O. Alvarez¹, C. Bayo¹, A. Berjón², V. Carreño¹, N. J. Castro¹, N. China^{2,8}, A. M. Cruz¹, M. Damas¹, V. Gómez-Trueba^{12*}, Y. González⁷, C. Guirado-Fuentes^{1,3*}, C. Hernández¹, S. F. León-Luís², R. López-Fernández¹, J. López-Solano², F. Parra^{1*}, J. Pérez de la Puerta^{1*}, M. Rodríguez-Valido¹³, C. Sálamo^{1*}, D. Santana¹⁴, F. Santo-Tomás¹, E. Sepúlveda^{1*} and A. Serrano¹

Editors:

Emilio Cuevas¹, Celia Milford¹ and Oksana Tarasova¹⁵

¹Izaña Atmospheric Research Center, State Meteorological Agency (AEMET), Tenerife, Spain

²TRAGSATEC, Madrid, Spain

³Atmospheric Optics Group, Valladolid University, Valladolid, Spain

⁴Institute for Meteorology and Climate Research, Karlsruhe Institute of Technology (KIT), Karlsruhe, Germany

⁵National Institute for Aerospace Technology (INTA), Torrejón de Ardoz, Madrid, Spain

⁶Universidad Autónoma de Barcelona (UAB), Barcelona, Spain

⁷Cimel Electronique, Paris, France

⁸SIELTEC, La Laguna, Tenerife, Spain

⁹Barcelona Supercomputing Centre, Barcelona, Spain

¹⁰Sand and Dust Storm Warning Advisory and Assessment Regional Centre, AEMET, Spain

¹¹Institute of Natural Products and Agrobiology, IPNA CSIC, Tenerife, Spain

¹²Air Liquide, Tenerife, Spain

¹³University of La Laguna (ULL), Tenerife, Spain

¹⁴LuftBlick Earth Observation Technologies, Innsbruck, Austria

¹⁵World Meteorological Organization, Geneva, Switzerland

*Now retired or with other organisation

November 2022

**Joint publication of State Meteorological Agency (AEMET)
and World Meteorological Organization (WMO)**

WMO/GAW Report No. 276



**World
Meteorological
Organization**

Weather • Climate • Water



**GLOBAL
ATMOSPHERE
WATCH**

Contents

Foreword.....	vii
1 Organization	1
2 Mission and Background	1
3 Facilities and Summary of Measurements	2
4 Greenhouse Gases and Carbon Cycle	19
5 Reactive Gases and Ozonesondes	26
6 Total Ozone Column and Ultraviolet Radiation	35
7 Fourier Transform Infrared Spectroscopy (FTIR)	45
8 In situ Aerosols	55
9 Column Aerosols	61
10 Radiation.....	69
11 Differential Optical Absorption Spectroscopy (DOAS)	75
12 Water Vapour	79
13 Meteorology.....	90
14 Aerobiology	102
15 ACTRIS	106
16 Regional Brewer Calibration Center for Europe (RBCC-E).....	109
17 Sand and Dust Storm Centres	117
18 GAW Tamanrasset twinning programme	126
19 WMO Testbed for Aerosols and Water Vapour Remote Sensing Instruments.....	130
20 Activities in collaboration with IAC.....	138
21 Capacity Building Activities.....	139
22 Scientific Communication	140
23 Publications	143
24 List of scientific projects	151
25 List of major national and international networks, programmes and initiatives	153
26 Staff	155
27 List of Acronyms	158
28 Acknowledgements.....	162

Foreword

The year 2020 was a complicated one for the whole world and for the Members and partners of the World Meteorological Organization (WMO). The beginning of 2020 was marked by the global pandemic of COVID-19 that impacted the work of organization through lockdowns and lack of access to the observational infrastructure. The report presented at the seventy-fifth session of the WMO Executive Council demonstrated that about 24% of activities were severely impacted by COVID-19. Despite these difficulties, the Izaña Atmospheric Research Center (IARC), which is part of the State Meteorological Agency of Spain (AEMET), continued its operations delivering outstanding science to the global atmospheric composition community.

IARC manages four observatories in Tenerife, including the high altitude Izaña Observatory, which was inaugurated in 1916 and has since carried out uninterrupted meteorological and climatological observations and become a WMO Centennial Station.

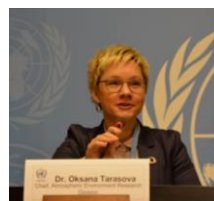
The Izaña Observatory has contributed to the Global Atmosphere Watch (GAW) Programme since its inception and is one of 30 GAW Global stations. It performs high-quality, long-term (multi-decade) measurements and analyses of atmospheric greenhouse gases, surface and column ozone, ultraviolet and solar radiation, in situ and column aerosols and selected reactive gases.

IARC supports the GAW quality assurance framework by operating the Regional Brewer Calibration Centre for Europe (RBCC-E), which calibrates Brewer spectrometers in Europe and North Africa, maintains the Brewer ozone reference and hosts the European Brewer Network (EUBREWNET). In addition, IARC operates for WMO a Testbed for Aerosols and Water Vapour Remote Sensing Instruments. It also supports the World Radiation Center by maintaining one of the World Optical Depth Research and Calibration Center (WORCC) Precision Filter Radiometer reference instruments at the Izaña Observatory. The Izaña Observatory is also one of three AERONET-EUROPE calibration facilities and ensures the calibration of more than 80 AERONET sites.

The Izaña Atmospheric Research Center also plays an important role in supporting international cooperation. For example, it contributes to activities of WMO Sand and Dust Storm Warning Advisory and Assessment System (SDS-WAS) Regional Center for Northern Africa, Middle East and Europe, focusing its efforts on dust observations and atmospheric processes. It also performs research in relation to sand and dust storm processes and their impacts on human health, ecosystem and economic activities.

The urgency of actions related to the state of climate and the environment requires that the public and decision-makers have access to the best available science and high-quality atmospheric composition data, and IARC is highly respected for the quality of the data it provides.

It is a pleasure for me to present this report summarizing the many activities of the Izaña Atmospheric Research Center. The Center's leadership in research and development regarding state-of-the-art measurement techniques, calibration and validation, as well as international cooperation have given it an outstanding reputation in weather, climate, hydrology and related environmental issues. I hope that it will inspire Members to consider becoming involved in the GAW Programme and in other WMO research activities.



Dr Oksana Tarasova

Head, Global Atmosphere Watch Programme

*Science and Innovation Department
World Meteorological Organization*



Julio González-Breña

Former Director of Planning, Strategy and Business Development (AEMET)

This report constitutes a detailed summary of the activities of the Izaña Atmospheric Research Center in the period 2019-2020, most of them of great international relevance. However, here I would like to highlight some of the extraordinary activities carried out by this Center, as they tell us a lot about its profile and character.

Writing a report like this is a complex and time-consuming task, but its publication has undoubtedly been beset with numerous challenges. In the period of time to which this report refers, and the subsequent period during its preparation and editing, extraordinary events took place that implied an additional workload and could have affected the operation of IARC, however, these challenges were met with resourcefulness and dedication.

In February 2020, the most intense Saharan dust outbreak so far recorded in the Canary Islands occurred. It was of such magnitude that, for the first time in history, the eight Canarian airports had to stop operations simultaneously, stranding thousands of people in the islands. This episode was addressed in a multidisciplinary and collaborative study led by IARC, and published by WMO, detailing different scientific aspects, but also evaluating the socio-economic impact of the dust outbreak in different sectors such as health, aviation and solar energy. It was a clear example of research work focused on the new vision of science for society.

Within days of this historic dust intrusion, the first wave of the COVID-19 epidemic occurred, resulting in a public health crisis and severe mobility restrictions. IARC personnel continued working physically at the Izaña Observatory in order to operate, maintain, and calibrate the numerous scientific instrumentation. Strict protocols were established while ensuring, at the same time, the continuity of the measurement programmes. My sincere thanks and appreciation go to the IARC personnel who made this possible.

In September 2021, the La Palma volcanic eruption took place, and IARC responded quickly by deploying a large amount of instrumentation on the island of La Palma, in collaboration with other national and international organisations with the sole purpose of helping to save lives and protect the population. Air quality equipment was installed and integrated into an expanded Canary Islands Government air quality network, and atmospheric profilers were set up around La Palma to monitor the volcanic plume height and composition. This is crucial

information used as input data for volcanic ash and gas dispersion models, essential for air traffic safety.

The fact that an emergency support unit was quickly formed from a research center, coordinating numerous external collaborations, was possible because it has highly qualified personnel accustomed to working with a tremendously flexible and versatile *modus operandi* provided by continuous national and international scientific collaborations. The overall response is a true example of the excellent results that can be achieved through international cooperation and personal and institutional involvement, leading to a significant contribution of science for society.

In addition, I would like to highlight the dedication of IARC and collaborating institutions in maintaining the high-quality, long-term measurement programmes, which now provide > 105 years of meteorological data, nearly 40 years of continuous greenhouse gas measurements (CO₂ and CH₄) and more than or close to 30 years of surface and column ozone, ultraviolet and solar radiation, in situ and column aerosols, water vapour and selected reactive gases. These long-term data series are invaluable and require commitment and a rigorous approach.

The summary of IARC's activities clearly explains the reason for the Center's relevance at an international level and the importance that AEMET (State Meteorological Agency and National Meteorological Service of Spain) gives to its work. I am confident that this is only a prologue to what awaits us in the coming years, in which we will see how IARC expands its historical and current activities to enhance what is already today part of the scientific heritage of humankind.

Finally, I would like to emphasise that, in addition to its outstanding scientific work, Izaña allows us to enjoy observing the atmosphere with all its energy and beauty in a unique place, showing meteorology in action in such a concise way that cannot be replicated in words. Over the years and from a distance, I have maintained a deep fondness for this place and a profound admiration and respect for the AEMET staff who serve there, fortunate enough to receive all that the job has to offer while contributing in return with their excellent scientific and personal dedication.

Consequently, it was an honour and a pleasure for me to have been able to join forces with them in supporting the development of IARC's R&D activities and contributing to the expansion of its logistical capabilities from my position as Director of Planning, Strategy and Business Development of AEMET.



1 Organization

The Izaña Atmospheric Research Center (IARC) is part of the Department of Planning, Strategy and Business Development of the State Meteorological Agency of Spain (AEMET). AEMET is an Agency of the Spanish Ministry for the Ecological Transition and the Demographic Challenge (MITECO).

2 Mission and Background

The Izaña Atmospheric Research Center conducts observations and research related to atmospheric constituents that are climate forcers in the Earth (greenhouse gases and aerosols), and may cause depletion of the global ozone layer, or play key roles in air quality from local to global scales. The IARC is an Associated Unit of the Spanish National Research Council (CSIC) through the Institute of Environmental Assessment and Water Research (IDAEA). The main goal of the Associated Unit “Group for Atmospheric Pollution Studies” is to perform air quality research in both rural and urban environments.

The IARC has contributed to the World Meteorological Organization (WMO) Global Atmosphere Watch (GAW) Programme since its establishment in 1989. GAW integrates a number of WMO research and monitoring activities in the field of atmospheric environment. The main objectives of GAW are to provide data and other information on the chemical composition and related physical characteristics of the atmosphere, its changes and the drivers of this change. These are required to improve our understanding of the behaviour of the atmosphere and its interactions with the oceans and the biosphere.

The Izaña Atmospheric Research Center also contributes to the Network for the Detection of Atmospheric Composition Change (NDACC). NDACC is an international network for monitoring atmospheric composition using remote measurement techniques. Originally, NDACC was created to monitor the physical and chemical changes in the stratosphere, with special emphasis on the evolution of the ozone layer and the substances responsible for its destruction known as Ozone Depleting Substances. The current objectives of NDACC are to observe and to understand the physicochemical processes of the upper troposphere and stratosphere, and their interactions, and to detect long-term trends of atmospheric composition. IARC also makes an important contribution to the WMO through the Global Climate Observing System and through the support of WMO Testbed for Aerosols and Water Vapour Remote Sensing Instruments.

Izaña Observatory was inaugurated in its present location on 1 January 1916, initiating uninterrupted meteorological and climatological observations, which constituted a 105-year record in 2020. In 1984, the observatory became a station of the WMO Background Atmospheric Pollution Monitoring Network (BAPMoN). In 1989, BAPMoN and GO3OS (Global Ozone Observing System) merged in the current Global Atmosphere Watch Programme, of which Izaña Observatory is one of 30 GAW Global stations (Figure 2.1). GAW Global stations serve as centres of excellence and perform extensive research on atmospheric composition change. Izaña Observatory is a key example of such a research facility.



Figure 2.1. WMO GAW Global stations.

3 Facilities and Summary of Measurements

The Izaña Atmospheric Research Center (IARC) manages four observatories in Tenerife (Fig. 3.1, Table 3.1): 1) Izaña Observatory (IZO); 2) Santa Cruz Observatory (SCO); 3) Botanic Observatory (BTO); and 4) Teide Peak Observatory (TPO).

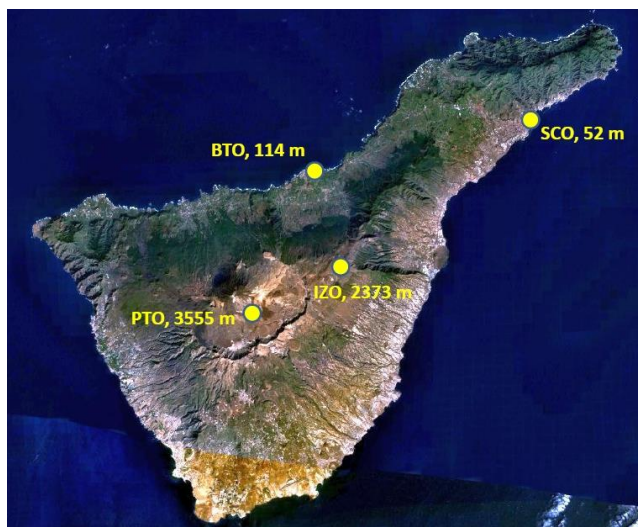


Figure 3.1. Location of IARC observatories on Tenerife.

Table 3.1. IARC observatories.

Observatory	Latitude	Longitude	Altitude (m a.s.l.)
IZO	28.309 °N	16.499 °W	2373
SCO	28.473 °N	16.247 °W	52
BTO	28.411 °N	16.535 °W	114
TPO	28.270 °N	16.639 °W	3555

3.1 Izaña Observatory

The Izaña Observatory (IZO) is located on the island of Tenerife, Spain, roughly 300 km west of the African coast. The observatory is situated on a mountain plateau, 15 km north-east of the volcano Teide (3718 m a.s.l.) (Figs 3.2 and 3.3). The local wind regime at the site is dominated by north-westerly winds. Clean air and clear sky conditions generally prevail throughout the year. IZO is normally above a temperature inversion layer, generally well established over the island, and below the descending branch of the Hadley cell.



Figure 3.3 Izaña Observatory (2373 m) with the volcano Teide (3718 m) to the left of the image.



Figure 3.2. Image of Izaña Observatory.

The station offers excellent conditions for trace gas and aerosol in situ measurements under “free troposphere” conditions, and for atmospheric observations by remote sensing techniques. The environmental conditions and pristine skies are optimal for calibration and validation activities of both ground-based and space-borne sensors. Due to its geographic location, it is particularly valuable for the investigation of dust transport from Africa to the North Atlantic, long-range transport of pollution from the Americas, and large-scale transport from the tropics to higher latitudes.

The Izaña Observatory facilities consist of three separate buildings: the main building, inaugurated in 1916; the aerosols lab, a small nearby building of the same period which was renamed “Joseph M. Prospero Aerosols Laboratory” on 8 April 2016; and the technical tower, completely rebuilt in early 2000, which hosts most of the instruments. Details of the IZO measurement programme are given in Table 3.2.

The main building is a two-storey building with a total area of 1420 m², which hosts the following facilities: office space, dining room, kitchen, library, conference hall with audio-visual system, meeting room, engine rooms, a mechanical workshop, and an electronics workshop. In addition, there is residential accommodation available for visiting scientists (seven double en-suite rooms).

The technical tower is a seven-storey building with a total area of 900 m². It includes 20 laboratories distributed among the different floors (Table 3.3, Fig. 3.8). All the laboratories are temperature-controlled.

Table 3.2. Izaña Observatory (IZO) measurement programme.

Parameter	Start date	Present Instrument	Data Frequency
Greenhouse Gases and Carbon Cycle			
CO ₂	Jun 1984	CRDS Picarro G2401 (Primary instrument) NDIR Licor 7000 (Secondary instrument)	2" 30"
CH ₄	Jul 1984	CRDS Picarro G2401 GC-FID Varian 3800	2" 4 samples/hour
N ₂ O	Jun 2007	GC-ECD Varian 3800 Los Gatos Research 913-0015	4 samples/hour 4"
SF ₆	Jun 2007	GC-ECD Varian 3800	4 samples/hour
CO	Jan 2008	CRDS Picarro G2401 GC-RGD Trace Analytical RGA-3 Los Gatos Research 913-0015	30" 3 samples/hour 4"
In situ Reactive Gases			
O ₃	Jan 1987	UV Photometry Teco 49-C (Previous Primary instrument) Teco 49-C (Secondary instrument) Teco 49-I (New Primary instrument)	1' 1' 1'
CO	Nov 2004	Non-dispersive IR absorption Thermo 48C-TL	1'
SO ₂	Jun 2006	UV fluorescence Thermo 43C-TL	1'
NO-NO ₂ -NO _x	Jun 2006	Chemiluminescence Thermo 42C-TL Chemiluminescence EcoPhysics CraNO _x II	1' 1'
Total Ozone Column and UV			
Column O ₃	May 1991	Brewer Mark-III #157 (Primary Reference) Brewer Mark-III #183 (for developments) Brewer Mark-III #185 (Travelling Reference)	~100/day ~100/day ~100/day
Spectral UV: 290-365 nm	May 1991	Brewer Mark-III #157 (Primary Reference) Brewer Mark-III # 183 (for developments) Brewer Mark-III #185 (Travelling Reference)	~30' ~30' ~30'
Spectral UV: 290-450 nm	May 1998	Bentham DM 150	Campaigns
Column SO ₂	May 1991	Brewer Mark-III #157 (Primary Reference) Brewer Mark-III # 183 (for developments) Brewer Mark-III #185 (Travelling Reference)	~100/day ~100/day ~100/day
Column O ₃	Oct 2011	Pandora 101 Pandora 121	10' 10'
Column NO ₂	Oct 2011	Pandora 101 Pandora 121	10' 10'

Parameter	Start date	Present Instrument	Data Frequency
Fourier Transform Infrared Spectroscopy (FTIR)			
Greenhouse gases, reactive gases, and O ₃ depleting substances (O ₃ , HF, HCN, HCl, ClONO ₂ , C ₂ H ₆ , HNO ₃ , CH ₄ , CO, CO ₂ , N ₂ O, NO, NO ₂ , H ₂ O, HDO, OCS)	Jan 1999 May 2007	Fourier Transform Infrared Spectroscopy Bruker IFS 120/5HR (co-managed with KIT) Middle infrared (MIR) solar absorption spectra Near infrared (NIR) solar absorption spectra	3 days/week (weather permitting)
Water vapour isotopologues (δD and δ ¹⁸ O)	Mar 2012- Apr 2019	Picarro L2120-I δD and δ ¹⁸ O Analyser	Continuous (2")
Greenhouse gases, and reactive gases (CO ₂ , CH ₄ , CO, H ₂ O)	May 2018	Fourier Transform Infrared Spectroscopy Bruker EM27/SUN	1 day/week (weather permitting)
In situ aerosols			
Chemical composition of particulate matter: PM _T ⁽¹⁾ PM ₁ ⁽²⁾ PM _{2.5} PM ₁₀	Jul 1987 Aug 2010 Apr 2002 Jan 2005	High-volume sampler custom built/MVC TM /MCZ TM Concentrations of soluble species by ion chromatography (Cl ⁻ , NO ₃ ⁻ and SO ₄ ²⁻) and FIA colorimetry (NH ₄ ⁺), major elements (Al, Ca, K, Na, Mg and Fe) and trace elements by ICP-AES and ICP-MS were determined at CSIC	8h sampling at night
Number of particles > 3 nm	Nov 2006 ⁽³⁾	TSI TM , UCPC 3025A	1'
Number of particles > 2.5 nm	Dec 2012	TSI TM , UCPC 3776	1'
Number of particles > 10 nm	Dec 2012	TSI TM , CPC 3010	1'
Size distribution of 10-400 nm	Nov 2006	TSI TM , class 3080 + CPC 3772	5'
Size distribution of 0.7-20 μm	Nov 2006	TSI TM , APS 3321	10'
Absorption coeff. 1λ (PM ₁₀)	Nov 2006	Thermo TM , MAAP 5012	1'
Attenuation 7λ (PM ₁₀)	Jul 2012	Magee TM , Aethalometer AE31-HS	1'
Scattering coeff. 3λ (PM ₁₀)	Jun 2008	TSI TM , Integration Nephelometer 3563	1'
PM ₁₀ concentration	Jun 2016 ⁽⁴⁾	Thermo, BETA 5014i	5'
PM _{2.5} and PM _{2.5-10} concentrations	Jun 2016	Thermo, TEOM 1405DF	6'

(1) Interrupted since 2017

(2) Usually only in summer (August)

(3) Not operational since June 2017

(4) Operating at SCO in 2019-2020

Parameter	Start date	Present Instrument	Data Frequency
Column aerosols			
AOD and Angstrom at 415, 499, 614, 670, 868, and 936 nm	Feb 1996-Dec 2018	YES Multi Filter-7 Rotating Shadow-Band Radiometer (MFRSR)	1'
AOD and Angstrom at 340, 380, 440, 500, 675, 870, 936, 1020 nm	Mar 2003	CIMEL CE318 sun photometer	~ 15'
Fine/Coarse AOD Fine mode fraction	Mar 2003	CIMEL CE318 sun photometer	~ 15'
Optical properties	Mar 2003	CIMEL CE318 sun photometer	~ 1h
AOD and Angstrom during night period	July 2012	CIMEL CE318-T sun-sky-lunar photometer	~ 15' during moon phases
AOD and Angstrom at 368, 412, 500 and 862 nm	July 2001	WRC Precision Filter Radiometer (PFR)	1'
AOD at 769.9 nm	July 1976	MARK-I (at the IAC)	AOD at 769.9 nm
Vertical Backscatter-extinction @523 nm, clouds altitude and thickness	Oct 2018	Micropulse Lidar MPL-3, SES Inc., USA (co-managed with INTA (www.inta.es))	1'
Radiation			
Global Rad. 285-2600nm	Jan 1977	2 CM-21 & CM-11 Kipp & Zonen Pyranom. (in parallel) and EKO MS-801	1'
Global Rad. 300-1100 nm	Feb 1996	YES MFRSR	1'
Estim. Direct Rad.	Feb 1996	YES MFRSR	1'
Direct Rad. 200-4000nm	Aug 2005	2 CH-1 Kipp & Zonen and EKO MS-56 Pyrhemometers	1'
Direct Rad. 200-4000nm	Jun 2014	Absolute Cavity Pyrhemometer PMO6	Calibration campaigns (1')
Spectral direct Radiation	Dec 2016	Spectrorradiometer EKO MS-711	1'
Spectral global and diffuse Radiation	Feb 2020	Spectrorradiometer EKO RSB	1'
Diffuse Rad.	Feb 1996	YES MFRSR	1'
Diffuse Rad. 285-2600nm	Aug 2005	2 CM-21 Kipp & Zonen Pyranometer (in parallel) and and EKO MS-801	1'
Downward Longwave Rad. 4.5-42µm	Mar 2009	2 CG-4 Kipp & Zonen Pyrgeometer (in parallel)	1'
UVB Radiation 315-400nm	Aug 2005	2 Yankee YES UVB-1 Pyranometer (in parallel)	1'
UVA Radiation 280-400nm	Mar 2009	Radiometers UVS-A-T	1'
PAR 400-700nm	Aug 2005	Pyranometer K&Z PQS1	1'
Net Radiation	Nov 2016	Net Radiometer EKO MR-60	1'
Luminance/Radiance	Nov 2020	EKO MS-321LR Sky Scanner	10'

Parameter	Start date	Present Instrument	Data Frequency
DOAS (managed by the Spanish National Institute for Aerospace Technology, INTA)			
Column NO ₂	May 1993	UV-VIS DOAS EVA and MAXDOAS RASAS II (INTA's homemade; www.inta.es)	Every ~20' during twilight
Column O ₃	Jan 2000	UV-VIS MAXDOAS RASAS II (INTA's homemade)	Every ~20' during twilight
Column BrO	Jan 2002	UV-VIS MAXDOAS ARTIST-II (INTA's homemade)	Every ~20' during twilight
Tropospheric O ₃	May 2010	UV-VIS MAXDOAS RASAS II (INTA's homemade)	Every ~20' during twilight
Tropospheric NO ₂	May 2010	UV-VIS MAXDOAS RASAS II (INTA's homemade)	Every ~20' during twilight
Tropospheric IO	May 2010	UV-VIS MAXDOAS RASAS II (INTA's homemade)	Every ~20' during twilight
Tropospheric HCHO	May 2015	UV-VIS MAXDOAS ARTIST II (INTA's homemade)	Every ~20' during twilight
Water Vapour			
Precipitable Water Vapour (PWV)	Feb 1996-Dec 2018	YES MFRSR-7 Radiometer (941 nm)	1'
PWV	Jul 2008 (ultra-rapid orbits) Jan 2009 (precise orbits)	GPS/GLONASS LEICA GRX1200GGPRO	15' (ultra-rapid orbits) and 1h (precise orbits)
Vertical relative humidity PWV Total Column and Profiles for layers from 2.4 km up to 12 km altitude	Dec 1963	Vaisala RS-40	Daily at 00 and 12 UTC
PWV	Mar 2003	CIMEL CE318 sun photometer	~ 15'
PWV	Jan 1999	Fourier Transform Infrared Spectroscopy	3 days/week when cloud-free conditions
Integrated Water Vapour (IWV)	May 2020	Microwave Radiometer LHATPRO G5	1''
Vertical Absolute Humidity (HPC)	May 2020	Microwave Radiometer LHATPRO G5	1''
Vertical Relative Humidity (HRC)	May 2020	Microwave Radiometer LHATPRO G5	1''
Liquid Water Path (LWP)	May 2020	Microwave Radiometer LHATPRO G5	1''
Liquid Water Profile (LPR)	May 2020	Microwave Radiometer LHATPRO G5	1''
Cloud Base Height (CBH)	May 2020	Microwave Radiometer LHATPRO G5	1''

Parameter	Start date	Present Instrument	Data Frequency
Meteorology			
Temperature	Jan 1916	THIES CLIMA 1.1005.54.700 3 VAISALA HMP45C (in parallel) VAISALA PTU300 THIES CLIMA 1.0620.00.000 (thermo-hygrograph) CAMPBELL SCIENTIFIC CS215 (Tower top)	1' 1' 1' Continuous 1'
Relative humidity	Jan 1916	THIES CLIMA 1.1005.54.700 3 VAISALA HMP45C (in parallel) VAISALA PTU300 THIES CLIMA 1.0620.00.000 (thermo-hygrograph) CAMPBELL SCIENTIFIC CS215 (Tower top)	1' 1' 1' Continuous 1'
Wind direction and speed	Jan 1916	Sonic anemometer Thies 2D 4.3820.31.401 Sonic anemometer FT Technologies FT742-D-DM Sonic anemometer FT Technologies FT742-D-DM (Tower Top)	1' 1' 1'
Pressure	Jan 1916	SETRA 470 VAISALA PTU 300 BELFORT 5/800AM/1 (Barograph) SETRA 470 (Tower top)	1' 1' Continuous 1'
Rainfall	Jan 1916	THIES CLIMA Tipping Bucket THIES CLIMA Tipping Bucket Hellman rain gauge Hellman pluviograph	1' 1' Daily Continuous
Sunshine duration	Aug 1916	KIPP & ZONEN CSD3 Campbell Stokes Sunshine recorder	10' Continuous
Present weather and visibility	Jul 1941	BIRAL 10HVJS	10'
Vertical profiles of T, RH, P, wind direction and speed, from sea level to ~30 km altitude	Dec 1963	RS92+GPS radiosondes launched at Güimar automatic radiosonde station (WMO GRUAN station #60018) (managed by the Meteorological Centre of Santa Cruz de Tenerife)	Daily at 00 and 12 UTC
Soil surface temperature	Jan 1953	2 THIES CLIMA Pt100 (in parallel)	10'
Soil temperature (20 cm)	Jan 2003	2 THIES CLIMA Pt100 (in parallel)	10'
Soil temperature (40 cm)	Jan 2003	2 THIES CLIMA Pt100 (in parallel)	10'
Atmospheric electric field	Apr 2004	Electric Field Mill PREVISTORM-INGESCO	10"
Lightning discharges	Apr 2004	Boltek LD-350 Lightning Detector	1'
Cloud cover	Sep 2008	Sieltec Canarias S.L. SONA total sky camera Sieltec Canarias S.L. SONA total sky camera (Model 201D, daytime) Sieltec Canarias S.L. SONA total sky camera (Model 502N, nighttime)	5' 5' 5'

Fog-rainfall	Nov 2009	THIES CLIMA Tipping Bucket with 20 cm ² mesh Hellman rain gauge with 20 cm ² mesh	1' Daily
Sea-cloud cover	Nov 2010	AXIS Camera: West View (Orotava Valley) AXIS Camera: South View (Meteo Garden) AXIS Camera: North View AXIS Camera: East View (Güimar Valley)	5' 5' 5' 5'
Drop size distribution and velocity of falling hydrometeors	May 2011	OTT Messtechnik OTT Parsivel	1'
Aerobiology			
Pollens and spores	Jun 2006	Hirst, 7-day recorder VPPS 2000 spore trap (Lanzoni S.r.l.). Analysis performed with a Light microscope, 600 X at the Laboratori d'Anàlisi Palinològiques, Universitat Autònoma de Barcelona	Continuous (1 h resolution) from April to October

On the ground floor of the technical tower, there are two storage spaces, one of them is for pressured cylinders (tested and certified at the Canary Islands Regional Council for Industry) and the other one is for cylinder filling using oil-free air compressors. This floor also includes the central system for supplying high purity gases (H₂, N₂, Ar/CH₄) and synthetic air to the different laboratories. On the second floor, there is a dark-room with the necessary calibration set-ups for the IZO radiation instruments. On the top of the technical tower there is a 160 m² flat horizon-free terrace for the installation of outdoor scientific instruments that need sun or moon radiation. It also has the East and West sample-inlets which supply the ambient air to in situ trace gas analysers set up in different laboratories.

The “Joseph M. Prospero Aerosol Research Laboratory” is a 40 m² building used as an on-site aerosol measurement laboratory. It has four sample-inlets connected to aerosol analysers. For more details, see Section 8. Outside Izaña Observatory there are the following facilities: 1) a 160 m² flat horizon-free platform with communications and UPS used for measurement field campaigns; 2) the meteorological garden, containing two fully-automatic meteorological stations (one of them is the SYNOP station and the second one is for meteorological research), manual meteorological gauges, a total sky camera, a GPS/GLONAS receiver, a lightning detector, and an electric field mill sensor; and 3) the Sky watch cabin hosting four cameras for cloud observations with corresponding servers. The following sections give further details of some of the facilities located at IZO.

Table 3.3. Izaña Observatory technical tower facilities.

Floor	Facilities	Description
Ground Floor	Mechanical Workshop	33 m ² room with the necessary tools to carry out first-step mechanical repairs.
	Electronics Workshop	25 m ² room equipped with oscilloscopes, power supplies, multimeters, soldering systems, etc. to carry out first-step electronic repairs.
	Heating system	Central heating and hot water 90 kW system.
	Air Conditioning System	Central air conditioning system for labs.
	Engine Room: Backup Generators	General electrical panel and two automatic start-up backup generators (400 kVA and 100 kVA, respectively).
	UPS room	Observatory's main UPS (40 kVA redundant) used for assuring the power of the equipment inside the building and an additional UPS (10 kVA) for the outside equipment.
	Compressor room	Room with clean oil-free air compressors used for calibration cylinders filling. It also contains the general pumps for the East and West sample inlets.
	Warehouse / Central Gas Supply System	30 m ² warehouse authorized for pressure cylinders. Central system for high purity gas (H ₂ , N ₂ , Ar/CH ₄) and synthetic air supply.
	Lift	6-floors. No lift access to roof terrace.
First Floor	Archive room	Archive of bands and historical records.
	Technical equipment warehouse	Spare parts for the Observatory's technical equipment.
	Meeting room	8 person meeting room
Second Floor	Optical Calibration Facility	30 m ² dark room hosting vertical and horizontal absolute irradiance, absolute radiance, angular response, and spectral response calibration set ups.
	T2.1 Laboratory	10 m ² lab with access to West sample inlet.
	T2.2 Laboratory	9 m ² lab with access to East sample inlet.
	T2.3 Laboratory	13 m ² lab hosting Picarro L2120-I δ D and δ^{18} O analyser with access to East sample inlet
Third Floor	Greenhouse Gases Laboratories	70 m ² shared in two labs hosting CO ₂ , CH ₄ , N ₂ O, SF ₆ and CO analysers with access to the East and West sample inlets.
Fourth Floor	All purpose laboratories	Three labs with access to the East and West sample inlets.
Fifth Floor	Reactive Gases Laboratory	10 m ² lab hosting NO-NO ₂ , CO, and SO ₂ analysers with access to West sample inlet.
	Communications room	Server room and WIFI connection with Santa Cruz de Tenerife headquarters.
	Brewer Laboratory	20 m ² lab for Brewer campaigns.
Sixth Floor	Surface Ozone Laboratory	10 m ² laboratory hosting surface O ₃ analysers with access to West sample inlet.
	Solar Photometry Laboratory	10 m ² maintenance workshop for solar photometers.
	Spectroradiometer Laboratory	25 m ² laboratory hosting two MAXDOAS and two spectroradiometers connected with optical fibre.
Roof	Instrument Terrace	160 m ² flat horizon-free terrace hosting outdoor instruments, East and West sample-inlets, wind, pressure, temperature and humidity sensors.

3.1.1 Optical Calibration Facility

The optical calibration facility at IZO has been developed within the framework of the Specific Agreement of Collaboration between the University of Valladolid and the IARC-AEMET: “To establish methodologies and quality assurance systems for programs of photometry, radiometry, atmospheric ozone and aerosols within the atmospheric monitoring programme of the World Meteorological Organization”. The main objective of the optical calibration facility is to perform Quality Assurance & Quality Control (QA/QC) assessment of the solar radiation instruments that support the ozone, aerosols, radiation, and water vapour programs of the IARC. The eight set-ups available are the following:

1) Set-up for the absolute irradiance calibration by calibrated standard lamps in a horizontally oriented position suitable for small radiometers (Fig. 3.4A). The basis of the absolute irradiance scale consists of a set of FEL-type 1000 W lamps traceable to the primary irradiance standard of the Physikalisch-Technische Bundesanstalt (PTB).

2) Set-up for the absolute irradiance calibration by calibrated standard lamps in a vertical oriented position suitable for relatively large spectrophotometers (Fig. 3.4B). The basis of the absolute irradiance scale consists of a set of DXW-type 1000 W lamps traceable to the primary irradiance standard of the PTB.

3) Set-up for the absolute radiance calibration by calibrated integrating sphere (Fig. 3.4C). The system is traceable to the AErosol RObotic NETwork (AERONET) standard at the Goddard Space Flight Center (Washington, USA). This set-up is mainly used by Cimel sun-photometers, but other instruments can also be calibrated.

4) At the end of 2017, in the framework of a competitive scientific infrastructure call of the National Plan for Research, Development and Innovation of Spain, a new integrating sphere was installed at Izaña for AERONET-Europe absolute radiance calibrations as well as optical tests required for QC/QA of reference instruments. The new integrating sphere has a 50.8 cm diameter, a 20.3 cm aperture, and 400 W power (Fig. 3.4G). This system is also traceable to the AERONET standard at the Goddard Space Flight Center.

5) Set-up for the angular response calibration (Fig. 3.4D). It is used to quantify the deviations of the radiometer’s angular response from an ideal cosine response. The relative angular response function is measured rotating the mechanical arm where the seasoned DXW-type 1000 W lamp is located. The rotation over $\pm 90^\circ$ is controlled by a stepper motor with a precision of 0.01° while the instrument is illuminated by the uniform and parallel light beam of the lamp.

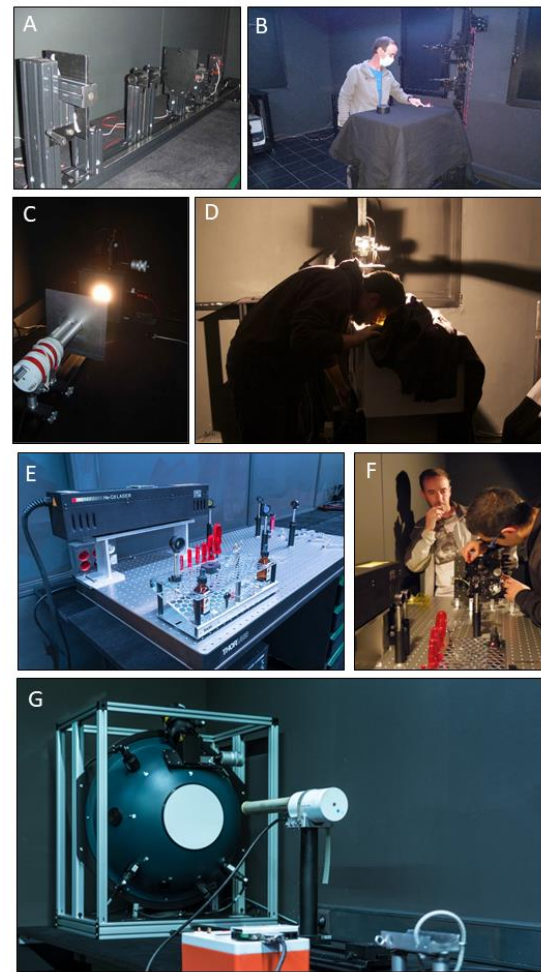


Figure 3.4. Images of the IZO Optical calibration facility. A) Horizontal absolute irradiance calibration set up, B) Three stages of a Brewer irradiance calibration with the vertical set up, C) Absolute radiance calibration of a Cimel CE318, D) Angular response function determination of a Brewer, E) Set up for Slit function determination, F) Alignment of a Brewer spectrophotometer optics, G) shows same set up as C) Absolute radiance calibration of a Cimel CE318.

6) Set-up for the spectral response calibration. It is used to quantify the spectral response of a radiometer. The light is scattered by an Optronic double monochromator OL 750 within the range from 200 to 1100 nm with a precision of 0.1 nm. An OL 740-20 light source positioned in front of the entrance slit acts as radiation source and two lamps, UV (200-400nm) and Tungsten (250-2500nm) are available.

7) Set-up for the slit function determination (Fig. 3.4E). The characterization of the slit function is performed illuminating the entrance slit of a spectrophotometer with the monochromatic light of a VM-TIM He-Cd laser. The nominal wavelength of the laser is 325 nm, its power is 6mW, and its beam diameter is 1.8 mm.

8) Set-up for the alignment of the Brewer spectrophotometer optics (Fig. 3.4F). It is suitable to perform adjustments of the optics without sending the instrument to the manufacturer.

3.1.2 In situ system used to produce working standards containing natural air

GAW requires very high accuracy in the atmospheric greenhouse gas mole fraction measurements, and a direct link to the WMO primary standards maintained by the GAW GHG CCLs (Central Calibration Laboratories), most of which are located at the National Oceanic and Atmospheric Administration-Earth System Research Laboratory-Global Monitoring Laboratory (NOAA-ESRL-GML). To accomplish these requirements, IARC uses Laboratory Standards prepared (using natural air) and calibrated by NOAA-ESRL-GML. Indeed, the Laboratory Standards used at IARC are WMO tertiary standards.

However, due to the fact that the consumption of standard and reference gases by the IARC GHG measurement systems is relatively high, an additional level of standard gases (working standards) prepared with natural air is used.

These working standards are prepared at IZO using an in-situ system (Fig. 3.5) and then calibrated against the Laboratory Standards using the IARC GHG measurement systems. The system used to fill the high pressure cylinders

(up to 120-130 bars) with dried natural air, takes clean ambient air from an inlet located on top of the IZO tower (30 m above ground), and pumps (using an oil-free compressor) it inside the cylinders after drying it (using magnesium perchlorate), achieving a H₂O mole fraction lower than 3 ppm.

Additionally, it is possible to modify slightly the CO₂ mole fraction of the natural air pumped inside the cylinders. To this end, air from a cylinder containing natural air with zero CO₂ mole fraction (prepared using the same system but adding a CO₂ absorber trap) or a tiny amount of gas from a spiking CO₂ cylinder (5% of CO₂ in N₂/O₂/Ar) is added to the cylinder being filled. This system is similar to that used by NOAA-ESRL-GML to prepare WMO secondary and tertiary standards, and it is managed and operated at IZO through a subcontractor (Air Liquide Canarias). The prepared working standards are mainly used in the GHG measurement programme, but some of them are used for other purposes, natural air for a H₂O isotopologue CRDS analyser located at Teide peak and for a CO NDIR analyser located at SCO.

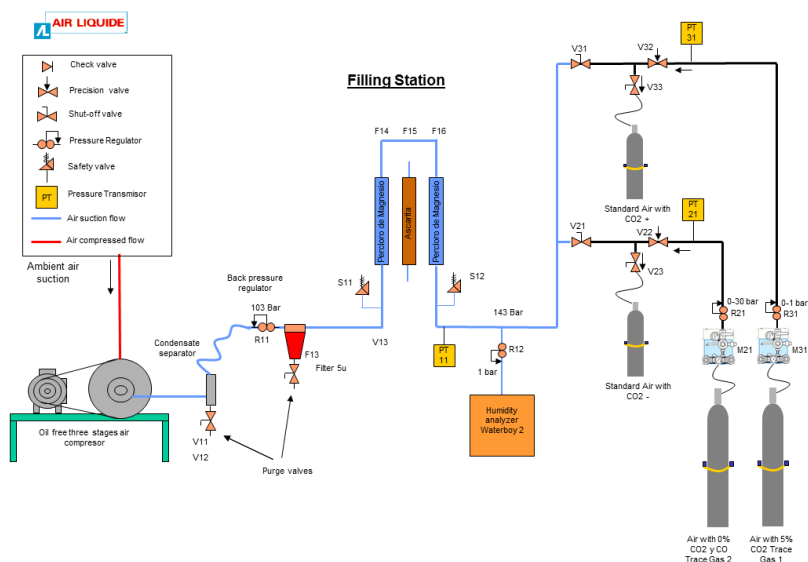


Figure 3.5. In situ system used to produce working standards containing natural air at Izaña Observatory.

3.1.3 Central Gas Supply System

There is a gas central facility located on the IZO tower ground floor for supplying support gases to the different instruments. This central facility supplies high purity: N₂ (used as carrier gas for the GC-FIDs, and for the IZO H₂O isotopologue Cavity Ring-Down Spectroscopy (CRDS) analyser), synthetic air (used as oxidizer in the FIDs, as carrier gas in the GC-RGD, as carrier gas in the IZO H₂O isotopologue CRDS analyser, and as diluting air used in the calibrations of the reactive gas instruments), 95% Ar / 5% CH₄ (used as carrier gas for the CD-ECD), and H₂ (used as combustible in the FIDs). The H₂O isotopologue CRDS

analyser located at Teide peak has its own dedicated high purity N₂ supply.

Additionally, other gases (provided by Air Liquide) are used at IZO: high purity CO₂ for the calibration of an aerosol nephelometer, high purity N₂O for FTIR instrumental line shape monitoring, liquid N₂ to cryocool the FTIR detectors, and calibrated concentrated gas standards in N₂ (19.4 ppm NO and 19.4 ppm NO₂, 1.01 ppm CO, 1.04 ppm CO, 99.9 ppm CO, 102 ppm SO₂, and 1 ppm SO₂) for the calibration of the instruments of the reactive gases programme.

3.1.4 Aerosol Filters Laboratory

The Aerosol Filters Laboratory at IZO is equipped with an auto-calibration microbalance (Mettler Toledo XS105DU) with a resolution of 0.01 mg, a set of standard weights, and an oven that reaches 300 °C. Filters are weighed following the requirements of the UNE-EN-12341-2015 standards. This filter weighing procedure is used for determination of concentrations of PM₁₀, PM_{2.5} and PM₁ by means of standardized methods, within a methacrylate chamber, which also contains the balance used for weighing the filters (Fig. 3.6).



Figure 3.6. IZO Aerosol Filters laboratory: temperature and relative humidity controlled chamber.

3.1.5 Modifications and improvements to the IZO facilities carried out in 2019-2020

In 2020, a new laboratory (Testbed#1), with a temperature stabilization system and UPS, was completed to house the Cimel CE-376 lidar (Fig. 3.7) (see Section 9.2.1 for more details).



Figure 3.7. New Lidar laboratory (Testbed#1) at IZO.

A room in the old meteorological kite hangar at IZO has been refurbished to house a new cosmic ray detector (ICaRO) (Fig. 3.8), an instrument from the University of Alcalá de Henares. The entire electrical system was renewed, conditioning of the floor and walls and a temperature control system were installed.



Figure 3.8. ICaRO cosmic ray detector.

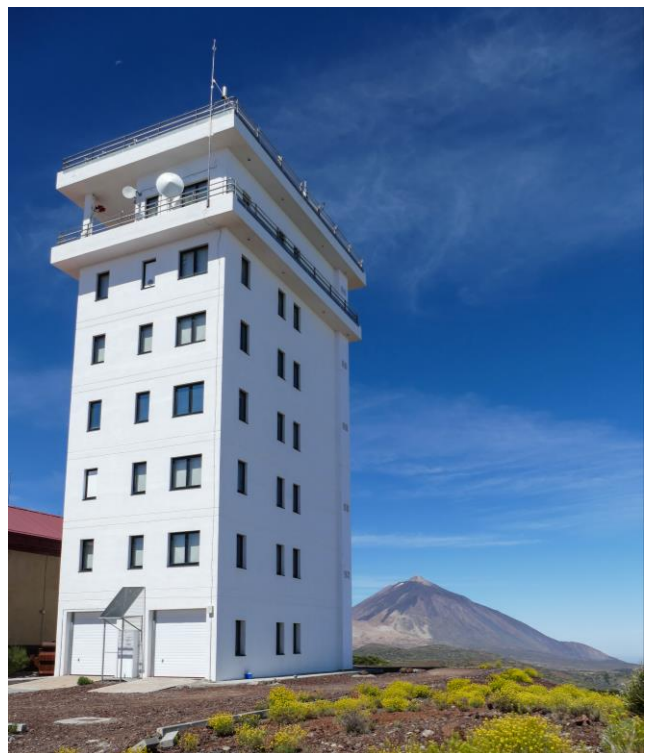


Figure 3.9. Images of IZO Instrument terrace and technical tower.

3.2 Santa Cruz Observatory

The Santa Cruz de Tenerife Observatory (SCO) is located on the roof of the IARC headquarters at 52 m a.s.l. in the capital of the island (Santa Cruz de Tenerife), close to the city harbour (Figs. 3.10 and 3.11). Details of the SCO measurement programme are given in Table 3.4.



Figure 3.10. Images of Santa Cruz Observatory (SCO).

This observatory has two main objectives: 1) to provide information on background urban pollution to support atmospheric research and to study contribution of the long-range pollution transport driven by trade winds or Saharan dust outbreaks on local air quality and 2) to perform complementary measurement programme to the one at IZO. The IARC headquarters include the following facilities:

- A laboratory for reactive gases measurements (surface O_3 , NO - NO_2 , CO and SO_2).
- A laboratory hosting Micro Pulse Lidar (MPL) and ceilometer VL-51.
- A laboratory for the preparation of ozonesondes.
- A 25 m² flat horizon-free terrace for radiation instruments and air intakes.

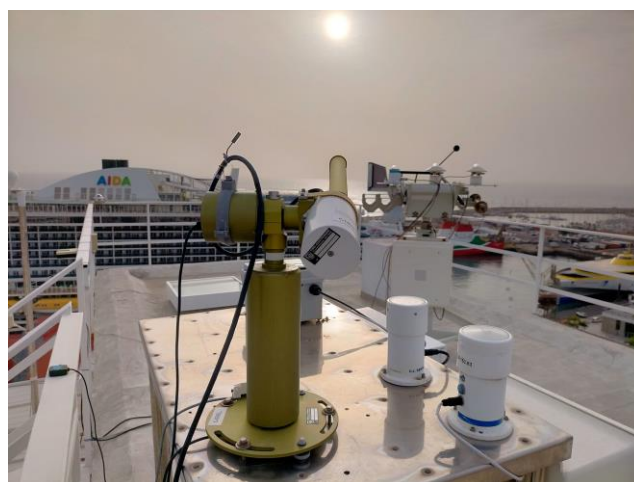


Figure 3.11. Image of SCO instrument terrace.

3.2.1 The Ozonesonde Laboratory

Advanced preparation of the Science Pump Corporation (SPC) Electrochemical Concentration Cell (ECC) ozone sensor (Model ECC-6A), together with digital Vaisala RS92 radiosonde and digital interface, is performed at the Ozonesonde Lab at SCO.

A Science Pump Corporation Model TSC-1 Ozonizer/Test Unit is used for ozonesonde preparation. This unit has been designed for conditioning of ECC ozonesondes with ozone, and for checking the performance of the sondes prior to balloon release. The Ozonizer/Test Unit uses synthetic air (air bottles) to produce ozone free air and an UV lamp to produce high concentration ozone. The sensing solution is prepared inside a hood in which ambient air is passed through an active charcoal filter to purify the air. The volumetric flow of the gas sampling pump of each ECC sonde is individually measured at the Ozonesonde Lab before flight. The pump flow rate of the sonde is measured with a bubble flow meter at the gas outlet of the sensing cell.

On the day of release, the ECC-6A ozonesonde is checked for proper operation, filled with the sensing solution and the background current measured. The ECC-sonde is transported to the Botanic Observatory ozonesonde launching station (30 km distance) where pre-launch tests are performed.

Table 3.4. Santa Cruz Observatory (SCO) measurement programme.

Parameter	Start date	Present Instrument	Data Frequency
In-situ Reactive Gases			
O ₃	Nov 2004	UV Photometry TECO 49-C	1'
CO	Mar 2006	Non-dispersive IR abs. Thermo 48C-TL	1'
SO ₂	Mar 2006	UV fluorescence Thermo 43C-TL	1'
NO-NO ₂ -NO _x	Mar 2006	Chemiluminescence Thermo 42C-TL	1'
O ₃ , NO ₂ , CO, PM _{2.5} , PM ₁₀	Mar 2017	Vaisala Air Quality Transmitter AQT420	1'
Ozone and UV (managed by the AEMET's Special Networks Service at the nearby Met Center)			
Column O ₃	Oct 2000	Brewer Mark-II#033	> ~20/day
Spectral UV	Oct 2000	Brewer Mark-II#033	~30'
SO ₂	Oct 2000	Brewer Mark-II#033	~30'
Column aerosols			
AOD and Angstrom at 340, 380, 440, 500, 675, 870, 936, 1020 nm	Jul 2004	CIMEL CE318 sun photometer	~ 15'
Fine/Coarse AOD	Jul 2004	CIMEL CE318 sun photometer	~ 15'
Vertical Backscatter-extinction @523 nm, clouds alt. and thickness	Nov 2005- Oct 2018	Micro Pulse Lidar MPL-3, SES Inc., USA (co-managed with INTA (www.inta.es)) <i>MPL-3 installed in IZO in Oct 2018</i>	1'
Vertical backscatter-extinction @910 nm, cloud alt. and thickness	Jan 2011	Vaisala CL-51 Ceilometer	36" + hourly and ten-minutes averages
Vertical Backscatter-extinction @500 and 800 nm, clouds alt. and thickness (with depolarization channels)	Dec 2015	CIMEL CE376 lidar	1'
Vertical Backscatter-extinction @532 nm, clouds alt. and thickness	May 2018	Micro Pulse Lidar MPL-4B, provided by NASA Goddard Space Flight Center MPLNET	1'
Radiation			
Global Radiation	Feb 2006	Pyranometer CM-11 Kipp & Zonen	1'
Direct Radiation	Feb 2006	Pyrheliometer EPPLEY	1'
Diffuse Radiation	Feb 2006	Pyranometer CM-11 Kipp & Zonen	1'
UV-B Radiation	Aug 2011	Yankee YES UVB-1 Pyranom. (managed by the AEMET's Special Networks Service at the nearby Met Centre)	1'
Water Vapour			
PWV Total Column and Profiles for 13 layers from surface up to 12 km of altitude	Dec 1963	Vaisala RS41	Daily at 00 and 12 UTC
Precipitable Water Vapour (PWV)	Mar 2003	CIMEL CE318 sun photometer	~ 15'

PWV	July 2008	GPS/GLONASS LEICA GR50 receiver	15' (ultra-rapid orbits)
PWV (total column) over SCO when cloudless skies. Cloud base heights when cloudy skies over SCO	Jun 2014	1 SIELTEC Sky Temperature Sensor (infrared thermometer prototype)	Every 30" during the complete day
Water vapour isotopologues (δD and $\delta^{18}O$)	May 2019	Picarro L2120-I δD and $\delta^{18}O$ Analyser	Continuous (2")
Meteorology*			
Vertical profiles of T, RH, P, wind direction and speed, from sea level to ~30 km altitude	Dec 1963	RS41+GPS radiosondes launched at Güimar automatic radiosonde station (WMO GRUAN station #60018) (managed by the Meteorological Centre of Santa Cruz de Tenerife)	Daily at 00 and 12 UTC
Temperature	Jan 2002	VAISALA HMP45C	1'
Relative humidity	Jan 2002	VAISALA HMP45C	1'
Wind Direction and speed	Jan 2002	RM YOUNG wind sentry 03002	1'
Pressure	Jan 2002	VAISALA PTB100A	1'
Rainfall	Jan 2002	THIES CLIMA Tipping Bucket	1'
Aerobiology			
Pollens and spores	Oct 2004	Hirst, 7-day recorder VPPS 2000 spore trap (Lanzoni S.r.l.).	Continuous (1 h resolution)

* Meteorological data from Santa Cruz de Tenerife Meteorological Center headquarters, 1 km distant, are also available since 1922.

3.3 Botanic Observatory

The Botanic Observatory (BTO) is located 13 km north of IZO at 114 m a.s.l. in the Botanical Garden of Puerto de la Cruz (Fig. 3.11). BTO is hosted by the Canary Institute of Agricultural Research (ICIA). The Botanic Observatory includes the following facilities:

- Ozone Sounding Monitoring Laboratory: equipped with a Digicora MW41 receiver with Vaisala data acquisition and processing software.
- Launch container: equipped with a Helium supply system used for ozonesonde balloons filling.

In addition to the ozonesonde measurements, there is a fully equipped automatic weather station (temperature, relative humidity, pressure, precipitation, wind speed and direction) and a global irradiance pyranometer. For details of the BTO measurement programme, see Table 3.5.



Figure 3.12. Image of Botanic Observatory (BTO).

Table 3.5. Botanic Observatory (BTO) measurement programme.

Parameter	Start date	Present Instrument	Data Frequency
Reactive Gases and ozonesondes			
Vertical profiles of O ₃ , pressure, temperature, humidity, wind direction and speed, from sea level to ~33 km altitude	Nov 1992	ECC-A6+RS41/GPS radiosondes	1/week (Wednesdays)
Radiation			
Global Radiation	May 2011	Pyranometer CM-11 Kipp & Zonen	1'
Column Water Vapour			
Precipitable Water Vapour	July 2008	GPS/GLONASS TRIMBLE NETR9 receiver	15' (ultra-rapid orbits)
Meteorology			
Temperature	Oct 2010	VAISALA F1730001	1'
Relative humidity	Oct 2010	VAISALA F1730001	1'
Wind direction and speed	Oct 2010	VAISALA WMT700	1'
Pressure	Oct 2010	VAISALA PMT16A	1'
Rainfall	Oct 2010	VAISALA F21301	1'

3.4 Teide Peak Observatory

The Teide Peak Observatory (TPO) is located at 3555 m a.s.l. at the [Teide Cable Car](#) terminal in the Teide National Park (Fig. 3.13). TPO was established as a satellite station of IZO primarily for radiation and aerosol observations at very high altitude. TPO station, together with Jungfraujoch (3454 m a.s.l.) in Switzerland, are the highest permanent radiation observatories in Europe.

This measurement site provides radiation and aerosol information under extremely pristine conditions and in conjunction with measurements at SCO and IZO allows us to study the variation of global radiation, UV-B and aerosol optical depth from sea level to 3555 m a.s.l. In addition to radiation and aerosol measurements, there is a meteorological station and a water vapour isotopologues analyser. Full details of the measurement programme are given in Table 3.6.



Figure 3.13. Measurements at Teide Peak Observatory.

Table 3.6. Teide Peak Observatory (TPO) measurement programme.

Parameter	Start date	Present Instrument	Data Frequency
Column aerosols			
AOD and Angstrom at 340, 380, 440, 500, 675, 870, 936 and 1020 nm	Jun 1997	CIMEL CE318 sun photometer (Co-managed with the University of Valladolid Atmospheric Optics Group)	~ 15' (during Apr-Oct)
Fine/Coarse AOD Fine mode fraction	Jun 1997	CIMEL CE318 sun photometer (Co-managed with the University of Valladolid Atmospheric Optics Group)	~ 15' (during Apr-Oct)
Radiation			
Global Radiation	Jul 2012	Pyranometer CM-11 Kipp & Zonen	1'
UVB Radiation	Jul 2012	Pyranometer Yankee YES UVB-1	1'
Global and diffuse radiation	Sep 2019	SPN1 Sunshine Pyranometer	1'
Water vapour			
Water vapour isotopologues (δD and $\delta^{18}O$)	June 2013	Picarro L2120-I δD and $\delta^{18}O$ analyser	2"
Precipitable Water Vapour	Feb 2020	GPS/GLONASS TRIMBLE NETR9 receiver	15 " (ultra-rapid orbits)
Meteorology			
Wind direction and speed	Oct 2011	THIES CLIMA Sonic 2D	1'
Temperature	Aug 2012	VAISALA HMP45C	1'
Relative humidity	Aug 2012	VAISALA HMP45C	1'
Pressure	Aug 2012	VAISALA PTB100A	1'

3.5 Computing Facilities and Communications

The computing facilities and communications form an integral component of all measurement programmes and activities in the Izaña Atmospheric Research Center. In the IARC headquarters there is a temperature-controlled room hosting server computers devoted to different automatic and continuous tasks (Network-Attached Storage (NAS), modelling, spectra inversion, etc.) for the research groups. Details of the computing facilities are given in Table 3.7.

Table 3.7. IARC computing facilities.

Computing Hardware				
	Storage	Virtualization	Modelling	Total
H.D.	34 TB	12 TB	10 TB	56 TB
Cores	7	28	68	105
RAM	12 GB	56 GB	46 GB	114 GB

A EUMETCast (European Organisation for the Exploitation of Meteorological Satellites (EUMETSAT) Broadcast System for Environmental Data) reception station is available at SCO. It consists of a multi-service dissemination system based on standard Digital Video Broadcast (DVB) technology. Most of the satellite information is received via this system (see Section 13 for more details).

Data communications were notably improved at the IARC in 2020 by its incorporation into the Advanced Communications Network for Spanish Research (IRIS NOVA network).

RedIRIS-NOVA is the high-capacity optical network of RedIRIS, which connects the regional networks of all the autonomous regions and the main research centers in Spain with the rest of international academic networks, especially the Portuguese academic and research networks and the European research network GÉANT. Fibre optics makes it possible to easily deploy 10Gbps or 40Gbps circuits, and soon 100Gbps, at a much lower cost than the network model based on capacity rental. RedIRIS-NOVA connects more than 50 Points of Presence with each other, making up a mesh network on which the RedIRIS IP Trunk Network and the regional networks are deployed. This network for research allows collaboration between researchers and the deployment of next-generation services.

IARC is the only AEMET unit that has IRIS NOVA Network communications due to its status as a research center.

IARC currently has two data networks, the AEMET network, with access from the central headquarters in Santa Cruz, and linked to the Izaña Observatory by a microwave link (Fig. 3.14), and the IRIS NOVA Network with a double entry. The IARC offices in Santa Cruz are linked to the IRIS NOVA network through a fibre optic connection to the IGN node located in the same building, and to the Izaña Observatory through a fibre optic connection, approximately 1 km long, with the IRIS NOVA node at the Teide Observatory of the Instituto de Astrofísica de Canarias (IAC) (Institute of Astrophysics of the Canary Islands).



Figure 3.14. Microwave link antenna between Santa Cruz (SCO) and the Izaña Observatory (IZO) of the AEMET data network.

3.6 Staff

Activities universal to all measurement programmes such as operation and maintenance of IARC facilities, equipment, instrumentation, communications and computing facilities are made by the following staff:

- Ramón Ramos (AEMET; Head of Scientific instrumentation and infrastructures)
- Enrique Reyes (AEMET; IT development specialist)
- Néstor Castro (AEMET; IT specialist)
- Antonio Cruz (AEMET; IT specialist)
- Rocío López (AEMET; IT specialist)
- Sergio Afonso (AEMET; Meteorological Observer-GAW Technician), retired in 2019
- Concepción Bayo (AEMET; Meteorological Observer-GAW Technician)
- Virgilio Carreño (AEMET; Meteorological Observer-GAW Technician)
- Cándida Hernández (AEMET; Meteorological Observer-GAW Technician)
- Antonio Alcántara (AEMET; Meteorological Observer-GAW Technician)

4 Greenhouse Gases and Carbon Cycle

4.1 Main Scientific Goals

The main goal of the Greenhouse Gases and Carbon Cycle programme conducted by IARC is to carry out highly accurate continuous in-situ measurements of long-lived greenhouse gas (GHG) in the atmosphere at IZO in order to contribute to the WMO/GAW programme, following the GAW recommendations and guidelines. Additional goals are: 1) to study with precision the long-term evolution of the GHGs in the atmosphere, as well as their daily, seasonal and inter-annual variability; 2) To incorporate continuously technical instrumental improvements and new data evaluation and calibration methodologies in order to reduce uncertainty and improve the accuracy of the GHG measurements; 3) to carry out research to study the processes that control the variability and evolution of the GHGs in the atmosphere; and 4) to contribute to international research and its documentation via recommendations and guidelines.

In addition, there has been a growing demand to provide reliable near-real-time GHG data for data assimilation by atmospheric models, to exchange data with the remote sensing community, and to inform policy makers since GHG information is now an object of great social interest and great media impact. Such data exchange requires an enormous effort and represents a technical challenge by having to combine the classic evaluation of very precise background few data (a task that can take at least 6 months) with the delivery of data of an acceptable quality and minimally validated within hours or minutes of being obtained.

4.2 Staff changes

Dr Emilio Cuevas coordinated the programme after the former PI left IARC. In 2020, Pedro Pablo Rivas-Soriano took over the programme as new PI. Vanessa Gómez left IARC subcontractor Air Liquide Canarias and Jaime Hernández-Estévez is now the person responsible. We thank sincerely Vanessa Gómez for the services provided to this programme and wish her all the best.

4.3 Measurement Programme

Table 4.1 gives details of the atmospheric greenhouse gases measurements currently performed at IZO using in-situ analysers (owned by AEMET) and some details about the measurement schemes. Details of the in-situ measurement systems and data processing can be found in Gomez-Pelaez et al. (2012, 2013, 2014, 2016 and 2019). Additional information can be found in the last IZO GHG GAW scientific audit reports: Scheel (2009), Zellweger et al. (2009, 2015 and 2020).

Additionally, weekly discrete flask samples have been collected at IZO for the National Oceanic and Atmospheric Administration-Earth System Research Laboratory-Global Monitoring Laboratory Carbon Cycle Greenhouse Gases Group (NOAA-ESRL-GML CCGG) [Cooperative Air Sampling Network](#) (since 1991). Weekly discrete flask samples are collected at IZO and subsequently shipped to NOAA-ESRL-GML.



Figure 4.1. IZO Gas Chromatograph measurement system for CH₄, N₂O and SF₆.

The air inside the flasks has been measured for the following gas specie mole fractions: 1) CO₂, CH₄, CO, and H₂ since 1991; N₂O and SF₆ since 1997 (NOAA/ESRL/GML CCGG); 2) Isotopic ratios Carbon-13/Carbon-12 and Oxygen-18/Oxygen-16 in carbon dioxide since 1991 (INSTAAR Stable Isotope Lab); 3) Methyl chloride, benzene, toluene, ethane, ethene, propane, propene, i-butane, n-butane, i-pentane, n-pentane, n-hexane and isoprene were measured from 2006 to 2018 (INSTAAR). Figure 4.2 shows the decline of ¹³CO₂ at Izaña Observatory during the period 1992-2014.

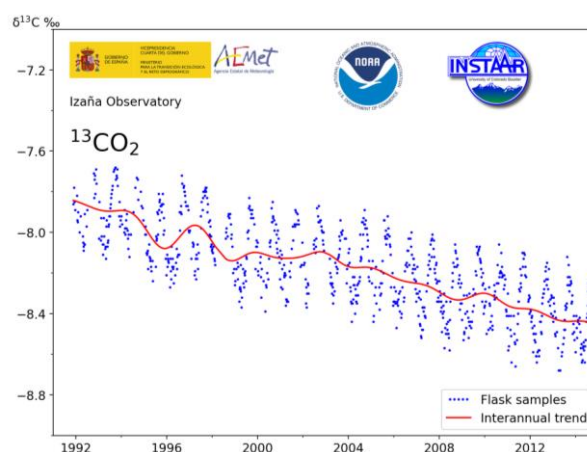


Figure 4.2. ¹³CO₂ data series (1992-2014) from the Stable Isotope Lab of INSTAAR (blue) and trend line using the NOAA/ESRL/GML curve fitting methods (red).

Two-week integrated samples of atmospheric carbon dioxide have also been collected for Heidelberg University (Institute of Environmental Physics, [Carbon Cycle Group](#)) since 1984 to measure the C-14 isotopic ratio in carbon dioxide, these data have been utilized in various carbon cycle modelling activities (e.g. Graven et al., 2017).

Table 4.1. Atmospheric greenhouse gases measured in situ at IZO and measurement schemes used.

Gas	Start Date	Analyser	Model	Ambient air measurement frequency	Reference gas/es and measurement frequency	Reference gas/es calibration frequency
CO ₂	1984	NDIR	Siemens Ultramat 3	10"	3 RG every hour	Biweekly using 4 LS
CO ₂	2007	NDIR	Licor 7000	1"	3 RG every hour	Biweekly using 4 LS
CO ₂	2008	NDIR	Licor 6252	1"	3 RG every hour	Biweekly using 4 LS
CH ₄	1984	GC-FID	Dani 3800	2 injections/h	1 RG every 30 min	Biweekly using 2 LS
CH ₄	2007	GC-FID	Varian 3800	4 injections/h	1 RG every 15 min	Biweekly using 2 LS
N ₂ O	2007	GC-ECD	Varian 3800	4 injections/h	1 RG every 15 min	Biweekly using 5 LS
SF ₆	2007	GC-ECD	Varian 3800	4 injections/h	1 RG every 15 min	Biweekly using 5 LS
CO	2008	GC-RGD	Trace Analytical RGA-3	3 injections/h	1 RG every 20 min	Biweekly using 5 LS
CO ₂ CH ₄ CO	2015	CRDS	Picarro G2401	2"	2 RG every 21 hours to study performance	Monthly using 4 LS
CO N ₂ O	2018	LGR	Los Gatos Research 907-0015	4"	2 RG every 4 hours, one as working gas and the other as a target gas	Monthly using 4 LS

Reference gas/es (RG), Laboratory Standard (LS)

4.4 Summary of remarkable activities during the period 2019-2020

This programme has continued performing continuous high-quality greenhouse gas measurements and annually submitting the data to the WMO GAW World Data Centre for Greenhouse Gases ([WDCGG](#)), where data are publicly available, as well as included in the data summaries (e.g., WDCGG, 2020).

The complete CO₂ time series is shown in Fig. 4.3. The growth rate of CO₂ throughout the period (1984-2020) is approximately 1.9 ppm/yr. However, the increase in CO₂ is accelerating, and is currently about 2.5 ppm/yr, significantly higher than the value of 1.8 ppm/yr which was recorded at the beginning of the CO₂ measurements at IZO in 1984.

The CH₄, N₂O, SF₆ and CO time series at IZO are shown in Fig. 4.4. All the collected data are used for analysis and investigation of the carbon cycle and understanding of the role of anthropogenic and natural factors that control GHG

variability. The curve fitting methods applied to the IZO time series are those used by NOAA/ESRL/GML (Thoning et al., 1989).

IARC has also continued contributing to the data products GLOBALVIEW and OBSPACK led by NOAA-ESRL-GML CCGG (e.g., Cooperative Global Atmospheric Data Integration Project, 2020), as well as collaborating with the associated CO₂ and CH₄ surface flux inversion products [CarbonTracker](#) (e.g. Chevallier et al., 2010; CarbonTracker Team, 2018; van der Velde et al., 2018; Jacobson et al., 2020) and [CarbonTracker Europe](#) (e.g. Tsuruta et al., 2017).

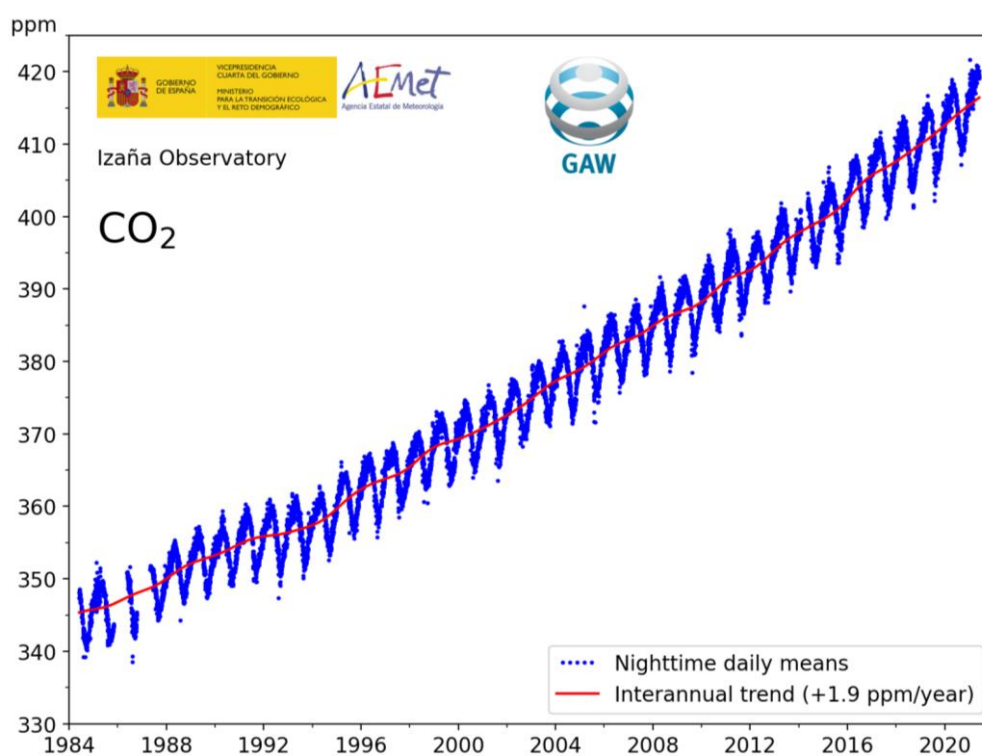


Figure 4.3. Izaña Observatory CO₂ time series (1984-2020).

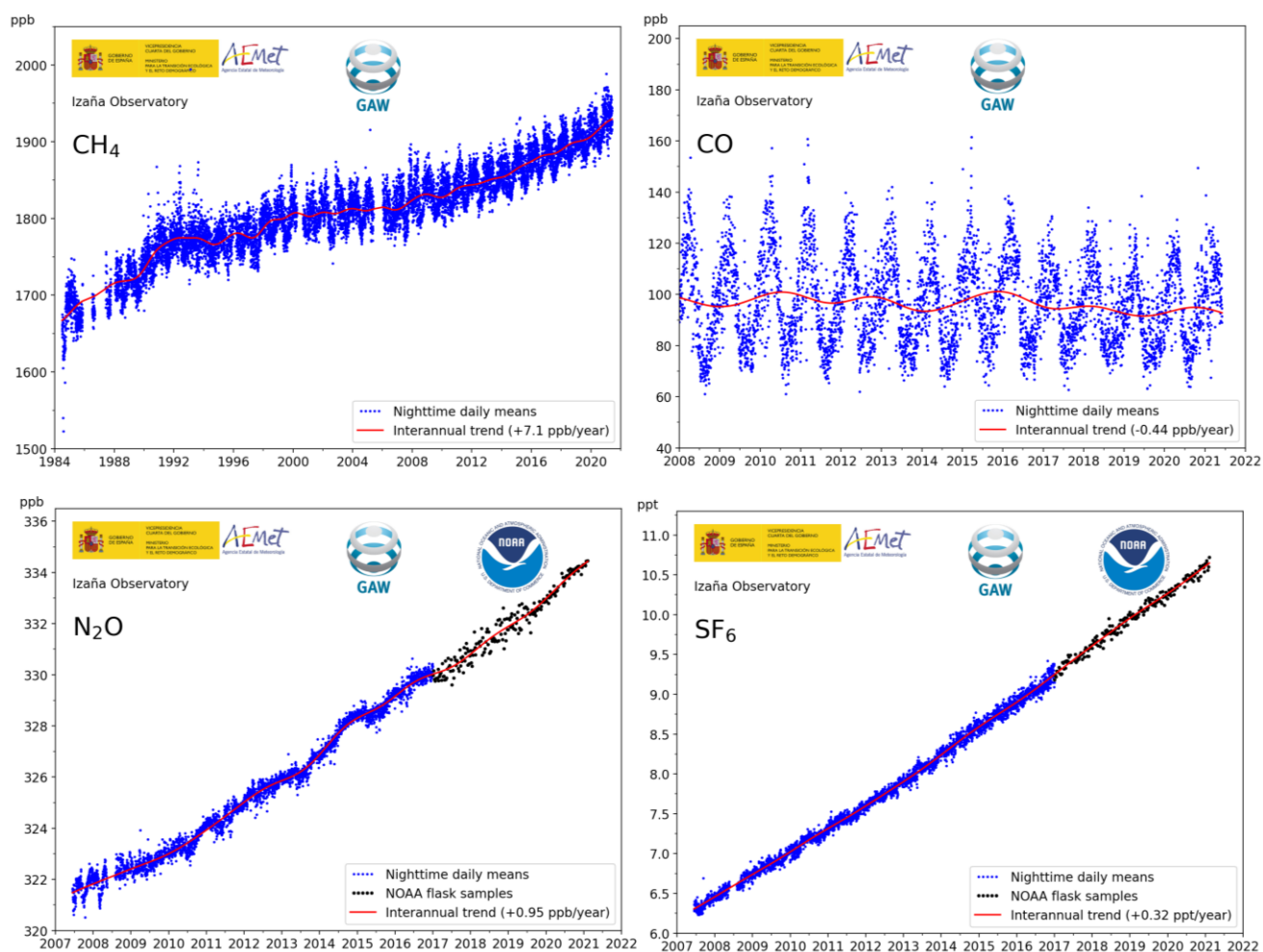


Figure 4.4. CH₄, CO, N₂O and SF₆ IZO time series. N₂O and SF₆ measurements by IZO analysers from year 2017 are temporarily unavailable due to technical problems and system updates. Data from 2017 to 2021 in these figures come from NOAA Cooperative Air Sampling Network and are shown as black points.

4.4.1 Analysers update

A Los Gatos Research LGR 907-0015 analyser was installed in 2018 at IZO to measure CO and N₂O. This instrument was acquired thanks to the project entitled “Equipment for the Monitoring and Research of the atmospheric components that cause and modulate climate change at the Izaña GAW (Global Atmosphere Watch) (Tenerife)” (contract: AEDM15-BE-3319). This R+D infrastructure project has been financed by the State Research Agency of the Ministry of Economy, Industry and Competitiveness, in the Call for projects for scientific equipment, co-financed with European Regional Development Fund (ERDF) funds.

The instrument is based on a cavity-enhanced absorption spectroscopy technique called Off-Axis Integrated Cavity Output Spectroscopy (OA-ICOS). It is still under a testing and software development phase, showing clearly better performance than our CRDS (cavity ringdown spectroscopy) based Picarro G2401 used for CO measurements and better performance than the gas chromatograph Varian 3800 used for N₂O measurements.

The calibration scheme consists of the measurement of four tanks containing CO and N₂O GAW world references provided by the NOAA Earth System Research Laboratory in Boulder, Colorado, USA, once a month. The system measures and registers atmospheric air every four seconds, and a working tank is measured every four hours in order to correct short term drifts. Additionally, a target tank with known CO and N₂O mole fractions is used to check long term drifts.

The last IZO GHG GAW scientific audit (Zellweger et al., 2020) checked the instrument, proved that it fully complies with WMO/GAW compatibility goals and recommended its use as the primary method to measure N₂O and CO, replacing the Varian GC and the Picarro CRDS, which will remain measuring these gases as backup instruments.

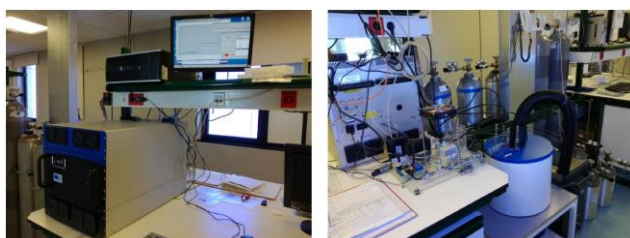


Figure 4.5. Front and rear view of the Los Gatos Research (LGR) CO/N₂O analyser at Izaña Observatory with the new designed plumbing including air samples cooling system.

In order to improve the IZO SF₆ data currently obtained by a Varian 3800 gas chromatograph, we decided to acquire a new system based on the GC-ECD three-column method

described in Hall et al. (2011), capable of improving the SF₆ measurement precision while maintaining the N₂O measurement performance.

The chosen instrument is an Agilent 8890 GC. At the moment of the publication of this report the analyser is installed at IZO and the first tests show an impressive uncertainty reduction of the SF₆ measurements with respect to the Varian 3800 GC.

Spain joined the Integrated Carbon Observation System, (ICOS) at the end of 2020 and consequently IZO will become a class 2 ICOS mountain atmosphere station. As a class 2 station, IZO is required to provide continuous in-situ CO₂ and CH₄ measurements, and the measurement of CO is recommended. Following the ICOS requirements for analysers, we acquired between the end of 2020 and the beginning of 2021 a new Picarro G2401 and a new LGR 907-0015 in order to measure the three aforementioned species and, additionally, N₂O. Both instruments will need to pass a test at the ICOS Atmospheric Thematic Center (ATC) Metrology Lab to be guaranteed to fulfill the ICOS data high quality standards.

4.4.2 System and performance audit by WCC-Empa

The 7th system and performance audit by WCC-Empa at the global GAW station Izaña was conducted from 15 to 21 May 2019 in agreement with the WMO/GAW quality assurance system. CO₂, CH₄, N₂O and CO analysers and also the surface ozone analysers (see Section 5) of IZO were audited on their performance measuring randomized levels of gas concentrations in WCC-Empa travelling standard tanks. The audit included parallel measurements of CO₂, CH₄ and CO with a WCC-Empa travelling Picarro G2401, running from 20 May through 01 July 2019. As part of the system audit, data within the scope of WCC-Empa available at WDCGG was reviewed.




















The audit concluded that most assessed measurements were of high quality and met the WMO/GAW network compatibility or extended compatibility goals in the relevant amount fraction range. Table 4.2 summarizes the results of the performance audit and the ambient air comparison with respect to the WMO/GAW network compatibility goals. A tick mark indicates that the compatibility goal (green) or extended compatibility goal (orange) was met on average. The tick mark in parenthesis mean that the goal was only partly reached in the relevant mole fraction. Table 4.3 summarizes the ranking of the station. Adequacy ranges from 0 (inadequate) through 5 (adequate). All primary instruments proved full adequacy. Detailed information can be found in Zellweger et al. (2020).

Table 4.2. Synthesis of the performance audit and ambient air comparison results. Reprinted from Zellweger et al. (2020).

Comparison type	O ₃ Analyser	O ₃ Calibrator	CO Picarro	CO LGR	CH ₄ GC/FID	CH ₄ Picarro	CO ₂ Li-COR	CO ₂ Picarro	N ₂ O GC/ECD	N ₂ O LGR
Audit with Time Series	✓	✓	✓	✓	✓	✓	✓	✓	(✓)	✓
Ambient air comparison	NA	NA	✓	✓	✓	✓	✓	✓	NA	NA

Not Available (NA)

Table 4.3. Summary ranking of the Izaña GAW station. Reprinted from Zellweger et al. (2020).

System Audit Aspect	Adequacy	Comment
Measurement programme	 (5)	Comprehensive programme covering all focal areas of GAW.
Access	 (5)	Year round access
Facilities		
Laboratory and office space	 (5)	Adequate, with space for additional research campaigns.
Internet access	 (5)	Sufficient bandwidth
Air Conditioning	 (5)	Fully adequate system
Power supply	 (5)	Reliable, backup UPS
General Management and Operation		
Organisation	 (5)	Well managed, clear responsibilities
Competence of staff	 (5)	Highly qualified staff
Air Inlet System	 (5)	Fully adequate systems
Instrumentation		
Ozone	 (5)	Adequate instrumentation
CH ₄ /CO ₂ /CO (Picarro)	 (5)	State of the art instrumentation
CO ₂ (LI-COR-7000)	 (4)	Adequate system
CH ₄ (Varian 3800 GC/FID)	 (3)	Quasi continuous, higher noise
CO and N ₂ O (LGR)	 (5)	State of the art instrumentation
N ₂ O (Varian 3800 GC/ECD)	 (3)	Quasi continuous, higher noise
Standards		
O ₃ , CO, CO ₂ , CH ₄ , N ₂ O	 (5)	NIST traceable (O ₃), NOAA and working standards available
Data Management		
Data acquisition	 (5)	Fully adequate system
Data processing	 (5)	Adequate procedures
Data submission	 (5)	Timely data submission of all parameters

4.5 Participation in international cooperative scientific studies

4.5.1 Fingerprint of the summer 2018 drought in Europe on ground-based atmospheric CO₂ measurements

IARC contributed with data to the study published in Philosophical Transactions of the Royal Society B (Ramonet et al., 2020). A widespread drought developed over Northern and Central Europe during the summer of 2018. The drought disturbed CO₂ exchange between the atmosphere and terrestrial ecosystems in various ways, such as a reduction of photosynthesis, changes in ecosystem respiration, and an increment of the fire frequency. The development of the ICOS network of atmospheric greenhouse gas monitoring stations in recent years enabled an unprecedented amount of data compared to previous drought events in 2003 and 2015.

This study analyzed the seasonal CO₂ cycles from 48 European stations for 2017 and 2018 and showed that the usual summer minimum in CO₂ mole fraction due to its biospheric uptake was reduced by 1.4 ppm in 2018 for the

10 stations located in the area most affected by the temperature anomaly, mostly in Northern Europe.

This was balanced by a CO₂ transition phase before and after July slower in 2018 compared to 2017, suggesting an extension of the growing season. Figure 4.6 shows the detrended CO₂ differences observed at several stations from May to September 2018 compared to the previous year (top panel plots), and compared to the average of the eight previous years, where data are available (lower panel plots). Top panel plots clearly show the development of a positive CO₂ difference (2018–2017) of around 2 to 4 ppm in July/August in the central and northern part of Europe that switches to negative values (–2 to –4 ppm) in September/October but remains positive for stations located further south. This CO₂ anomaly was compared with the anomaly observed in previous European droughts in 2003 and 2015. Considering the areas most affected by the temperature anomalies, a higher CO₂ anomaly was found in 2003 (+3 ppm averaged over 4 sites), and a smaller anomaly in 2015 (+1 ppm averaged over 11 sites) compared to 2018.

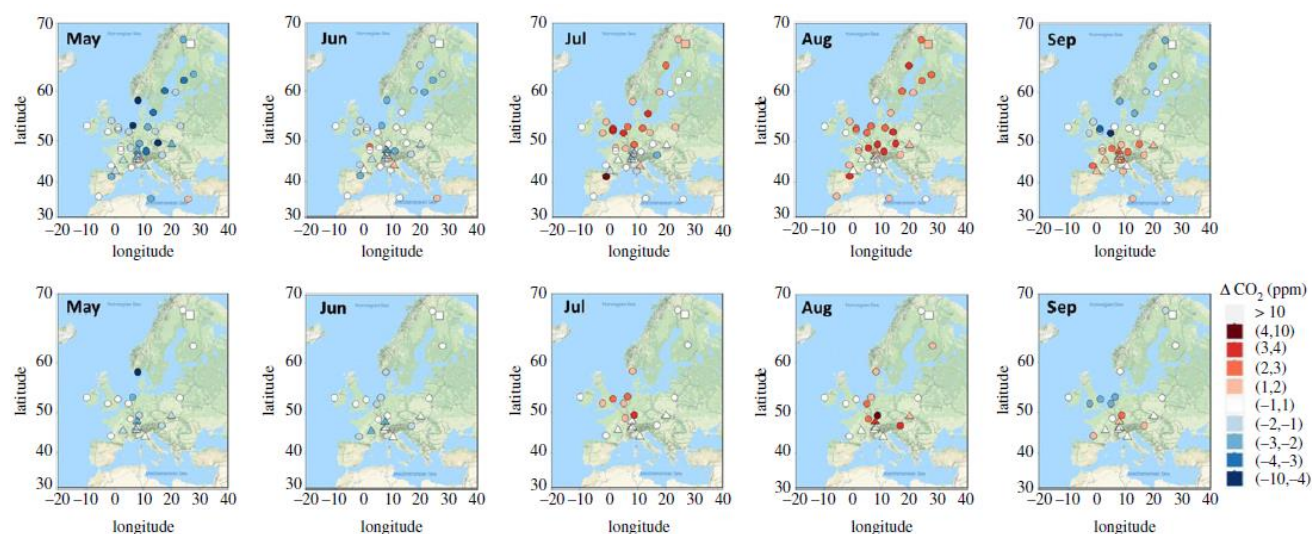


Figure 4.6. Map of the monthly mean CO₂ mole fraction differences from May (left) to September (right). Circles represent surface stations in lowlands. Triangles indicate the mountain sites, and the square indicates a total column measurement station (TCCON). Top panels show the differences between 2018 and 2017. Bottom panels show differences between 2018 and averaged multi-annual mean of 2010–2017. Reprinted from Ramonet et al. (2020).

4.6 References

Chevallier, F., P. Ciais, T. J. Conway, T. Aalto, B. E. Anderson, P. Bousquet, E. G. Brunke, L. Ciattaglia, Y. Esaki, M. Fröhlich, A. Gomez, A. J. Gomez-Pelaez, L. Haszpra, P. B. Krummel, R. L. Langenfelds, M. Leuenberger, T. Machida, F. Maignan, H. Matsueda, J. A. Morguí, H. Mukai, T. Nakazawa, P. Peylin, M. Ramonet, L. Rivier, Y. Sawa, M. Schmidt, L. P. Steele, S. A. Vay, A. T. Vermeulen, S. Wofsy, D. Worthy, CO₂ surface fluxes at grid point scale estimated from a global 21 year

reanalysis of atmospheric measurements, *J. Geophys. Res.*, 115, D21307, doi:10.1029/2010JD013887, 2010.

Cooperative Global Atmospheric Data Integration Project; (2020): Multi-laboratory compilation of atmospheric carbon dioxide data for the period 1957–2019; obspack_co2_1_GLOBALVIEWplus_v6.1_2021-03-01; NOAA Global Monitoring Laboratory. <https://search.datacite.org/works/10.25925/20201204>

Gomez-Pelaez, A.J., R. Ramos, V. Gomez-Trueba, R. Campo-Hernandez, E. Dlugokencky, T. Conway "New improvements in the Izaña (Tenerife, Spain) global GAW station in-situ

- greenhouse gases measurement program" in GAW report (No. 206) of the "16th WMO/IAEA Meeting on Carbon Dioxide, Other Greenhouse Gases, and Related Measurement Techniques (GGMT-2011) (Wellington, New Zealand, 25-28 October 2011)", edited by Gordon Brailsford, World Meteorological Organization, 76-81, 2012.
- Gomez-Pelaez, A. J., Ramos, R., Gomez-Trueba, V., Novelli, P. C., and Campo-Hernandez, R.: A statistical approach to quantify uncertainty in carbon monoxide measurements at the Izaña global GAW station: 2008–2011, *Atmos. Meas. Tech.*, 6, 787–799, doi:10.5194/amt-6-787-2013, 2013.
- Gomez-Pelaez, A.J., R. Ramos, V. Gomez-Trueba, R. Campo-Hernandez, E. Reyes-Sanchez: "Izaña Global GAW station greenhouse-gas measurement programme. Novelties and developments during October 2011-May 2013" in GAW report (No. 213) of the "17th WMO/IAEA Meeting on Carbon Dioxide, Other Greenhouse Gases, and Related Measurement Techniques (Beijing, China, June 10-14, 2013)", edited by P. Tans and C. Zellweger, World Meteorological Organization, 77-82, 2014.
- Gomez-Pelaez, A.J., R. Ramos, V. Gomez-Trueba, R. Campo-Hernandez, E. Reyes-Sanchez: "GGMT-2015 Izaña station update: instrumental and processing software developments, scale updates, aircraft campaign, and plumbing design for CRDS" in GAW report (No. 229) of the "18th WMO/IAEA Meeting on Carbon Dioxide, Other Greenhouse Gases, and Related Measurement Techniques (GGMT) (La Jolla, CA, USA, 13-17 September, 2015)", edited by P. Tans and C. Zellweger, World Meteorological Organization, 125-131, 2016.
- Gomez-Pelaez, A. J., Ramos, R., Cuevas, E., Gomez-Trueba, V., and Reyes, E.: Atmospheric CO₂, CH₄, and CO with the CRDS technique at the Izaña Global GAW station: instrumental tests, developments, and first measurement results, *Atmos. Meas. Tech.*, 12, 2043–2066, <https://doi.org/10.5194/amt-12-2043-2019>, 2019.
- Hall, B. D., Dutton, G. S., Mondeel, D. J., Nance, J. D., Rigby, M., Butler, J. H., Moore, F. L., Hurst, D. F., & Elkins, J. W. (2011). Improving measurements of SF₆ for the study of atmospheric transport and emissions. *Atmospheric Measurement Techniques*, 4(11), 2441–2451. <https://doi.org/10.5194/amt-4-2441-2011>
- Graven, H., Allison, C. E., Etheridge, D. M., Hammer, S., Keeling, R. F., Levin, I., Meijer, H. A. J., Rubino, M., Tans, P. P., Trudinger, C. M., Vaughn, B. H., and White, J. W. C.: Compiled records of carbon isotopes in atmospheric CO₂ for historical simulations in CMIP6, *Geosci. Model Dev.*, 10, 4405–4417, <https://doi.org/10.5194/gmd-10-4405-2017>, 2017
- Jacobson, A. R., Schuldt, K. N., Miller, J. B., Oda, T., Tans, P., Arlyn Andrews, Mund, J., Ott, L., Collatz, G. J., Aalto, T., Afshar, S., Aikin, K., Aoki, S., Apadula, F., Baier, B., Bergamaschi, P., Beyersdorf, A., Biraud, S. C., Bollenbacher, A., ... Mirosław Zimnoch. (2020). CarbonTracker Documentation CT2019B release. NOAA Global Monitoring Laboratory. <https://doi.org/10.25925/20201008>
- Ramonet, M., P. Ciais, F. Apadula, J. Bartyzel, A. Bastos, P. Bergamaschi, P. E. Blanc, D. Brunner, L. Caracciolo di Torchiarolo, F. Calzolari, H. Chen, L. Chmura, A. Colomb, S. Conil, P. Cristofanelli, E. Cuevas, R. Curcoll, M. et al.: The fingerprint of the summer 2018 drought in Europe on ground-based atmospheric CO₂ measurements, *Philosophical Transactions of the Royal Society B: Biological Sciences*, Royal Society, The, 375 (1810), pp.20190513. [ff10.1098/rstb.2019.0513](https://doi.org/10.1098/rstb.2019.0513), 2020.
- Scheel, H.E. (2009), System and Performance Audit for Nitrous Oxide at the Global GAW Station Izaña, Tenerife, Spain, November 2008, WCC-N2O Report 2008/11, http://www.aemet.izana.org/publications/Rep_WCCN2O_2008_IZOaudit.pdf
- Thoning, K.W., P.P. Tans, and W.D. Komhyr; Atmospheric carbon dioxide at Mauna Loa Observatory, 2. Analysis of the NOAA/GMCC data, 1974 1985. *J. Geophys. Res.*, 94, 8549–8565, 1989.
- Tsuruta, A., Aalto, T., Backman, L., Hakkarainen, J., van der Laan-Luijkx, I. T., Krol, M. C., Spahni, R., Houweling, S., Laine, M., Dlugokencky, E., Gomez-Pelaez, A. J., van der Schoot, M., Langenfelds, R., Ellul, R., Arduini, J., Apadula, F., Gerbig, C., Feist, D. G., Kivi, R., Yoshida, Y., and Peters, W.: Global methane emission estimates for 2000–2012 from CarbonTracker Europe-CH4 v1.0, *Geosci. Model Dev.*, 10, 1261–1289, doi:10.5194/gmd-10-1261-2017, 2017.
- van der Velde, I. R., Miller, J. B., van der Molen, M. K., Tans, P. P., Vaughn, B. H., White, J. W. C., Schaefer, K., and Peters, W.: The CarbonTracker Data Assimilation System for CO₂ and δ¹³C (CTDAS-C13 v1.0): retrieving information on land–atmosphere exchange processes, *Geosci. Model Dev.*, 11, 283–304, <https://doi.org/10.5194/gmd-11-283-2018>, 2018.
- Zellweger, C., J. Klausen, B. Buchmann, H.-E. Scheel (2009), System and Performance Audit of Surface Ozone, Carbon Monoxide, Methane and Nitrous Oxide at the Global GAW Station Izaña, Spain, March 2009, WCC-Empa Report 09/1, <https://www.empa.ch/documents/56101/250799/Izana09.pdf/8dd7d439-c6cb-4122-bcea-bc3fcd5a367>
- Zellweger, C., M. Steinbacher, B. Buchmann, R. Steinbrecher (2015), System and Performance Audit of Surface Ozone, Methane, Carbon Dioxide, Nitrous Oxide and Carbon Monoxide at the Global GAW Station Izaña, September 2013. WCC-Empa Report 13/2, <https://www.empa.ch/documents/56101/250799/Izana13.pdf/d8bbb9f-8623-404e-bdab-6949d6e16282>
- Zellweger, C., M. Steinbacher, B. Buchmann, R. Steinbrecher (2020), System and Performance Audit of Surface Ozone, Carbon Monoxide, Methane, Carbon Dioxide and Nitrous Oxide at the Global GAW Station Izaña, Spain, May 2019. WCC-Empa Report No. 19/2, <https://www.empa.ch/documents/56101/250799/Izana+2019/a2d85ce-12d1-4c30-a53d-b4d7f70ed913>
- World Data Centre for Greenhouse Gases (WDCGG), WMO WDCGG Data Summary, GAW Data (Volume IV-Greenhouse and Related Gases), WDCGG No. 44, Japan Meteorological Agency in Co-operation with World Meteorological Organization, 2020.

4.7 Staff

- Pedro Pablo Rivas Soriano (AEMET; Head of programme)
- Ramón Ramos (AEMET; Head of Infrastructure and instrumentation)
- Enrique Reyes (AEMET; Software and data processing)
- Dr Sergio León-Luís (TRAGSATEC; ICOS)
- Dr Rosa García (TRAGSATEC/UVA)
- Jaime Hernández-Estévez (Air Liquide)

5 Reactive Gases and Ozonesondes

5.1 Main Scientific Goals

The main scientific objectives of this programme are:

- Long-term high-quality observations and analysis of tropospheric O₃ in both the free troposphere (FT) and the Marine Boundary Layer (MBL).
- Long-term high-quality observations of reactive gases (CO, NO_x, SO₂) in the FT and in the MBL to support other measurement programmes at IARC.
- Air quality studies in urban and background conditions.
- Analysis of long-range transport of pollution (e.g. transport of anthropogenic and wildfire pollution from North America).
- Study of the impact of dust and water vapour on tropospheric O₃.
- Characterization of the vertical profile of ozone in subtropical latitudes.
- Analysis and characterization of the Upper Troposphere-Lower Stratosphere (UTLS).
- Analysis of Stratosphere-Troposphere Exchange processes.

5.2 Measurement Programme

The measurement programme of reactive gases (O₃, CO, NO_x and SO₂) includes long-term observations at IZO, SCO and BTO (see Tables 3.2, 3.4 and 3.5) and ozonesonde vertical profiles at Tenerife (now at BTO). In addition, IARC (through AEMET and INTA) has a long-term collaboration with the Argentinian Meteorological Service (SMN) and in the framework of this collaboration, ozone vertical profiles are measured at Ushuaia GAW Global station (Argentina). Surface O₃ measurements started in 1987, CO in 2004, and SO₂ and NO_x measurements were implemented since 2006 at IZO. At SCO, surface O₃

measurements started in 2001, and CO, SO₂ and NO_x programmes were also implemented since 2006.

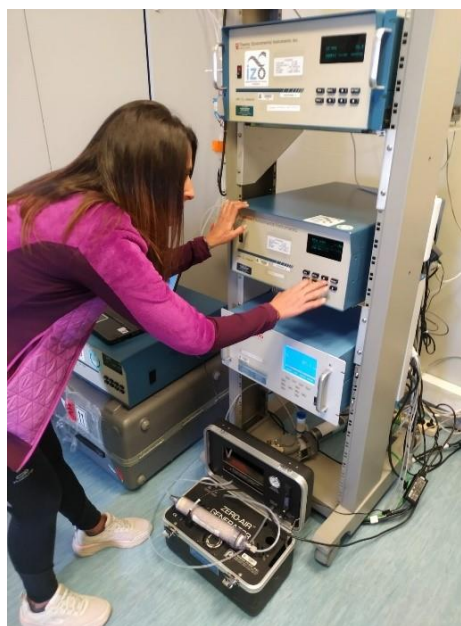


Figure 5.2. Ozone analysers at Izaña Observatory: comparison of the analysers with primary ozone standard (TEI 49C-PS).

Details of the reactive gases and ozonesondes measurement programme are described in González (2012) and Cuevas et al. (2013).

5.2.1 Reactive gases

The surface ozone measurement programme is developed within the framework of the GAW-WMO programme for the measurement of reactive gases, and its main objectives are high-quality monitoring of surface ozone, as well as other reactive gases, under background conditions in the free atmosphere at IZO, and the analysis of chemical and transport processes in which the ozone is involved. The almost uninterrupted 34-year time series of surface O₃ at IZO is shown in Fig. 5.1.

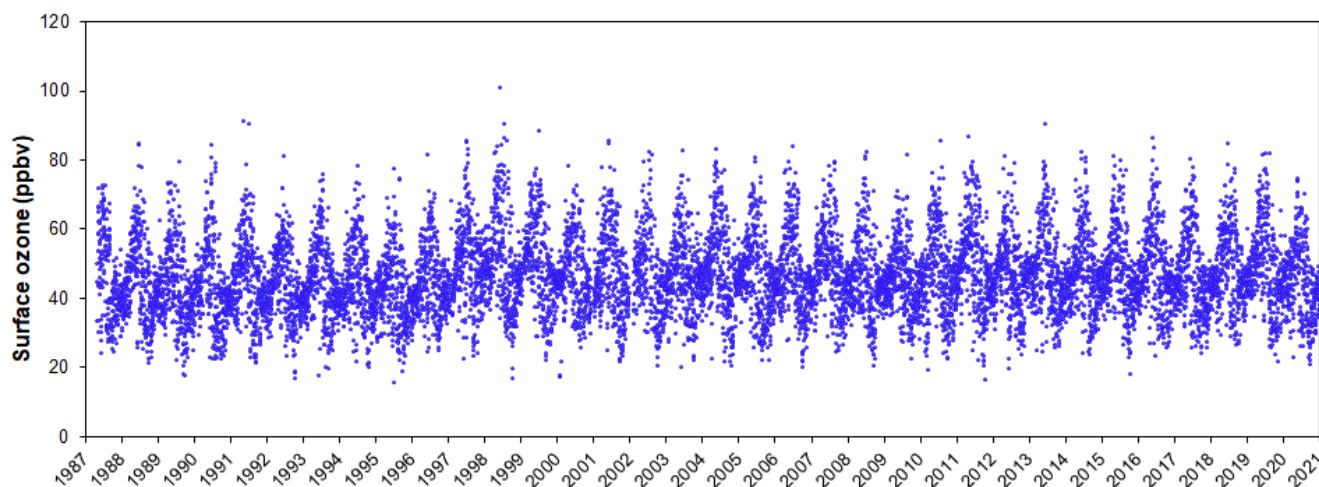


Figure 5.1. Long-term daily (night period) surface O₃ at IZO (1987-2020).

At present, ozone is measured with two ozone analyzers main and auxiliary, which are measuring simultaneously. A third reserve analyzer is used in case any of the two operational analyzers have a problem. All analyzers determine the ozone mixing ratio by UV absorption; this is the recommended measurement technique for analyzers which are part of the GAW-WMO programme (WMO, 2013). The main analyzer belongs to the new series of Thermo Scientific 49i analyzers, and the other two (auxiliary and reserve) belong to the old series of Thermo Scientific 49C analyzers. All analyzers are compared every three months with the IARC primary ozone standard (Thermo Scientific 49C-PS, since August 2008) (Figure 5.2), which has previously been calibrated against a reference equipment (SRP#15) from the [World Calibration Centre](#) for Surface Ozone, Carbon Monoxide, Methane and Carbon Dioxide (WMO/WCC-Empa) to check if there is any drift in the instruments. The error must be less than 1% to ensure that the analyzer has not changed and therefore maintains the WCC-Empa calibration.

In addition, all analyzers and their installation are audited every 2-3 years by the WCC-Empa to check if the calibration has been maintained over time. This redundancy of equipment, together with the rigorous verification and calibration protocols, are necessary to maintain the quality and continuity of ozone measurements required by the the GAW Programme.

The surface O₃ programme at IZO has been audited by the WCC-Empa in 1996, 1998, 2000, 2004, 2009, 2013 and 2019. All Empa's audit reports are available in the link: <https://www.empa.ch/web/s503/wcc-empa>.

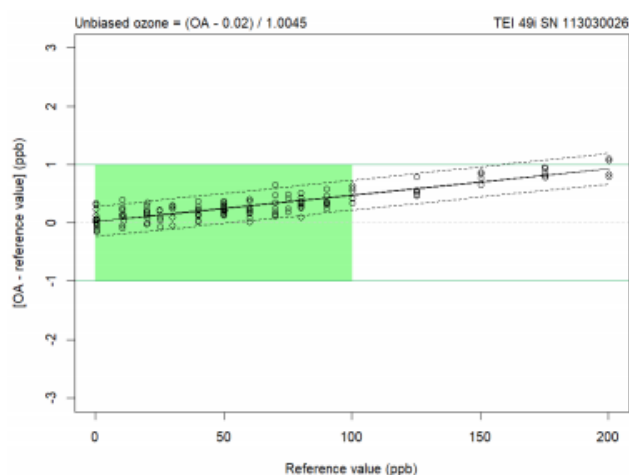


Figure 5.3. Bias of the IZO ozone analyser (TEI 49i #1153030026, principal analyser) with respect to the SRP as a function of mole fraction. Each point represents the average of the last five 1-minute values at a given level. The green area corresponds to the relevant mole fraction range, while the DQOs are indicated with green lines. The dashed lines about the regression lines are the Working-Hotelling 95% confidence bands (WMO, 2020).

During the last audit (May 2019) the three IZO analysers (TEI 49i #1153030026, TEI 49C #72491-371 and #62900-337) and the primary ozone standard (TEI 49C-PS #56085-306) were compared against the WCC-Empa travelling standard (TS) with traceability to a Standard Reference Photometer (SRP). Good agreement between the WCC-Empa travelling instrument and the IZO calibrator was found, which confirms the validity of the last calibration made at Empa in 2017. The ozone analysers were all in agreement within 1 ppb at the relevant mole fraction range from 0-100 ppb ozone (Fig. 5.3), which confirms that the quality control and maintenances made periodically in IZO are appropriate.

On the other hand, the WCC-Empa 2019 audit noted that the C-Series instruments (TEI 49C) are reaching the end of their lifetime and these instruments should be replaced within the next two years. These instruments will be replaced by analysers of I-Series (TEI 49i) during 2021-2022 and the reserve analyser will be installed at the Teide Peak Observatory. The final WCC/Empa Audit report No 19/2 “System and performance audit of surface ozone, carbon monoxide, methane, carbon dioxide and nitrous oxide at the global GAW station Izaña, Spain May 2019, was published as a GAW report No 251 (WMO 2020).

NO_x and SO₂ instruments at IZO usually operate below the detection limit (50 ppt) during the night-time period when we can ensure background conditions. However, these measurements are quite useful for studies of local or regional pollution during daytime, when concentrations are modulated by valley-mountain breeze, and help to understand the impact of regional pollution and of long-range transport of pollution on the background atmosphere.

In order to lend continuity to the NO_x measurement programme in IZO, improving the quality of measurements and increasing precision, the EcoPhysics CraNO_x II analyzer was acquired, as part of the project “Equipment for Monitoring and Research from the Global Atmospheric Watch station at Izaña (Tenerife) of Atmospheric Parameters and Components that modulate Climate Change (MICA)” (EQC2018-004376-P). The infrastructure project was approved at the end of 2018, and the new equipment was installed in October 2020 (Fig. 5.4).



Figure 5.4. Start-up of the EcoPhysics CraNO_x II analyser at the Izaña Observatory.

CO is measured with high accuracy at IZO by the Greenhouse Gases and Carbon Cycle Programme, following the GAW recommendations (see Section 4 for more details). CO measurements are also performed at SCO with the non-dispersive IR absorption technique and are utilized for air quality research.

5.2.2 CraNOx II analyzer

The CraNOx analyser is a high-performance device based on a chemiluminescence detection principle (O₃-CLD, Ozone Chemiluminescence Detection), which detects NO directly and NO₂ after converting it into NO with a photolytic converter (PLC, Photolytic Converter). This NO measurement technique is recommended by GAW at its NO_x measurement stations (WMO, 2011 and 2017) given its reliability, linearity and proven reproducibility in a wide range of conditions. The technique consists of enriching the air sample, whose concentration of NO is to be studied, with O₃, which produces a set of reactions resulting in the generation of NO₂ and release of radiation proportional to the initial concentration of NO. This radiation is measured using a photomultiplier tube (PMT) with a signal proportional to NO in the initial sample.

In order to obtain the concentration of NO₂ in the sample, all the NO₂ must first be converted into NO, and then subsequently, the same direct NO measurement process is repeated with the O₃-CLD detector. There are several methods to produce NO₂ from NO, e.g. using a photolytic converter or a heated molybdenum converter. In GAW stations, photolytic conversion is recommended (WMO, 2011) since it is a more selective method, avoiding the overestimation of NO₂, by preventing other nitrogen compounds in the air from being transformed into NO during the process. The air sample is irradiated in a photolytic cell and a fraction of the NO₂ is converted into NO, depending on an efficiency factor related to the intensity and type of lamp, e.g. mercury or xenon arc lamp or UV-LEDs.

The CraNOx II installed in the Izaña Observatory complies with GAW recommendations in terms of measurement technique, precision and detection limit for the measurement of NO and NO₂ in background conditions (WMO, 2011 and 2017). It is a compact instrument consisting of a double O₃-CLD detector for the simultaneous measurement of NO and NO_x, with a pre-chamber, to minimise interference due to the reaction of ozone with other compounds present in the air, and uses a photolytic converter with a metal halide lamp (200W). For the ozone required in the O₃-CLD chemiluminescence detector, the analyser has an internal ozone generator. This ozone is generated by applying an electrical discharge to a constant flow of oxygen (O₂), taken from a bottle, breaking the O₂ molecules down into more unstable atoms, which recombine to form ozone. Thanks to this design, the analyser allows the measurement of NO and NO₂

concentrations < 25 ppt, with great stability and precision (Fig 5.5).

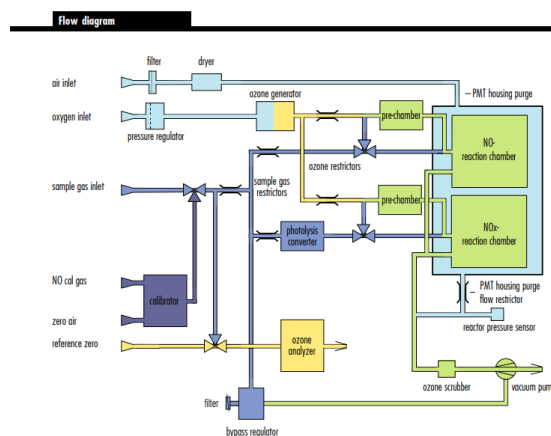


Figure 5.5. Flow diagram of the EcoPhysics CraNOx II (<https://www.ecophysics.com/environmental/supreme-line/cranox-ii/>).

The CraNOx II also incorporates an internal calibration module that allows the automatic verification/calibration of the analyser: NO-zero (synthetic air with zero NO mole fraction), NO-span (measurement of a known dilute amount of NO) and efficiency of the PLC converter. The high degree of instrument automation always allows control of both the quality of the measurement and of the equipment itself. The CraNOx II is completed with an internal O₃ analyzer, by UV photometric absorption, which measures O₃ mole fraction of the air sample simultaneously with the NO and NO₂ measurements, which will allow the detailed study of how the chemical reactions that connect these three compounds occur under background conditions.

5.2.3 Ozonesonde vertical profiles

The ozone vertical profile measurements were initiated in November 1992 using the ECC ozonesonde technique. The equipment and launching stations used in this programme are listed in Table 5.1. Launches are performed once a week (Wednesday). The frequency of ozone soundings in this station is significantly increased during intensive campaigns.

At the start of the programme, the ozonesondes were launched from Santa Cruz Station and since 2011 they have been launched from BTO (Fig. 5.6 and 5.7). This programme provides ozone profiles from the ground to the burst level (generally between 30 and 35 km) with a resolution of about 10 metres. A constant mixing ratio above burst level is assumed for the determination of the residual ozone if an altitude equivalent to 17 hPa has been reached.



Figure 5.6. Inflating the balloon with helium at BTO.

Ozonesondes are checked before launching with a Ground Test with Ozonizer/Test Unit TSC-1 (see Section 3.2.1). The ECC-ozone sensor used is an electrochemical cell consisting of two half cells, made of Teflon, which serve as cathode and anode chambers, respectively. Both half cells contain platinum mesh electrodes. They are immersed in a KI-solution, always with the same sensing solution type (SST1.0: 1.0% KI & full pH-buffer) since the beginning of the Ozonesonde Programme (Nov 1992). The two chambers are linked together by an ion bridge in order to provide an ion pathway and to prevent mixing of the cathode and anode electrolytes.

The main features of the ozonesonde system currently in use (see Table 5.1) are the following:

- Sensor: ECC-6A
- Balloon: TOTEX TA 1200
- Radiosonde: RS-41
- Receiver: DigiCora MW41
- Wind system: GPS



Figure 5.7. a) Preparing the balloon and the ozonesonde for launch at BTO, b) Ozonesonde in air launched from BTO.

Table 5.1. Ozonesonde Programme equipment used in different time periods and launching stations since November 1992.

Instrument manufacturer and model	Frequency	Period/Launching station
OZONESONDES: Nov 1992 – Sep 1997: Science Pump Corp. Model ECC-5A Sep 1997 – present: Science Pump Corp. Model ECC-6A GROUND EQUIPMENT: Nov 1992 – Oct 2010: VAISALA DigiCora MW11 Rawinsonde Oct 2010 – Feb 2018: VAISALA DigiCora MW31 Mar 2018 – present: VAISALA DigiCora MW41 RADIOSONDES: Nov 1992 – Oct 1997: VAISALA RS80-15NE (Omega wind data) Oct 1997 – Sep 2006: VAISALA RS80-15GE (GPS Wind data) Sep 2006 - Dec 2018: VAISALA RS92-SGP (GPS Wind data) Dec 2018 - present: VAISALA RS41-SGP (GPS Wind data)	1/week (Wed)	Nov 1992 – Oct 2010: From Santa Cruz Station (28.46°N, 16.26°W; 36 m a.s.l.) Oct 2010 – Feb 2011: From Santa Cruz/ BTO (In alternate launches) Feb 2011 – present: From BTO Station (28.41°N, 16.53°W; 114 m a.s.l.)

5.3 Summary of remarkable results during the period 2019-2020

5.3.1 Software for the evaluation of reactive gases data (O_3 , NO_x , SO_2 , CO)

The software for reactive gases data evaluation was developed during 2015 and 2016, and is improved each year. This software makes it possible to carry out the evaluation and processing of the data of the reactive gases programme (surface O_3 , NO_x , SO_2 and CO). The software works in a web environment that facilitates consultations with the database and data processing.

The raw data are acquired by a CR1000 Campbell datalogger, which interrogates each instrument every minute. The data are automatically stored in a database, zeros, span and calibration coefficients of the analysers are also recorded. The software uses all this information to process data automatically and it allows us to choose the desired component to evaluate and visualize its record along with that of another component and/or together with the meteorological information (temperature, relative humidity, pressure and wind).

5.3.2 World Data Center for Reactive Gases (WDCRG)

The World Data Center for Reactive Gases (WDCRG) is the data repository and archive for reactive gases of the GAW Programme and is managed by NILU. The WDCRG was established on 1 January 2016 and takes over the responsibility of RG data archiving from the Japan Meteorological Agency, which continues to host the World Data Centre on Greenhouse Gases (WDCGG). Some of the reactive gases hosted at WDCRG are SO_2 , oxidized nitrogen species, surface O_3 and VOCs. We have developed the necessary software to edit surface O_3 data in the Ebas NASA-Ames format required by the WDCRG. Hourly surface O_3 data from 2014 to 2020 have been submitted directly to WDCRG (<http://ebas.nilu.no>) and O_3 data from 1987 to 2013 have been transferred from the WDCGG to WDCRG in the Ebas format.

5.3.3 Network for the Detection of Atmospheric Composition Change (NDACC)

In 2004, the Izaña Atmospheric Research Center joined the Network for the Detection of Atmospheric Composition Change and began routinely archiving the ozonesonde data into the NDACC database; in addition, all the ozonesonde records since 1995 were uploaded to the NDACC at this time. Ozonesonde data archived in the NDACC database must meet certain quality criteria. Currently 96% of the ozone soundings performed in the period 1995-2020 are available in the NDACC database (Figure 5.8). Ozonesonde data from the early period (November 1992-1994) need to be reprocessed and reanalysed carefully. At present

NDACC is working in the homogenization of the ozone soundings of all NDACC-stations and implementation of a new data format.

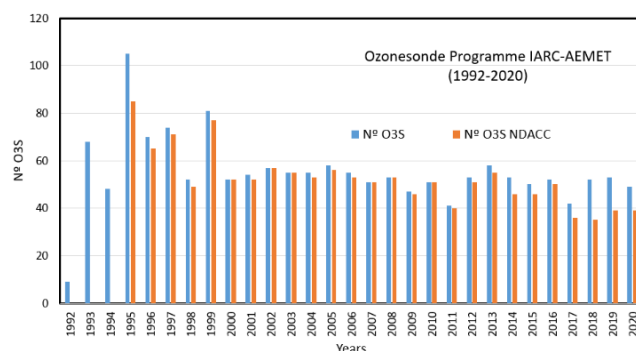


Figure 5.8. Number of ozone soundings (O3S) since the beginning of the programme and the number of ozonesonde datasets recorded in the NDACC database that meet the quality assurance criteria (1992-2020).

5.3.4 Ozonesonde data homogenization activity

An Ozonesonde Data Quality Assessment (O3S-DQA) activity was initiated in 2011 to identify changes in the ozonesondes and in their preparation that introduce inhomogeneities in the long-term ozonesonde records and to formulate correction functions to resolve these artefacts. This activity was part of SI2N (SPARC [Stratosphere-troposphere Processes And their Role in Climate], IO3C [International Ozone Commission] and IGACO-O3 [Integrated Global Atmospheric Chemistry Observations] and NDACC) initiative on “Past Changes in the Vertical Distribution of Ozone”.

An Ozonesonde Data Quality Assessment (O3S-DQA) activity was initiated in 2011 to homogenize temporal and spatial ozonesonde data records under the framework of the SI2N (SPARC [Stratosphere-troposphere Processes And their Role in Climate], IO3C [International Ozone Commission], and NDACC) initiative on “Past Changes in the Vertical Distribution of Ozone”. The aim of this homogenization is to correct for biases related to instrumental (such as sonde type or sensing solution strength) or processing changes to reduce the uncertainty (from 10–20% down to 5–10 %), and to provide an uncertainty estimate for every single ozone partial pressure measurement in the profile.

In this context, some O_3 -sounding stations, one of them being the IZO station, were selected to be involved in the homogenization process, following the “Guidelines for Homogenization of Ozone Sonde Data” (Smit et. al, 2012) prepared by the O3S-DQA panel members. The reprocessing carried out in IZO station is being supervised by Dr H. Smit (FZJ, Germany), leader of the O3S-DQA panel, and Dr R. Van Malderen (KMI, Belgium).

In our case, although there have not been any changes in ECC ozonesonde manufacturer (Vaisala ECC-SPC) or

changes in sensing solution type (STT 1.0% KI & full pH-buffer) since the beginning of the Ozonesonde Programme (Nov 1992), some non-uniformity in ozonesonde and data processing could have occurred during the programme implementation period: changes in the ozonesonde type (ECC5A, Nov.92 to Sep.97 and ECC6A, Sep97 to present), in the pump temperature measurement, in the background current, in the correction (temperature and humidity) of the pump flow or the method of determining the ozone residual.

All this can lead to some inhomogeneities in time series and may influence the trends derived from such data dramatically. The Assessment of Standard Operating Procedures for Ozonesondes (ASOPOS, Smit et al., 2013) demonstrated that, after standardization and homogenization, improvement of precision and accuracy by about a factor of two might be achieved.

5.3.5 COVID-19 crisis reduces Free Tropospheric Ozone across the Northern Hemisphere

During the spring-summer of 2020, the global crisis associated with COVID-19 caused all countries to take drastic measures to contain the spread of the virus, such as confining the population to their homes and, in many countries, the reduction of a great part of non-essential industrial, commercial and transport activity. These measures brought about a significant reduction in the emission of gases, not only in the lower layers of the atmosphere, but also throughout the troposphere due to the reduction of emissions associated with air transport. Faced with this situation, the international scientific community has questioned what effects this reduction in gas emissions has had on the environment and how it has affected the average distribution of certain gases in the free atmosphere, such as in the case of tropospheric ozone.

In order to find out how ozone in the free atmosphere responded during the emission reduction caused by the COVID-19 crisis throughout spring and summer 2020, the scientific community working on the measurement of tropospheric ozone has collaborated on the comparison and analysis of vertical profiles of ozone obtained using three different measurement techniques: ozone sounding, Fourier Transform Infrared Spectrometers (FTIR) and tropospheric LIDAR (Light Detection and Ranging). This collaboration of more than 30 institutions in 16 countries has resulted in the publication of the article “Did the COVID-19 Crisis Reduce Free Tropospheric Ozone across the Northern Hemisphere?” (Steinbrecht et al., 2020), which gives the keys to understanding the behaviour of ozone in the free troposphere during the period. IARC-AEMET took part in the work, contributing with IARC-FTIR measurements at Izaña Observatory and with ozone profile soundings carried out at Tenerife.

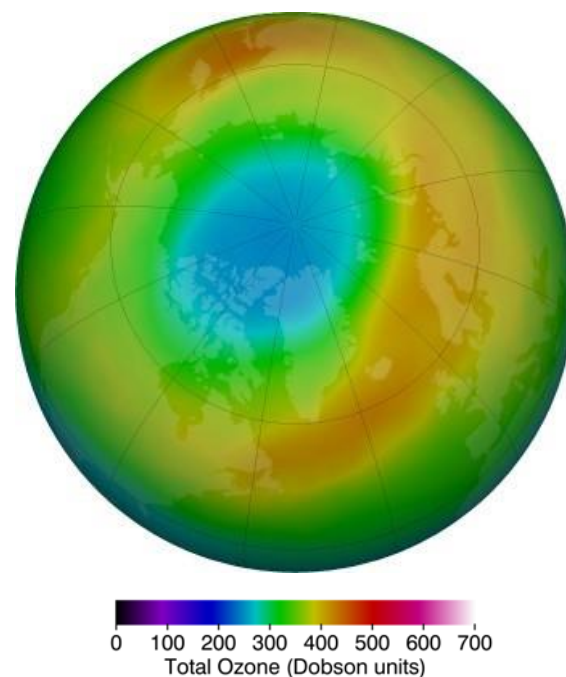


Figure 5.9. Image of the monthly average of the total ozone content over the Arctic region during March 2020, obtained from satellite data. Image from NASA Ozone Watch, GSFC (<https://ozonewatch.gsfc.nasa.gov/NH.html>).

The spring-summer of 2020 was not only atypical due to the crisis associated with COVID-19, which caused a reduction in gas emissions on a global scale, but also concerning the atmospheric circulation, since this same period was characterized by a record decrease of the ozone levels in the Arctic (Figure 5.9). This decrease in ozone in the stratosphere, for which the causes were mainly meteorological, was due to the fact that during the winter period a very strong, persistent polar vortex with very low temperatures in the stratosphere hovered over the Arctic. This “blocking” situation favoured the concentration of compounds that accelerate ozone depletion reactions, which meant that, from spring onwards, more ozone was depleted with the increase in solar radiation in the region. Circulation itself caused these ozone-poor air masses to drift to latitudes lower than normal. A similar situation occurred in 2011, when very low levels of ozone were detected in the stratosphere over Europe and Canada, with an increase in the UV index at the surface.

For the analysis of tropospheric ozone in 2020 during the reduction in emissions associated with the COVID-19 crisis, ozone soundings from 31 stations were used. Only the stations that carried out at least one sounding per month from the year beginning of 2000 to July 2020 were included in the analysis. Ozone soundings provide information on the vertical distribution of ozone in the troposphere and in the stratosphere up to an approximate altitude of 30 km, with a vertical resolution of about 100 m and ozone content accuracy of 5% -15% in the troposphere and 5% in the stratosphere (Smit et al., 2013). In addition, vertical ozone profiles obtained from FTIR spectrometers at 12 stations

were used which, although they have lower vertical resolution than the soundings, give a similar degree of accuracy (5%-10%, Vigouroux et al., 2015), and data from two tropospheric LIDARs, which provide ozone profiles between 3 and 12 km, with comparable accuracy (5% -10%, Leblanc et al., 2018) were also included.

Comparison of the vertical profiles of ozone anomalies averaged from April to August for each station for the years 2011 and 2020 in which, as indicated above, the greatest reduction in stratospheric ozone is associated with the polar vortex in the Arctic, demonstrates a clear difference. In 2011, the average reduction of the anomaly is observed above 9 km, whilst below that it is minimal, so the reduction of stratospheric ozone seems to have little influence on the concentration of tropospheric ozone, whilst in 2020, the negative anomaly is observed at all levels (Figure 5.10). Anomalies were defined as the relative deviation (in percent) from the 2000-2020 climatological mean.

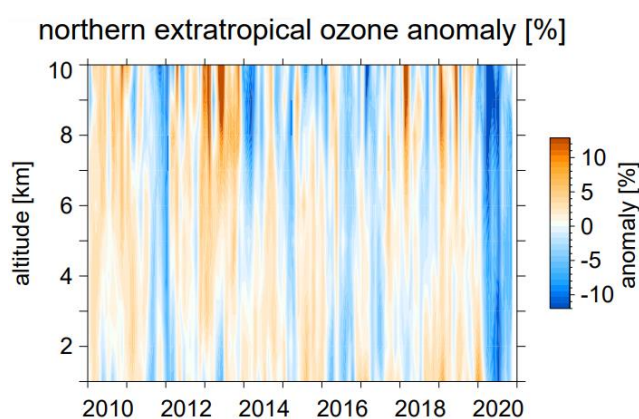


Figure 5.10. Vertical distribution of the average tropospheric ozone anomalies for the extra-tropical region in the northern hemisphere during the spring-summer period 2010-2020. A blue band is observed in 2020 corresponding to low ozone levels throughout the free troposphere. This remarkable reduction in tropospheric ozone is mainly caused by global gas emission reductions due to the economic downturn, a consequence of COVID-19. Credit: Steinbrecht et al., (2020).

When evaluating the CAMS reanalysis for 2011, a very similar result is obtained for the model analysis and for averages of anomalies obtained with observations: a larger negative anomaly in the stratosphere than in the free troposphere where the negative anomaly is smaller and closer to zero. However, although the CAMS analysis for 2020 reproduces a situation equivalent to that for 2011, with a minimum of stratospheric ozone and little influence on the free troposphere, it does not coincide with the anomalies obtained from the ozone profiles in the free troposphere. Taking into account that the CAMS 2020 analysis used pre-set emissions that did not reflect the reduction in gas emissions due to the COVID crisis, it seems that a large part of the reduction of tropospheric ozone in the free atmosphere (1 to 8 km) during 2020 was mainly due to the reduction in emissions due to the COVID crisis. In addition, the anomaly observed is consistent with simulations of

chemical-climate models, in which a reduction in emissions similar to the one of 2020 was assumed (Weber et al., 2020).

From the analysis of all the data, it is concluded that, between April and August 2020, the extra-tropical stations of the northern hemisphere measured an average of 7% (~ 4 nmol / mol = ppb) less tropospheric ozone (between 1 and 8 km) than normal (reference average 2000-2020) (Fig. 5.10). Specifically, the average anomaly observed in that period in Tenerife (Izaña Observatory) with FTIR was -6.3% (0.0% CAMS anomaly) and -1.6% (0.0% CAMS anomaly) in the ozone soundings. The decrease in ozone, observed over several consecutive months and simultaneously at a large number of extra-tropical stations in the northern hemisphere, had not occurred in recent years, at least since the year 2000. The reduction, on average of 7% in the free troposphere, contrasts with the increase of 10%-30% in surface ozone observed in polluted urban areas, coinciding with the reduction in emissions due to COVID-19, which has been reflected in various studies carried out on this subject.

5.3.6 The TOAR project: Final phase-I and start phase-II



As of February 2020, TOAR (Tropospheric Ozone Assessment Report: Global metrics for climate change, human health and crop/ecosystem research) Activity of the International Global Atmospheric Chemistry Project (IGAC), has entered its second phase (TOAR-II), the first phase having been completed in 2019.

TOAR-I (2014-2019) delivered on its goals of producing the first tropospheric ozone assessment report and building the world's largest database of surface ozone metrics (Fig. 5.11), calculated consistently for over 9000 surface ozone time series worldwide (Schultz et al., 2017). (Further details are given in section 5.3.5 of Izaña Activity Report 2017-2018, Cuevas et al, 2019). TOAR's accomplishments were made possible by the collective efforts of the international research community, drawing on the expertise of 230 scientists and air quality specialists from 36 nations, representing research on all seven continents.

TOAR-I has published its findings as a series of peer-reviewed manuscripts made available through a Special Feature of the open-access, non-profit journal, Elementa: Science of the Anthropocene, and IARC has collaborated in several of these publications: Gaudel et al., 2018 (Section 5.3.6 of Izaña Activity Report 2017-2018, Cuevas et al.,

2019); Tarasick et al., 2019 (Section 7, Fourier Transform Infrared Spectroscopy), and Cooper et al., 2020.

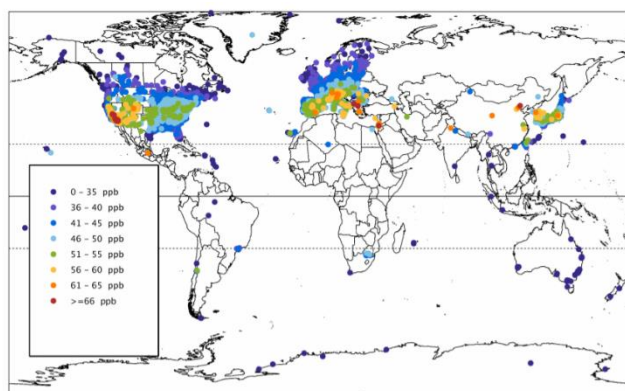


Figure 5.11. Present-day (2010-2014) values of the 6-month average (April-September in the N. Hemisphere, October-March in the S. Hemisphere) of maximum daily 8-hr average ozone, at all available sites (4801 total sites) in the TOAR database. Values are further averaged across the 5-yr period, 2010-2014.

The TOAR mission continues, with TOAR-II providing updated and extended information on tropospheric ozone (2020-2024). In the second phase, the goals of TOAR-II are:

1. TOAR Ozone Data Portal: Update the ozone observations in the TOAR surface ozone database to include all recent observations (since 2014), and include data from new sites and regions, as well as ozone precursor and meteorological data. Develop methods for including historical data (pre-1975) and create working links to repositories of free tropospheric observations.
2. TOAR publications: Exploit the new observational datasets collected by Goal 1 (with data through 2020) to provide an updated state of the science related to ozone's global distribution and trends relevant to climate, human health and vegetation. Extend the statistical toolbox and metrics of the TOAR trend analyses.
3. Involve scientists from the atmospheric sciences community, as well as statisticians and scientists who focus on broader issues of global change and sustainability, to identify outstanding science questions in relation to tropospheric ozone. The range of topics can be expanded beyond the scope of the original TOAR effort to investigate the impacts of tropospheric ozone on climate, human health and vegetation, and to address urban-scale issues in addition to the regional and global scale.
4. Maximize exploitation of the TOAR Surface Ozone Database by, 1) helping scientists around the world, beyond the TOAR effort, to apply the database to new analyses, and 2) exploring new data science methods to improve the analysis of global ozone trends and their attribution.

The TOAR-II virtual workshop organized in late January and early February 2021, was designed to gather the community and develop the working groups that will produce the papers for the TOAR-II Community Special Issue (the first step of the second Tropospheric Ozone Assessment Report), as well as identify new datasets for the assessment of tropospheric ozone and its impact on climate, health and vegetation. The working groups that were set up will focus on: Chemical Reanalysis, East Asia, Harmonization and Evaluation of Ground Based Instruments for Free Tropospheric Ozone Measurements (HEGIFTOM), Ozone over the Oceans, Ozone and Precursors in the Tropics (OPT), Radiative Forcing, Satellite Ozone, Statistics, and Urban Ozone.

IARC will participate in TOAR-II within the HEGIFTOM working group with surface ozone measurements, ozonesonde profiles and FTIR ozone profiles (for further details refer to Section 7). The HEGIFTOM working group will bring together different networks of ground-based instruments measuring free tropospheric ozone, not only to strengthen, speed up, and expand existing activities of harmonization of instruments, but also to compare Quality Assurance/Quality Control (QA/QC) procedures and reports, and harmonization efforts between the different networks.

5.4 References

- Cooper, O.R, Schultz, MG, Schröder, S, Chang, K-L, Gaudel, A, Benítez, GC, Cuevas, E, Fröhlich, M, Galbally, IE, Molloy, S, Kubistin, D, Lu, X, McClure-Begley, A, Nédélec, P, O'Brien, J, Oltmans, SJ, Petropavlovskikh, I, Ries, L, Senik, I, Sjöberg, K, Solberg, S, Spain, GT, Spangl, W, Steinbacher, M, Tarasick, D, Thouret, V and Xu, X. : Multi-decadal surface ozone trends at globally distributed remote locations., *Elem Sci Anth* 2020, 8: 23. DOI: <https://doi.org/10.1525/elementa.420>.
- Cuevas, E., González, Y., Rodríguez, S., Guerra, J. C., Gómez-Peláez, A. J., Alonso-Pérez, S., Bustos, J., and Milford, C.: Assessment of atmospheric processes driving ozone variations in the subtropical North Atlantic free troposphere, *Atmos. Chem. Phys.*, 13, 1973-1998, doi:10.5194/acp-13-1973-2013, 2013.
- Cuevas, E., Milford, C., Bustos, J. J., R., García, O. E., García, R. D., Gómez-Peláez, A. J., Guirado-Fuentes, C., Marrero, C., Prats, N., Ramos, R., Redondas, A., Reyes, E., Rivas-Soriano, P. P., Rodríguez, S., Romero-Campos, P. M., Torres, C. J., Schneider, M., Yela, M., Belmonte, J., del Campo-Hernández, R., Almansa, F., Barreto, A., López-Solano, C., Basart, S., Terradellas, E., Werner, E., Afonso, S., Bayo, C., Berjón, A., Carreño, V., Castro, N. J., Chinea, N., Cruz, A. M., Damas, M., De Ory-Ajamil, F., García, M.I., Gómez-Trueba, V., Hernández, C., Hernández, Y., Hernández-Cruz, B., León-Luís, S. F., López-Fernández, R., López-Solano, J., Parra, F., Rodríguez, E., Rodríguez-Valido, M., Sálamo, C., Sanromá, E., Santana, D., Santo Tomás, F., Sepúlveda, E., and Sosa, E.: Izaña Atmospheric Research Center Activity Report 2017-2018. (Eds. Cuevas, E., Milford, C. and Tarasova, O.), State Meteorological Agency (AEMET), Madrid, Spain and World Meteorological Organization, Geneva, Switzerland, WMO/GAW Report No. 247, 2019.

- Gaudel, A., O. R. Cooper, G. Ancellet, B. Barret, A. Boynard, J. P. Burrows, C. Clerbaux, P.-F. Coheur, J. Cuesta, E. Cuevas, S. Doniki, G. Dufour, F. Ebojje, G. Foret, O. Garcia, M. J. Granados-Muñoz, J. W. Hannigan, F. Hase, B. Hassler, G. Huang, D. Hurtmans, D. Jaffe, N. Jones, P. Kalabokas, B. Kerridge, S. Kulawik, B. Latter, T. Leblanc, E. Le Flochmoën, W. Lin, J. Liu, X. Liu, E. Mahieu, A. McClure-Begley, J. L. Neu, M. Osman, M. Palm, H. Petetin, I. Petropavlovskikh, R. Querel, N. Raupach, A. Rozanov, M. G. Schultz, J. Schwab, R. Siddans, D. Smale, M. Steinbacher, H. Tanimoto, D. W. Tarasick, V. Thouret, A. M. Thompson, T. Trickl, E. Weatherhead, C. Wespes, H. M. Worden, C. Vigouroux, X. Xu, G. Zeng, J. Ziemke: The Tropospheric Ozone Assessment Report: Present-day distribution and trends of tropospheric ozone relevant to climate and global atmospheric chemistry model evaluation, *Elem Sci Anth*, 6: 39. DOI: <https://doi.org/10.1525/elementa.291>, 2018.
- González, Y., Levels and origin of reactive gases and their relationship with aerosols in the proximity of the emission sources and in the free troposphere at Tenerife, PhD Thesis, Technical Note N° 12, AEMET, NIPO 281-12-016-1, July 2012.
- Leblanc, T., Brewer, M. A., Wang, P. S., Granados-Muñoz, M. J., Strawbridge, K. B., Travis, M., et al. (2018). Validation of the TOLNet lidars: the Southern California Ozone Observation Project (SCOOP). *Atmospheric Measurement Techniques*, 11, 6137–6162. <https://doi.org/10.5194/amt-11-6137-2018>.
- Schultz, M. G., Schröder, S., Lyapina, O., Cooper, O. R., Galbally, I., Petropavlovskikh, I., von Schneidemesser, E., Tanimoto, H., et al.: Tropospheric Ozone Assessment Report, links to Global surface ozone datasets. PANGAEA, <https://doi.org/10.1594/PANGAEA.876108>, Supplement to: Schultz, MG et al. (2017): Tropospheric Ozone Assessment Report: Database and Metrics Data of Global Surface Ozone Observations, *Elementa - Science of the Anthropocene*, 5:58, 26 pp, <https://doi.org/10.1525/elementa.244>, 2017.
- Smit, H. G. J., Oltmans, S., Deshler, T., Tarasick, D., Johnson, B., Schmidlin, F., Stübi, R., and Davies, J.: SI2N/O3S-DQA Activity: Guide Lines for Homogenization of Ozone Sonde Data, version 19 November 2012, available at: http://www-das.uwyo.edu/~deshler/NDACC_O3Sondes/O3s_DQA/O3S-DQA-Guidelines%20Homogenization-V2-19November2012.pdf, 2012.
- Smit, H.G.J., and the Panel for the Assessment of Standard Operating Procedures for Ozone sondes (ASOPOS), Quality Assurance and Quality Control for Ozone sonde Measurements in GAW, GAW Report No. 201, World Meteorological Organization (WMO), 92 pp, 2013.
- Steinbrecht, W., Kubistin, D., Plass-Dulmer, C., Tarasick, D.W., Davies, J., Gathen, P.V., Deckelmann, H., Jepsen, N., Kivi, R., Lyall, N., Palm, M., Notholt, J., Kois, B., Oelsner, P., Allaart, M., Piders, A., Gill, M., Malderen, R.V., Delcloo, A.W., Sussmann, R., Mahieu, E., Servais, C., Romanens, G., Stubi, R., Ancellet, G., Godin-Beekmann, S., Yamanouchi, S., Strong, K., Johnson, B., Cullis, P., Petropavlovskikh, I., Hannigan, J., Hernandez, J.L., Rodriguez, A.D., Nakano, T., Chouza, F., Leblanc, T., Torres, C., Garcia, O., Rohling, A., Schneider, M., Blumenstock, T., Tully, M., Jones, N., Querel, R., Strahan, S., Inness, A., Engelen, R., Chan, K.L., Cooper, O.R., Stauffer, R.M., Thompson, A.M., Did the COVID-19 Crisis Reduce Free Tropospheric Ozone across the Northern Hemisphere?, *Earth and Space Science Open Archive*, 20, doi:10.1002/essoar.10505226.1, 2020.
- Tarasick, D., Galbally, I.E., Cooper, O.R., Schultz, M.G., Ancellet, G., Leblanc, T., Wallington, T.J., Ziemke, J., Liu, X., Steinbacher, M., Staehelin, J., Vigouroux, C., Hannigan, J.W., García, O., Foret, G., Zanis, P., Weatherhead, E., Petropavlovskikh, I., Worden, H., Osman, M., Liu, J., Chang, K.-L., Gaudel, A., Lin, M., Granados-Muñoz, M., Thompson, A.M., Oltmans, S.J., Cuesta, J., Dufour, G., Thouret, V., Hassler, B., Trickl, T. and Neu, J.L., 2019. Tropospheric Ozone Assessment Report: Tropospheric ozone from 1877 to 2016, observed levels, trends and uncertainties. *Elem Sci Anth*, 7(1), p.39. DOI: <http://doi.org/10.1525/elementa.376>, 2019.
- Vigouroux, C., Blumenstock, T., Coffey, M., Errera, Q., García, O., Jones, N.B., et al. Trends of ozone total columns and vertical distribution from FTIR observations at eight NDACC stations around the globe. *Atmospheric Chemistry and Physics*, 15, 2915–2933. <https://doi.org/10.5194/acp-15-2915-2015>, 2015.
- Weber, J., Shin, Y. M., Staunton Sykes, J., Archer-Nicholls, S., Abraham, N. L., & Archibald, A. T. Minimal climate impacts from short-lived climate forcers following emission reductions related to the COVID-19 pandemic. *Geophysical Research Letters*, 47, e2020GL090326, 2020. <https://doi.org/10.1029/2020GL090326>.
- WMO, 2011: WMO/GAW Expert Workshop on Global Long-term Measurements of Nitrogen Oxides and Recommendations for GAW Nitrogen Oxides Network, Hohenpeissenberg, Germany, 8-9 October 2009, GAW Report 195, (WMO/TD-No. 1570), Geneva.
- WMO, 2013: Guidelines for Continuous Measurements of Ozone in the Troposphere, WMO TD No. 1110, GAW Report No. 209, World Meteorological Organization, Geneva, Switzerland.
- WMO, 2017: Report of the WMO/GAW Expert Meeting on Nitrogen Oxides and International Workshop on the Nitrogen Cycle, 12-14 April 2016, York, UK, GAW Report No. 232.
- WMO, 2020: Research Infrastructure Quality Assurance, System and Performance Audit of Surface Ozone, Carbon Monoxide, Methane, Carbon Dioxide and Nitrous Oxide at the Global GAW Station Izaña, Spain, May 2019, WCC-Empa Report No. 19/2, GAW Report No. 251.

5.5 Staff

Carlos Torres (AEMET; Head of programme)

Dr Emilio Cuevas (AEMET)

Dr Natalia Prats (AEMET)

Ramón Ramos (AEMET; Head of Infrastructure)

Sergio Afonso (AEMET; Meteorological Observer-GAW Technician), retired in 2019

Virgilio Carreño (AEMET; Meteorological Observer-GAW Technician)

Nayra Chinae (SIELTEC Canarias / TRAGSATEC; Calibrations and ozonesonde technician)

6 Total Ozone Column and Ultraviolet Radiation

6.1 Main Scientific Goals

The main scientific objective of this programme is to obtain the total ozone column (TOC) and ultraviolet (UV) spectral radiation with the highest precision and long-term stability that the current technology and scientific knowledge allows to achieve. To reach this objective the group uses three interconnected areas: instrumentation, modelling and dissemination. The basis of the research is the instrumentation supported by strict QA/QC protocols, laboratory calibrations and theoretical modelling. Finally, web-oriented [databases](#) are developed for dissemination of the observational data.

6.2 Measurement Programme

Measurements of total ozone and spectral ultraviolet radiation began in May 1991 in IZO with the installation of Brewer spectrometer #033. Ozone profile measurements were added in September 1992 with two daily (sunrise and sunset) vertical ozone profiles obtained with the Umkehr technique. In July 1997, a double Brewer #157 was installed at IZO and it ran in parallel with Brewer #033 for six months. In 2003, a second double Brewer #183 was installed, and it was designated the travelling reference of the Regional Brewer Calibration Center for Europe (RBCC-E).



Figure 6.1. Members of the Total Ozone and UV radiation programme with the RBCC-E Brewer spectrophotometer triad located at IZO. Left to right: Virgilio Carreño, Francisco Parra Rojas, Alberto Redondas, Sergio León Luis, and Javier López Solano.

In 2005, a third double Brewer #185 was installed, and it completes the reference triad of the RBCC-E (Fig. 6.1). The measurement programme was complemented with the installation of a Pandora spectroradiometer in October 2011. The technical specifications of both Brewer and Pandora instruments are summarized in Table 6.1.

Table 6.1. Spectrometer specifications.

Brewer	
Slit Wavelengths	O ₃ (nm): 303.2 (Hg slit), 306.3, 310.1, 313.5, 316.8, 320.1
Mercury-calibration (O ₃ mode)	302.15 nm
Resolution	0.6 nm in UV; approx 1nm in visible
Stability	±0.01 nm (over full temperature range)
Precision	0.006 ± 0.002 nm
Measurement range (UVB)	286.5 nm to 363.0 nm (in UV)
Exit-slit mask cycling	0.12 sec/slit, 1.6 sec for full cycle
O ₃ measurement accuracy	±1% (for direct-sun total ozone)
Ambient operating temperature range	0°C a +40°C (no heater) -20°C a +40°C (with heater option) -50°C a +40°C (with complete cold weather kit)
Physical dimensions (external weatherproof container)	Size: 71 by 50 by 28 cm Weight: 34 kg
Power requirements Brewer and Tracker	3A @ 80 to 140 VAC (with heater option) 1.5A @ 160 to 264 VAC 47 to 440 Hz
Pandora	
Instrument spectral range	265-500 nm
Spectral window for NO ₂ fit	370-500 nm
Spectral resolution	±0.4 nm
Total integration time	20 s
Number of scans per cycle	50-2500
Spectral sampling	3 pixels per Full Width at Half Maximum (FWHM)

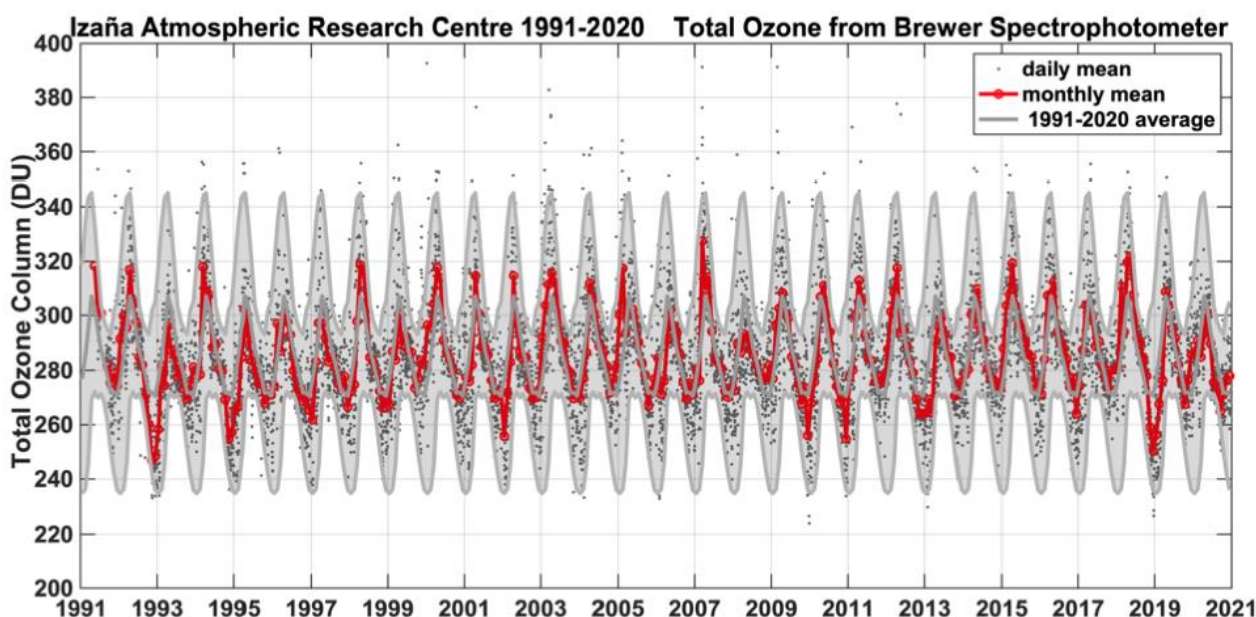


Figure 6.2. Total Ozone series at Izaña Observatory (1991-2020), daily mean (in grey dots) and monthly mean (in red), the long-term daily mean from the period 1991-2020 is also shown (grey line) with the shaded area corresponding to the standard deviation in the long-term mean.

The spectral UV measurements are routinely quality controlled using IZO calibration facilities. The stability and performance of the UV calibration is monitored by 200W lamp tests twice a month. Every six months the Brewers are calibrated in a laboratory darkroom, against 1000W DXW lamps traceable to the World Radiation Center (WRC) standards. The [SHICrvm](#) software tool is used to analyse quality aspects of measured UV-spectra before data transfer to the databases. In addition, LibRadtran model to measurements comparisons are regularly done. Every year the Brewer #185 is compared with the Quality Assurance of Spectral Ultraviolet Measurements (QASUME) International portable reference spectroradiometer from Physikalisch-Meteorologisches Observatorium Davos, World Radiation Center ([PMD/WRC](#)).

Concerning total ozone, the Brewer triad has an exhaustive quality control in order to assure its performance, with routine calibrations performed on a monthly basis. With this procedure, we have achieved a long-term agreement between the instruments of the triad with a precision better than 0.25% in ozone.

The Total Ozone programme is a part of the NDACC programme. The total ozone series for 1991-2020 is shown in Fig. 6.2 and is available at the NDACC [website](#) and at the World Ozone and Ultraviolet Data Center ([WOUDC](#)). Fig. 6.3 shows the UV index calculated on the basis of UV observations from Brewer spectrophotometer #157, available also at the WOUDC.

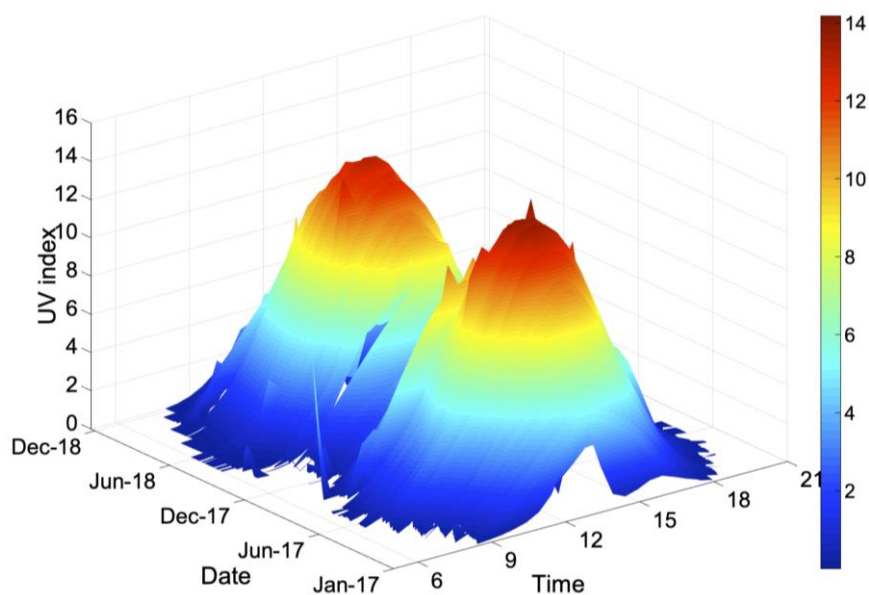


Figure 6.3. UV index during 2019-2020, calculated on the basis of measurements from Brewer #157, at Izaña Observatory.

6.3 Summary of remarkable results during the period 2019-2020

The participation in scientific projects of this measurement programme is intertwined with the activities of the Regional Brewer Calibration Center for Europe (RBCC-E) (see Section 16 for more details).

6.3.1 EUBREWNET

The Vienna Convention for the Protection of the Ozone Layer and the subsequent Montreal Protocol on Substances that Deplete the Ozone Layer have been among the most successful environmental agreements the nations of the world have entered into and have now almost completely eliminated the production of Ozone Depleting Substances. This has led to the halting of the rapid decline of stratospheric ozone observed in the 1980s and 1990s, with some promising early indications of ozone recovery now being apparent. It is therefore important to continue to measure carefully the state of the global ozone layer in the coming decades, noting also that stratospheric conditions are expected to change with the projected increasing concentration of greenhouse gases, and the fact that stratospheric ozone itself has a significant effect on the atmospheric radiation balance and surface climate. For this reason, the Vienna Convention obliges signatory countries to maintain programmes to systematically monitor stratospheric ozone.

The Brewer Ozone Spectrophotometer has, for the last 30 years, been the instrument of choice for ground station measurements of ozone and, in an effort to significantly improve the quality and timeliness of the data. The European Cooperation in Science and Technology (COST) Action (ES1207) was active from April 2013 to July 2017 to form a European Brewer Network – [EUBREWNET](#). The results of this COST Action have been presented in Rimmer, Redondas, and Karppinen (2018).

Since the end of 2018, support to EUBREWNET has been provided by AEMET. The activities carried out are overseen by a committee within the WMO Scientific Advisory Group (SAG) for Ozone and UV, which includes M. Tully (O₃ - UV SAG Chair), J. Rimmer (University of Manchester, UK), A. Redondas (IARC-AEMET, Spain), T. Kralidis (WOUDC) and C. Sinclair (O₃-UV SAG member). Further input is provided by EUBREWNET's Management Committee, consisting of J. Rimmer (University of Manchester, UK), A. Redondas (IARC-AEMET, Spain), A.F. Bais (Aristotle University of Thessaloniki, Greece), J. Gröbner (PMOD/WRC, Switzerland), T. Karppinen (Finnish Meteorological Institute, Arctic Research Center, Finland), and V. de Book (Royal Meteorological Institute of Belgium, Belgium).

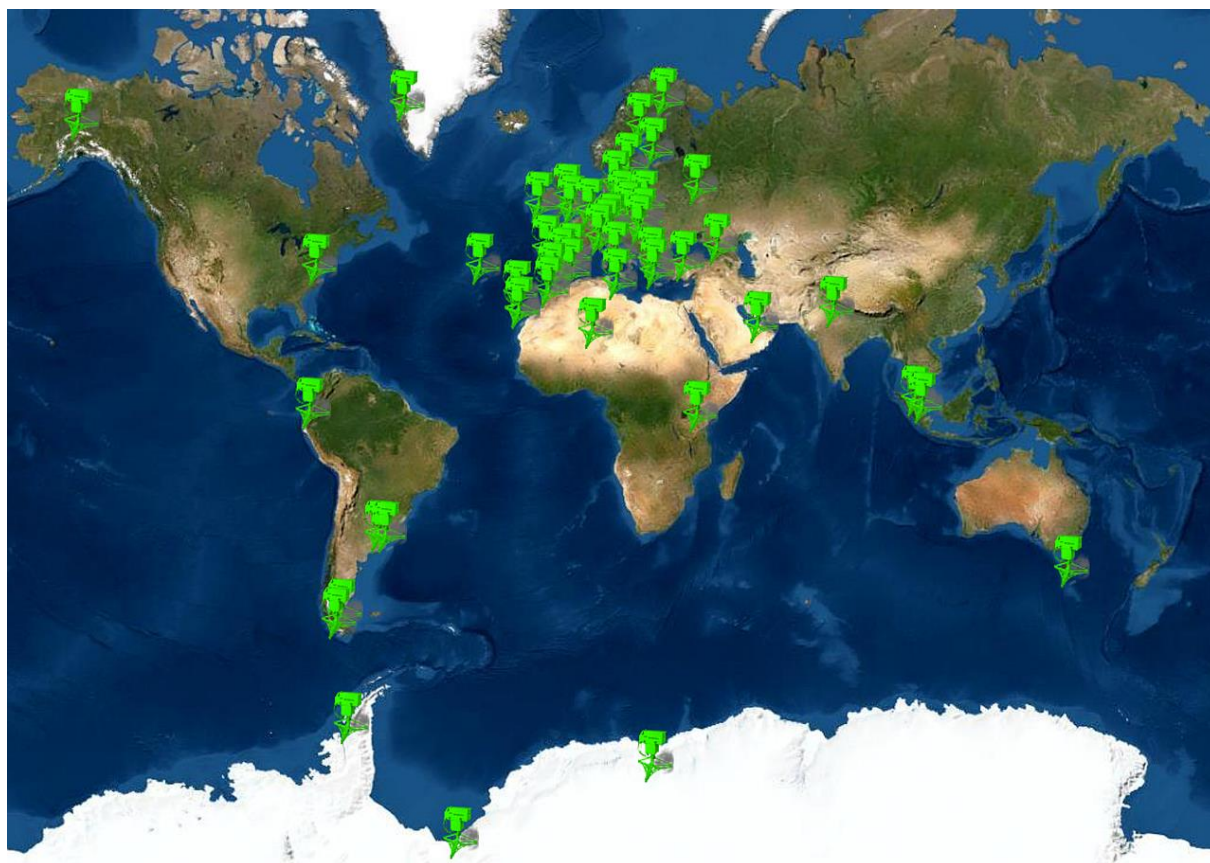


Figure 6.4. Location of Brewer stations currently participating in EUBREWNET. The network started as a European network but now includes close to 60 stations located world-wide.

EUBREWNET relies on the work of two European calibration Centers, the RBCC-E and the WRC. The RBCC-E plays a key role in EUBREWNET, coordinating the standardization of operation, characterization and calibration of the network instruments as well as providing the Brewer database. Now recognised by the WMO and the International Ozone Commission (IO3C), it represents an extremely valuable network of ground station data points without which the space-borne instruments would not be able to function with any degree of accuracy. In the current times when we are trying to identify ozone recovery rates of 1% per decade, it is highly important that data are both accurate and consistent across all stations.

The purpose of EUBREWNET is to harmonise observations, data processing, calibrations and operating procedures so that a measurement at one station is entirely consistent with measurements at all the others. Additionally, the Brewer spectrophotometers are also used to measure spectral UV irradiance, the sulphur dioxide column and aerosol optical depth. Some Brewer spectrophotometers are also able to measure the nitrogen dioxide column. This harmonised Brewer network (Fig. 6.4) constitutes the largest harmonised ground-based UV network in the world, available for assimilation into satellite retrievals and models to greatly improve accuracy of the satellite data and ozone and UV radiation forecasting. Another important point is the link to climate change where tropospheric ozone and aerosols are still regarded as having the largest effect on uncertainties in climate models. The Brewer instruments are suitable for the measurement of total column ozone which includes both tropospheric and stratospheric ozone whereas satellites struggle with the lower altitudes.

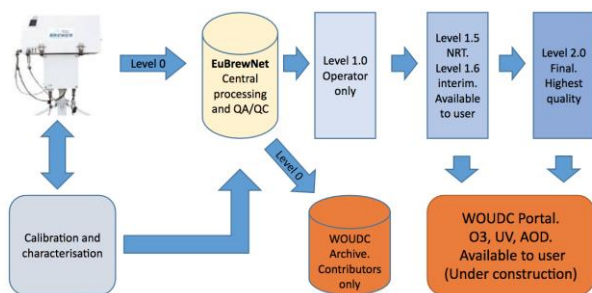


Figure 6.5. EUBREWNET database architecture.

The actual implementation of the network can be summarized as follows:

- Automated data transfers to central database (Fig. 6.5) started in September 2014. Data submission now became automatic with little operator involvement so improving overall submission rates.
- Calibration data are stored in a central database. This allows for central processing of all stations' data so ensuring consistency and use of up-to-date calibration and processing.

- Site characterisation. Central data processing in addition to data processing at the stations: including part of QC by comparison with near instruments and state of the art algorithms.
- Central re-processing. Historical data or changes in constants recommended by WMO Ozone and UV SAG.
- Central QA/QC systems (QA/QC validated in one place): stations with a problem can be easily identified.
- Near Real Time (NRT) data. Essential for NRT validation of satellite data and model assimilations.

As mentioned previously, support to EUBREWNET has been provided by AEMET since the end of the year 2018. The activities during 2019 were mostly devoted to tasks related to improving EUBREWNET's server stability and capabilities. The latter includes, for example, the capability to export data in the WOUDC and NDACC file formats. During 2020, two new products were implemented: version 2 of the ozone algorithm (including updated ozone cross-sections, airmass calculation, and Rayleigh coefficients), and a new Aerosol Optical Depth product. Furthermore, thanks to funding by ESA under the umbrella of the TROPOMI Mission Performance Centre, work has started on the implementation of the error budget of the Brewer ozone spectrophotometer in EUBREWNET that was developed during the ATMOZ project. During 2021, work will be focused on UV radiation, continuing with the development started by Kaisa Lakkala and Sergio León-Luis on the UV near real time product.

As a result of the work carried out during 2019 and 2020, EUBREWNET total ozone observations are now accessible from the [WOUDC](#) website. Users can search for EUBREWNET data from the Data Search / Download page (see Fig. 6.6) and download the resulting data directly from the EUBREWNET data server. Note that downloading data from EUBREWNET requires authentication.

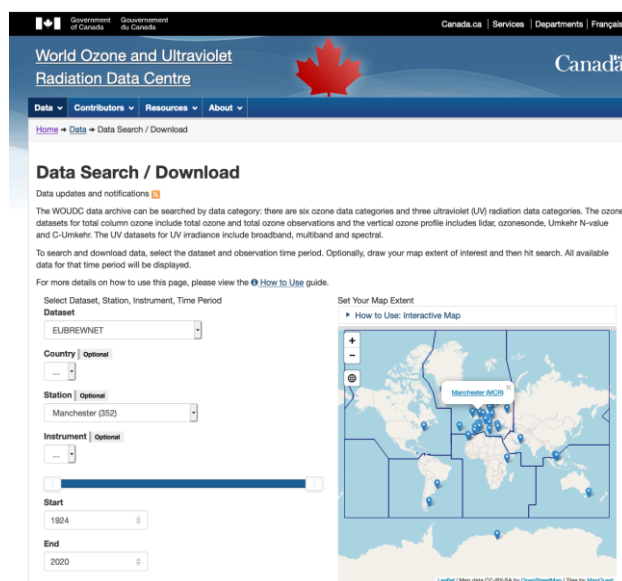


Figure 6.6. The WOUDC search page provides access to EUBREWNET data.

During the 2019 meeting of the WMO Ozone and UV Scientific Advisory Group, the Maturity Index Matrix for the EUBREWNET Network was also presented (Fig. 6.7). The maturity matrix has been developed within the Horizon 2020 (H2020) GAIA-CLIM project for different data products and networks, see Thorne et al. (2017). The idea behind this is to provide a framework and tool to semi-objectively classify measurement capabilities. The idea is also to identify and characterise mature data sets and include them in the Virtual Observatory developed within GAIA-CLIM to be used for satellite to non-satellite data comparisons. The EUBREWNET Maturity Index Matrix, which summarize the maturity of the network, was evaluated by Karin Kreher with good results, and EUBREWNET is now considered a Fiducial Reference Network for total ozone measurements.

Metadata	Documentation	Uncertainty characterization	Public access, feedback and update	Usage	Sustainability	Software (optional)
Standards	Formal Description of Measurement Methodology	Traceability	Access	Research	Siting environment	Coding standards
Collection level	Formal Validation Report	Comparability	User feedback mechanism	Public and commercial exploitation	Scientific and expert support	Software documentation
File level	Formal Measurement Series User Guidance	Uncertainty Quantification	Updates to record		Programmatic support	Portability and numerical reproducibility
		Routine Quality Management	Version control			Security
			Long term data preservation			
Legend						
1	2	3	4	5	6	Not applicable

Figure 6.7. EUBREWNET Maturity Index Matrix.

A cooperative agreement between EUBREWNET and NDACC networks was also presented during the NDACC meeting in 2020. This agreement mutually recognized both networks, reinforcing the cooperation between them while maintaining their own data policy. The stations/PI that participate in both networks with the same measurements continue to submit the observations to both networks. IARC (Spain) and Uccle (Belgium) stations which take part in both networks are developing the real time submission of the Brewer V2 total ozone to NDACC using EUBREWNET.

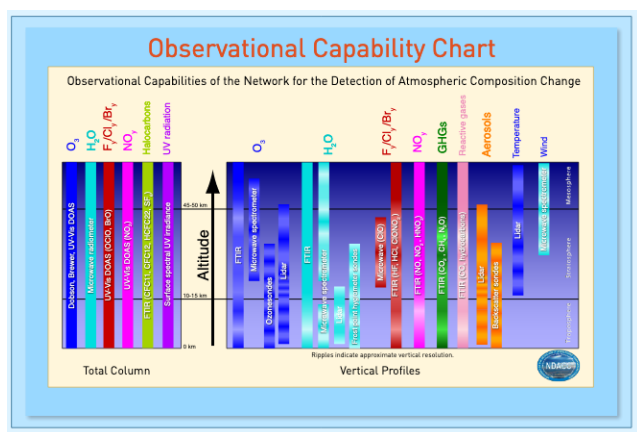


Figure 6.8. Observational capabilities of NDACC indicating Brewer data in Total Ozone Column measurements.

Furthermore, within the reorganization of WMO a new structure of “Expert Teams” has been created. The Expert Teams within GAW are now responsible for the advances in the research infrastructure in collaboration with SAG and the Infrastructure commission.

The Expert Team on Atmospheric Composition Measurement Quality (ET-ACMQ) deals with the QA/QC of GAW measurements, and in the case of Total Ozone the new group will combine activities that were part of O₃-UV SAG and SC-MINT (Standing Committee on Measurement, Instrumentation and Traceability) the former CIMO.

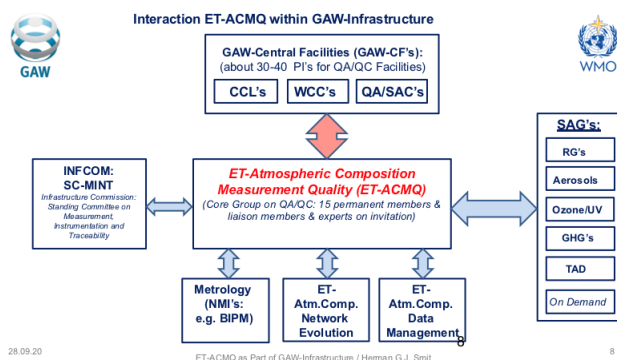


Figure 6.9. Interaction of the ET-ACMQ within GAW & WMO Infrastructure.

One of the objectives of these Expert Teams is to guarantee the quality of every GAW stored measurement based on the following principles:

- The measurement value is obtained following the Standard Operating Procedure (SOP).
- The overall uncertainty is reported and the traceability uncertainty chain is documented.
- Flag Code providing the state of processing /validation, reliability and representativeness is included in data reporting.
- Metadata sufficient for data reprocessing from raw data are provided.

It is clear that the Brewer total ozone observations have a lot of work to do by finalizing SOP's, addressing the lack of uncertainty budget, traceability documentation, and in the case of WUODC the impossibility to reprocess Brewer data starting from raw observations due to a lack of metadata.

Associated with this Expert Team, a Total Column Ozone (including Umkehr) Task Force has been created with two co-chairs: Irina Petropavlovsky (Dobson) and Alberto Redondas (Brewer) with the following key topics to address:

- Introduction of the new ozone cross-section and the temperature dependence.
- Uncertainty chain, traceability and metadata.
- New instrumentation.
- The Brewer documentation gaps as mentioned above.

EUBREWNET activities that were coordinated by O₃-UV-SAG are now under the umbrella of the ET-ACQM. The Ozone task force will bridge the NDACC and EUBREWNET total ozone activities.

Finally, it should be noted that EUBREWNET, in conjunction with WMO/UNEP, is very active in the areas of capacity building, particularly in Article 5 Vienna Convention countries. This includes the organization of operator courses and workshops, which provide expert instruction and knowledge exchange using the considerable expertise within EUBREWNET.

6.3.2 Updated V2 Brewer Algorithm

During 2020, a preliminary Version 2 of the ozone data processing was implemented in EUBREWNET. This processing is an update of the previous work of the Brewer community and it includes the following elements:

- New ozone cross-sections (from Bremen University).
- Ozone layer effective height and effective temperature for air mass calculation and ozone cross-sections correction.
- Rayleigh coefficients from (Nicolet, 1984).

The preliminary version 2 of the EUBREWNET ozone processing can be accessed from the Process function available [here](#). The parameters needed to process the data can be included in the Brewer configuration using the user interface available [here](#). See Fig. 6.10 for a V2 configuration example.

Figure 6.10. V2 processing software configuration parameters.

This V2 algorithm is now being tested in collaboration with the EUBREWNET stations of Davos, El Arenosillo, Izaña, Madrid, Sodankylä, Tamanrasset, Thessaloniki and Uccle.

6.3.3 Aerosol Optical Depth in EUBREWNET

A new Aerosol Optical Depth (AOD) product was implemented in EUBREWNET in 2020. AOD is determined from the standard Direct Sun (DS) ozone measurements following the method described in López-Solano et al. (2018).

This new AOD product has the same capabilities and functionality as the L1.5 ozone product with regard to

automatic and manual processing, and database insertion and retrieval. More information is available at the EUBREWNET [wiki](#).

AOD configurations and data for the El Arenosillo 2013, 2015, 2017, and 2019 campaigns are already available in EUBREWNET database. Fig. 6.11 shows a comparison of the AOD at 320 nm during the last three days of these campaigns. The calibrations of the 2017 and 2019 campaigns are still to be completed.

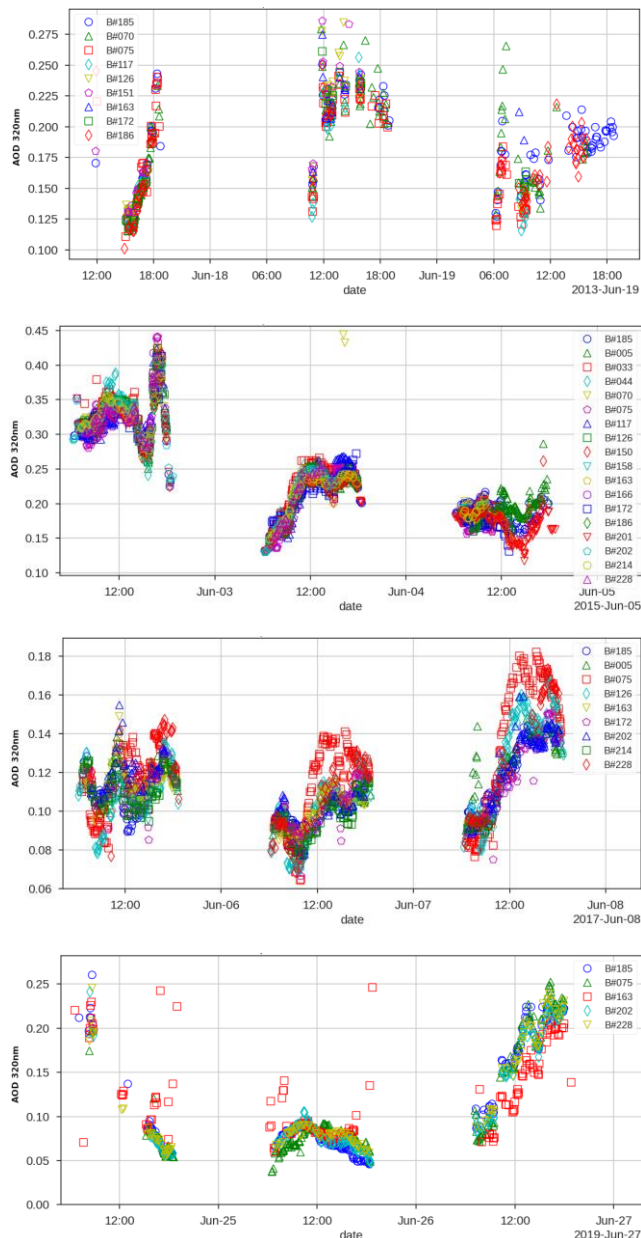


Figure 6.11. 320nm AOD during the last three days of the El Arenosillo 2013, 2015, 2017, and 2019 campaigns.

6.3.4 Brewer Total Ozone Error Budget in EUBREWNET

Funded by ESA under the umbrella of the TROPOMI Mission Performance Centre, the total ozone error budget of the Brewer ozone spectrophotometer developed during the ATMOZ project is being implemented in EUBREWNET. The final report of the ATMOZ project (Gröbner et al., 2017) is available [here](#).

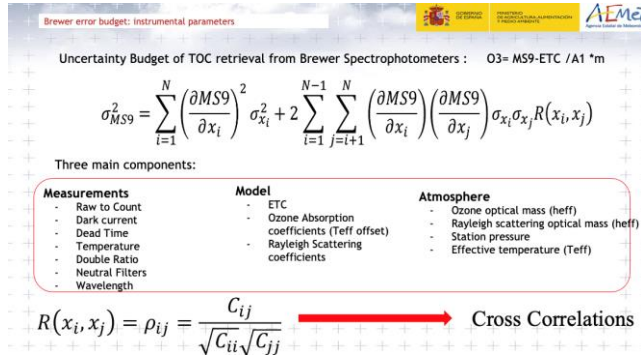


Figure 6.12. Cross-correlated standard uncertainty for Brewer spectrophotometer. The correlations are obtained through the covariances of the variables.

The model includes the effects of three main sources of uncertainty: measurements, atmosphere and model. It also considers the cross-correlations between the different parameters.

The measurement factors and calibration transfer errors were studied during the first phase of the project using the ATMOZ 2016 campaign for testing. The first results indicated that the major factor of the uncertainty, when the Extra Terrestrial Constant (ETC) is obtained with Langley calibration, is the Ozone Absorption Coefficient due to errors in ozone cross-section, followed by Solar Zenith Angle, the Calibration Transfer and finally the measurement errors.

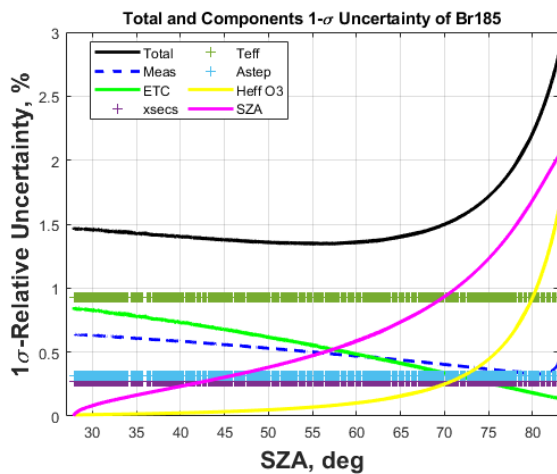


Figure 6.13. Non-correlated standard 1 σ -uncertainty and its components for Brewer 185 evaluated for 21 September 2017. The ETC uncertainty has been obtained through Langley Calibration.

The 1 σ uncertainties obtained for the ATMOZ 2016 campaign data at noon, using the standard algorithm are 1.5% for the reference instrument (BR#185, Fig. 6.13) and 2.2% for the network instrument (Br#157, Fig.6.14), where the most important component is the ETC Transfer Calibration followed by the Solar Zenith Angle.

The contributions of the Rayleigh scattering coefficients, pressure, AOD, Rayleigh effective altitude and the integration method to get the Ozone absorption coefficients are negligible.

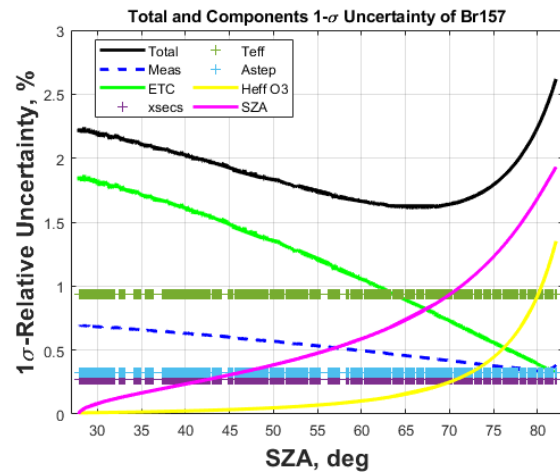


Figure 6.14. Non-correlated standard 1 σ -uncertainty and its components for Brewer 157 evaluated for 21 September 2017. The ETC uncertainty has been obtained through Transfer Calibration from Brewer 185.

Other important result of this first stage of the project is that some of the uncertainties required for the error budget calculation are not available in the calibration reports. This includes the errors of the temperature coefficients and filter attenuation and the uncertainty of the measurement (MS9) due to wavelength that can be extracted from the sun-scan measurements.

A python library that deals with the error budget calculation is under development for the implementation in EUBREWNET.

6.3.5 TROPOMI S5P total ozone column global validation within the VALTOZ project

The observations of individual Brewer spectrophotometers of EUBREWNET have been used for the validation of the TROPOMI Sentinel 5P ozone measurements (Garane et al. 2019). This was the first time EUBREWNET data was used for satellite validation. A similar future comparison is planned for NASA EPIC ozone observations. Only the high frequency EUBREWNET observations have sufficient time resolution to operationally validate the diurnal ozone variation as provided by TROPOMI and EPIC.

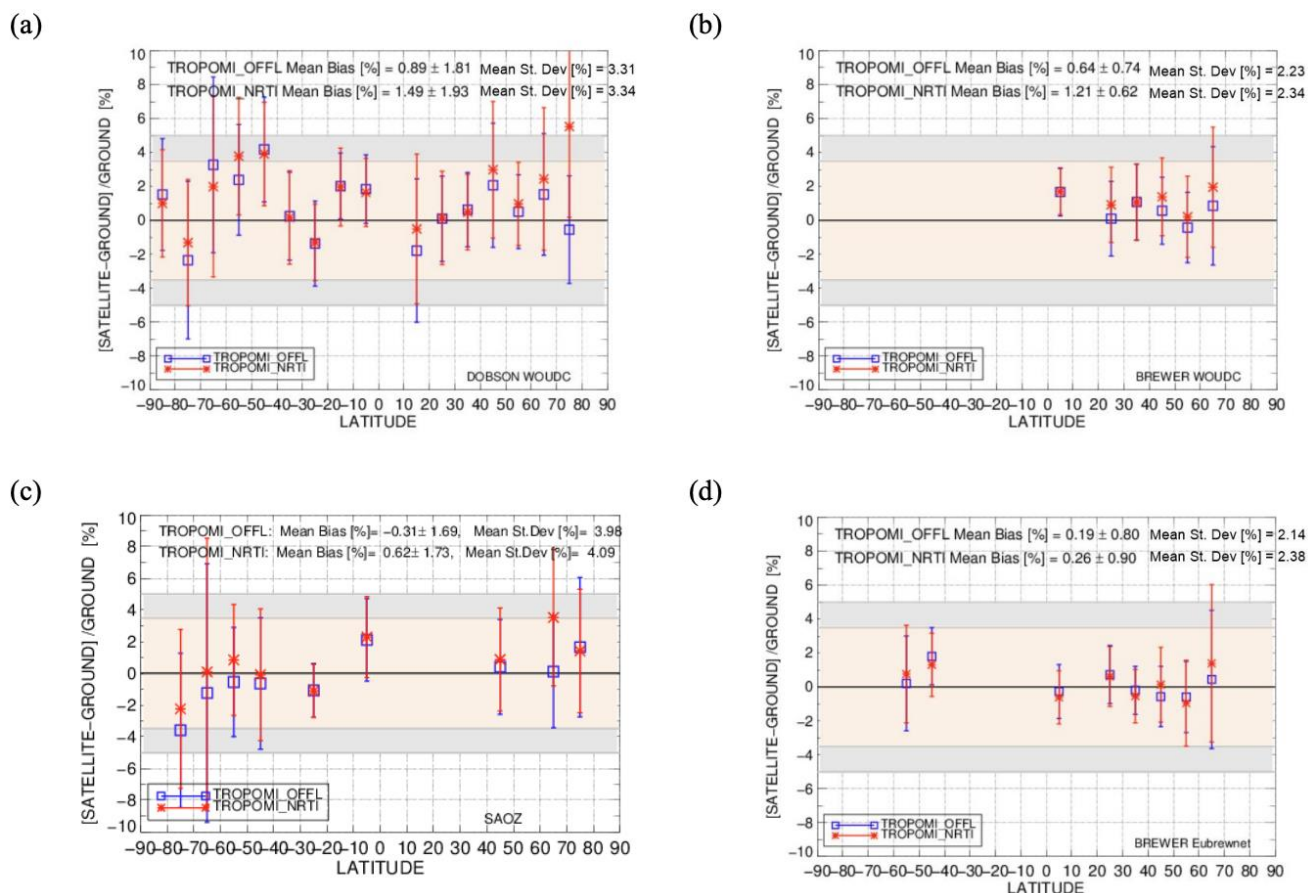


Figure 6.15. The latitudinal dependency of the mean percentage differences (panels a: Dobson and b: Brewer from WOUDC, panel c: SAOZ and panel d: Brewer from Eubrewnet) and their standard deviations for the two TROPOMI TOC products (blue line: OFFL, red line: NRTI). Reprinted from Garane et al. (2019).

6.3.6 Pandonia Global Network

The Pandora Spectrometer System is a ground-based, sun/sky/lunar passive remote sensing instrument for the retrieval of trace gases in the UV/Vis spectral wavelengths. It was developed in 2005 by NASA and the Sciglob company, and since that time the Pandora spectrometer system has evolved, with the participation in a series of field campaigns such as DISCOVER-AQ (Deriving Information on Surface conditions from Column and Vertically Resolved Observations Relevant to Air Quality), CINDI (Cabauw Intercomparison of Nitrogen Dioxide Measuring Instruments) 1&2, ATMOZ 2016, and the 2018 OWLETS (Ozone Water-Land Environmental Transition Study and LISTOS (Long Island Sound Tropospheric Ozone Study)). The Pandonia Network, funded by ESA through the LuftBlick company, has unified the operating and calibration procedures for the Pandora instruments since 2011.

NASA and ESA are currently collaborating to expand the global network of standardized, calibrated Pandora instruments focused on atmospheric composition. Through this collaboration the Pandonia Network has become the [Pandonia Global Network](#) (PGN), which emphasizes:

homogeneous calibration of instrumentation, low instrument manufacturing and operation costs, remote operative assistance, and central data processing and formatting for near real time delivery of final data products.

A major joint objective is to support the validation and verification of more than a dozen of Low Earth Orbit (LEO) and Geostationary Orbit (GEO) satellites, most notably Sentinel 5P, TEMPO, GEMS and Sentinel 4. PGN participants are primarily comprised of governmental and academic researchers and technicians. The launch of the PGN in early 2018 represents a programmatic shift by NASA and ESA away from primarily operating and supporting the research and field campaign operations, to establishing long-term fixed locations that are focused on providing long-term quality observations of total column and vertically resolved concentrations of a range of trace gases. The major trace gases observed by the Pandora systems across the range of 280 - 530 nm include: O_3 , NO_2 , $HCHO$, SO_2 and BrO .



Figure 6.16. Daniel Santana and the Pandora 121 mounted at IZO.

The Izaña Observatory is one of the most important Pandora instrument testing sites together with the Innsbruck Atmospheric Observatory of the University of Innsbruck, Austria. Two Pandora instruments were in operation at Izaña during 2019-2020, the Pandora 101 (1S model, UV, 270-530nm) owned by the Izaña Observatory, Fig.6.17, and the Pandora 121 (2S model, UV 270-530nm + VIS 400-900nm) owned by LuftBlick (Fi. 6.16). The Pandora 121 was dismantled from Izaña around 11 Jan 2019 to participate in an ATMOZ intercomparison campaign in Huelva, and after the campaign it was shipped to LuftBlick laboratories for recalibration.

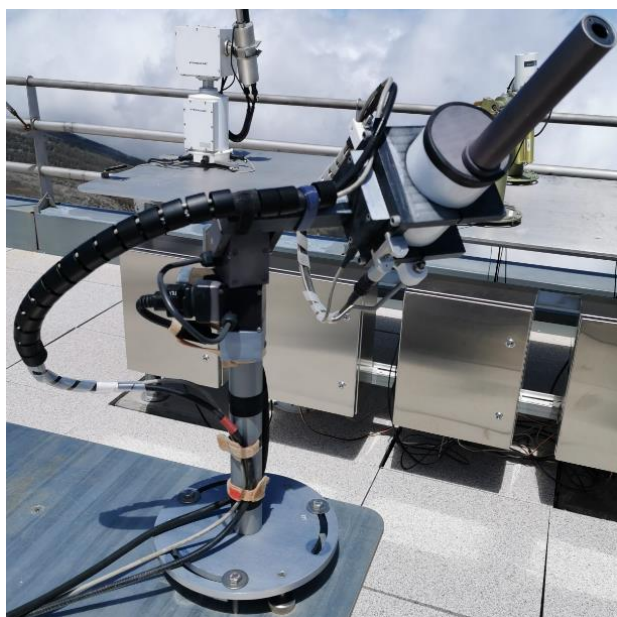


Figure 6.17. Pandora 101 mounted at IZO.

Both instruments have received funds from the PGN operational project from ESA to go through an important hardware upgrade which includes a new tracker model allowing to improve significantly the pointing accuracy. This upgrade is currently being applied to P121, and will be applied to P101 as soon as P121 is operational again at Izaña. Also, funds have been received through ESA to purchase and test a third instrument for Izaña, which will include a new set of filters and a new technology of high-

speed low noise Complementary Metal-oxide-Semiconductor (CMOS) spectrometers (Avantes EVO).

Izaña is an invaluable PGN testing location, not only for testing the performance of the hardware, but also for data intercomparison (e.g. total ozone column) and algorithm development due to its remote location, the large fleet of auxiliary datasets and highly experienced staff.

Trace gas column amounts from Pandora data are retrieved utilizing a DOAS like algorithm, where the gas absorption features in a measured spectrum are compared to an absorption-free reference spectrum.

The standard method to process total ozone column in PGN is based on the use of a theoretical reference spectrum, assuming a fixed effective ozone temperature in the atmosphere. This leads to seasonal differences of up to 1% and a 3 % bias between the standard Pandora and Brewer TOC data (Zhao et al., 2016). Currently, updated total ozone column algorithms are being implemented within the PGN. The first algorithm is similar to the current standard but includes the correction of the effective ozone temperature by using the TOMS v8 ozone profile climatology. The second algorithm relies on a novel calibration technique to create an absorption-free synthetic reference spectrum for the retrieval and also derives the effective ozone temperature explicitly.

The current activities at Izaña related to PGN are focused on maintaining the operation of the instruments, testing new hardware improvements on demand, and to serve as a testbed for algorithm refinement and development.

6.4 References

- Cede, A., Manual for Blick Software Suite 1.6, available at http://pandonia.net/media/documents/BlickSoftwareSuite_Manual_v11.pdf, 2019.
- Garane, K., Koukoulis, M.-E., Verhoelst, T., Lerot, C., Heue, K.-P., Fioletov, V., Balis, D., Bais, A., Bazureau, A., Dehn, A., Goutail, F., Granville, J., Griffin, D., Hubert, D., Keppens, A., Lambert, J.-C., Loyola, D., McLinden, C., Pazmino, A., Pommereau, J.-P., Redondas, A., Romahn, F., Valks, P., Van Roozendael, M., Xu, J., Zehner, C., Zerefos, C., Zimmer, W., TROPOMI/SSP total ozone column data: global ground-based validation and consistency with other satellite missions, *Atmospheric Measurement Techniques*, 10(12):5263–5287, 2019.
- Gröbner, J., Redondas, A., Weber, M., Bais, A. Final Publishable Report Traceability for atmospheric total column ozone (ENV59, ATMOZ). EURAMET; 2017. (Available at: <https://www.euramet.org/research-innovation/search-research-projects/details/project/traceability-for-atmospheric-total-column-ozone/>)
- Lakkala, K., Kujanpää, J., Brogniez, C., Henriot, N., Arola, A., Aun, M., Auriol, F., Bais, A.F., Bernhard, G., De Bock, V., Catalfamo, M., Deroo, C., Diémoz, H., Egli, L., Forestier, J.-B., Fountoulakis, I., Garane, K., Garcia, R.D., Gröbner, J., Hassinen, S., Heikkilä, A., Henderson, S., Hülsen, G., Johnsen, B., Kalakoski, N., Karanikolas, A., Karppinen, T., Lamy, K., León-Luis, S.F., Lindfors, A.V., Metzger, J.-M., Minvielle, F.,

- Muskatel, H.B., Portafaix, T., Redondas, A., Sanchez, R., Siani, A.M., Svendby, T., Tamminen, J.: Validation of the TROPOspheric Monitoring Instrument (TROPOMI) surface UV radiation product. *Atmospheric Measurement Techniques*, 13(12) 6999-7024, DOI: 10.5194/amt-13-6999-2020, 2020.
- López-Solano, J., Redondas, A., Carlund, T., Rodríguez-Franco, J. J., Diémoz, H., León-Luis, S. F., Hernández-Cruz, B., Guirado-Fuentes, C., Kouremeti, N., Gröbner, J., Kazadzis, S., Carreño, V., Berjón, A., Santana-Díaz, D., Rodríguez-Valido, M., De Bock, V., Moreta, J. R., Rimmer, J., Smedley, A.R.D., Boulkelia, L., Jepsen, N., Eriksen, P., Bais, A. F., Shiroto, V., Vilaplana, J. M., Wilson, K. M., and Karppinen, T., Aerosol optical depth in the European Brewer Network, *Atmospheric Chemistry and Physics*, 18, 3885-3902, 2018.
- Nicolet, M., On the molecular scattering in the terrestrial atmosphere: an empirical formula for its calculation in the homosphere, *Planet. Space Sci.*, 32, 1467–1468, [https://doi.org/10.1016/0032-0633\(84\)90089-8](https://doi.org/10.1016/0032-0633(84)90089-8), 1984.
- Rimmer, J., A. Redondas, and T. Karppinen, EuBrewNet – A European Brewer network (COST Action ES1207), an overview, *Atmospheric Chemistry and Physics*, 18, 10347–10353, 2018.
- Thorne, P. W., Madonna, F., Schulz, J., Oakley, T., Ingleby, B., Rosoldi, M., Tramutola, E., Arola, A., Buschmann, M., Mikalsen, A. C., Davy, R., Voces, C., Kreher, K., De Maziere, M., and Pappalardo, G. Making better sense of the mosaic of environmental measurement networks: a system-of-systems approach and quantitative assessment, *Geoscientific Instrumentation, Methods and Data Systems*, 2(6):453–472, 2017.
- Zhao, Xiaoyi, Vitali Fioletov, Alexander Cede, Jonathan Davies, and Kimberly Strong. 2016. “Accuracy, Precision, and Temperature Dependence of Pandora Total Ozone Measurements Estimated from a Comparison with the Brewer Triad in Toronto.” *Atmospheric Measurement Techniques* 9 (12): 5747–61. <https://doi.org/10.5194/amt-9-5747-2016>.

A list of publications involving EUBREWNET is available [here](#).

A list of publications involving the Pandonia Global Network is available [here](#).

6.5 Staff

Alberto Redondas Marrero (AEMET; Head of programme)
 Virgilio Carreño (AEMET; Meteorological Observer-GAW Technician)
 Dr Francisco Parra Rojas (AEMET; Research Scientist)
 Dr Sergio León Luis (TRAGSATEC; Research Scientist)
 Daniel Santana Díaz (Sieltec/LuftBlick; Pandonia Global Network Operator/Research Scientist)
 Dr Alberto Berjón (TRAGSATEC; Research Scientist)
 Dr Javier López Solano (TRAGSATEC; Research Scientist)

7 Fourier Transform Infrared Spectroscopy (FTIR)

7.1 Main Scientific Goals

Earth observations are fundamental for understanding the drivers of climate change and thus for supporting decisions on adaptation and mitigation strategies. Atmospheric remote sounding from space and ground are essential components of the observational strategy. In this context, the Fourier transform infrared spectroscopy (FTIR) programme at the IARC was established with the main goals of long-term monitoring of atmospheric gas composition (ozone related species and greenhouse gases) and for the validation of satellite remote sensing measurements and climate models. Much effort within the FTIR programme has been put in developing new strategies for observing tropospheric water vapour isotopologues from ground and space-based remote sensors, since these observations play a fundamental role in understanding atmospheric water cycle and its links to the global energy and radiation budgets.

The FTIR programme at the IARC is the result of the close and long-lasting collaboration of more than a decade between the IARC-AEMET and the [IMK-ASF-KIT](#) (Institute of Meteorology and Climate Research-Atmospheric Trace Gases and Remote Sensing, Karlsruhe Institute of Technology, Germany). The IMK-ASF has operated high-resolution ground-based FTIR systems for almost two decades and they are leading contributors in developing FTIR inversion algorithms and quality control of FTIR solar measurements. As a result of this collaboration, the FTIR observations at IZO has contributed to the prestigious international networks NDACC and TCCON since 1999 and 2007, respectively.

7.2 Measurement Programme

A ground-based high-resolution FTIR experiment (HR FTIR in the following) for atmospheric composition monitoring has two main components (Figure 7.1): a precise solar tracker that captures the direct solar light beam and a high-resolution Michelson interferometer (IFS). IARC's FTIR activities started in 1999 with a Bruker IFS 120M spectrometer, which was replaced by a Bruker IFS 120/5HR spectrometer in 2005 (see technical specifications in Table 7.1).

In order to derive trace gas concentrations from the recorded FTIR solar absorption spectra, synthetic spectra are calculated by the line-by-line radiative transfer model PRFWD (Schneider and Hase, 2009). Then, the synthetic spectra are fitted to the measured ones by the software package PROFFIT (PROFile FIT, Hase et al., 2004).



Figure 7.1. The ground-based FTIR experiment at the IARC (scientific container is shown on the upper panel, and the Michelson interferometer is shown on the lower panel).

PROFFIT allows to retrieve volume mixing ratio (VMR) profiles and to scale partial or total VMR profiles of several species simultaneously. There have been a lot of efforts for assuring and even further improving the high quality of the FTIR data products: e.g., monitoring the instrumental line shape (Hase et al., 1999), monitoring and improving the accuracy of the applied solar trackers (Gisi et al., 2011), as well as developing sophisticated retrieval algorithms (Hase et al., 2004). The good quality of these long-term ground-based FTIR data sets has been extensively documented by theoretical and empirical validation studies (e.g., Schneider et al., 2008; Schneider et al., 2010; García et al., 2012; Sepúlveda et al., 2012).

In 2018 a portable and low-resolution FTIR spectrometer (LR FTIR in the following), the Bruker EM27/SUN, was acquired by the IARC within the Spanish infrastructure programme (project no. AEDM15-BE-3319). This instrument operates within the Collaborative Carbon Column Observing Network (COCCON) (Frey et al., 2019a, Dubravica et al., 2019) (see section 7.3.2).

Table 7.1. Technical Specifications for Bruker IFS 120/5HR (in brackets, if different for 120M).

Manufacturer, Model	Bruker, IFS 120/5HR [IFS 120M]
Spectral range (cm ⁻¹)	700 - 4250 (NDACC) and 3500 - 9000 (TCCON) Optional: 20 - 43000
Apodized spectral resolution (cm ⁻¹)	0.0025 [120M: 0.0035]
Resolution power ($\lambda/\Delta\lambda$)	$2 \cdot 10^5$ at 1000 cm ⁻¹
Typical Scan velocity (cm/s)	2.5 (scan time about 100 s @ 250 cm of Optical Path Difference)
Field of view (°)	0.2
Detectors	MCT and InSb (NDACC); InGaAs (TCCON)
Size (cm)/Weight (kp)/Mobility	320 x 160 x 100 [120M: 200 x 80 x 30] 550 + 70 (Pump) [120M: 100 + 30 (Electronics)] Installed inside container, limited mobility
Quality assurance system	Routine N ₂ O and HCl cell calibrations to determinate the Instrumental Line Shape

The FTIR programme at the IARC is complemented by two Picarro L2120-I δD (standardized ratio between H₂¹⁶O and HD¹⁶O) and $\delta^{18}O$ (standardized ratio between H₂¹⁶O and H₂¹⁸O) analysers installed at IZO and TPO (for more details see González et al., 2016). The IZO instrument was moved to SCO station in May 2019 to monitor the isotopic footprint of the maritime boundary layer. The Picarro spectrometers are based on the Wavelength-Scanned Cavity Ring-Down Spectroscopy (WS-CRDS) technology and are calibrated by injecting liquid standards in a Standard Delivery Mode (SDM) from Picarro. The 0.6 Hz-precision of the analyser on δD is <13.5‰ at 500 ppmv H₂O and is <2‰ for 4000 ppmv. The absolute uncertainty for δD is <13.7‰ at 500 ppmv and <2.3‰ at 4500 ppmv. The error estimation accounts for instrument precision as well as errors due to the applied data corrections (Standards Delivery Module (SDM) effects + instrumental drifts <1‰, liquid standard bias <0.7‰, calibration bias <0.5‰) for δD .

7.3 Summary of remarkable results during the period 2019-2020

The FTIR activities from 2019 to 2020 have been focused on ground and space-based remote sensing FTIR spectrometry as well as in-situ spectrometry.

7.3.1 Ground-based high-resolution FTIR spectrometry

The ground-based HR FTIR observations have a large potential to support analysis of the composition of the troposphere, the stratosphere and their exchange processes. This is fundamental to monitor and study, for example, the sources and sinks of greenhouse gases or the evolution of the ozone layer. Routinely, the IARC HR FTIR have contributed to NDACC with C₂H₆, ClONO₂, CO, CH₄, COF₂, HCl, HCN, HF, H₂CO, HNO₃, N₂O, NO₂, NO, O₃ and OCS observations (total column amounts and VMR vertical profiles) since 1999. So, the first 20 years of operation of the NDACC IZO FTIR programme were reached in 2019 (García et al., 2019a). Within TCCON, total column-averaged abundances of CO₂, N₂O, CH₄, HF, CO, H₂O and HDO have been measured since 2007 (Fig. 7.2).

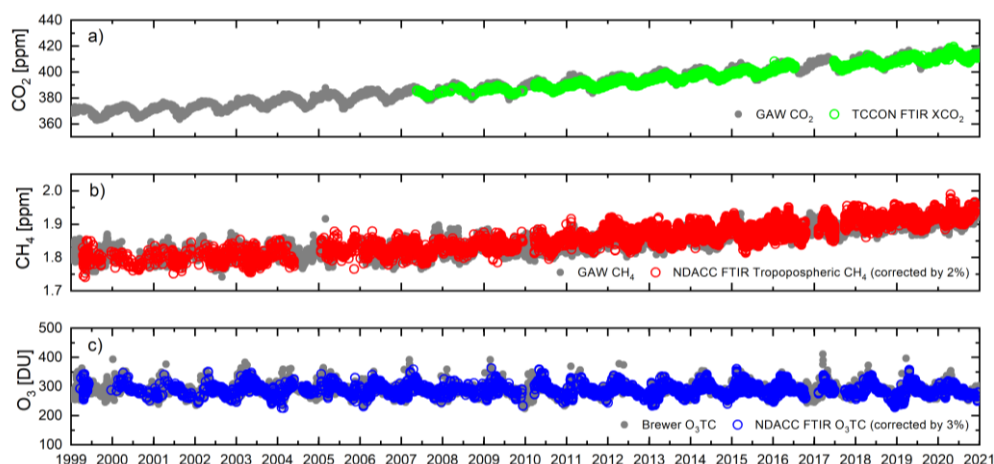


Figure 7.2. Time series of the total column-averaged abundances of a) carbon dioxide (XCO₂) in the framework of TCCON, b) tropospheric methane (CH₄) and c) ozone total column (O₃TC) amounts in the framework of NDACC as observed by the IARC FTIR. For comparison, the time series of these trace gases as observed by other high-quality measurement techniques available at the IARC are also displayed (GAW in-situ records for CO₂ and CH₄, and Brewer O₃TC amounts for O₃).

With these refined time series, we have participated in numerous studies at a global scale. For example, the IARC HR FTIR station has been one of the 20 NDACC FTIR stations used to investigate the level of optical resonances (“channeling”) of each FTIR spectrometer within NDACC (Blumenstock et al., 2020). Dedicated spectra were recorded using a laboratory mid-infrared source and two operational detectors. In the indium antimonide (InSb) detector domain (1900–5000 cm^{-1}), the amplitude of the most pronounced channeling frequency amounts from 0.1‰ to 2.0‰ of the spectral background level. In the mercury cadmium telluride (HgCdTe) detector domain (700–1300 cm^{-1}), stronger effects were documented with the largest amplitude ranging from 0.3‰ to 21‰ (see Fig. 7.3). The observed channeling frequencies were found to be caused by the optical thickness of the beam splitter substrate, and the air gap in between the beam splitter and compensator plate. A new beam splitter design was proposed to potentially reduce channeling impacts on the NDACC FTIR spectrometers, thereby increasing the quality of recorded spectra across the network (Blumenstock et al., 2020).

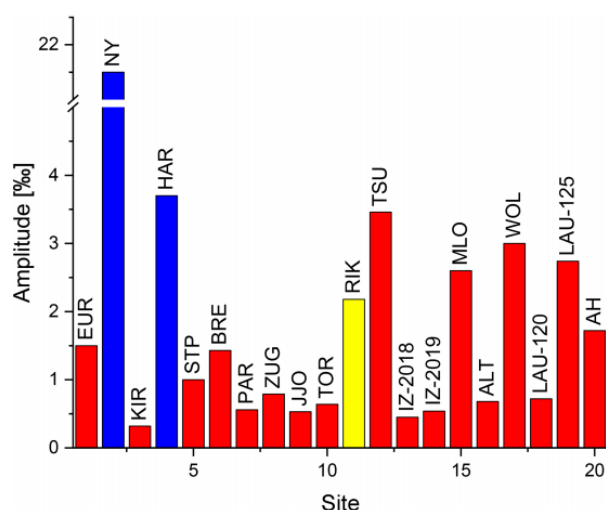


Figure 7.3. Amplitude of channeling in the HgCdTe spectrum. Red, yellow, and blue bars indicate channeling due to the beam splitter air gap, beam splitter substrate, and detector window, respectively. Note that IZO NDACC station is named as “IZ”. Reprinted from Blumenstock et al. (2020).

Other works have addressed the assessment of consistency between different NDACC and TCCON products, which allows both HR FTIR data sets to be used with high confidence. Zhou et al. (2019a, 2019b) presented the intercomparison of total column-averaged nitrous oxide (XN_2O) and carbon monoxide (XCO) between TCCON and NDACC FTIR measurements at different stations (including IZO among them). This comparison demonstrated that the NDACC XCO measurements are about 5.5% higher than the TCCON data at Northern Hemisphere stations, while the absolute bias is within 2% at Southern Hemisphere sites. This hemispheric dependence is mainly attributed to the smoothing errors of the TCCON and NDACC products (caused by the different a priori profiles

and vertical sensitivities). It was also found that TCCON XCO measurements are 6–8% smaller than coincident AirCore profile measurements, pointing out that further investigations should be carried out to determine the correct scaling factor to be applied to the TCCON XCO data (Zhou et al., 2019a).

Regarding XN_2O , the comparison reveals that mean differences between TCCON and NDACC are between 1.1%–0.5% with standard deviations between 0.5%–1.6%, which are within the uncertainties of the two data sets (Zhou et al., 2019b). The comparison to GEOS-Chem model and ground-level records also documents that the XN_2O trends from the GEOS-Chem a posteriori simulation are close to those from the NDACC and surface flask samples, while the XN_2O trends from the GEOS-Chem a priori simulation are significantly larger (see Fig. 7.4). This confirms that the N_2O fluxes from the a priori inventories are overestimated.

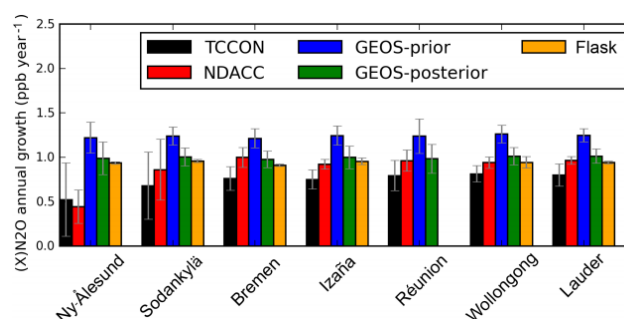


Figure 7.4. XN_2O trends from TCCON and NDACC measurements, a priori and a posteriori model simulations, and surface N_2O trend from flask samples at different NDACC/TCCON sites. Reprinted from Zhou et al. (2019b). Note that GEOS model output and flask sample data are both for the 2007–2014 period, whereas all available FTIR measurements are from the 2007–2017 period.

In addition, we have investigated long-term changes in key elements participating in the creation and destruction of ozone (O_3) in the atmosphere, such as nitric acid (HNO_3), hydrogen chloride (HCl) or O_3 itself across the globe. As recently pointed out by Strahan et al. (2020), analyses of NDACC HNO_3 and HCl columns at a global scale (including IZO among them) allowed to detect changes in the extratropical stratospheric transport circulation from 1994 to 2018.

The HNO_3 and HCl analyses combined with the age of air from a simulation using the MERRA2 reanalysis show that the Southern Hemisphere lower stratosphere has become one month per decade younger relative to the Northern Hemisphere, largely driven by the changes in Southern Hemisphere transport circulation. The analysis reveals multiyear anomalies with a 5 to 7 years period driven by interactions between the circulation and the quasi-biennial oscillation in tropical winds (see Fig. 7.5). Given that the amplitude of this short-term dynamical variability is larger than the long-term trend records, it may lead to biased O_3 trend estimations.

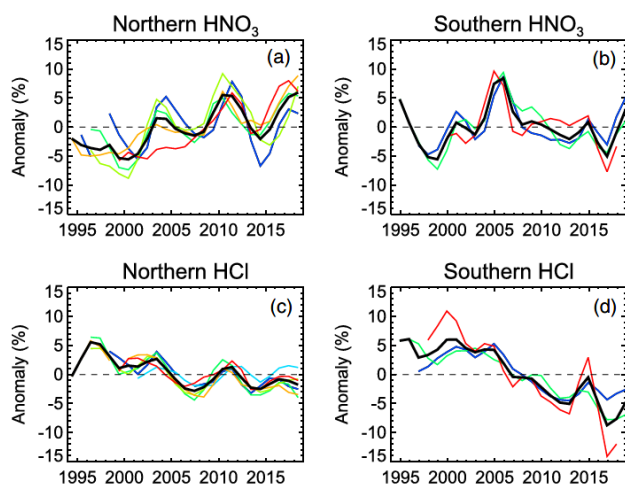


Figure 7.5. NDACC FTIR annual mean total column anomalies as a percent of each site's long-term mean, 1994-2018, for (a) HNO_3 from five Northern Hemisphere sites (IZO in red), (b) HNO_3 from three Southern Hemisphere sites, (c) and (d) as for (a) and (b), but for HCl columns. Hemispheric means are shown in black. Reprinted from Strahan et al. (2020).

Regarding O_3 and focused on the troposphere, the IARC HR FTIR O_3 time series have also contributed to the first Tropospheric Ozone Assessment Report (see Section 5.3.6). The first phase of TOAR offered remarkable results. For example, in Tarasick et al. (2019), various O_3 measurement methods and O_3 data sets are reviewed and selected for inclusion in the historical record of background O_3 levels, based on the relationship of the measurement technique to the modern UV absorption standard, absence of interfering pollutants, representativeness of the well-mixed boundary layer and expert judgement of their credibility. This overview work concludes that the great majority of validation and intercomparison studies of free tropospheric O_3 measurement methods use ECC ozonesondes as reference.

Compared to UV-absorption measurements, ECC ozonesondes show a modestly high ($\sim 1\text{--}5\% \pm 5\%$) bias in the troposphere, but no evidence of a change with time. Umkehr, lidar, and FTIR methods all show modestly low biases relative to ECCs, and so, using ECC sondes as a transfer standard, all appear to agree to within one standard deviation with the modern UV-absorption standard. In relation to space-based observations, biases and standard deviations of satellite retrieval are often 2–3 times larger than those of other free tropospheric measurements.

As detailed in Section 5.3.5, Steinbrecht et al (2020) conducted an analysis addressing whether the COVID-19 crisis reduced the Free Tropospheric ozone across the Northern Hemisphere and the IARC-FTIR measurements at Izaña Observatory contributed to this study (for further details see Section 5.3.5).

In the framework of IZO activities as a WMO Commission on Infrastructure, Testbed for Aerosols and Water Vapour

Remote Sensing Instruments, the first long-term time series (1-year) of aerosol properties generated consistently in the NIR and SWIR ranges from ground-based FTIR spectrometry have been developed (Barreto et al., 2020). The new aerosol dataset has shown the enhanced multi-parameter capability of the FTIR technique for atmospheric monitoring (simultaneous trace gas and aerosol retrievals), providing important additional information to estimate the radiative effects of aerosols and trace gases on climate. Other remarkable activities within WMO-CIMO are related to the validation of new instrumentation for measuring water vapour content (e.g. ZEN radiometer, Almansa et al. 2020). For further details see Section 19.3.

7.3.2 Ground-based low-resolution FTIR spectrometry

The EM27/SUN spectrometer shares the same working principles as HR FTIR and, by covering the near infrared spectral range from 5000 to 11000 cm^{-1} with a spectral resolution of 0.5 cm^{-1} , it is able to measure total column-averaged amounts of O_2 , CO_2 , CH_4 , CO and H_2O . In the framework of the COCCON infrastructure, the performance of an ensemble of the 30 EM27/SUN spectrometers, including the IARC EM27/SUN, was recently tested and found to be very uniform (Frey et al., 2019a). The EM27/SUN instrument long-term stability and capability to provide very precise XCO_2 and XCH_4 observations by comparing to coincident TCCON HR FTIR spectrometers were confirmed.

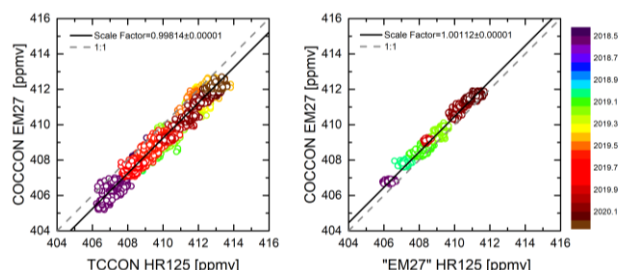


Figure 7.6. XCO_2 and XCH_4 comparison between EM27/SUN and TCCON observations at IZO (1-minute coincident pairs). The left and right panels correspond to the HR FTIR measurements taken with TCCON and EM27 configurations, respectively. The coloured bar denotes the acquisition time.

As an example, Fig. 7.6 displays the comparison of the coincident EM27/SUN and HR FTIR observations taken at IZO between 2018 and 2020 within COCCON activities. To analyze the impact of spectral resolution on retrieved data, the HR FTIR data were acquired using both the TCCON and EM27 configuration (with spectral resolution of 0.02 and 0.5 cm^{-1} , respectively).

MEGEI

COCCON EM27/SUN instruments are a useful complement to the existing TCCON HR network in remote areas as its data can be used for the quantification of local sinks/sources and fluxes of greenhouse gases. With this idea, the IARC is

leading the Spanish project, Monitoring greenhouse Gas EmIssions (MEGEI), to monitor greenhouse gas concentrations to evaluated fluxes in different environments by using the COCCON LR spectrometers. MEGEI activities are mainly focused on performing routine measurements at IARC IZO (background conditions) and SCO stations and in addition, on carrying out field campaigns under different atmospheric conditions.

In June 2019, the IARC EM27/SUN instrument participated in the “XIV Campaña Internacional de Calibración e Intercomparación de Instrumentos para la medida de Ozono Total y Radiación Solar Ultravioleta”, carried out in Arenosillo station (Huelva, Spain). This MEGEI activity was focused on identifying potential greenhouse gas hot-spots, taking observations under low surface albedo conditions (strongly required for satellite validation purposes), and testing the capability of EM27/SUN spectrometers to monitor ozone concentrations.

In addition, in September 2019, the second phase of the MEGEI-MAD experiment was carried out in the Madrid metropolitan area in order to characterise the CH₄ emission sources detected during the first MEGEI-MAD field campaign performed in 2018 (García et al., 2019b, c, d; Frey et al., 2019b). The methodology to quantify CH₄ emissions from waste disposal sites near the city of Madrid using ground- and space-based observations of COCCON, TROPOMI and IASI is described in Tu et al. (2022) for the first phase of the MEGEI-MAD campaign. Figure 7.7 displays the time series of XCO₂, XCH₄, XCO and XH₂O column averaged abundances observed by COCCON EM27/SUN spectrometers during the two phases of the MEGEI-MAD experiment in 2018 and 2019. During both campaigns, strong CH₄ plumes were detected around the Madrid urban area with increases by about 10% with respect to the regional background. These emissions are likely due to the combined impact of several waste treatment plants located in the surrounding Madrid area.

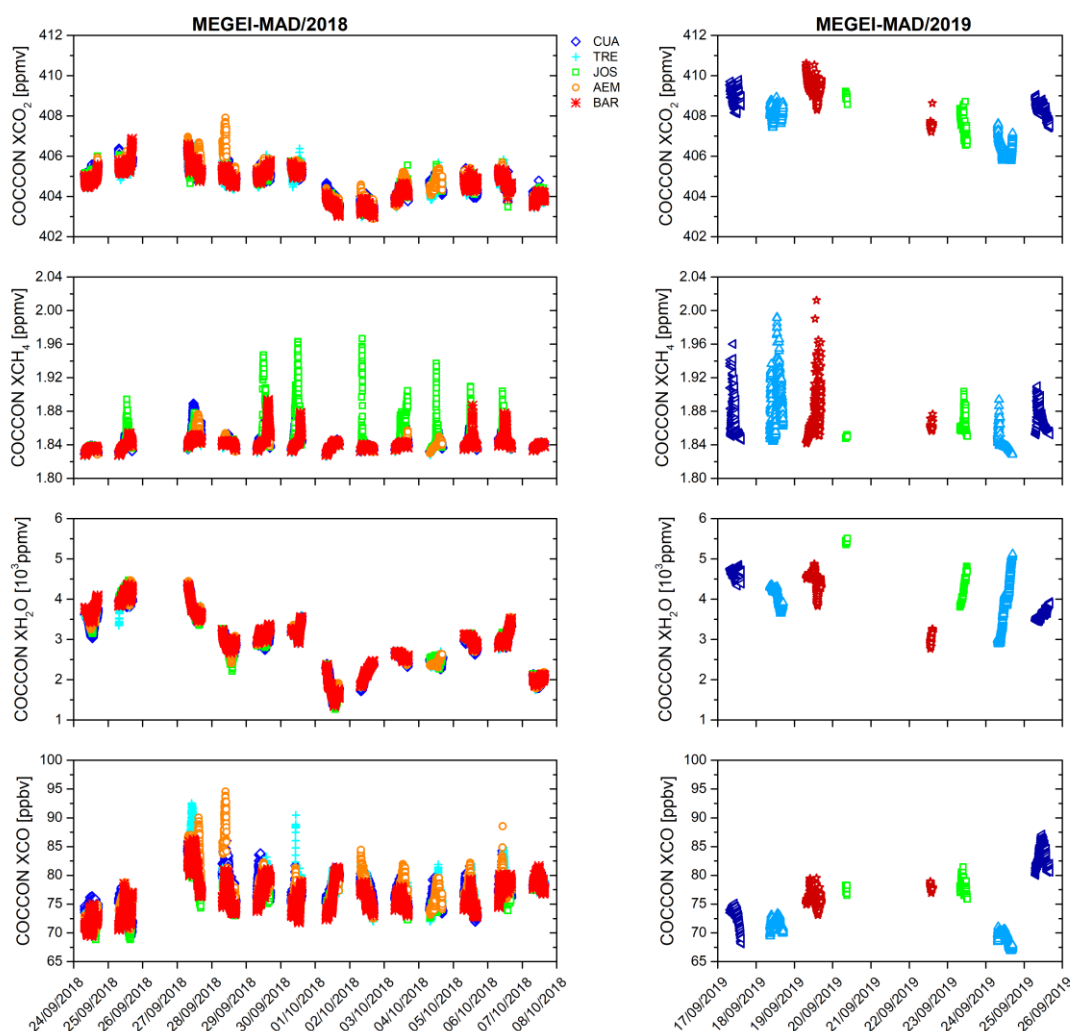


Figure 7.7. Time series of the total column-averaged abundances of carbon dioxide (XCO₂), methane (XCH₄), water vapour (XH₂O) and carbon monoxide (XCO), as observed by COCCON EM27/SUN spectrometers during MEGEI-MAD field campaigns in 2018 and 2019.

MAPP

In June 2020, the Metrology for aerosol optical properties (MAPP) project (19ENV04) started, supported by the European Metrology Programme for Innovation and Research (EMPIR). With a consortium of thirteen European organisations (AEMET-IARC among them), the overall goal of MAPP is to enable the SI-traceable measurement of column-integrated aerosol optical properties for assessing the radiative forcing impact on climate. These properties are retrieved from the passive remote sensing of the atmosphere using solar and lunar radiation measurements that are largely lacking traceability to the SI. A secondary objective is to evaluate the retrieval of aerosol optical properties from emerging technologies such as solar and lunar spectroradiometers. The IARC FTIR programme will contribute to this activity by developing the methodology required to retrieve aerosol properties from EM27/SUN instruments. For further details about MAPP project and the IARC contributions refer to Section 9 (Column Aerosols).

EIONET

To protect the integrity of the Paris Agreement, the European Union is currently elaborating a measurement-based system to independently monitor fossil fuel CO₂ emissions of nation states, large cities and even industrial complexes. The foreseen “Copernicus CO₂ Monitoring and Verification Support (MVS) capacity” constitutes a unique and unprecedented inverse modelling framework that will rely heavily on a space-based observation component (Matthews et al., 2020).

In this context, the European Environment Information and Observation Network (EIONET), supported by the European Environmental Agency (EEA), represents a relevant *in situ* network due to the CO₂ MVS capacity needed for urban measurement data on co-emitted species. The IARC FTIR programme, along with the Greenhouse Gas and Carbon Cycle programme, has participated in the “EIONET Group of Copernicus In Situ Data Experts” (Negotiated procedure No. EEA/IDM/R0/17/008, 2018-2020), which aims at advising and assisting the EEA regarding its cross-cutting coordination of the Copernicus In Situ Component. This EIONET expert group has examined how EIONET in its current form could be *exploited*, and how it could be *extended* to help contribute to needed urban *in situ* observation data to the Copernicus CO₂ MVS capacity, resulting in a technical report entitled “Report on how EIONET and EEA can contribute to the urban *in situ* requirements of a future Copernicus anthropogenic CO₂ observing system” (Matthews et al., 2020). This report furthermore examines *in situ* contribution opportunities for the EEA given the EEA’s responsibility for developing EIONET and for coordinating urban and non-GHG activities under the Copernicus programme.

7.3.3 Space-based FTIR spectrometry

The IARC’s high quality HR FTIR data have been extensively applied for many years for the validation of trace gases measured by different satellite instruments. During the period 2019-2020, particularly, IARC participated in the validation of HCHO, HCCOH, CH₃COOH, CH₄, CO₂, H₂O/HDO, and CO observations from space-based platforms like the TROPOMI, GOSAT, OCO-II, and MOPITT (Franco et al., 2019; Hedelius et al., 2019; Kivimäki et al., 2019; Kulawik et al., 2019; Röhling et al., 2019a, 2019b; Dogniaux et al., 2020; Schneider et al., 2020a; Sha et al., 2020a, 2020b; Vigouroux et al., 2020).

Within space-based FTIR spectrometry, the activities of the group are mainly focused on the Infrared Atmospheric Sounding Interferometer (IASI) on board MetOp/EUMETSAT satellites through the Spanish project INMENSE (IASI for surveying methane and nitrous oxide in the troposphere) and the German project MOTIV (MOisture Transport pathways and Isotopologues in water Vapour).

MOTIV

The MOTIV project aims at using water vapour isotopologues as a diagnostic tool to investigate moisture pathways and evaluate the representation of moist processes in weather and climate models. For this purpose, this project combines high-resolution IASI isotopologue observations, retrieved with the MUSICA processor (Schneider et al., 2016) with high-resolution modelling. The combination of simulations and MUSICA products provides insight into the diurnal cycle, small-scale variations and effects of large-scale circulation on the moisture in the atmosphere. Within MOTIV, the space-based isotopologue observations are complemented by the *in-situ* continuous measurements recorded at IZO and PTO since 2012.

INMENSE

The Spanish project INMENSE aims to improve understanding of the atmospheric budgets of two of the most important greenhouse gases, CH₄ and N₂O. Knowledge of the atmospheric CH₄ and N₂O distributions, from local to global scales, as well as their variability in time is essential for a better understanding of their sinks and sources, and for predicting their evolution in the atmosphere. In order to achieve this core objective, INMENSE has generated a new global observational data set of middle/upper tropospheric mole fractions of CH₄ and N₂O with high and well-documented quality by using the IASI processor developed during the project MUSICA. By integrating IASI observations and model estimates, INMENSE has investigated the kind of CH₄ and N₂O sink/source signals that can be captured by high-quality IASI observations (García et al., 2020). As an example, Figures 7.8 and 7.9 summarize the comparison between the IASI observations and MOCAGE (Modèle de Chimie Atmosphérique de

Grande Echelle) chemical transport simulations over the Iberian Peninsula for CH₄ and N₂O, for 2017, assessing the degree of agreement between both datasets. It is found that both data sets are not comparable in the lower troposphere. However, the new IASI products appear to capture the dynamics of the upper troposphere similarly to the MOCAGE simulations, which is in agreement with the experimental validation carried out with independent reference observations (García et al., 2018).

Within MOTIV and in collaboration with the INMENSE team, the potential synergetic use of IASI and TROPOMI space borne sensors for generating a tropospheric CH₄ profile product has been evaluated (Schneider et al., 2020b). The proposed method uses the output of the individual satellite retrievals and combines them a-posteriori in an

optimal sense. This approach is largely equivalent to applying thermal (TIR) and short-wave infrared (SWIR) spectra together in a single retrieval procedure, but with the substantial advantage of being applicable to any existing TIR and SWIR retrieval processor, of being very time efficient, and of benefiting from the high quality and most recent improvements of the specific TIR and SWIR retrievals. The combination of IASI and TROPOMI information can detect better the CH₄ tropospheric variations than those by IASI or TROPOMI observations alone. The resulting advantage has been documented theoretically as well as empirically by comparisons to independent free tropospheric in-situ reference data obtained within the frameworks of GAW, and NDACC and TCCON FTIR networks.

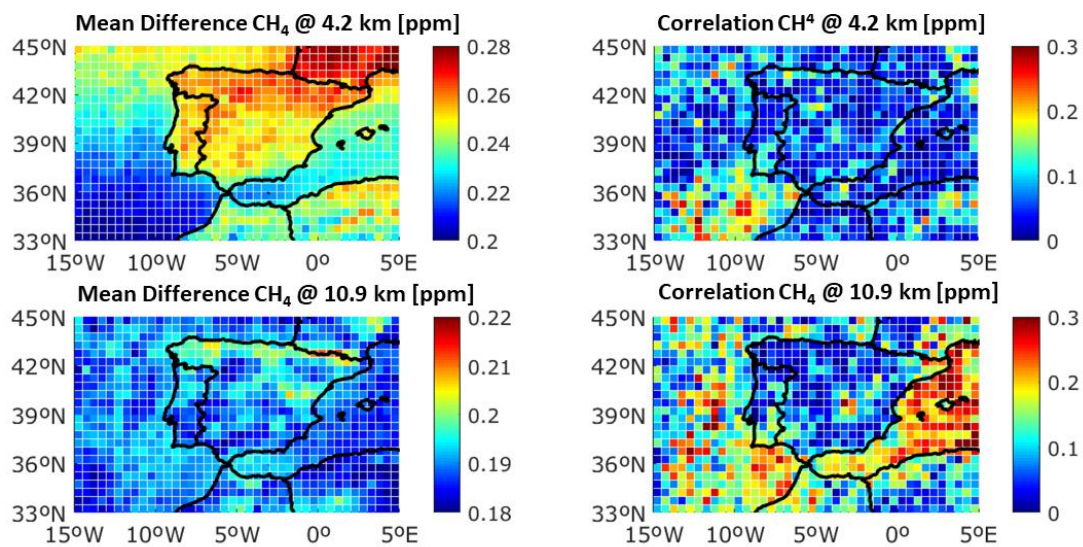


Figure 7.8. Mean difference for CH₄ mole fractions (IASI-MOCAGE, in ppm) in the free troposphere (at 4.2 km a.s.l.) and tropopause region (at 10.9 km a.s.l.) (left panels) and Pearson correlation between IASI and MOCAGE estimates at the same altitude levels (right panels) over the Iberian Peninsula. Reprinted from García et al. (2020).

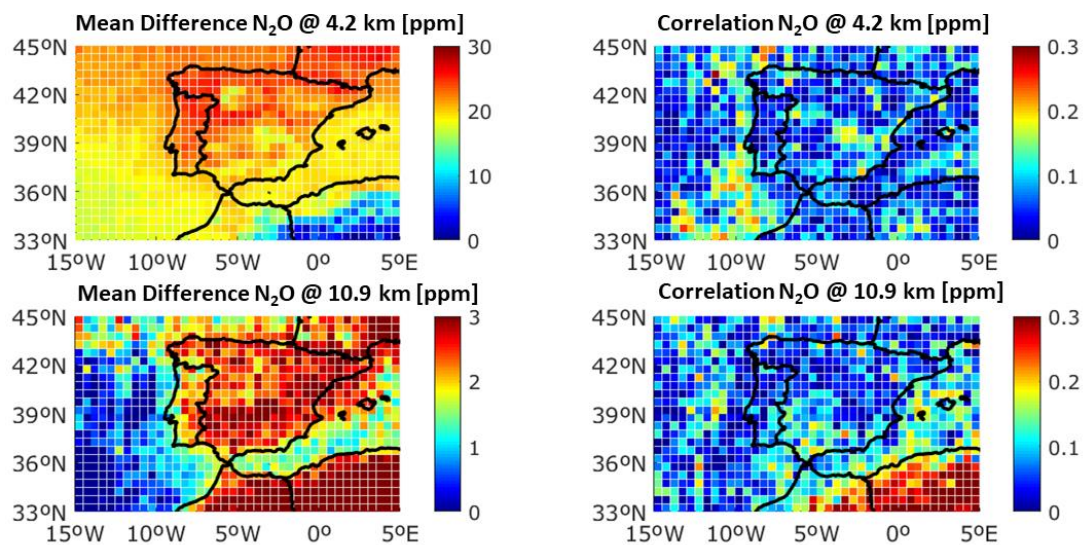


Figure 7.9. As for Figure 7.8, but for N₂O concentrations. Reprinted from García et al. (2020).

7.3.4 In situ spectrometry

Over the last two decades, the infrared laser spectroscopy technique has been successfully used to measure the isotopic composition of water vapour near the Earth's surface. In this context, Wei et al. (2019) presented for the first time the Stable Water Vapor Isotope Database (SWVID), which assembles a global database of high temporal resolution stable water vapour isotope ratios ($\delta^{18}\text{O}$ and δD) observed using this measurement technique. The database includes data collected at 35 sites in 15 Köppen climate zones from the years 2004 to 2017 (Figure 7.10), including the IARC IZO and PTO stations. To support interpretation of the isotopologue data, synchronized time series of standard meteorological variables from in situ observations and ERA5 reanalyses are also provided. The SWVID is intended to serve as a centralized platform allowing researchers to share their vapour isotope datasets, thus facilitating investigations that transcend disciplinary and geographic boundaries.

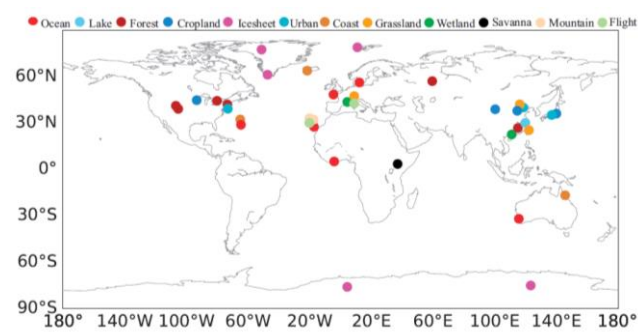


Figure 7.10. Map of SWVID measurement sites. Reprinted from Wei et al. (2019).

7.4 References

- Almansa, A.F.; Cuevas, E.; Barreto, Á.; Torres, B.; García, O.E.; Delia García, R.; Velasco-Merino, C.; Cachorro, V.E.; Berjón, A.; Mallorquín, M.; López, C.; Ramos, R.; Guirado-Fuentes, C.; Negrillo, R.; de Frutos, Á.M: Column Integrated Water Vapor and Aerosol Load Characterization with the New ZEN-R52 Radiometer, *Remote Sens.* 2020, 12, 1424.
- Barreto, Á.; García, O.E.; Schneider, M.; García, R.D.; Hase, F.; Sepúlveda, E.; Almansa, A.F.; Cuevas, E.; Blumenstock, T. Spectral Aerosol Optical Depth Retrievals by Ground-Based Fourier Transform Infrared Spectrometry. *Remote Sens.*, 12, 3148, 2020.
- Blumenstock, T., Hase, F., Keens, A., Czurlok, D., Colebatch, O., Garcia, O., Griffith, D. W. T., Grutter, M., Hannigan, J. W., Heikkinen, P., Jeseck, P., Jones, N., Kivi, R., Lutsch, E., Makarova, M., Imhasin, H. K., Mellqvist, J., Morino, I., Nagahama, T., Notholt, J., Ortega, I., Palm, M., Raffalski, U., Rettinger, M., Robinson, J., Schneider, M., Servais, C., Smale, D., Stremme, W., Strong, K., Sussmann, R., Té, Y., and Velazco, V. A.: Characterization and potential for reducing optical resonances in Fourier transform infrared spectrometers of the Network for the Detection of Atmospheric Composition Change (NDACC), *Atmos. Meas. Tech. Discuss.*, <https://doi.org/10.5194/amt-2020-316>, 2020.
- Dogniaux, M., Crevoisier, C., Armante, R., Capelle, V., Delahaye, T., Cassé, V., De Mazière, M., Deutscher, N. M., Feist, D. G., Garcia, O. E., Griffith, D. W. T., Hase, F., Iraci, L. T., Kivi, R., Morino, I., Notholt, J., Pollard, D. F., Roehl, C. M., Shiomi, K., Strong, K., Té, Y., Velazco, V. A., and Warneke, T.: The Adaptable 4A Inversion (SAI): Description and first XCO₂ retrievals from OCO-2 observations, *Atmos. Meas. Tech. Discuss.*, <https://doi.org/10.5194/amt-2020-403>, 2020.
- Dubravica, D., M. Frey, F. Hase, T. Blumenstock, J. Orphal, and the COCCON team, The Collaborative Carbon Column Observing Network (COCCON): Current status, *Geophysical Research Abstracts Vol. 21, EGU2019-9754*, EGU General Assembly, Vienna (Austria), 7-12 April, 2019.
- Franco, B., Clarisse, L., Stavrakou, T., Müller, J.-F., Taraborrelli, D., Hadji-Lazaro, J., et al. (2020). Spaceborne measurements of formic and acetic acids: A global view of the regional sources. *Geophysical Research Letters*, 47, e2019GL086239. <https://doi.org/10.1029/2019GL086239>, 2019.
- Frey, M., Sha, M. K., Hase, F., Kiel, M., Blumenstock, T., Harig, R., Surawicz, G., Deutscher, N. M., Shiomi, K., Franklin, J. E., Bösch, H., Chen, J., Grutter, M., Ohya, H., Sun, Y., Butz, A., Mengistu Tsidu, G., Ene, D., Wunch, D., Cao, Z., Garcia, O., Ramonet, M., Vogel, F., and Orphal, J.: Building the Collaborative Carbon Column Observing Network (COCCON): long-term stability and ensemble performance of the EM27/SUN Fourier transform spectrometer, *Atmos. Meas. Tech.*, 12, 1513-1530, <https://doi.org/10.5194/amt-12-1513-2019a>.
- Frey, M., Hase, F., Blumenstock, T., Orphal, J., Vogel, F., Stauffer, J., Broquet, G., Ciais, P., Xueref-Remy, I., Chelin, P., Te, Y., Garcia, O., Sepúlveda, E., Ramos, R., Torres, C., Leon, S., Cuevas, E., Butz, A., Schneider, C., and the COCCON Paris team, The COCCON city campaigns: Monitoring greenhouse gas emissions of Paris and Madrid, *Geophysical Research Abstracts Vol. 21, EGU2019-5197*, EGU General Assembly, Vienna (Austria), 7-12 April, 2019b.
- García, O. E., Schneider, M., Redondas, A., González, Y., Hase, F., Blumenstock, T., and Sepúlveda, E.: Investigating the long-term evolution of subtropical ozone profiles applying ground-based FTIR spectrometry, *Atmos. Meas. Tech.*, 5, 2917-2931, [doi:10.5194/amt-5-2917-2012](https://doi.org/10.5194/amt-5-2917-2012), 2012.
- García, O. E., Schneider, M., Ertl, B., Sepúlveda, E., Borger, C., Diekmann, C., Wiegele, A., Hase, F., Barthlott, S., Blumenstock, T., Raffalski, U., Gómez-Peláez, A., Steinbacher, M., Ries, L., and de Frutos, A. M.: The MUSICA IASI CH₄ and N₂O products and their comparison to HIPPO, GAW and NDACC FTIR references, *Atmos. Meas. Tech.*, 11, 4171-4215, <https://doi.org/10.5194/amt-11-4171-2018>, 2018.
- García, O., M. Schneider, E. Sepúlveda, F. Hase, T. Blumenstock, E. Cuevas, A.J. Gómez-Peláez, R.D. García, E. Reyes, R. Ramos, A. Redondas, V. Carreño, S.F. León-Luis, P.M. Romero-Campos, M. Navarro, M. Yela, 20 years of Fourier Transform Spectrometry at the Izaña Atmospheric Observatory, 2019 Joint NDACC-IRWG and TCCON Meeting, Wanaka, New Zealand, 20th-24th May, 2019a.
- García, O., E. Sepúlveda, J.-A. Morgui, C. Estruch, R. Curcoll, M. Frey, C. Schneider, R. Ramos, C. Torres, S.F. León-Luis, F. Hase, A. Butz, C. Toledano, E. Cuevas, T. Blumenstock, C. Marrero, J.J. Bustos, J. López-Solano, V. Carreño, C. Pérez García-Pando, M. Guevara, O. Jorba, Monitoring of Urban Greenhouse Gases Emissions combining COCCON EM27 spectrometers and in-situ records (MEGEI-MAD), 2019 Joint

- NDACC-IRWG and TCCON Meeting, Wanaka, New Zealand, 20th-24th May, 2019b.
- García, O., J.-A. Morgui, R. Curcoll, C. Estruch, E. Sepúlveda, R. Ramos, E. Cuevas, Characterizing methane emissions in Madrid City within the MEGEI-MAD project: the temporal and spatial ground-based mobile approach, 8th International Symposium on Non-CO₂ Greenhouse Gases (NCGG8), Amsterdam (The Netherlands), June 12-14, 2019c.
- García, O., Sepúlveda, E., Morgui, J.A., Frey, M., Schneider, C., Curcoll, R., Estruch, C., Ramos, R., Torres, C., León, S., Hase, F., Butz, A., Toledano, C., Cuevas, E., Blumenstock, T., Pérez, C., Guevara, M., Jorba, O., Marrero, C., Bustos, J.J., López-Solano, J., Romero-Campos, P.M., Medida de las Concentraciones de Gases de Efecto Invernadero en Madrid (MEGEI-MAD), XVIII Congreso de la Asociación Española de Teledetección, Valladolid (Spain), 24-27 September, 2019d.
- García, O., Schneider, M., Ertl, B., Sepúlveda, E., Borger, C., Diekmann, C., Hase, F., Krosraw, F., Cansado, A., and Allué, M.: Monitoring of atmospheric methane and nitrous oxide concentrations from Metop/IASI. *Revista de Teledetección*, [S.l.], n. 57, p. 1-11, ISSN 1988-8740, doi:<https://doi.org/10.4995/raet.2020.13290>, 2020.
- Gisi, M., F. Hase, S. Dohe, and T. Blumenstock: Camtracker: a new camera controlled high precision solar tracker system for FTIR-spectrometers, *Atmos. Meas. Tech.*, 4, 47-54, 2011.
- González, Y., Schneider, M., Dyroff, C., Rodríguez, S., Christner, E., García, O. E., Cuevas, E., Bustos, J. J., Ramos, R., Guirado-Fuentes, C., Barthlott, S., Wiegeler, A., and Sepúlveda, E.: Detecting moisture transport pathways to the subtropical North Atlantic free troposphere using paired H₂O- δ D in situ measurements, *Atmos. Chem. Phys.*, 16, 4251-4269, doi:[10.5194/acp-16-4251-2016](https://doi.org/10.5194/acp-16-4251-2016), 2016.
- Hase, F., T. Blumenstock, C. Paton-Walsh: Analysis of the instrumental line shape of high-resolution Fourier transform IR spectrometers with gas cell measurements and new retrieval software, *Appl. Opt.* 38, 3417-3422, 1999.
- Hase, F., J.W. Hannigan, M.T. Coffey, A. Goldman, M. Höpfner, N.B. Jones, C.P. Rinsland, S.W. Wood: Intercomparison of retrieval codes used for the analysis of high-resolution, ground-based FTIR measurements, *Journal of Quantitative Spectroscopy & Radiative Transfer* 87, 25-52, 2004.
- Hedelius, J. K., He, T.-L., Jones, D. B. A., Baier, B. C., Buchholz, R. R., De Mazière, M., Deutscher, N. M., Dubey, M. K., Feist, D. G., Griffith, D. W. T., Hase, F., Iraci, L. T., Jeseck, P., Kiel, M., Kivi, R., Liu, C., Morino, I., Notholt, J., Oh, Y.-S., Ohyama, H., Pollard, D. F., Rettinger, M., Roche, S., Roehl, C. M., Schneider, M., Shiomu, K., Strong, K., Sussmann, R., Sweeney, C., Té, Y., Uchino, O., Velasco, V. A., Wang, W., Warneke, T., Wennberg, P. O., Worden, H. M., and Wunch, D.: Evaluation of MOPITT Version 7 joint TIR-NIR XCO retrievals with TCCON, *Atmos. Meas. Tech.*, 12, 5547-5572, <https://doi.org/10.5194/amt-12-5547-2019>, 2019.
- Kivimäki, E.; Lindqvist, H.; Hakkarainen, J.; Laine, M.; Sussmann, R.; Tsuruta, A.; Detmers, R.; Deutscher, N.M.; Dlugokencky, E.J.; Hase, F.; Hasekamp, O.; Kivi, R.; Morino, I.; Notholt, J.; Pollard, D.F.; Roehl, C.; Schneider, M.; Sha, M.K.; Velasco, V.A.; Warneke, T.; Wunch, D.; Yoshida, Y.; Tamminen, J. Evaluation and Analysis of the Seasonal Cycle and Variability of the Trend from GOSAT Methane Retrievals. *Remote Sens.*, 11, 882. <https://doi.org/10.3390/rs11070882>, 2019.
- Kulawik, S. S., Crowell, S., Baker, D., Liu, J., McKain, K., Sweeney, C., Biraud, S. C., Wofsy, S., O'Dell, C. W., Wennberg, P. O., Wunch, D., Roehl, C. M., Deutscher, N. M., Kiel, M., Griffith, D. W. T., Velasco, V. A., Notholt, J., Warneke, T., Petri, C., De Mazière, M., Sha, M. K., Sussmann, R., Rettinger, M., Pollard, D. F., Morino, I., Uchino, O., Hase, F., Feist, D. G., Roche, S., Strong, K., Kivi, R., Iraci, L., Shiomu, K., Dubey, M. K., Sepúlveda, E., García Rodríguez, O. E., Té, Y., Jeseck, P., Heikkinen, P., Dlugokencky, E. J., Gunson, M. R., Eldering, A., Crisp, D., Fisher, B., and Osterman, G. B.: Characterization of OCO-2 and ACOS-GOSAT biases and errors for CO₂ flux estimates, *Atmos. Meas. Tech. Discuss.*, <https://doi.org/10.5194/amt-2019-257>, 2019.
- Matthews, B., O. E. García, E. Cuevas, W. Spangl, and P. Castro: Report on how EIONET and EEA can contribute to the urban in situ requirements of a future Copernicus anthropogenic CO₂ observing system, European Environment Agency (EEA) – Negotiated procedure No EEA/IDM/R0/17/008, 2020.
- Röhling, N. A., T. Blumenstock, U. Cayoglu, O. E. Garcia, F. Hase, T. Kerzenmacher, U. Raffalski, and E. Sepúlveda, Validation of Tropomi/Sentinel-5 Precursor Satellite Data Using Time Series of Ground-Based FTIR Sites at Different Latitudes, ESA S5P Validation Team Meeting, Frascati (Italy), 12 November 2019.
- Röhling, N. A., Hase, F., Raffalski, U., Garcia, O.E., Sepúlveda, E. and Blumenstock, T., Evaluation of Trace Gases Using Time Series of Ground-Based FTIR Observations for the Validation of Tropomi/Sentinel-5 Precursor Satellite Data, Living Planeta Symposium, ESA, Milan (Italy), 13-17 May 2019.
- Schneider, A., Borsdorff, T., van de Brugh, J., Aemisegger, F., Feist, D. G., Kivi, R., Hase, F., Schneider, M., and Landgraf, J.: First data set of H₂O/HDO columns from the Tropospheric Monitoring Instrument (TROPOMI), *Atmos. Meas. Tech.*, 13, 85-100, <https://doi.org/10.5194/amt-13-85-2020>, 2020a.
- Schneider, M., Diekmann, C., Ertl, B., Khosrawi, F., Röhling A., Hase, F., García, O.E., Sepúlveda, E., Landgraf, J., Meinhardt, F., Steinbacher, M., Synergetic use TROPOMI and IASI for generating a tropospheric CH₄ product, 16th international workshop on greenhouse gas measurements from space, online meeting, 2-5 June, 2020b.
- Schneider, M., A. Redondas, F. Hase, C. Guirado, T. Blumenstock, and E. Cuevas: Comparison of ground-based Brewer and FTIR total O₃ monitoring techniques, *Atmos. Chem. Phys.*, 8, 5535-5550, 2008.
- Schneider, M., P. M. Romero, F. Hase, T. Blumenstock, E. Cuevas, and R. Ramos: Continuous quality assessment of atmospheric water vapour measurement techniques: FTIR, Cimel, MFRSR, GPS, and Vaisala RS92, *Atmos. Meas. Tech.*, 3, 323-338, 2010.
- Schneider, M., Wiegeler, A., Barthlott, S., González, Y., Christner, E., Dyroff, C., García, O. E., Hase, F., Blumenstock, T., Sepúlveda, E., Mengistu Tsidu, G., Takele Kenea, S., Rodríguez, S., and Andrey, J.: Accomplishments of the MUSICA project to provide accurate, long-term, global and high-resolution observations of tropospheric {H₂O, δ D} pairs – a review, *Atmos. Meas. Tech.*, 9, 2845-2875, doi:[10.5194/amt-9-2845-2016](https://doi.org/10.5194/amt-9-2845-2016), 2016.
- Sepúlveda, E., Schneider, M., Hase, F., García, O. E., Gomez-Pelaez, A., Dohe, S., Blumenstock, T., and Guerra, J. C.: Long-term validation of total and tropospheric column-averaged CH₄ mole fractions obtained by mid-infrared ground-based FTIR spectrometry, *Atmos. Meas. Tech.*, 5, 1425-1441, doi:[10.5194/amt-5-1425-2012](https://doi.org/10.5194/amt-5-1425-2012), 2012.
- Sha, M.K., Bavo Langerock, M. De Mazière, Minqiang Zhou, Yang Yang, D. G. Feist, R. Sussmann, F. Hase, M. Schneider,

- T. Blumenstock, J. Notholt, T. Warneke, C. Petri, R. Kivi, Y. Té, P. O. Wennberg, D. Wunch, L. Iraci, K. Strong, D. W. T. Griffith, N.M. Deutscher, V. Velazco, I. Morino, H. Ohyama, O. Uchino, K. Shiomi, T. Y. Goo, D. F. Pollard, Pucal Wang, T. Borsdorff, H. Hu, O. Hasekamp, J. Landgraf, C. Roehl, M. Kiel, G. Toon, TCCON team & NDACC-IRWG team, Validation results of S-5P methane and carbon monoxide products using TCCON and NDACC-IRWG data, 2020 Joint NDACC-IRWG and TCCON Meeting, online meeting, 12-14 May 2020.
- Sha, M.K., Bavo Langerock, Martine De Mazière, Dietrich G. Feist, Ralf Sussmann, Frank Hase, Matthias Schneider, Thomas Blumenstock, Justus Notholt, Thorsten Warneke, Rigel Kivi, Yao Té, Paul O. Wennberg, Debra Wunch, Laura Iraci, Kimberly Strong, David W. T. Griffith, Nicholas M. Deutscher, Voltaire Velazco, Isamu Morino, Hirofumi Ohyama, Osamu Uchino, Kei Shiomi, Tae-Young Goo, David F. Pollard, Minqiang Zhou, Yang Yang, Pucal Wang, Alba Lorente, Haili Hu, Tobias Borsdorff, Otto Hasekamp, Jochen Landgraf, Coleen Roehl, Matthäus Kiel, Geoffrey Toon and TCCON and NDACC-IRWG team, Lessons learned from 2.5 years of Sentinel-5P methane validation using global TCCON and NDACC-IRWG data, 16th international workshop on greenhouse gas measurements from space, online meeting, 2-5 June 2020.
- Steinbrecht, W., Kubistin, D., Plass-Dulmer, C., Tarasick, D.W., Davies, J., Gathen, P.V., Deckelmann, H., Jepsen, N., Kivi, R., Lyall, N., Palm, M., Notholt, J., Kois, B., Oelsner, P., Allaart, M., PETERS, A., Gill, M., Malderen, R.V., Delcloo, A.W., Sussmann, R., Mahieu, E., Servais, C., Romanens, G., Stubi, R., Ancellet, G., Godin-Beekmann, S., Yamanouchi, S., Strong, K., Johnson, B., Cullis, P., Petropavlovskikh, I., Hannigan, J., Hernandez, J.L., Rodriguez, A.D., Nakano, T., Chouza, F., Leblanc, T., Torres, C., Garcia, O., Rohling, A., Schneider, M., Blumenstock, T., Tully, M., Jones, N., Querel, R., Strahan, S., Inness, A., Engelen, R., Chan, K.L., Cooper, O.R., Stauffer, R.M., Thompson, A.M., Did the COVID-19 Crisis Reduce Free Tropospheric Ozone across the Northern Hemisphere?, Earth and Space Science Open Archive, 20, doi:10.1002/essoar.10505226.1, <https://doi.org/10.1002/essoar.10505226.1>, 2020.
- Strahan, S. E., Smale, D., Douglass, A. R., Blumenstock, T., Hannigan, J. W., Hase, F., Jones, N., Mahieu, E., Notholt, J., Oman L.D., Ortega, I., Palm, M., Prignon, M., Robinson, J., Schneider, M., Sussmann, R. and Velazco, V.A. Observed hemispheric asymmetry in stratospheric transport trends from 1994 to 2018. *Geophysical Research Letters*, 47, <https://doi.org/10.1029/2020GL088567>, 2020.
- Tarasick, D., Galbally, I.E., Cooper, O.R., Schultz, M.G., Ancellet, G., Leblanc, T., Wallington, T.J., Ziemke, J., Liu, X., Steinbacher, M., Staehelin, J., Vigouroux, C., Hannigan, J.W., García, O., Foret, G., Zanis, P., Weatherhead, E., Petropavlovskikh, I., Worden, H., Osman, M., Liu, J., Chang, K.-L., Gaudel, A., Lin, M., Granados-Muñoz, M., Thompson, A.M., Oltmans, S.J., Cuesta, J., Dufour, G., Thouret, V., Hassler, B., Trickl, T. and Neu, J.L., 2019. Tropospheric Ozone Assessment Report: Tropospheric ozone from 1877 to 2016, observed levels, trends and uncertainties. *Elem Sci Anth*, 7(1), p.39. DOI: <http://doi.org/10.1525/elementa.376>, 2019.
- Tu Q., Hase, F., Schneider, M., García, O., Blumenstock, T., Borsdorff, T., Frey, M., Khosrawi, F., Lorente, A., Alberti, C., Bustos, J. J., Butz, A., Carreño, V., Cuevas, E., Curcoll, R., Diekmann, C. J., Dubravica, D., Ertl, B., Estruch, C., León-Luis, S. F., Marrero, C., Morgui, J.-A., Ramos, R., Scharun, C., Schneider, C., Sepúlveda, E., Toledano, C., and Torres, C.: Quantification of CH₄ emissions from waste disposal sites near the city of Madrid using ground- and space-based observations of COCCON, TROPOMI and IASI, *Atmos. Chem. Phys.*, 22, 295–317, <https://doi.org/10.5194/acp-22-295-2022>, 2022.
- Wei, Z., X. Lee, F. Aemisegger, M. Benetti, M. Berkelhammer, M. Casado, K. Caylor, E. Christner, C. Dyroff, O. García, Y. González, T. Griffis, N. Kurita, J. Liang, M.-C. Liang, G. Lin, D. Noone, K. Gribanov, N. C. Munksgaard, M. Schneider, F. Ritter, H. C. Steen-Larsen, C. Vallet-Coulomb, X. Wen, J. S. Wright, W. Xiao, and K. Yoshimura: A global database of water vapor isotopes measured with high temporal resolution infrared laser spectroscopy, *Scientific Data* volume6, Article number: 180302, doi.org/10.1038/sdata.2018.302, 2019.
- Vigouroux, C., Langerock, B., Bauer Aquino, C. A., Blumenstock, T., Cheng, Z., De Mazière, M., De Smedt, I., Grutter, M., Hannigan, J., Jones, N., Kivi, R., Loyola, D., Lutsch, E., Mahieu, E., Makarova, M., Metzger, J.-M., Morino, I., Murata, I., Nagahama, T., Notholt, J., Ortega, I., Palm, M., Pinardi, G., Röhling, A., Smale, D., Stremme, W., Strong, K., Sussmann, R., Té, Y., van Roozendael, M., Wang, P., and Winkler, H.: TROPOMI–Sentinel-5 Precursor formaldehyde validation using an extensive network of ground-based Fourier-transform infrared stations, *Atmos. Meas. Tech.*, 13, 3751–3767, <https://doi.org/10.5194/amt-13-3751-2020>, 2020.
- Zhou, M., Langerock, B., Vigouroux, C., Sha, M. K., Hermans, C., Metzger, J.-M., Chen, H., Ramonet, M., Kivi, R., Heikkinen, P., Smale, D., Pollard, D. F., Jones, N., Velazco, V. A., García, O. E., Schneider, M., Palm, M., Warneke, T., and De Mazière, M.: TCCON and NDACC XCO measurements: difference, discussion and application, *Atmos. Meas. Tech.*, 12, 5979–5995, <https://doi.org/10.5194/amt-12-5979-2019>, 2019a.
- Zhou, M., Langerock, B., Wells, K. C., Millet, D. B., Vigouroux, C., Sha, M. K., Hermans, C., Metzger, J.-M., Kivi, R., Heikkinen, P., Smale, D., Pollard, D. F., Jones, N., Deutscher, N. M., Blumenstock, T., Schneider, M., Palm, M., Notholt, J., Hannigan, J. W., and De Mazière, M.: An intercomparison of total column-averaged nitrous oxide between ground-based FTIR TCCON and NDACC measurements at seven sites and comparisons with the GEOS-Chem model, *Atmos. Meas. Tech.*, 12, 1393–1408, <https://doi.org/10.5194/amt-12-1393-2019>, 2019b.

7.5 Staff and collaborators

The FTIR research group (listed below) is composed of researchers and specialist technicians from IARC-AEMET, from IMK-ASF-KIT, and from GOA-UVA:

Dr Omaira García (AEMET; Head of programme)

Dr Eliezer Sepúlveda (AEMET; Research Scientist) left IARC in 2020

Dr Sergio León-Luis (TRAGSATEC, Research Scientist)

Ramón Ramos (AEMET; Head of Infrastructure)

Dr Matthias Schneider (IMK-ASF-KIT; Head of the MUSICA group)

Dr Thomas Blumenstock (IMK-ASF-KIT; Head of Ground-based remote-sensing using Fourier-transform interferometers (BOD) group)

Dr Frank Hase (IMK-ASF-KIT; Research Scientist, BOD group)

Dr Matthias Frey (IMK-ASF-KIT; Research Scientist, BOD group)

8 In situ Aerosols

8.1 Main Scientific Goals

Atmospheric aerosol is composed of a mixture of natural (e.g. sea salt, desert dust or biogenic material) and anthropogenic (e.g. soot, industrial sulphate, nitrate, metals or combustion linked carbonaceous matter) airborne particles whose size range from a few nanometres (nm) to tens of microns (μm). Aerosols contribute to deterioration of air quality with impacts on human health due to cardiovascular, cerebrovascular and respiratory diseases such as asthma and chronic obstructive pulmonary disease; they also influence climate by scattering and absorbing radiation and by influencing cloud formation and rainfall.

The activities of the In situ Aerosols programme (AIS group, *Aerosol In-Situ*) are developed within the scientific priorities of the Global Atmosphere Watch programme. One of the main tasks of this group is to maintain the long-term observations of aerosols at IZO. The group focuses its research on: 1) Long-term multi-decadal variability and trends of aerosols; 2) Aerosols and climate interaction and 3) Aerosols and air quality interaction.

8.2 Measurement Programme

The long-term in situ aerosols observation program of Izaña Observatory includes measurements of aerosol mass and number concentration, chemical composition, size distribution and optical properties by in-situ techniques. Instruments are placed in the so-called Aerosols Research Laboratory (ARL) renamed as the Joseph M. Prospero Aerosols Research Laboratory, as a tribute to the pioneer of dust research, in 2016 (Fig. 8.1). The laboratory is equipped with a whole air inlet for aerosol sampling for the on-line analysers (CPCs, SMPS, APS, MAAP, aethalometer, nephelometer), two additional PM_{10} and $\text{PM}_{2.5}$ inlets for the aerosol filter samplers and also two additional inlets for TEOM (PM_{10} and $\text{PM}_{2.5}$) and BETA (PM_{10}) analysers respectively. The interior of the Aerosols Research Laboratory is maintained at 22 °C. Driers are not needed during the sampling because of the low relative humidity (RH) of the outdoor ambient air (RH percentiles 25th, 50th and 75th are 15%, 31% and 55%, respectively). Measurements of number concentration, size distribution and optical properties of aerosols are performed with high time resolution (Table 3.2).

Despite the adverse circumstances due to the COVID crisis, and the resulting restrictions, the operation in the laboratory has remained practically unchanged.



Figure 8.1. Joseph M. Prospero Aerosols Research Laboratory at Izaña Observatory (upper panel: building; lower panel: C. Bayo, operator of the AIS group working in the ARL).

For the automatic instruments in the aerosol laboratory, the QA/QC activities include:

- <daily checks> of the data and status of the instruments.
- <weekly checks> of the airflows and leak tests for some instruments (e.g. SMPS).
- <quarterly checks> includes measurements of the instrumental zero (24h filtered air) for all the instruments (CPCs, SMPS, APS, MAAP, aethalometer nephelometer) and calibration checks (e.g. nephelometer).
- <annual intercomparisons> for some instruments.
- participation in intercomparisons, e.g. those performed annually between 2010 and 2012 for CPCs and SPMS at El Arenosillo - Huelva (Gómez-Moreno et al., 2015) and those in the World Calibration Centre for Aerosols Physics (WCCAP) in Leipzig – Germany for CPCs (Sep 2012) and absorption photometers (Nov 2005; Müller et al., 2011).
- <regular> calibration of the instruments at the WCCAP. In October 2017, the instruments of the ARL (SMPS, CPCs, MAAPs, nephelometer and aethalometer) were recalibrated at the WCCAP. All devices obtained the calibration certificate.

These activities follow the recommendations of the GAW programme for aerosols (GAW Report n°227, 2016).

During 2019 and 2020 a dedicated internal database for all aerosol in-situ parameters measured at ARL was developed and improved. This database is particularly useful with respect to the annual reporting of data to the GAW World Data Centre for Aerosols (WDCA). During the 2019-2020 period, R-routines have been developed for reporting aerosol scattering (nephelometer) and absorption (MAAP) PM₁₀ data.

In addition, this database is useful for monitoring in real-time the performance of the instruments, detection of special events, etc. A series of GRAFANA® panels (an open-source analytics and monitoring tool for visualization of data in databases) were designed to this purpose.

The aerosols chemical composition programme is based on:

- the collection of aerosol samples on filters. Samples are collected at night to avoid the diurnal upslope winds that may bring material from the boundary layer,
- the determination of the aerosol mass concentrations by the gravimetric method. Filters are weighed, before and after sampling, at 20 °C temperature and 30-35 % relative humidity in the Aerosol Filters Laboratory of the Izaña Atmospheric Research Centre (see Section 3.1.4). The procedure for weighing filters is similar to that described in EN-14907, except that we use a lower relative humidity (30-35 %) due to the relative humidity of the ambient air at IZO being much lower than the 50% stated by EN-14907.
- the determination of chemical composition which currently includes elemental composition (those detected by IPC-AES, i.e. Al, Ca, Fe, Mg, K, Na,...), salts (SO₄²⁻, NO₃⁻, NH₄⁺, Cl⁻), organic carbon, elemental carbon and trace elements (those detected by IPC-MS, i.e. P, V, Ni, Cd, As, Sb, Sn,...).

The QA/QC procedure for the aerosol chemical composition programme includes:

- airflow checks and calibrations.
- the collection of blank field filters for gravimetry and chemical analysis.
- intercomparison exercises.

The IARC Aerosol In-Situ group has participated in the ACTRIS data QA and submission workshop, held online during 15-17 September 2020 to get the most out of the data and to make it available to the scientific community.

The AIS group is also responsible for the measurements of different passive samplers, for mercury and persistent organic pollutants. These programmes are led by the Environment and Climate Change Canada and the Spanish National Research Council (CSIC).

8.3 Summary of remarkable results during the period 2019-2020

During the 2019-2020 biennium, the scientific activities of the In situ Aerosols group were focused in finalizing results of the AEROATLAN project (CGL2015-66299-P, funded by the Ministry of Economy and Competitiveness of Spain and the European Regional Development Fund), and continuing the research activities on dust and the transatlantic transport of aerosols with implications for climate. International cooperation has allowed the group to enter the emerging field of PM_x-Low Cost Sensors (Peltier et al., WMO Report N°1215, 2021), testing some of them with the aim of providing the best cost-performance option to the CREWS (Climate Risk and Early Warning System) West Africa project and MAC-CLIMA initiatives (Madeira-Azores-Canarias-CLIMA). Further details are given in Section 17.5.4 (Sand and Dust Storms Centres). Contributions to wider studies based on data regularly reported to WDCA continued, these results are presented in the next section.

8.3.1 Focus on Dust Research

In the framework of the AEROATLAN project, a study about rapid changes of dust geochemistry in the Saharan Air Layer linked to sources and meteorology was published (Rodríguez et al., 2020).

In this study, 1-hour resolution measurements of elemental composition of dust in the Saharan Air Layer were performed. Rapid variations of dust composition were observed (ratios of elemental composition of dust to aluminium); some elemental ratios changed by a factor 2 in a few (5–8) hours. This variability was induced by the meteorologically modulated, alternating contributions of three of the large North African dust sources: NE Algeria (rich in evaporite minerals bearing Ca, S, Sr, K and Mg and in illite mineral), Western Sahara to Bechar region (containing Na, S and Cl rich Yermosol soils) and SW Sahara – Western Sahel (rich in illite and hematite).

The changes in large-scale meteorology were traced by using the North African Dipole Intensity (NAFDI), i.e. the strength of the subtropical North African high, at Morocco, to the monsoon tropical low at Nigeria (Rodríguez et al., 2015). The change of phase of NAFDI, from negative to positive, is associated with westward propagating Harmattan pulses, the associated westward shifts of the Saharan Heat Low and convection, including processes embedded within the monsoon inflow. This resulted in the alternated activation and export of dust from the different sources and a correlation between NAFDI and dust composition was found. Moderate values of NAFDI (0 to +2.5) are associated with Ca, K, Na, Mg and S rich dust (linked to Northern Sahara sources) in the Atlantic Saharan Air Layer (SAL), higher NAFDI values (+2.5 to +4) are associated with Fe rich dust in the SAL (linked to Southern

Sahara), whereas negative values of NAFDI promoted (Ca, K, Na, Mg and S rich) dust export to the Mediterranean (Figure 8.2).

This study also shows that trace metals (Br, Cr, Ni, Zn and Zr) of industrial emissions in North Africa are transported with dust in the Saharan Air Layer.

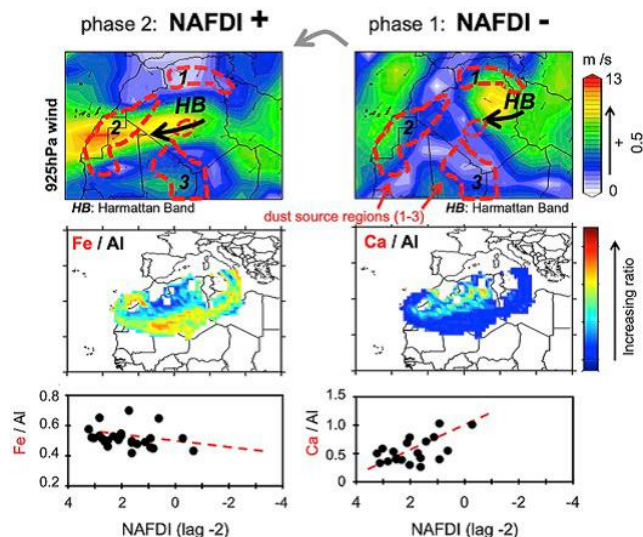


Figure 8.2. NAFDI phase and elemental ratios associated with different dust sources. Reprinted from Rodríguez et al. (2020).

8.3.2 Focus on transatlantic transport of aerosols

As a result of the AEROATLAN project, an article about tracking the changes of iron solubility and air pollutants traces as African dust transits the Atlantic in the Saharan dust outbreaks was published (Rodríguez et. al., 2021). The main conclusions from this study are:

- Iron solubility increases from ~0.7% to 4.7% as Saharan dust fronts transit from Africa to the Americas.
- Dust, heavy fuel oil combustion and atmospheric processing are identified as sources of soluble iron.
- Fresh dust accounts for 63, 43 and 9% of soluble iron in Tenerife, Barbados and Miami.
- Aged dust accounts for 26, 45 and 74% of soluble iron in Tenerife, Barbados and Miami.
- Oil combustion accounts for 10, 12 and 16% of soluble iron in Tenerife, Barbados and Miami.

8.4 Participation in Scientific Projects and Studies/Experiments

8.4.1 REDMAAS 2019 Campaign

The In-Situ Aerosols research group has also participated in the REDMAAS (Red Española de DMAs Ambientales) 2019 campaign.

The campaign was carried out in the facilities of the Center for Energy, Environmental and Technological Research (CIEMAT) in Madrid from 4 - 8 March 2019 (Fig.8.3). The

following REDMAAS network members participated: CIEMAT; Institute of Environment of the University of A Coruña (IUMA-UDC); IARC-AEMET; Institute of Investigation of the Earth System in Andalusia, University of Granada (IISTA-UGR) and IDAEA-CSIC as well as an instrument provided by the TSI company for this campaign.

The purpose of REDMAAS is to facilitate the exchange of knowledge between the groups, also to promote cooperation among them in order to create synergies and to optimize the use and the coordination of scientific-technological infrastructures of common interest.

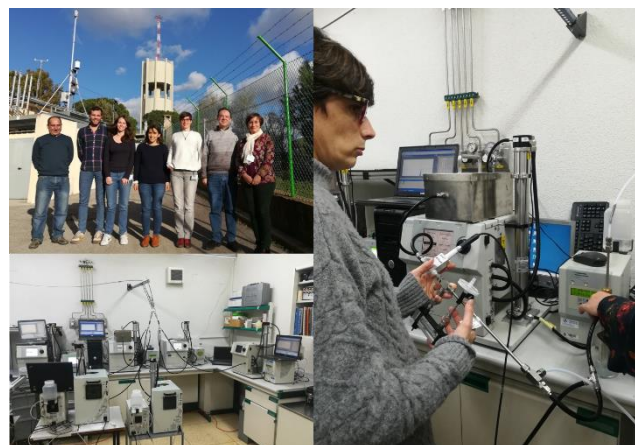


Figure 8.3. Top left: participants in the REDMAAS 2019 campaign. Bottom left: instruments during intercomparison at CIEMAT facilities. Right: N. Prats, head of the AIS group at IARC, testing the efficiency in discrimination 200nm size particles.

The objective of this campaign was the intercomparison of aerosol particle size analyzers of the SMPS type (Scanning Mobility Particle Sizer) and to check that the instruments are quality controlled to ensure the validity of the measurements and their traceability. The campaign was successful and confirmed that in the size range from 20-800 nm, ARL SMPS system was within +/-10% of the mean values of all instruments' data including the corrections for aerosol flow, diffusion losses and the CPC efficiency (Fig.8.4), which is well in agreement with WCCAP and ACTRIS recommendations.

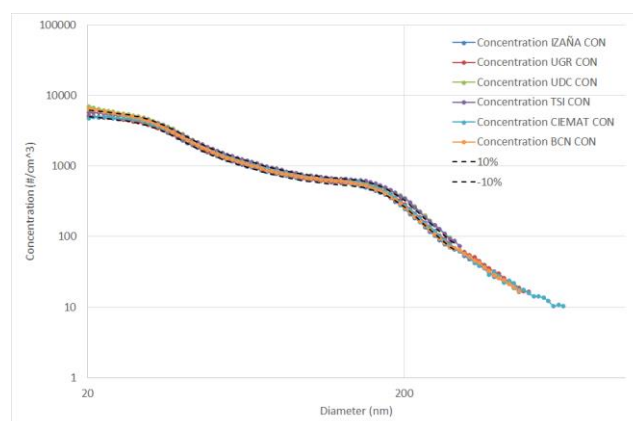


Figure 8.4. Results of the REDMAAS 2019 intercomparison.

IARC contributed to a series of scientific papers related to global trend analysis of climate relevant aerosol properties, in particular, in-situ aerosol radiative properties thanks to its effort in maintaining and reporting high quality data.

8.4.2 Hosting measurements of the AEROPOLSOL project (Agustín de Betancourt Program)

The AEROPOLSOL project (through the Agustín de Betancourt program) aims to standardize methods for determining the insoluble fraction of aerosols and the soluble fraction of iron and other compounds of environmental interest in samples of desert dust aerosols.

During summer 2019, samples were taken at IZO in cellulose filters, for later analysis at the Atomic Absorption Spectroscopy Laboratory of the General Research Support Services of the University of La Laguna. Part of the results of the project were already shown in Section 8.3.2 (Rodríguez et al., 2021).

8.4.3 Contribution of IZO Aerosol In-Situ data to climatological works.

The long-term in-situ aerosol monitoring data at the IZO GAW-Station was included in the work led by Laj et al. (2020) in which they presented a global analysis of climate-relevant aerosol properties retrieved from the network of GAW near-surface observatories. The paper provides the widest effort so far to document variability of climate-relevant in situ aerosol properties (namely wavelength dependent particle light scattering and absorption coefficients, particle number concentration and particle number size distribution) from all sites connected to the GAW network. High-quality data from almost 90 stations worldwide were collected and controlled for quality and are reported for a reference year in 2017, providing a very extended and robust view of the variability of these variables worldwide.

The range of variability observed worldwide for light scattering and absorption coefficients, single-scattering albedo, and particle number concentration were presented together with preliminary information on their long-term trends and comparison with model simulations for the different stations. In addition, the scope of the paper was to provide the necessary suite of information to understand data availability, quality and useability. It delivers to users of the World Data Centre for Aerosols, the required confidence in data products in the form of a fully characterized value chain, including uncertainty estimation and requirements for contributions to the global climate observing system.

Associated with this work, a series of companion papers was published, such as Collaud Coen et al. (2020) where long-term climatological trends were derived for the optical aerosol properties, showing for the first time an unequivocal decrease in scattering and absorption coefficient in Europe,

following a tendency already detectable in the US several years ago. The IZO Aerosol Research Laboratory was one of the stations that contributed to this work.

The results of the study, considering the lack of information from many WMO regions, provide evidence that the aerosol load has significantly decreased over the last 2 decades in North America and Europe. The low number of stations on the other continents means global tendencies cannot be assessed and the results are more variable.

The mean aerosol property trends are decreasing for all parameters (scattering coefficient σ_{sp} , backscattering coefficient σ_{bsp} and absorption coefficient σ_{ap}) in all regions apart from the σ_{sp} trend in the South Pacific and in the polar regions (for detailed information see Table 4 of Collaud Coen et al., 2020). These decreases in aerosol burden are assumed to be a direct consequence of decreases in primary particles emission and particulate precursors such as SO_4 and NO_x due to pollution abatement policies. This assumption is supported by trend results for the USA, where the inflection point between not statistically significant and statistically significant decreasing σ_{sp} 10-year trends consistently occurred over the same time period (2009–2012) for all central and eastern stations. While the annual σ_{ap} decrease (-2.5 to -5 % yr^{-1} for the ss trends in all regions) is larger than that for σ_{sp} , the σ_{ap} time series are not long enough to detect the beginning of σ_{ap} decreasing 10-year trends.

Also, it is worthy to highlight from this work of Collaud et al. (2020), the recommendations based on the results of this study and with a view toward future trend analyses, concerning the improvement of aerosol optical time series (in line with the GAW objectives and applied for all atmospheric composition monitoring):

- The station history, metadata and logbooks should be detailed and handled with great care, since they are absolutely necessary to evaluate long-term trends on homogenized time series.
- Time series are affected not only by the instrument type or inlet changes, but also by replacement by instruments of the same type and by shifts in calibrations.
- A rotation between instruments in a network (e.g., to enable repairs) will decrease potential missed data losses but has a potential to increase breakpoints in the time series, particularly in the wavelength dependence of the parameters.
- The scattering and backscattering coefficients, the backscattering fraction and the scattering Ångström exponents are very sensitive to the humidity conditions in the nephelometers due to the hygroscopic growth of particles even at low RH. The nephelometer humidity sensors should be better checked and characterized in order to assess long-term trends of dry particles.

- Long-term trend analysis should not be computed on time series shorter than 10 years, since short datasets lead to a larger probability of false trend detection because of the low number of elements in the time series.
- Stations with long-term records have to be sustained and their funding should be assured in order to study the future impact of aerosol on climate change. Station maintenance as well as new station creation in regions with a low spatial coverage (Africa, South America, Asia and Oceania) should be particularly encouraged.

8.4.4 Ongoing studies regarding COVID-19 lockdown impact

The AIS group made multiple contributions to studies regarding the impact of lockdowns due to the COVID-19 Crisis, not only over Europe but also across the Northern Hemisphere. These activities were mostly conducted in the second half of 2020 and some results were already published at the time of writing of this report (Evangelizou et al., 2021).

8.5 References

- Collaud Coen, M., Andrews, E., Alastuey, A., Arsov, T. P., Backman, J., Brem, B. T., Bukowiecki, N., Couret, C., Eleftheriadis, K., Flentje, H., Fiebig, M., Gysel-Beer, M., Hand, J. L., Hoffer, A., Hooda, R., Hueglin, C., Joubert, W., Keywood, M., Kim, J. E., Kim, S.-W., Labuschagne, C., Lin, N.-H., Lin, Y., Lund Myhre, C., Luoma, K., Lyamani, H., Marinoni, A., Mayol-Bracero, O. L., Mihalopoulos, N., Pandolfi, M., Prats, N., Prenni, A. J., Putaud, J.-P., Ries, L., Reisen, F., Sellegri, K., Sharma, S., Sheridan, P., Sherman, J. P., Sun, J., Titos, G., Torres, E., Tuch, T., Weller, R., Wiedensohler, A., Zieger, P., and Laj, P.: Multidecadal trend analysis of in situ aerosol radiative properties around the world, *Atmos. Chem. Phys.*, 20, 8867–8908, <https://doi.org/10.5194/acp-20-8867-2020>, 2020.
- Evangelizou, N., Platt, S. M., Eckhardt, S., Lund Myhre, C., Laj, P., Alados-Arboledas, L., Backman, J., Brem, B. T., Fiebig, M., Flentje, H., Marinoni, A., Pandolfi, M., Yus-Diez, J., Prats, N., Putaud, J. P., Sellegri, K., Sorribas, M., Eleftheriadis, K., Vratolis, S., Wiedensohler, A., and Stohl, A.: Changes in black carbon emissions over Europe due to COVID-19 lockdowns, *Atmos. Chem. Phys.*, 21, 2675–2692, <https://doi.org/10.5194/acp-21-2675-2021>, 2021.
- Gómez-Moreno, F.J., Alonso, E., Artíñano, B., Juncal-Bello, V., Iglesias-Samitier, S., Piñeiro Iglesias, M., López Mahía, P., Pérez, N., Pey, J., Ripoll, A., Alastuey, A., de la Morena, B.A., García, M.I., Rodríguez, S., Sorribas, M., Titos, G., Lyamani, H., Alados-Arboledas, L., Latorre, E., Tritscher, T., Bischof, O.F. Intercomparisons of Mobility Size Spectrometers and Condensation Particle Counters in the Frame of the Spanish Atmospheric Observational Aerosol Network. *Aerosol Science and Technology*, 49, 9, 2015.
- Laj, P., Bigi, A., Rose, C., Andrews, E., Lund Myhre, C., Collaud Coen, M., Lin, Y., Wiedensohler, A., Schulz, M., Ogren, J. A., Fiebig, M., Gliß, J., Mortier, A., Pandolfi, M., Petäjä, T., Kim, S.-W., Aas, W., Putaud, J.-P., Mayol-Bracero, O., Keywood, M., Labrador, L., Aalto, P., Ahlberg, E., Alados Arboledas, L., Alastuey, A., Andrade, M., Artíñano, B., Ausmeel, S., Arsov, T., Asmi, E., Backman, J., Baltensperger, U., Bastian, S., Bath, O., Beukes, J. P., Brem, B. T., Bukowiecki, N., Conil, S., Couret, C., Day, D., Dayantolis, W., Degorska, A., Eleftheriadis, K., Fetfatzis, P., Favez, O., Flentje, H., Gini, M. I., Gregorič, A., Gysel-Beer, M., Hallar, A. G., Hand, J., Hoffer, A., Hueglin, C., Hooda, R. K., Hyvärinen, A., Kalapov, I., Kalivitis, N., Kasper-Giebl, A., Kim, J. E., Kouvarakis, G., Kranjc, I., Krejci, R., Kulmala, M., Labuschagne, C., Lee, H.-J., Lihavainen, H., Lin, N.-H., Löschan, G., Luoma, K., Marinoni, A., Martins Dos Santos, S., Meinhardt, F., Merkel, M., Metzger, J.-M., Mihalopoulos, N., Nguyen, N. A., Ondracek, J., Pérez, N., Perrone, M. R., Petit, J.-E., Picard, D., Pichon, J.-M., Pont, V., Prats, N., Prenni, A., Reisen, F., Romano, S., Sellegri, K., Sharma, S., Schauer, G., Sheridan, P., Sherman, J. P., Schütze, M., Schwerin, A., Sohmer, R., Sorribas, M., Steinbacher, M., Sun, J., Titos, G., Toczko, B., Tuch, T., Tulet, P., Tunved, P., Vakkari, V., Velarde, F., Velasquez, P., Villani, P., Vratolis, S., Wang, S.-H., Weinhold, K., Weller, R., Yela, M., Yus-Diez, J., Zdimal, V., Zieger, P., and Zikova, N.: A global analysis of climate-relevant aerosol properties retrieved from the network of Global Atmosphere Watch (GAW) near-surface observatories, *Atmos. Meas. Tech.*, 13, 4353–4392, <https://doi.org/10.5194/amt-13-4353-2020>, 2020.
- Müller, T., J. S. Henzing, G. de Leeuw, A. Wiedensohler, A. Alastuey, H. Angelov, M. Bizjak, M. Collaud Coen, J. E. Engström, C. Gruening, R. Hillamo, A. Hoffer, K. Imre, P. Ivanow, G. Jennings, J. Y. Sun, N. Kalivitis, H. Karlsson, M. Komppula, P. Laj, S.-M. Li, C. Lunder, A. Marinoni, S. Martins dos Santos, M. Moerman, A. Nowak, J. A. Ogren, A. Petzold, J. M. Pichon, S. Rodriguez, S. Sharma, P. J. Sheridan, K. Teinilä, T. Tuch, M. Viana, A. Virkkula, E. Weingartner, R. Wilhelm, and Y. Q. Wang. Characterization and intercomparison of aerosol absorption photometers: result of two intercomparison workshops. *Atmos. Meas. Tech.*, 4, 245–268, doi:10.5194/amt-4-245-2011, 2011
- Peltier R.E., Castell, N., Clements A.L., Dye T., Hüglin C., Kroll J.S., Ning Z., Parsons M., Penza M., Reisen F., von Schneidmesser E., Arfire A., Boso A., Fu Q., Hagan D., Henshaw G., Jayaratne R., Jones R., Kelly K., Kilaru V., Mead I., Morawska L., Papale D., Polidori A., Querol X., Seddon J., Schneider P., Tarasova O. An Update on Low-cost Sensors for the Measurement of Atmospheric Composition, Ed. by Richard E. Peltier, WMO- No. 1215, 2021
- Rodríguez, S., Cuevas, E., Prospero, J. M., Alastuey, A., Querol, X., López-Solano, J., García, M. I., and Alonso-Pérez, S.: Modulation of Saharan dust export by the North African dipole, *Atmos. Chem. Phys.*, 15, 7471–7486, 2015.
- Rodríguez, S., Calzolari, G., Chiari, M., Nava, S., García, M.I., Lopez-Solano, J., Marrero, C., Lopez-Darias, J., Cuevas, E., Alonso-Perez, S., Prats, N., Amato, F., Lucarelli, F., Querol, X.: Rapid changes of dust geochemistry in the Saharan Air Layer linked to sources and meteorology, *Atmospheric Environment* 2020, <https://doi.org/10.1016/j.atmosenv.2019.117186>
- Rodríguez, S., Prospero, J.M., López-Darias, J., García-Alvarez, M. I., Zuidema, P., Nava, S., Lucarelli, F., Gaston, C.J., Galindo, L., Sosa, E.: Tracking the changes of iron solubility and air pollutants traces as African dust transits the Atlantic in the Saharan dust outbreaks, *Atmospheric Environment*, 118092, ISSN 1352-2310, <https://doi.org/10.1016/j.atmosenv.2020.118092>, 2021.
- WMO/GAW Report n° 227, Aerosol Measurement Procedures, Guidelines and Recommendations, 2016.

8.6 Staff

Dr Natalia Prats (AEMET; Head of programme)

Concepción Bayo-Pérez (AEMET; Meteorological
Observer-GAW Technician)

Ramón Ramos (AEMET; Head of Infrastructure)

Dr Javier López Solano (AEMET until March 2019, now
at TRAGSATEC; Research Scientist)

Nayra Chinaa (SIELTEC Canarias; laboratory technician)

9 Column Aerosols

9.1 Main Scientific Goals

The main scientific goals of this programme are:

- Long-term high-quality measurements of column aerosol properties in the FT and the MBL.
- Aerosol characterization in the Saharan Air Layer and the MBL.
- Development of new methodologies and instrumentation for column aerosols and water vapour observations, as well as new calibration techniques.
- Mineral dust model validation.
- Satellite borne aerosol data validation.
- Provision of accurate sun and lunar photometer calibrations and intercomparisons.

9.2 Measurement Programme

The measurement programme is very extensive, including photometric, lidar and ceilometer observations.

Photometric observations are performed at three of the IARC stations, IZO, SCO and TPO (see Tables 3.2, 3.4 and 3.6). Two of the most important parameters for long-term monitoring of the evolution of atmospheric aerosol are AOD, which accounts for the aerosol loading in the atmospheric column, and the Angström Exponent (AE) which gives information on the size and type of the particles. Both parameters have been measured at IZO since 2004 and SCO since 2005, as AERONET-Cimel stations and at IZO also within the WMO Global Atmosphere Watch - Precision Filter Radiometer (GAW-PFR) network since July 2001.

AOD observations at Izaña can be also dated back to 1982 (Fig. 9.1) when they were performed with the Astronomical Potassium-based Resonance Scattering Spectrometer Mark-I (Barreto et al., 2014).

An IARC collaborative station at Roque de los Muchachos (La Palma) was established in 2019 to extend the monitoring of atmospheric aerosol at key sites.

IARC manages not only the AERONET sites of IZO (Fig. 9.2), SCO (Fig. 9.3), TPO and collaborative stations in Spain, but also collaborates closely and provides technical assistance to AERONET-Africa sites, such as Tamanrasset (Algeria), Cairo (Egypt) and Carthage (Tunis). These observations near dust sources over the Sahara provide key information for the SDS-WAS Regional Center (see Section 17) for dust modelling, verification and validation of satellite-based aerosol products.

IZO is a reference calibration site for radiometric observations and calibrations using the Langley plot technique (since 2011) due to the pristine and relatively stable atmospheric conditions at this site. Together with Mauna Loa (Hawaii), IZO is the site for absolute calibration of the GAW-PFR network of the World Radiation Center (Wehrli, 2000, 2005).

Moreover, reference instruments belonging to AERONET, AERONET-Europe and the China Aerosol Remote Sensing NETwork (CARSNET), managed by the China Meteorological Administration (CMA; Key Laboratory of Atmospheric Chemistry, Centre for Atmosphere Watch and Services, Chinese Academy of Meteorological Sciences), are periodically calibrated at Izaña Observatory (Che et al., 2009; Toledano et al., 2018). The absolute calibration of Cimel instruments is complemented with laboratory radiance calibration using the integrating sphere of the Optical calibration facility at IZO (Guirado et al., 2012).

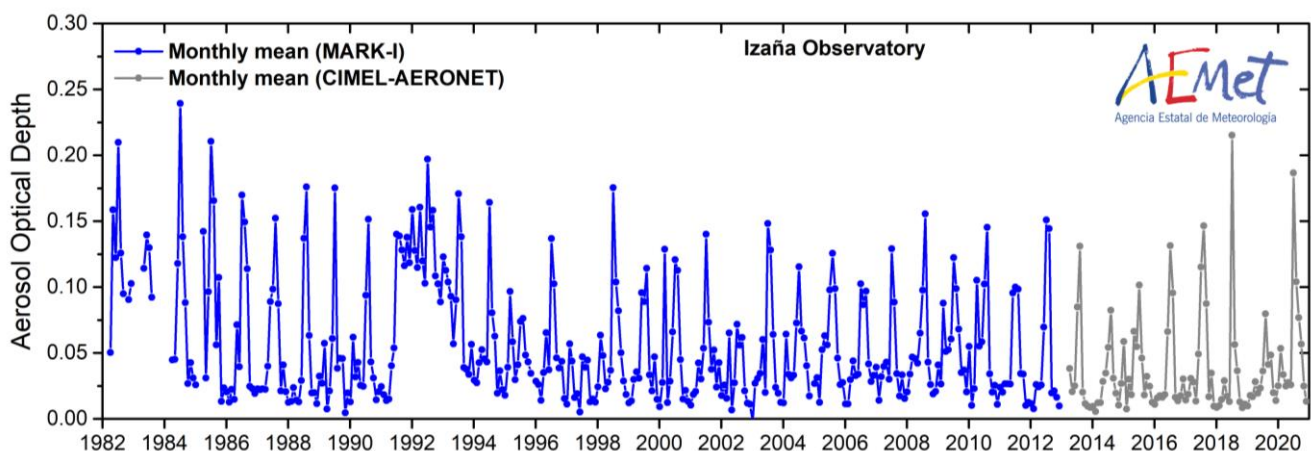


Figure 9.1. Monthly AOD measured at Izaña (in blue) between 1982 and 2012 with the Mark-I spectrometer. AOD measured with Cimel CE318 photometers within AERONET (<https://aeronet.gsfc.nasa.gov/>) are also included, completing the series between 2012 and 2020 (in grey).



Figure 9.2. Cimel reference instruments of the AERONET-Europe Calibration Facility at Izaña Observatory.



Figure 9.3. Cimel at Santa Cruz Observatory (SCO). On the right, a ZEN radiometer and on the left a tube to prevent direct sunlight and reflections in the NASA-MPLNet Lidar located in the room below.

9.2.1 Lidar observations

The IARC and the Spanish Institute for Aerospace Technology (PI: Dr Margarita Yela) co-manage a Micropluse lidar (MPL-3) aerosols programme, belonging to the NASA Micro-Pulse Lidar Network (MPLNET), which started a long-term observation programme in 2005. This instrument is part of the NASA MPLNET worldwide aerosol lidar network and operates in full-time continuous mode (24 hours a day / 365 days a year). This instrument operating at SCO can be considered the unique aerosol lidar in Northern Africa that provides regular and long-term information about the vertical structure of the Saharan Air Layer over the North Atlantic.

This lidar was replaced in May 2018 by a new MPL-4B lidar provided by NASA Goddard Space Flight Center MPLNET. The new MPL-4B lidar provides common features of the previous MPL-3 version in addition to dual polarization backscatter measurements allowing researchers to discriminate between aerosol types and clouds phase. A ferroelectric liquid crystal (FLC) is used in these new systems for faster data rates in addition to a slightly modified measurement strategy to accommodate the difference in polarizer properties. The main technical characteristics of the MPL-4B are detailed in Table 9.1.

Table 9.1. Technical characteristics of the Micro-Pulse Lidar (MPL) at Santa Cruz de Tenerife Observatory.

Micro-Pulse Lidar version 4 (MPL-4B)	
Transmitter	
Laser	Nd:YAG
Wavelength	532 nm
Pulse repetition rate	2500 Hz
Pulse energy	6-8 μ J
Receiver	
Type	Maksutov Cassegrain
Diameter	18 cm
Focal	240 mm
Field of view	Dual field of view configuration: Narrow FOV: 100 μ rad Wide FOV: 2 mrad
Polarization	Co-polar and cross-polar components
Detector	
Type	Avalanche photodiode (APD)
Mode	Photocounting

Another MPL-4B was acquired by IARC and installed in the Testbed#2 lidar facility at IZO (Fig. 9.4) in order to provide simultaneous measurements with two MPLs, one located at sea level, and one located in Izaña (2373 m a.s.l.), along with measurements of their co-located AERONET sun photometric measurements. These two pieces of information are useful for the characterization of the Saharan Air Layer, its effects in lower (marine boundary layer) and higher (free troposphere) layers and also its impact on mid and high cloud formation.



Figure 9.4 Lidar facility (Testbed#2) at IZO.

In addition to the two MPL-4B lidars, a Cimel CE376 lidar is also installed at IZO. This instrument performs observations at two wavelengths (532 & 808 nm) with two depolarization channels, complementing the existing MPL database with NIR measurements. This instrument is still subject to adjustments and calibrations at IZO where it is expected to be permanently in operation from 2021.

As part of the WMO Testbed for Aerosols and Water Vapour Remote Sensing Instruments, IZO carries out some activities related to column aerosol measurements specifically focusing on methodological and instrument developments aspects (see Section 19 for more details).

9.2.2 Ceilometer observations

The Vaisala CL51 ceilometer was installed in SCO in 2011. It has a single channel centered at 910 nm. Every 36 s, it provides atmospheric backscatter profiles up to 15 km altitude as well as cloud base heights at three different altitude levels.

Daily extinction and AOD profiles at 910 nm (centered at 12:00 UTC and averaged over one hour and over ten minutes) are generated by applying the iterative Fernald-Klett inversion algorithm (Fernald, 1984; Klett, 1981; Klett, 1985) to the backscatter profile of CL51, following the procedure and guidelines set out in Córdoba et al. (2008). The humidity, temperature and pressure values of the daytime soundings in Tenerife as well as AERONET AOD 910 nm values at SCO and IZO are utilised in this process.

Each type of profile, hourly or ten-minute, of extinction or AOD, is constructed in two different ways: 1) adjusting the algorithm to a single AOD value in the SCO (monolayer atmosphere), or 2) simultaneously adjusting two AOD values, one at SCO and another at IZO, considering a two-layer atmosphere. Fig. 9.5 presents the backscatter, extinction and AOD profiles at 910 nm for 27 December 2020. The profiles shown were fitted according to the two-layer atmosphere model mentioned above.

Until 8 November 2020, AOD from AERONET corresponding to Level 1.5 and Version 2 were used to adjust the algorithm. Since 9 November 2020, the Level 1.5 Version 3 AERONET AOD are used.

In addition, the CL51 ceilometer also detects the height of the first aerosol layer every 16 s, which is useful to obtain the height of the mixing layer (ML) in quasi-real time. This calculation is performed with a temporal resolution of half an hour following the criteria indicated in Lotteraner and Piringer (2016). The mixing layer is defined as the height of the layer adjacent to the ground over which pollutants or any constituents emitted within the layer itself, or that penetrate it from outside, are vertically dispersed by convection or mechanical turbulence within a timescale of approximately 1 hour (Seibert et al., 2000). This layer provides information on the volume available for the dispersion of pollutants. Hence, its calculation from CL51 can be used as input in dispersion models. Fig. 9.6 presents the quasi-real time mixing layer height obtained from the CL51 in SCO on 22 September 2019.

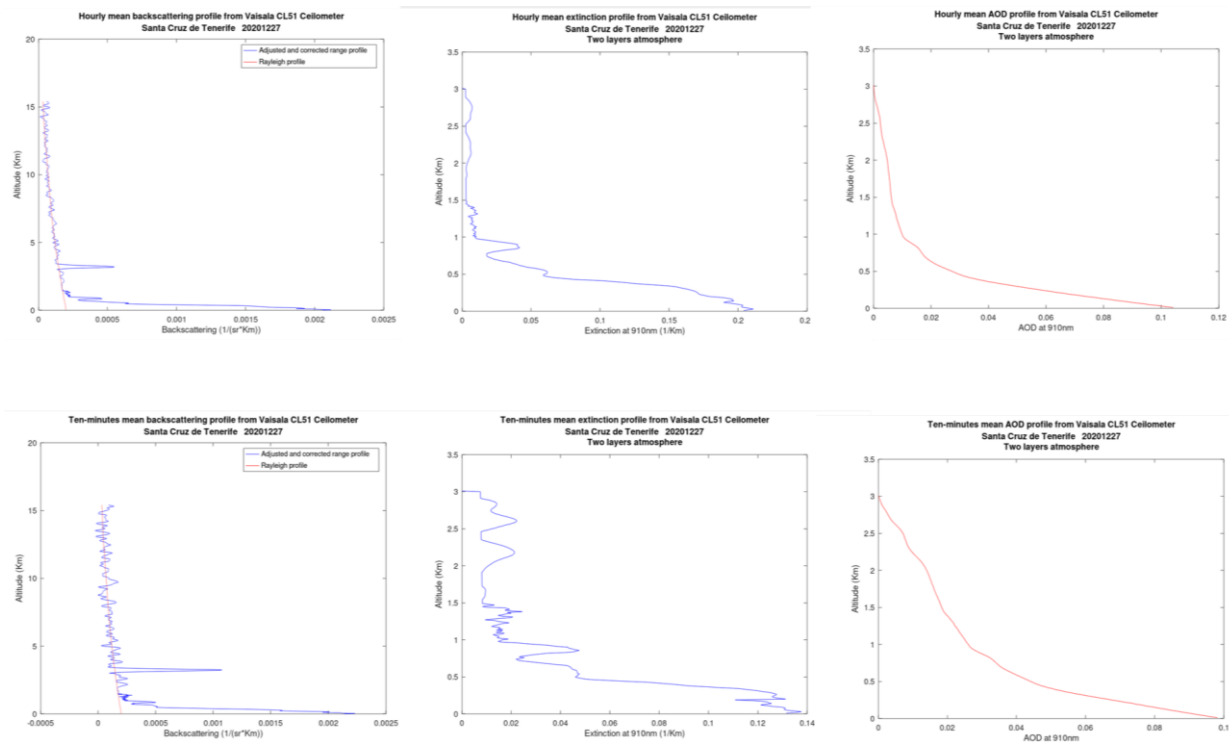


Figure 9.5. Backscatter, extinction and AOD (910 nm) profiles from CL51 ceilometer on 27 December 2020.

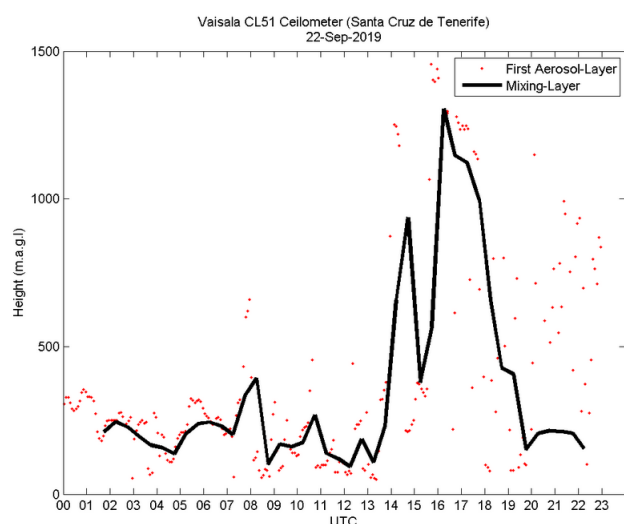


Figure 9.6. CL51 ceilometer results of Mixing Layer height at SCO on 22 September 2019.

The Vaisala CL51 ceilometer was integrated into the Automatic Ceilometer and Lidars Network (ALC; www.eumetnet.eu) within the framework of the EUMETNET Profiling Programme ([E-PROFILE](#)) on 24 April 2018.

9.3 Summary of remarkable results during the period 2019-2020

The most relevant results obtained during the reporting period are summarized hereinafter.

9.3.1 Spectral Aerosol Optical Depth Retrievals by Ground-Based FTIR Spectrometry

Atmospheric aerosol is a key constituent in the atmosphere as it influences the radiative balance in the ultraviolet to infrared (IR) region. The WMO Global Climate Observing System (GCOS) considers it as an Essential Climate Variable (ECV). Consequently, aerosol research and monitoring have recently been promoted to improve knowledge on aerosol–climate interactions, which is especially challenging in the IR, where aerosol spectral information is particularly scarce.

The first long-term (1-year) series of aerosol optical depth and Angström Exponent in the near infrared (NIR) and the short-wave infrared (SWIR) spectral regions has been retrieved from ground-based high-quality spectroscopic measurements at Izaña (Barreto et al., 2020). These results were obtained by means of a Fourier Transform Infrared spectrometer originally devoted to high-resolution and high-quality atmospheric trace gas monitoring. The lack of absolute photometric stability of the FTIR system required for aerosol monitoring was addressed in this study by means of a continuous Langley–Plot procedure based on 29 different Langley–Plots smoothed with a spline smoothing method. This procedure revealed a linear degradation rate in the FTIR absolute calibration up to 1.75% month⁻¹, confirming that the FTIR absolute calibration is very sensitive to the surface degradation or dirtiness deposited on the FTIR external optical mirrors.

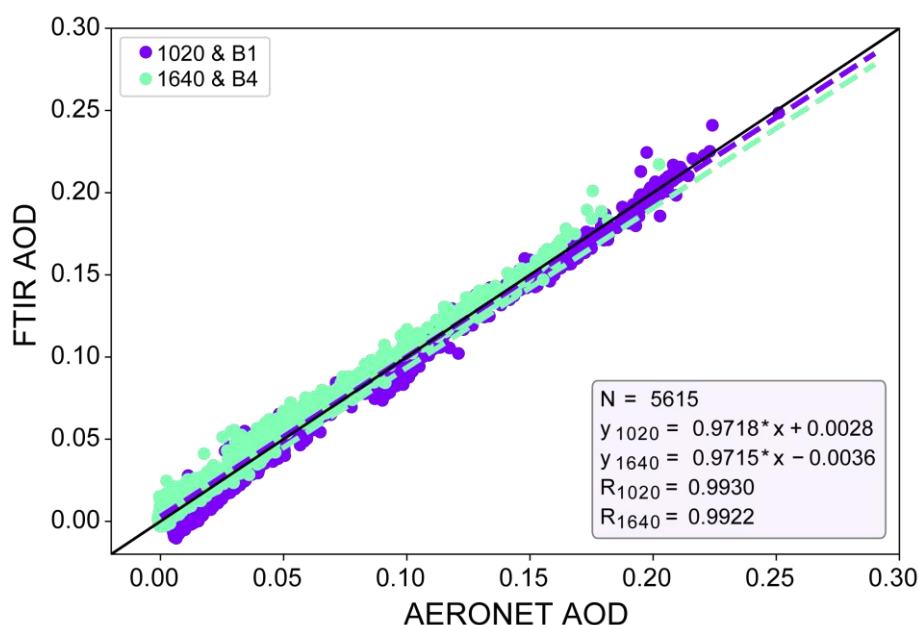


Figure 9.7 Scatterplot for the coincident AERONET-FTIR AOD values from May 2019 to May 2020 considering the FTIR B1 and B4 micro-windows: the number of coincidences (N), the fitting parameters and correlation coefficient (R) are displayed in the legend. Reprinted from Barreto et al. (2020).

A cross-validation of the 1-year spectral AOD series extracted from the FTIR was performed using co-located Cimel CE318-T photometric observations in the framework of AERONET. The results showed an excellent agreement between both AOD products (Fig. 9.7). The reliability of the FTIR dataset was additionally ensured by means of a subsequent cross-validation with the Modeled optical properties of ensembles of aerosol particles (MOPSMAP) package (Gasteiger and Wiegner, 2018).

With this recent study we have taken the first step to extend the operation of the FTIR to monitor aerosols, therefore providing important additional information for the validation and subsequent improvement of satellite aerosol products as well as enhancing the sensitivity to large particles in the existing databases, required to improve the estimation of the aerosols' radiative effect on climate. This new methodology for aerosol retrieval will open the door for broader application of portable low-resolution FTIR instruments, with a potentially higher spatial coverage for atmospheric monitoring.

9.3.2 EURAMET/EMPIR project “Metrology for aerosol optical properties” (MAPP)

The MAPP EURAMET project is coordinated by PMOD/WRC as a consortium of 14 partners (6 National Metrological Institutes and 8 external partners), in which AEMET is included. The project started in June 2020 and has a duration of 36 months.

Passive remote sensing currently which is currently broadly used for the determination of column-integrated aerosol, using solar and lunar radiation measurements, lacks traceability to the SI units. The main goal of this EMPIR/MAPP project is to develop methods and SI-traceable devices for both laboratory and in-field calibrations of the current radiometers used in aerosol monitoring along with the validation of these new or improved methods linking ground-based measurements to satellite-based data.

The EMPIR/MAPP project aims to reduce the radiometer calibration chain, the downtime of monitoring networks as well as to generate traceable data regarding aerosol. AEMET is assigned in this project the tasks of organizing a field campaign at Izaña, operating sun/moon radiometers and a Bruker EM27/SUN spectrometer and validating the ROLO and RIMO lunar irradiance models.

9.3.3 The 2nd nocturnal multi-instrumental campaign for aerosol optical depth measurements at Ny-Alesund (Svalbard)

Arctic amplification, which means that the largest temperature increase due to global warming in the world is found in the Arctic region (Graßl et al., 2019), as well as other phenomena such as retreating sea ice or permafrost melting, have boosted Arctic research in the last decades. One remarkable example is the Multidisciplinary drifting Observatory for the Study of Arctic Climate (MOSAIC) expedition, the largest polar expedition in history. For this reason, long-term aerosol monitoring in the Arctic is currently considered a key activity for climate change studies.

Lunar and star photometry are considered as viable techniques for monitoring aerosols at night, even in polar regions. The first nighttime inter-comparison campaign, jointly organized by AEMET and University of Valladolid, was conducted at Izaña Observatory during June 2017 in order to evaluate the performance of the different instruments capable of monitoring aerosol at night.

The second nighttime inter-comparison campaign was held in Ny-Ålesund (Svalbard) during February 2020 (Fig. 9.8). This campaign was a collaboration between different institutions strongly involved in polar activities (Alfred-Wegener Institut of Germany (AWI), National Research Council of Italy (CNR) and NOAA, among others) as a part of the Svalbard Integrated Arctic Earth Observing System (SIOS) access programme (also included as a part of the MOSAIC activities on land). A scientist from the IARC Column Aerosols research group participated in this field campaign and subsequent workshop. In this comparison campaign different instruments were included: different types of lunar photometers (Cimel, precision filter radiometer –PFR- and Prede), all-sky cameras, camera lidar and lidar. The goal of this comparison activity was to improve instruments performance, to share and compare the different processing procedure and to adopt common processing procedures to homogenize and make comparable the outputs of lunar and stellar photometry.



Figure 9.8. The camera lidar laser deployed on the roof of the Alfred-Wegener Institut (AWI) observatory and the beam from the AWI lidar (on the left). Photo credit: Gregory Tran. On the right is the Lunar PFR during this campaign. Photo credit: <https://images.app.goo.gl/9UTSaTZqAu9NADNM8>.

9.3.4 The 3rd nocturnal multi-instrumental campaign for aerosol optical depth measurements at Lindenberg (Germany)

The third lunar/stellar AOD intercomparison campaign was carried out in Lindenberg (Germany) during 26 August - 9 September 2020 (Fig. 9.9). This campaign, organized by the German Meteorological Service (DWD) with the collaboration of the University of Valladolid, IARC-AEMET, PMOD-WRC, CNR, National Institute of Polar Research of Japan (NIPR), Pulkovo Observatory Sankt Petersburg, Dr. Schulz & Partner GmbH, Meteo Swiss, ETH Zurich, University of Sherbrooke, and others, took place at Meteorologisches Observatorium Lindenberg - Richard Aßmann-Observatorium (MOL-RAO).

The Summer Campaign for Intercomparison of Lunar measurements of Lindenberg's Aerosol (SCILLA) involved synchronous measurements from three different types of lunar photometers and one kind of stellar photometer. Some other aerosol remote sensing observations were also included in SCILLA thanks to the wide variety of measurements provided at the MOL-RAO supersite (vertical profiles from Raman lidars and ceilometers, COBALD radiosondes and an all-sky camera). This field campaign, together with the field campaign carried out in Ny-Alesund in February 2020, have been conceived within the Polar-AOD community as critical field tests to verify the capability of the current remote sensing techniques to extend the aerosol monitoring during the nocturnal period, which is of special interest for polar studies.



Figure 9.9. Different photometers installed in Lindenberg during the 2020 field campaign. Photo credit: Lionel Doppler.

9.3.5 New developments using GRASP algorithm

Recent developments in remote sensing have allowed a complete day-to-night aerosol characterization, especially in terms of aerosol microphysical properties (Perez-Ramírez et al., 2012; Barreto et al., 2016). A new study conducted by Benavent-Oltra et al. (2019) evaluates the potential of the Generalized Retrieval of Aerosol and Surface Properties (GRASP) algorithm to retrieve continuous day-to-night aerosol properties (both column-integrated and vertically resolved) combining remote-sensing measurements as input data during an intense Saharan dust event that occurred during the Sierra Nevada Lidar aerosol Profiling Experiment I (SLOPE I) field campaign. This synergetic approach includes measurements with an elastic lidar, solar

and lunar measurements with a CE318-T, which allows us to derive the day- and night-time AOD (Barreto et al., 2013, 2016; Giles et al., 2019), and sky camera images, which allow us to obtain the normalized sky radiance from the lunar aureole (Román et al., 2017).

The three schemes proposed in this study for the GRASP AOD night-time retrievals are the following: 1) the use of lidar night-time measurements in combination with the interpolation of sun–sky daytime measurements (N0 scheme); 2) night-time aerosol optical depth obtained by lunar photometry are used in addition to intensive properties of the aerosol (such as complex refractive index or spherical particle fraction) retrieved during sun–sky daytime measurements (N1 scheme); and finally 3) sky camera images are used to retrieve the Moon aureole radiance (N2 scheme). The results of the three schemes were validated by considering the coherence of day-to-night evolutions as well as in-situ measurements as reference.

In general, GRASP N0 and N1 schemes provide better results than the GRASP N2 scheme, with the exception of the analysis based on volume concentration, in which the GRASP N2 shows the lowest differences against in situ measurements (around 10 %) for high aerosol optical depth values. Given the fact that the N2 scheme provides a stand-alone way to retrieve intensive and extensive aerosol properties at night in cases with high values of AOD and high Moon irradiance (at least between the first and last Moon quarters) independent of daytime information, this scheme usually presents higher differences than the reference values. However, as summarized in Benavent-Oltra et al. (2019), a more complete data set that includes at least different aerosol types is needed to ensure these findings, in addition to more detailed investigations on the accuracy and uncertainty of the retrieved GRASP products obtained with the proposed schemes.

9.4 References

- Barreto, A., Cuevas, E., Pallé, P., Romero, P. M., Guirado, C., Wehrli, C. J., and Almansa, F.: Recovering long-term aerosol optical depth series (1976–2012) from an astronomical potassium-based resonance scattering spectrometer, *Atmos. Meas. Tech.*, 7, 4103–4116, <https://doi.org/10.5194/amt-7-4103-2014>, 2014.
- Barreto, Á., Cuevas, E., Granados-Muñoz, M. J., Alados-Arboledas, L., Romero, P. M., Gröbner, J., Kouremeti, N., Almansa, A. F., Stone, T., Toledano, C., Román, R., Sorokin, M., Holben, B., Canini, M., and Yela, M.: The new sun-sky-lunar Cimel CE318-T multiband photometer – a comprehensive performance evaluation, *Atmos. Meas. Tech.*, 9, 631–654, <https://doi.org/10.5194/amt-9-631-2016>, 2016.
- Barreto, Á., García, O.E., Schneider, M., García, R.D., Hase, F., Sepúlveda, E., Almansa, A.F., Cuevas, E., Blumenstock, T. Spectral Aerosol Optical Depth Retrievals by Ground-Based Fourier Transform Infrared Spectrometry. *Remote Sens.* 2020, 12, 3148. <https://doi.org/10.3390/rs12193148>.
- Benavent-Oltra, J. A., Román, R., Casquero-Vera, J. A., Pérez-Ramírez, D., Lyamani, H., Ortiz-Amezcu, P., Bedoya-Velásquez, A. E., de Arruda Moreira, G., Barreto, Á., Lopatin, A., Fuertes, D., Herrera, M., Torres, B., Dubovik, O., Guerrero-Rascado, J. L., Goloub, P., Olmo-Reyes, F. J., and Alados-Arboledas, L.: Different strategies to retrieve aerosol properties at night-time with the GRASP algorithm, *Atmos. Chem. Phys.*, 19, 14149–14171, <https://doi.org/10.5194/acp-19-14149-2019>, 2019.
- Che, H., Qi, B., Zhao, H., Xia, X., Eck, T. F., Goloub, P., Dubovik, O., Estelles, V., Cuevas-Agulló, E., Blarel, L., Wu, Y., Zhu, J., Du, R., Wang, Y., Wang, H., Gui, K., Yu, J., Zheng, Y., Sun, T., Chen, Q., Shi, G., and Zhang, X.: Aerosol optical properties and direct radiative forcing based on measurements from the China Aerosol Remote Sensing Network (CARSNET) in eastern China, *Atmos. Chem. Phys.*, 18, 405–425, <https://doi.org/10.5194/acp-18-405-2018>, 2018.
- Córdoba, C., Gil, M. El lidar micropulsado MPL (‘Micro Pulse Lidar’). Métodos de cálculo y algoritmo de inversión de los datos. Doc. N°: LI/DSC/4720/002/INTA. Instituto Nacional de Técnica Aeroespacial. Secretaría de Estado de Defensa. Ministerio de Defensa. Edición: 01. Mayo 2008.
- Fernald, F. G. Analysis of atmospheric lidar observations: some comments. *Applied Optics*, 23, 652–653, 1984.
- Gasteiger, J.; Wiegner, M. MOPSMAP v1.0: A versatile tool for the modeling of aerosol optical properties. *Geosci. Model Dev.* 2018, 11, 2739–2762.
- Giles, D. M., Sinyuk, A., Sorokin, M. G., Schafer, J. S., Smirnov, A., Slutsker, I., Eck, T. F., Holben, B. N., Lewis, J. R., Campbell, J. R., Welton, E. J., Korkin, S. V., and Lyapustin, A. I.: Advancements in the Aerosol Robotic Network (AERONET) Version 3 database – automated near-real-time quality control algorithm with improved cloud screening for Sun photometer aerosol optical depth (AOD) measurements, *Atmos. Meas. Tech.*, 12, 169–209, <https://doi.org/10.5194/amt-12-169-2019>, 2019.
- Klett, J. D. Lidar inversion with variable backscatter/extinction ratios. *Applied Optics*, 24, 1638–1643, [doi:10.1364/AO.24.001638](https://doi.org/10.1364/AO.24.001638), 1985.
- Klett, J. D. Stable analytical inversion solution for processing lidar returns. *Applied Optics*, 20, 211–220, [doi:10.1364/AO.20.000211](https://doi.org/10.1364/AO.20.000211), 1981.
- Lotteraner, C., Piringer M. (2016). Mixing-Height Time Series from Operational Ceilometer Aerosol-Layer Heights. *Boundary-Layer Meteorol.* DOI: 10.1007/s10546-016-0169-2.
- Pérez-Ramírez, D., Lyamani, H., Olmo, F. J., Whiteman, D. N., and Alados-Arboledas, L.: Columnar aerosol properties from sun-and-star photometry: statistical comparisons and day-to-night dynamic, *Atmos. Chem. Phys.*, 12, 9719–9738, <https://doi.org/10.5194/acp-12-9719-2012>, 2012.
- Román, R., Torres, B., Fuertes, D., Cachorro, V. E., Dubovik, O., Toledano, C., Cazorla, A., Barreto, A., Bosch, J. L., Lapyonok, T., González, R., Goloub, P., Perrone, M. R., Olmo, F. J., de Frutos, A., and Alados-Arboledas, L.: Remote sensing of lunar aureole with a sky camera: Adding information in the nocturnal retrieval of aerosol properties with GRASP code, *Remote Sens. Environ.*, 196, 238–252, <https://doi.org/10.1016/j.rse.2017.05.013>, 2017.
- Seibert P., Beyrich F., Gryning SE., Joffre S., Rasmussen A., Tercier P. Review and intercomparison of operational methods for the determination of the mixing height. *Atmos Environ* 34: 1001–1027, 2000.
- Toledano, C., González, R., Fuertes, D., Cuevas, E., Eck, T. F., Kazadzis, S., Kouremeti, N., Gröbner, J., Goloub, P., Blarel, L.,

- Román, R., Barreto, Á., Berjón, A., Holben, B. N., and Cachorro, V. E.: Assessment of Sun photometer Langley calibration at the high-elevation sites Mauna Loa and Izaña, *Atmos. Chem. Phys.*, 18, 14555-14567, <https://doi.org/10.5194/acp-18-14555-2018>, 2018.
- Wehrli, C.: Calibrations of filter radiometers for determination of atmospheric optical depth, *Metrologia*, 37, 419, <https://doi.org/10.1088/0026-1394/37/5/16>, 2000.
- Wehrli, C.: GAWPFR: A network of aerosol optical depth observations with precision filter radiometers, *GLOBAL ATMOSPHERE WATCH*, p. 36, 2005.

9.5 Staff

- Dr África Barreto (AEMET; Head of programme)
- Dr Emilio Cuevas (AEMET)
- Ramón Ramos (AEMET; Head of Infrastructure)
- Dr Rosa García (TRAGSATEC/UVA; Research Scientist)
- Dr Sergio León Luis (TRAGSATEC; Research Scientist)
- Dr Fernando Almansa (CIMEL/UVA; Research Scientist)
- Dr Yenny González (CIMEL; Research Scientist)
- Óscar Alvarez Losada (AEMET; Research Scientist)
- Pedro Miguel Romero (AEMET; Research Scientist)
- Dr Carmen Guirado Fuentes (UVA/AEMET; Research Scientist) left IARC in September 2019
- Dr Victoria Cachorro (University of Valladolid; Head of Atmospheric Optics Group)
- Dr Ángel de Frutos (University of Valladolid Atmospheric Optics Group; Research Scientist)
- Dr Margarita Yela (INTA; Co-PI in MPL sub-programme)

10 Radiation

The radiation programme, and specifically the implementation of its core component, the Baseline Surface Radiation Network (BSRN) programme, has been performed in close collaboration with the [University of Valladolid Atmospheric Optics Group](#).

10.1 Main Scientific Goals

The main scientific goals of this programme are:

- To conduct high quality measurement of radiation parameters.
- To investigate the variations of the solar radiation balance and other solar energy parameters at the three radiation stations managed by the IARC.
- To investigate aerosols radiative forcing with a particular focus on the role played by dust taking advantage of the privileged situation of the Canary Islands to analyse dust outbreaks over the North Atlantic and the unique local radiation network with stations at different altitudes (from sea level to 3555 m a.s.l.).
- To recover, digitize and analyse historical radiation data in order to reconstruct long-term radiation series that allow us to make precise studies concerning sky darkening and brightening, and relate radiation and cloud cover and solar flux.
- To conduct the spectral characterization of the solar radiation with respect to impacts of different types of clouds, aerosols, especially mineral dust, and precipitable water vapour.

10.2 Measurement Programme

Direct radiation records from an Abbot silver-disk pyrheliometer are available since 1916, although this information has not yet been analysed. Global solar radiation records from a bimetallic pyranograph are available both in bands and as daily integrated values in printed lists, since 1977. This information has been digitized, recalibrated and processed. The results show an excellent agreement between the bimetallic pyranograph and the BSRN CM21 pyranometer, which allowed the successful reconstruction of a long-term global radiation data series (since 1977), after a careful analysis of historical data (Figure 10.1).

Global and direct radiation measurements started in 1992 as part of a solar radiation project of the Canary Islands Government. In 2005, IZO joined the Spanish radiation network managed by the AEMET National Radiation Center (CNR). Since 2009, IZO has been a BSRN station providing the basic set of radiation parameters. In addition, other parameters, including shortwave and long wave upward radiation, UV-A and UV-B radiation are also

measured within the BSRN Programme. Later, some basic radiation measurements were implemented at the other three IARC measurement stations (SCO, TPO and BTO).

Radiation measurements are tested against physically possible and globally extremely rare limits, as defined and used in the BSRN recommended data quality control. Shortwave downward radiation (SDR) measurements are compared daily with SDR simulations, which are modelled with the LibRadtran model. This information has been created and shared on the web page <http://bsrn.aemet.es/>, where real time measurements of global, direct, diffuse and UV-B radiation are shown.

Measurements of spectral direct solar radiation (spectral direct normal irradiance) performed with an EKO MS-711 spectroradiometer (Fig. 10.2) started in 2016. This instrument covers a wavelength range from 300 to 1100 nm, exhibiting a Full Width at Half Maximum < 7 nm. It is equipped with its own built-in entrance optics, and the housing is temperature-stabilized at $25^{\circ} \pm 5^{\circ}$ (Egli et al., 2016). The main specifications of the EKO MS-711 are given in Table 10.1.

Table 10.1. Main specifications of the EKO MS-711 spectroradiometer

EKO MS-711 spectroradiometer	
Wavelength range	300 to 1100 nm
Wavelength interval	0.3 - 0.5nm
Optical resolution FWHM	< 7 nm
Wavelength accuracy	+/- 0.2 nm
Cosine Response (Zenith: 0 ~ 80°)	< 5%
Temp. dependency (-10°C to 50°C)	< 2 %
Temp. Control	25°C ± 5°C
Operating temperature	-10 to 50°C
Exposure time	10 msec – 5 sec Automatic adjustment
Dome material	Synthetic Quartz Glass
Communication	RS-422 (Between sensor and power supply)
Power requirement	12VDC, 50VA (from the power supply)

The EKO MS-711 spectroradiometer has been mounted on an Owel INTRA 3 sun-tracker (Fig. 10.2), an intelligent tracker which combines the advantages of automatic-tracking operation (automatic alignment with the system of astronomical coordinates follows after a few days), and actively-controlled tracking (a 4-quadrant sun sensor). It is constructed for use under extreme weather conditions; its operational temperature range is between -20 and +50 °C.

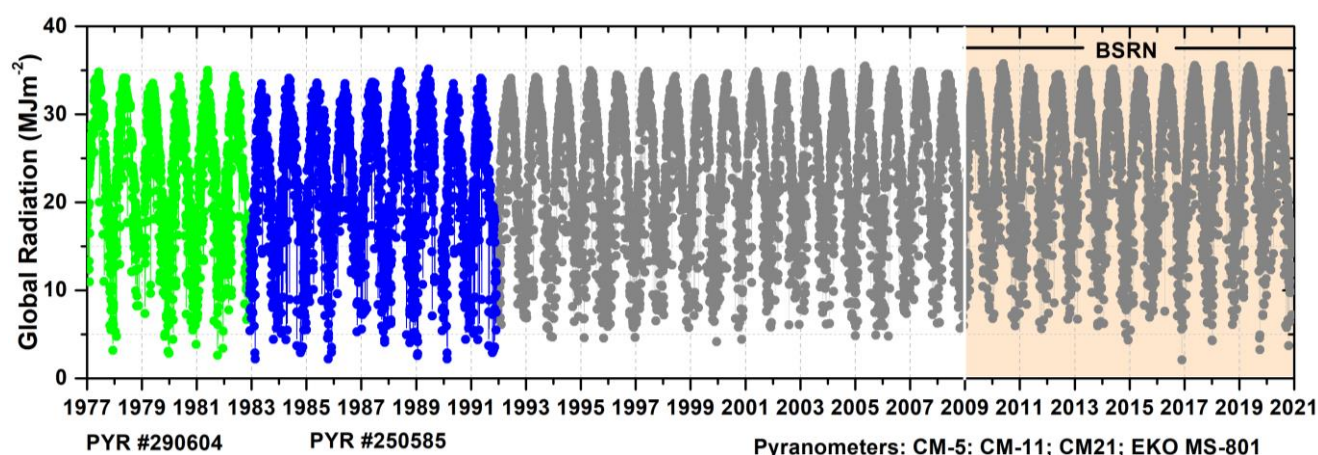


Figure 10.1. Daily GSR_H data time series between 1977 and 2020 at IZO. The green and blue dots correspond to the measurements performed with PYR #290609 and #250585, respectively, between 1977 and 1991, and the grey dots represent the measurements performed with different pyranometers (CM-5, CM-11, CM-21 and EKO MS-801) between 1992 and 2020 (García et al., 2014; 2017; 2019).

It can sustain about 50 kg of a carefully balanced load. The tracker motors have a special grease for use in low temperatures. The drive unit has an azimuth rotation $> 360^\circ$. It moves back to the start (morning) position at the corresponding midnight. The drive unit has a zenith rotation $> 90^\circ$. The unit has an angular resolution $\leq 0.1^\circ$, an angular repeatability of $\leq \pm 0.05^\circ$ and an angular velocity $\geq 1.5^\circ/\text{s}$ on the outgoing shafts. The maximum speed is $2.42^\circ/\text{s}$.

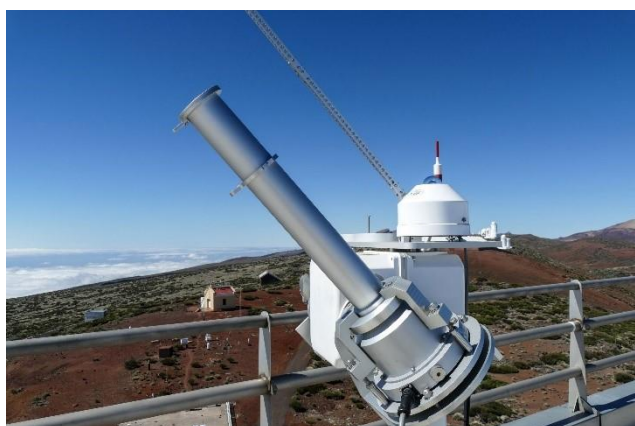


Figure 10.2. The EKO MS-711 spectroradiometer installed at IZO.

The spectral direct solar radiation measurements have been complemented since February 2020 by global and diffuse solar radiation measurements performed with an EKO RSB spectroradiometer (Fig. 10.3). This instrument covers a wavelength range from 300 to 1100 nm. The main specifications of the EKO RSB are given in Table 10.2.

The atmospheric transmission is a data product that is produced since 2014, it was also processed retrospectively back until 2009, and it has been updated until December 31st 2020 (Fig. 10.4). It is available at the IZO BSRN web page. The atmospheric transmission is derived from broadband (0.2 to $4.0 \mu\text{m}$) direct solar irradiance BSRN observations. Data are for clear-sky mornings between solar elevations of 11.3° and 30° .

Table 10.2. Main specifications of the EKO RSB spectroradiometer

EKO RSB spectroradiometer	
Wavelength range	300 to 1100 nm
Wavelength accuracy	$\pm 0.2 \text{ nm}$
Directional response	$< 5^\circ$
Measurement time	10-5000 ms
Precision of Shadow Band Position	$\pm 2^\circ$
Measurement Frequency	1 rotation / minute
Operating temperature	$-10 \text{ to } 50^\circ\text{C}$
Temperature control	$25^\circ \pm 2^\circ\text{C}$
Shielding Angle	5°
Field of view	180°



Figure 10.3. The EKO RSB spectroradiometer installed at IZO.

A summary of the radiation measurement programme managed by the IARC is shown in Table 10.3.

Table 10.3. Details of IARC radiation measurement programme.

Instrument	Measurements	Spectral Range
Izaña historical records (2373 m a.s.l.) Start Date: Different dates		
Abbot silver-disk pyrheliometer	Direct Radiation (1916)	~0.3 to ~3.0 μm
Bimetallic pyranograph (analog.)	Global Radiation (Jan 1977)	~0.3 to ~3.0 μm
YES Multi Filter Rotating Shadow-band Radiometer	Global, diffuse and estimated direct radiation (Feb 1996)	300-1200 nm
K&Z CM5 pyranometer	Global radiation (Jan 1992)	310-2800 nm
Izaña BSRN Station (2373 m a.s.l.) Start Date: March 2009		
Pyranometer K&Z CM-21, EKO MS-801	Global and Diffuse Radiation	285-2600 nm
Pyrheliometer K&Z CH-1, EKO MS-56	Direct Radiation	200-4000 nm
Pyrgeometer K&Z CG-4	Longwave Downward Radiation	4500-42000 nm
Net Radiometer, EKO MR-60	Net Radiation	
Pyranometer K&Z UV-A-S-T	UV-A Radiation	315-400 nm
Pyranometer Yankee YES UVB-1	UV-B Radiation	280-400 nm
Absolute Cavity Pyrheliometer PMO6	Direct Radiation	-
Spectroradiometer EKO MS-711	Spectral Direct Radiation	300-1100 nm
Spectroradiometer EKO RSB	Spectral Global and Diffuse Radiation	300-1100 nm
EKO MS-321LR Sky Scanner	Luminance/Radiance	-
Izaña National Radiation Center (CNR) Station (2373 m a.s.l.) Start Date: August 2005		
Pyranometer K&Z CM-21	Global and Diffuse Radiation	285-2600 nm
Pyrheliometer K&Z CH-1	Direct Radiation	200-4000 nm
Pyrgeometer K&Z CG-4	Longwave Downward Radiation	4500-42000 nm
Pyranometer Yankee YES UVB-1	UV-B Radiation	280-400 nm
Pyranometer K&Z PQS1	Photosynthetically Active Radiation (PAR)	400-700 nm
SCO (52 m a.s.l.) Start Date: February 2006		
Pyranometer K&Z CM-11	Global and Diffuse Radiation	310-2800 nm
Pyrheliometer EPPLY	Direct Radiation	200-4000 nm
BTO (114 m a.s.l.) Start Date: 2009		
Pyranometer K&Z CM-11	Global and Diffuse Radiation	310-2800 nm
TPO (3555 m a.s.l.) Start Date: July 2012		
Pyranometer K&Z CM-11, CM-21	Global and Diffuse Radiation	310-2800 nm
Pyranometer Yankee YES UVB-1	UV-B Radiation	280-400 nm
SPN1 Sunshine Pyranometer	Global and Diffuse Radiation	400-2700 nm

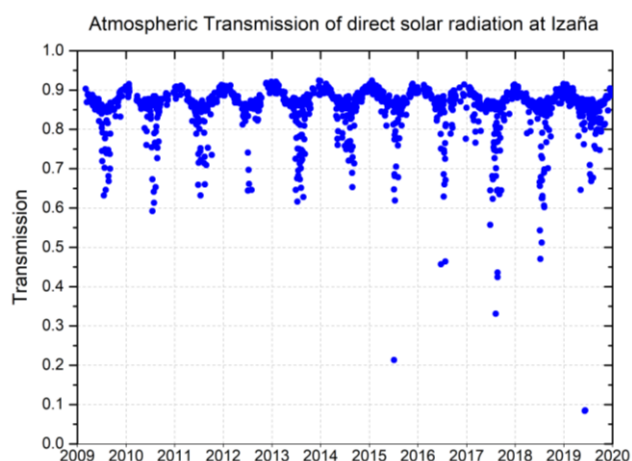


Figure 10.4. Daily atmospheric transmission data (2009-2020) at IZO computed for clear-sky mornings between solar elevations of 11.3° and 30°.

Sky images from SONA total-sky cameras at IZO and SCO, meteorological vertical profiles from radiosondes, AOD and AE from Cimel and PFR sunphotometers, column water vapour from Cimel and GPS/GLONASS, column NO₂ from DOAS, and total O₃ from Brewer spectrophotometer are used as ancillary data and/or as input data in LibRadtran SDR simulations.

10.3 New instrumentation: Sky scanner

In late 2020, an EKO sky scanner model MS 321-LR was installed at IZO (Figure 10.5a). This instrument is provided with two sensors, one measures the sky luminance (Kcd/m²) and the other measures the sky radiance (W/m²sr) (Figure 10.5b). The sensors are mounted on a tracker. Data from the sky scanner is obtained in 10 min. intervals during daylight (each scan takes up to 4.5 min.). The distribution of both luminance and radiance, is obtained by dividing the sky dome in 145 patches with field of view of 11° (Figure 10.5b). The main specifications of the EKO MS 321-LR are listed in Table 10.4.

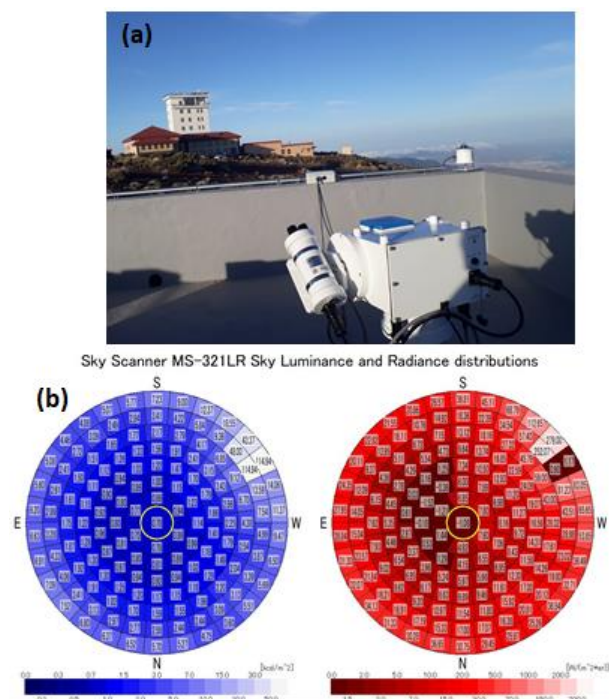


Figure 10.5. (a) The sky scanner EKO MS-321 LR installed at IZO. (b) An example of sky luminance (blue colour) and radiance (red colour) distribution measurements.

Table 10.4. Main specifications of the EKO MS 321-LR sky scanner.

EKO MS 321-LR		
Luminance Sensor	Spectral response	VISIBLE response (CIE)
	Illuminance	0 - 50 Kcd/m ²
	Field of view	11°
	Slope angle	1°
Radiance Sensor	Linearity	0.3%
	Spectral response	0.3 – 3 μm
	Range	0 – 300 W/m ² sr
	Field of view	11°
	Slope angle	1°
	Linearity	0.5%

10.4 Participation in Scientific Projects and Campaigns/Experiments

10.4.1 Calibration campaign of BSRN instruments with a PMO6 Absolute Cavity Pyrheliometer

As part of the radiation quality assurance system a calibration campaign of BSRN pyranometers and pyrheliometer took place in summers 2019 and 2020 using an Absolute Cavity Pyrheliometer PMO6 as reference (Fig. 10.6). The PMO6 was calibrated in the World Radiation Center, Davos. The BSRN instruments were calibrated following the ISO 9059:1990 (E) and ISO 9846:1993(E), delivering the corresponding official calibration certificates.



Figure 10.6. Absolute cavity radiometer (PMO6) installed at IZO during summers 2019 and 2020 on the BSRN sun-tracker.

10.5 Future activities

The main on-going and future activities of the radiation programme are focused on:

- Characterization of CIE standard sky types at Izaña station from sky scanner measurements.
- Accurate determination of cloud attenuation impact on global, direct and diffuse spectral radiation performed with EKO RSB spectroradiometer from SCO and IZO.
- Reconstruction and accurate analysis of a new long-term GSR data series (since 1916) in which newly recovered observation data are being incorporated. Long-term records of aerosols (AOD), cloudiness, and solar flux will be compared with GSR data.
- Accurate determination of cloud attenuation impact on global radiation using GSR from SCO and BTO.
- Accurate analysis of UV-B broadband data from the vertical transect formed by SCO (52 m a.s.l.), IZO (2373 m a.s.l) and TPO (3555 m a.s.l.) observatories, with complementary information on cloudiness, AOD and O₃ vertical profiles (ECC O₃ sondes).

10.6 References

- Driemel, A., Augustine, J., Behrens, K., Colle, S., Cox, C., Cuevas-Agulló, E., Denn, F. M., Duprat, T., Fukuda, M., Grobe, H., Haeffelin, M., Hodges, G., Hyett, N., Ijima, O., Kallis, A., Knap, W., Kustov, V., Long, C. N., Longenecker, D., Lupi, A., Maturilli, M., Mimouni, M., Ntsangwane, L., Ogihara, H., Olano, X., Olefs, M., Omori, M., Passamani, L., Pereira, E. B., Schmithüsen, H., Schumacher, S., Sieger, R., Tamlyn, J., Vogt, R., Vuilleumier, L., Xia, X., Ohmura, A., and König-Langlo, G.: Baseline Surface Radiation Network (BSRN): structure and data description (1992–2017), *Earth Syst. Sci. Data*, 10, 1491–1501, <https://doi.org/10.5194/essd-10-1491-2018>, 2018.
- Egli, L., Gröbner, J., Hülsen, G., Bachmann, L., Blumthaler, M., Dubard, J., Khazova, M., Kift, R., Hoogendijk, K., Serrano, A., Smedley, A., and Vilaplana, J.-M.: Quality assessment of solar UV irradiance measured with array spectroradiometers, *Atmos. Meas. Tech.*, 9, 1553–1567, [doi:10.5194/amt-9-1553-2016](https://doi.org/10.5194/amt-9-1553-2016), 2016.
- García, R. D., Cuevas, E., García, O. E., Cachorro, V. E., Pallé, P., Bustos, J. J., Romero-Campos, P. M., and de Frutos, A. M.: Reconstruction of global solar radiation time series from 1933 to 2013 at the Izaña Atmospheric Observatory, *Atmos. Meas. Tech.*, 7, 3139–3150, [doi:10.5194/amt-7-3139-2014](https://doi.org/10.5194/amt-7-3139-2014), 2014.
- García, R. D., Cuevas, E., García, O. E., Ramón, R., Romero-Campos, P. M., de Ory, F., Cachorro, V. E., and de Frutos, A.: Compatibility of different measurement techniques. Long-term global solar radiation observations at Izaña Observatory, *Atmos. Meas. Tech.*, 10, 731–743, [doi:10.5194/amt-10-731-2017](https://doi.org/10.5194/amt-10-731-2017), 2017.
- García, R. D., Barreto, A., Cuevas, E., Gröbner, J., García, O. E., Gómez-Peláez, A., Romero-Campos, P. M., Redondas, A., Cachorro, V. E., and Ramos, R.: Comparison of observed and modeled cloud-free longwave downward radiation (2010–2016) at the high mountain BSRN Izaña station, *Geosci. Model Dev.*, 11, 2139–2152, <https://doi.org/10.5194/gmd-11-2139-2018>, 2018.
- García, R. D., Cuevas, E., Ramos, R., Cachorro, V. E., Redondas, A., and Moreno-Ruiz, J. A.: Description of the Baseline Surface Radiation Network (BSRN) station at the Izaña Observatory (2009–2017): measurements and quality control/assurance procedures, *Geosci. Instrum. Method. Data Syst.*, 8, 77–96, <https://doi.org/10.5194/gi-8-77-2019>, 2019.
- García, R. D., Cuevas, E., Barreto, Á., Cachorro, V. E., Pó, M., Ramos, R., and Hoogendijk, K.: Aerosol retrievals from the EKO MS-711 spectral direct irradiance measurements and corrections of the circumsolar radiation, *Atmos. Meas. Tech.*, 13, 2601–2621, <https://doi.org/10.5194/amt-13-2601-2020>, 2020.
- García, R.D.; Cuevas, E.; Cachorro, V.E.; García, O.E.; Barreto, Á.; Almansa, A.F.; Romero-Campos, P.M.; Ramos, R.; Pó, M.; Hoogendijk, K.; Gross, J: Water Vapor Retrievals from Spectral Direct Irradiance Measured with an EKO MS-711 Spectroradiometer-Intercomparison with Other Techniques, *Remote Sens.*, 13, 350. <https://doi.org/10.3390/rs13030350>, 2021.
- Kaisa Lakkala, Jukka Kujanpää, Colette Brogniez, Nicolas Henriot, Antti Arola, Margit Aun, Frédérique Auriol, Alkiviadis F. Bais, Germar Bernhard, Veerle De Bock, Maxime Catalfamo, Christine Deroo, Henri Diémoz, Luca Egli, Jean-Baptiste Forestier, Ilias Fountoulakis, Katerina Garane, Rosa Delia Garcia, Julian Gröbner, Seppo Hassinen, Anu Heikkilä, Stuart Henderson, Gregor Hülsen, Björn Johnsen, Niilo

Kalakoski, Angelos Karanikolas, Tomi Karppinen, Kevin Lamy, Sergio F. León-Luis, Anders V. Lindfors, Jean-Marc Metzger, Fanny Minvielle, Harel B. Muskatel, Thierry Portafaix, Alberto Redondas, Ricardo Sanchez, Anna Maria Siani, Tove Svendby, and Johanna Tamminen.: Validation of the TROPOspheric Monitoring Instrument (TROPOMI) surface UV radiation product Atmos. Meas. Tech., 13, 6999–7024, <https://doi.org/10.5194/amt-13-6999-2020>, 2020.

10.7 Staff

Dr Emilio Cuevas (AEMET; Head of programme)

Dr Rosa García (TRAGSATEC/AEMET/UVA; Co-PI)

Ramón Ramos (AEMET; Head of Infrastructure)

Dr Omaira García (AEMET; Research Scientist)

Dr Sergio León (TRAGSATEC; Research Scientist)

Dr Victoria Cachorro (University of Valladolid; Head of Atmospheric Optics Group)

Dr Ángel de Frutos (University of Valladolid Atmospheric Optics Group; Research Scientist)

11 Differential Optical Absorption Spectroscopy (DOAS)

11.1 Main Scientific Goals

Differential Optical Absorption Spectroscopy (DOAS) and Multi Axis Differential Optical Absorption Spectroscopy (MAXDOAS) techniques allow the determination of atmospheric trace gases present in very low concentrations. The long-term monitoring of atmospheric trace gases is of a great interest for trend studies and satellite validation. The detection of gases using DOAS or MAXDOAS technique allows the study of mutual interaction between gases even when detection limits of the gases are low.

The main scientific goals of the DOAS and MAXDOAS programme are:

- To improve the knowledge of the distribution, seasonal behaviour and long-term trends of minor constituents related to ozone equilibrium such as NO₂, BrO and IO and their distribution in the subtropical atmosphere.
- To obtain a climatology of stratospheric NO₂ and BrO in subtropical regions and to study its dependence on environmental and climatic variables.
- To study the seasonal variations of NO₂, O₃, formaldehyde (HCHO) and IO in the free troposphere and their interaction with environmental factors such as Saharan dust amongst others.
- To contribute to validation of NO₂ and O₃ satellite products (GOME, GOME2, SCIAMACHY, OMI, TROPOMI) and in the improvement of the methodology to perform comparisons of DOAS and MAXDOAS with satellite products.

11.2 Measurement Programme

The DOAS technique (Platt and Stutz, 2008) is a method to determine the atmospheric trace gases column density by measuring their absorption structures in the near ultraviolet and visible spectral region.



Figure 11.1. RASAS II and ARTIST II MAXDOAS (UV-VIS) spectroradiometers at IARC.

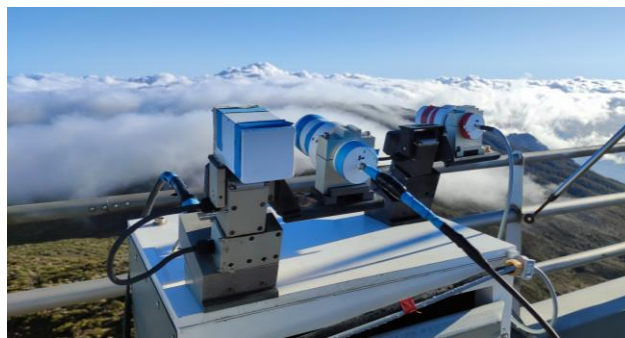


Figure 11.2. DOAS instruments outdoor optics with sky trackers.

The technique is based on measurement of atmospheric absorption of solar radiation at selected wavelength bands where the gas under consideration shows a structured and known absorption cross-section. For stratospheric observations the instrument is pointed at zenith during the twilights.

Although the DOAS technique was developed for stratospheric research, during the last few years it has been largely employed in tropospheric environment and pollution episodes studies. In particular, the so called Multi Axis Differential Optical Absorption Spectroscopy approach allows to infer vertical distribution of minor species from spectrometric measurements of solar scattered light at given angles of elevation (off-axis measurements). The analysis technique makes use of the Optical Estimation Method (Rodgers, 2000) by putting together the off-axis measurements and a radiative transfer algorithm to get the best solution for all used elevation angles.

The instruments (see Figures 11.1 and 11.2) automatically take spectra from an AM SZA = 96° to PM SZA = 96°, every day. As the instrument must work with a stabilized room temperature and also with a stabilized internal temperature and humidity, those parameters are monitored and recorded in data files. Calibration of the instrument grating is performed approximately every year. Calibration of the elevation angle is performed once a month. After the spectral inversion, a quality control of data is carried out. The acquired data are filtered on the basis of the analysis and instrumental error, aerosol optical thickness and the solar zenith angles, to ensure quality.

INTA has performed measurements of stratospheric O₃ and NO₂ at IARC since 1993. Data have been used for the study of stratospheric O₃ and NO₂ distribution in the subtropical region (Gil et al., 2008, Gil et al., 2012 and Yela et al., 2017) and for validation of satellite products (Hendrick et al., 2011, Robles-Gonzalez et al., 2016, Yela et al., 2017). In 2003, the installation of an ultraviolet DOAS spectrometer expanded the measurements of stratospheric gases to the near ultraviolet region, allowing the monitoring of stratospheric BrO and the estimation of the concentration of BrO in the free troposphere. In 2010, the instruments were adapted to MAXDOAS measurements, allowing the

detection of free tropospheric trace gases, such as IO and NO₂ (Puentedura et al, 2012, Gomez et al., 2014, Gil-Ojeda et al., 2015) in the visible region and of BrO and HCHO in the ultraviolet region. Prior to the installation at IZO in 2009, the VIS-MAXDOAS instrument participated in the international blind NO₂ MAXDOAS intercomparison campaign CINDI (Cabauw Intercomparison campaign Nitrogen Dioxide measuring Instrument) (Piters et al., 2012, Pinardi et al., 2013). During the AMISOC campaign in 2013, extensive measurements of IO were performed at three different altitude levels on Tenerife.

11.3 Participation in Scientific Projects and Campaigns/Experiments

11.3.1 Contribution to NDACC data base

The Network for Detection of Atmospheric Composition Change (De Mazière et al., 2018) is one of the most important global networks which primary goal is to

establish long-term databases for detecting changes and trends in the chemical and physical state of the atmosphere and to assess the coupling of such changes with climate and air quality. INTA, with DOAS measurements of O₃ and NO₂ at IZO, have contributed to NDACC since 1998. Participation in NDACC requires compliance with strict measurement and data protocols to ensure that the network data are of high and consistent quality. NO₂ and O₃ results are shown in Figures 11.3 and 11.4.

11.3.2 Contribution to CAMS27

The Copernicus Atmosphere Monitoring Service (CAMS) is an integrated service within the Copernicus program that provides information on the atmospheric composition. CAMS27 provides CAMS or high-quality atmospheric data in HDF GEOMS format within a few weeks after measurements acquisition from selected NDACC stations, such as the DOAS measurements at IARC from INTA.

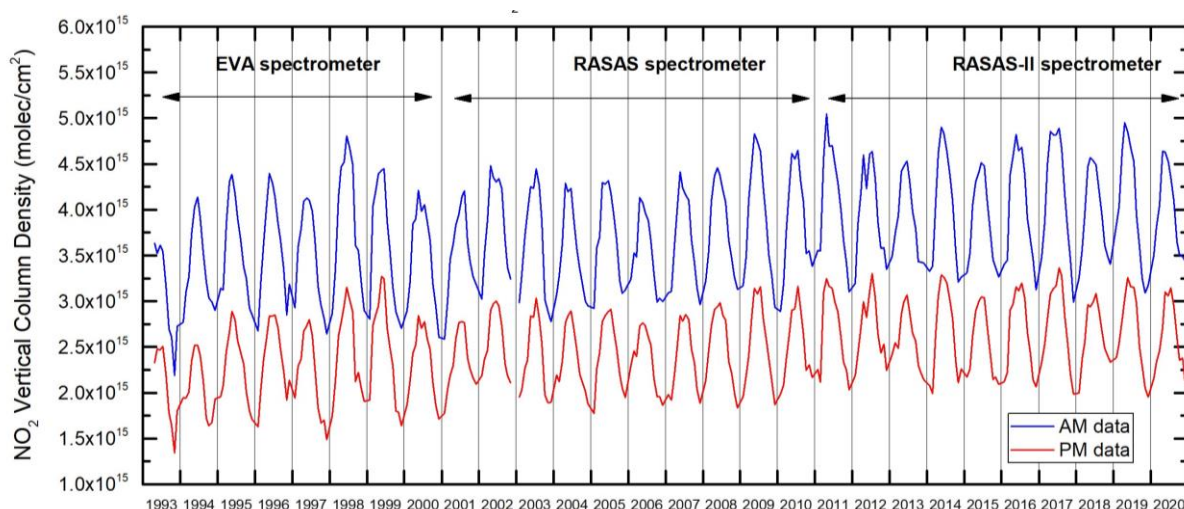


Figure 11.3. Time series of reanalyzed stratospheric NO₂ 1993-2020.

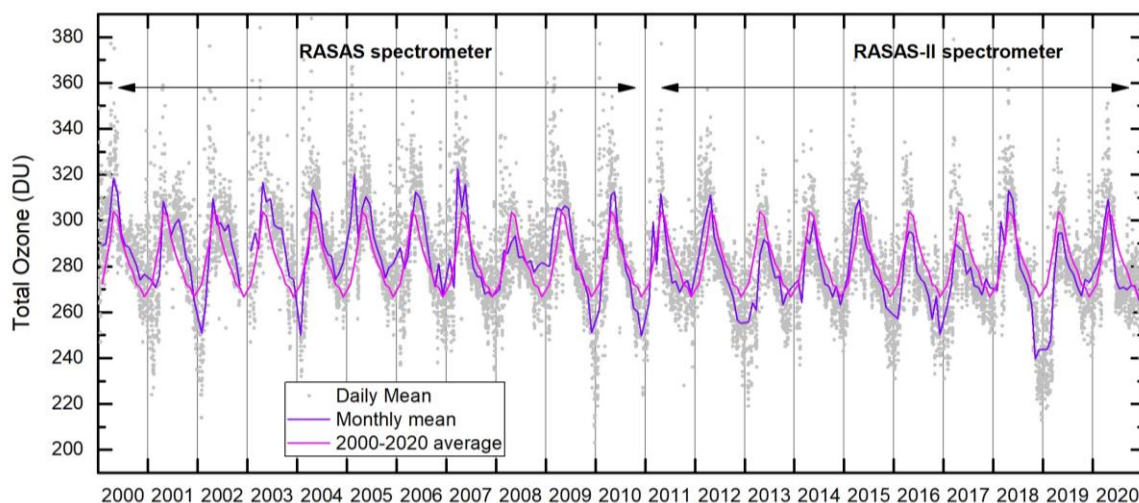


Figure 11.4. Time series of reanalyzed stratospheric O₃ 2000-2020.

11.3.3 S5P Nitrogen Dioxide and Formaldehyde Validation (NIDFORVal) using NDACC and complementary FTIR and UV-Vis DOAS ground-based remote sensing data

NIDFORVal is an ESA proposal (ID28607) led by the Royal Belgian Institute for Space Aeronomy (BIRA-IASB) that started in 2016 and extends to 2024. The aim of this project is to establish a network of observations supporting validation for tropospheric products of the Sentinel-5 Precursor (Sentinel-5P). The INTA-MAXDOAS instruments installed at IARC are part of the Sentinel-5P Calibration and Validation Team for NO₂.

11.3.4 Contribution to FRM4DOAS

Fiducial Reference Measurements (FRM) can be defined as a suite of independent, fully characterized, and traceable ground measurements that follow the guidelines outlined by the project Quality Assured Data for Earth Observation communities (QA4EO). These FRM provide the maximum return on investment for a satellite mission by delivering to users the required confidence in data products, in the form of independent validation of results and satellite measurement uncertainty estimation, over the entire end-to-end duration of a satellite mission. A number of FRM projects have been set up in the past by ESA to build up FRM for different satellites and measurement types.

FRM4DOAS (FRM for DOAS) is an ESA proposal, led by BIRA-IASB, that started in 2016 and ended in 2020. During FRM4DOAS, several activities related to the MAXDOAS measurement technique were carried out with three main objectives: the specification of best practices for MAXDOAS instrumentation operation, the evaluation of the different existing MAXDOAS analysis algorithms, and finally, the development and implementation of a central and automatic processing system in near real time for the delivery of harmonized MAXDOAS data products and with an exhaustive quality control (NDACC MAXDOAS Service).

The VIS-MAXDOAS instrument installed at IARC is part of the FRM4DOAS project providing NO₂ and O₃ DOAS/MAXDOAS data products.

11.4 Summary of remarkable results during the period 2019-2020

11.4.1 Satellite validation

The Izaña VIS-MAXDOAS instrument measurements have participated in two validation studies of TROPOMI Sentinel-5P (S5P) NO₂ products.

Marais et al. (2021) utilised Izaña VIS-MAXDOAS tropospheric NO₂ column data to compare and evaluate upper tropospheric NO₂ TROPOMI observations from June 2019 to February 2020. The MAXDOAS instrument at

IARC, as a high altitude free tropospheric monitoring site, is a good candidate for this intercomparison. Upper tropospheric NO₂ TROPOMI products are retrieved using cloud-slicing retrieval technique.

Verhoelst et al. (2021) compared tropospheric, stratospheric and total NO₂ column from TROPOMI S5P to globally distributed correlative measurements collected by 19 MAXDOAS, 26 NDACC zenith DOAS, and 25 Pandora Global Network instruments, in the frame of the NIDFORVal project. Izaña VIS-DOAS zenith NO₂ has participated in this work with the data used for comparison with stratospheric NO₂ column product from TROPOMI S5P.

11.5 References

- De Mazière, M., Thompson, A. M., Kurylo, M. J., Wild, J. D., Bernhard, G., Blumenstock, T., Braathen, G. O., Hannigan, J. W., Lambert, J.-C., Leblanc, T., McGee, T. J., Nedoluha, G., Petropavlovskikh, I., Seckmeyer, G., Simon, P. C., Steinbrecht, W., and Strahan, S. E.: The Network for the Detection of Atmospheric Composition Change (NDACC): history, status and perspectives, *Atmos. Chem. Phys.*, 18, 4935-4964, <https://doi.org/10.5194/acp-18-4935-2018>, 2018.
- Gil-Ojeda, M., M. Navarro-Comas, A. Redondas, O. Puertedura, F. Hendrick, M. Van Roozendaal, J. Iglesias and E. Cuevas. Título: Total ozone measurements from the NDACC Izaña Subtropical Station: Visible spectroscopy versus Brewer and satellite instruments. Quadrennial Ozone Symposium, (QOS 2012). Toronto, Canada. 27-31 August 2012.
- Gil-Ojeda, M. Navarro-Comas, L. Gómez-Martín, J. A. Adame, A. Saiz-Lopez, C. A. Cuevas, Y. González, O. Puertedura, E. Cuevas, J.-F. Lamarque, D. Kinnison, S. Tilmes, NO₂ seasonal evolution in the north subtropical free troposphere, *Atmos. Chem. Phys.*, 15, pp. 10569-10579, doi:10.5194/acp-15-10567-2015, 2015.
- Gil, M., M. Yela, L. N. Gunn, A. Richter, I. Alonso, M. P. Chipperfield, E. Cuevas, J. Iglesias, M. Navarro, O. Puertedura, and S. Rodriguez, NO₂ climatology in the northern subtropical region: diurnal, seasonal and interannual variability *Atmos. Chem. Phys.* 8, 1635–1648, 2008.
- Gomez, L., Navarro-Comas, M., Puertedura, O., Gonzalez, Y., Cuevas, E., and Gil-Ojeda, M.: Long-path averaged mixing ratios of O₃ and NO₂ in the free troposphere from mountain MAX-DOAS, *Atmos. Meas. Tech.*, 7, 3373-3386, doi:10.5194/amt-7-3373-2014, 2014.
- Hendrick, F., J.-P. Pommereau, F. Goutail, R. D. Evans, D. Ionov, A. Pazmino, E. Kyrö, G. Held, P. Eriksen, V. Dorokhov, M. Gil, and M. Van Roozendaal, NDACC/SAOZ UV-visible total ozone measurements: improved retrieval and comparison with correlative ground-based and satellite observations, *Atmos. Chem. Phys.*, 11, 5975-5995, 2011.
- Marais, E. A., Roberts, J. F., Ryan, R. G., Eskes, H., Boersma, K. F., Choi, S., Joiner, J., Abuhassan, N., Redondas, A., Grutter, M., Cede, A., Gomez, L., and Navarro-Comas, M.: New observations of NO₂ in the upper troposphere from TROPOMI, *Atmos. Meas. Tech.*, 14, 2389–2408, <https://doi.org/10.5194/amt-14-2389-2021>, 2021.
- Pinardi, G., Van Roozendaal, M., Abuhassan, N., Adams, C., Cede, A., Clémer, K., Fayt, C., Frieß, U., Gil, M., Herman, J., Hermans, C., Hendrick, F., Irie, H., Merlaud, A., Navarro

- Comas, M., Peters, E., Piters, A. J. M., Puertedura, O., Richter, A., Schönhardt, A., Shaiganfar, R., Spinei, E., Strong, K., Takashima, H., Vrekoussis, M., Wagner, T., Wittrock, F., and Yilmaz, S.: Erratum: MAX-DOAS formaldehyde slant column measurements during CINDI: intercomparison and analysis improvement (Atmospheric Measurement Techniques (2013) 6 (167-185)), *Atmos. Meas. Tech.*, 6 (2), 219, doi: 10.5194/amt-6-219-2013, 2013.
- Piters, A. et al.: The Cabauw Intercomparison campaign for Nitrogen Dioxide measuring Instruments (CINDI): design, execution, and early results, *Atmos. Meas. Tech.*, 5, 457-485, doi:10.5194/amt-5-457-2012, 2012.
- Platt and Stutz, *Differential Optical Absorption Spectroscopy, Principles and Applications*, Springer, 2008.
- Puertedura, O., Gil, M., Saiz-Lopez, A., Hay, T., Navarro-Comas, M., Gómez-Pelaez, A., Cuevas, E., Iglesias, J., and Gomez, L.: Iodine monoxide in the north subtropical free troposphere, *Atmos. Chem. Phys.*, 12, 4909-4921, doi:10.5194/acp-12-4909-2012, 2012.
- Robles-Gonzalez, C., Navarro-Comas, M., Puertedura, O., Schneider, M., Hase, F., Garcia, O., Blumenstock, T., and Gil-Ojeda, M.: Intercomparison of stratospheric nitrogen dioxide columns retrieved from ground-based DOAS and FTIR and satellite DOAS instruments over the subtropical Izana station, *Atmos. Meas. Tech.*, 9, 4471-4485, doi:10.5194/amt-9-4471-2016, 2016.
- Rodgers, C.D., *Inverse methods for Atmospheric Sounding: Theory and Practice*, World Scientific, Series on Atmospheric, Oceanic and Planetary Physics, Vol. 2, 2000.
- Verhoelst, T., Compennolle, S., Pinardi, G., Lambert, J.-C., Eskes, H. J., Eichmann, K.-U., Fjæraa, A. M., Granville, J., Niemeijer, S., Cede, A., Tiefengraber, M., Hendrick, F., Pazmiño, A., Bais, A., Bazureau, A., Boersma, K. F., Bogner, K., Dehn, A., Donner, S., Elokhorov, A., Gebetsberger, M., Goutail, F., Grutter de la Mora, M., Gruzdev, A., Gratsea, M., Hansen, G. H., Irie, H., Jepsen, N., Kanaya, Y., Karagkiozidis, D., Kivi, R., Kreher, K., Levelt, P. F., Liu, C., Müller, M., Navarro Comas, M., Piters, A. J. M., Pommereau, J.-P., Portafaix, T., Prados-Roman, C., Puertedura, O., Querel, R., Remmers, J., Richter, A., Rimmer, J., Rivera Cárdenas, C., Saavedra de Miguel, L., Sinyakov, V. P., Stremme, W., Strong, K., Van Roozendael, M., Veefkind, J. P., Wagner, T., Wittrock, F., Yela González, M., and Zehner, C.: Ground-based validation of the Copernicus Sentinel-5P TROPOMI NO₂ measurements with the NDACC ZSL-DOAS, MAX-DOAS and Pandonia global networks, *Atmos. Meas. Tech.*, 14, 481-510, <https://doi.org/10.5194/amt-14-481-2021>, 2021.
- Yela, M., Gil-Ojeda, M., Navarro-Comas, M., Gonzalez-Bartolomé, D., Puertedura, O., Funke, B., Iglesias, J., Rodríguez, S., García, O., Ochoa, H., and Deferrari, G.: Hemispheric asymmetry in stratospheric NO₂ trends, *Atmos. Chem. Phys.*, 17, 13373-13389, <https://doi.org/10.5194/acp-17-13373-2017>, 2017. Yela, M., Gil-Ojeda, M., Navarro-Comas, M., Gonzalez-Bartolomé, D., Puertedura, O., Funke, B., Iglesias, J., Rodríguez, S., García, O., Ochoa, H., and Deferrari, G.: Hemispheric asymmetry in stratospheric NO₂ trends, *Atmos. Chem. Phys.*, 17, 13373-13389, <https://doi.org/10.5194/acp-17-13373-2017>, 2017.

11.6 Staff

The DOAS research group is composed of researchers and specialist technicians from INTA and IARC-AEMET.

Dr Margarita Yela González (INTA; Head of programme)

Dr Olga Puertedura Rodríguez (INTA; Research Scientist)

Dr Mónica Navarro Comas (INTA; Research Scientist)

Javier Iglesias Méndez, (INTA; Research Scientist)

Dr Laura Gómez Martín (INTA; Research Scientist)

Ramón Ramos (AEMET; Head of Infrastructure)

12 Water Vapour

12.1 Main Scientific Goals

The main scientific goals of this programme are:

- To conduct high quality observations and to study precipitable water vapour (PWV) total column content and vertical profile.
- To analyse intra-hourly variability as well as daily and annual mean cycles of PWV for different locations and altitudes of Tenerife and La Palma islands.
- To study radiative forcing due to water vapour and clouds.
- To study monthly and annual mean series, analyzing their homogeneity and evaluating their anomalies and evolution over time to detect possible trends.
- To contribute to the European Meteorological Network (EUMETNET) Water Vapour Programme within the framework of the E-PROFILE Atmospheric Profiling Programme with measurements from the Vaisala CL51 Ceilometer at SCO and from the RPG-LHATPRO-G5 series microwave radiometer, recently acquired and installed at IZO.

12.2 Measurement Programme

Several instruments and measurement techniques are used in this programme as detailed below.

12.2.1 Global Navigation Satellite System technique

The Global Navigation Satellite System (GNSS) technique consists in determining PWV in the atmospheric column from the observed delay in radio signals at two different frequencies emitted by a network of Global Positioning System (GPS) and Global Navigation Satellite System (GLONASS) satellites received by a GNSS receiver (Fig. 12.1).



Figure 12.1. Global Navigation Satellite System receiver at Izaña Observatory.

Currently, the group works with 11 GNSS receiver stations (Fig. 12.2) at different altitudes, ten of them in Tenerife and one in La Palma. Las Cañadas and Teide are the names of the last two GNSS receiving stations that were incorporated into the routine evaluation on 4 February 2020.

The atmospheric pressure in places where the GNSS antennas are located is a key parameter for obtaining the PWV from the zenith total delay (ZTD) and zenith hydrostatic delay (ZHD). The Spanish National Geographic Institute (IGN) is in charge of managing the GNSS network and data acquisition, as well as the calculation of the ZTD from the GNSS signals using the Bernese 5.2 software applied for both ultra-fast and precise orbits.

The ZHD calculation depends on the temperature and pressure at the GNSS antenna sites. However, atmospheric pressure plays a more important role in determination of PWV than temperature. An uncertainty of 1 hPa in pressure produces, approximately, the same uncertainty in determination of PWV (0.33 mm to 0.36 mm) as an uncertainty of 5K in temperature (Hagemann et al., 2003).

The PWV is calculated from ZTD and pressure values at the different GNSS stations. One of the most important tasks carried out is to estimate the pressure at the GNSS sites where surface pressure measurements are not available due to the absence of barometric sensors. To do this, based on the perfect gas law and the hydrostatic equation, a precise value of pressure as a function of altitude and temperature is calculated for each GNSS station using a grid of ten automatic meteorological stations (EMA) equipped with barometric and temperature sensors, located at different altitudes (Fig. 12.2).

The values of the PWV column are obtained in quasi-real time at each GNSS station from the ZTD from ultra-fast GNSS orbits, which have a temporal resolution of 15 minutes and are available approximately every two hours. Values are plotted as contour maps (Fig. 12.3a). Together with these maps, profiles are obtained that represent the amount of PWV comprised in layers located between GNSS stations. Fig. 12.3b shows one of these profiles.

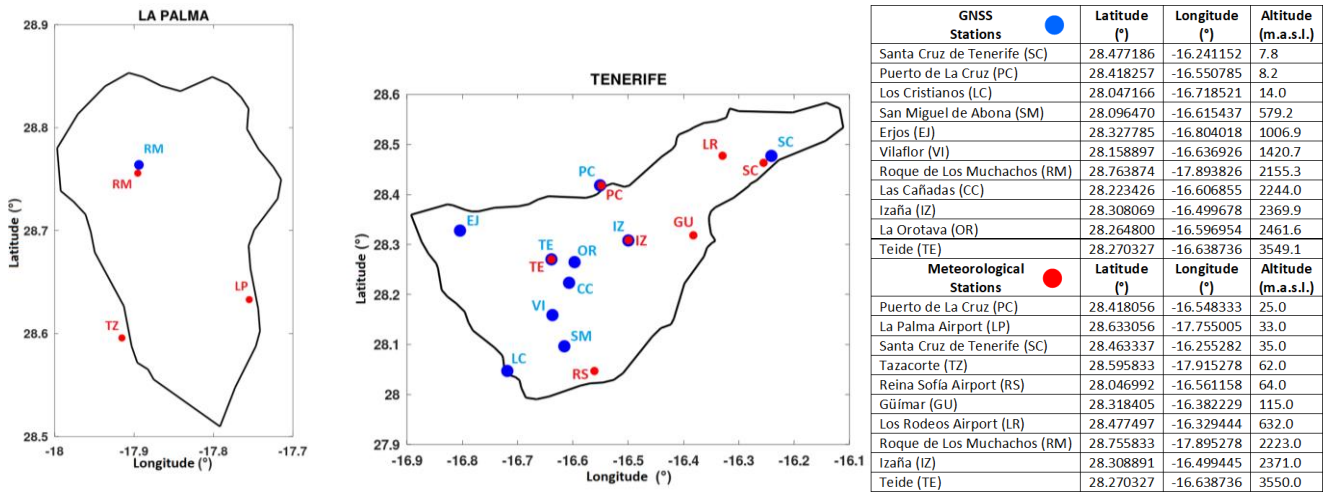


Figure 12.2. Locations of Global Navigation Satellite System stations and automatic meteorological stations in La Palma and Tenerife.

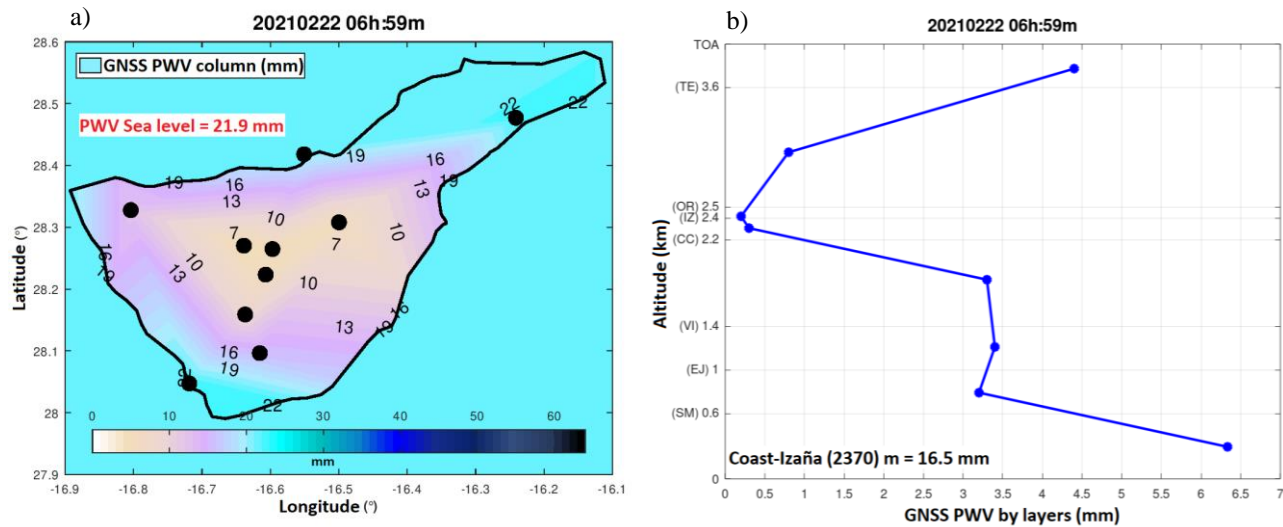


Figure 12.3. PWV at the GNSS stations in Tenerife obtained in quasi-real time at 6:59 UTC on 22 February 2021. a) PWV column values and b) PWV profile between stations.

12.2.2 Daily 24-hour PWV GNSS forecast

A daily 24-hour forecast of the PWV GNSS column and profile is generated at IARC with the same resolution and in the same format as those shown for the quasi-real-time measurements in Fig 12.3 for different locations and altitudes (Romero Campos et al., 2016). All this information is very valuable for operations at airports, as well as for meteorological and astronomical observatories.

The 24-hour forecast is based on the calculation of atmospheric refractivity and ZTD using the GNSS equations. The input values for the GNSS PWV prediction are pressure, temperature, specific humidity and geopotential supplied by ECMWF and the latitude, longitude and time values associated with each station in the GNSS network.

12.2.3 Radiosondes

From the vertical profiles of relative humidity obtained with Vaisala RS-40 radiosondes, precipitable water content in the atmospheric column is calculated by integrating numerically (using the trapezoidal rule) the density function of atmospheric water vapour for the base and top of each atmospheric layer. The integration is performed from ground level to 12 km altitude. By default, the PWV profile is supplied for the following layers: 1) from ground up to 1.5 km; 2) from 1.5 km to 3 km altitude in layers of 0.5 km thickness; 3) from 3 km altitude up to 12 km in layers of 1 km thickness.

The use of RS-40 radiosonde sounding started on Tenerife on 13 December 2017 and it has a temporal resolution of 1 s. Prior to this date RS-92 radiosondes were used from 1995-2017, with a temporal resolution of 2 s. This high resolution of RS-40 radiosondes provides a large number of

levels in the vertical profiles of pressure, temperature, humidity and wind.

However, at high altitudes (~14 km in the stratosphere), we have occasionally detected a weak decrease in reported altitude in the RS-40 Vaisala Tenerife radiosonde data. It could be due to the combination of an excessively high temporal resolution and longer response times and errors of the different meteorological sensors and GNSS. For these reasons, the erroneous records are filtered from the files before they are evaluated.

12.2.4 Microwave Radiometer

In 2019, a high precision microwave radiometer (MWR) was acquired to measure tropospheric temperature and humidity vertical profiles, with high temporal resolution, at the Izaña Observatory. It was installed at IZO on 29 April 2020. The Low Humidity and Temperature Profiling (LHATPRO-G5 series) microwave radiometer (Radiometer Physics GmbH) is specially designed to make humidity measurements under low humidity conditions such as those in the free troposphere above IZO. The radiometer obtains vertical profiles of humidity and tropospheric temperature up to 10 km of altitude with a spatial resolution of 200 m to 400 m depending on the altitude level and a temporal resolution of 1 s.

The microwave radiometer operates with two channels at different frequencies: the 60 GHz oxygen absorption line for temperature profiling and the 183 GHz water vapour line for humidity and water vapour profiles from the brightness temperature measurement. The instrument is also equipped with a single channel coupled infrared radiometer (IRR), a GPS receiver and a conventional weather station with a rain sensor. Through the radiometer's RPG software, using an artificial neural network (ANN) algorithm, derivative products can be obtained such as the Liquid Water Path (LWP), column integrated water vapour, zenith, total, hydrostatic and wet zenith delays of GPS signals, infrared temperatures, atmospheric stability indices, cloud base height, height and temperature profiles of the planetary boundary layer (PBL) and atmospheric attenuation. Fig. 12.4 shows an example of the 24-hour history of the main types of MWR measurements on 5 February 2021.

The MWR is a robust instrument, with a high degree of autonomy, especially designed for outdoor measurements in high mountain conditions that require minimal maintenance. The most important maintenance task is calibration. The equipment requires an absolute calibration with liquid nitrogen every six months. The last such calibration took place on 14 October 2020 at IZO (Fig. 12.5).

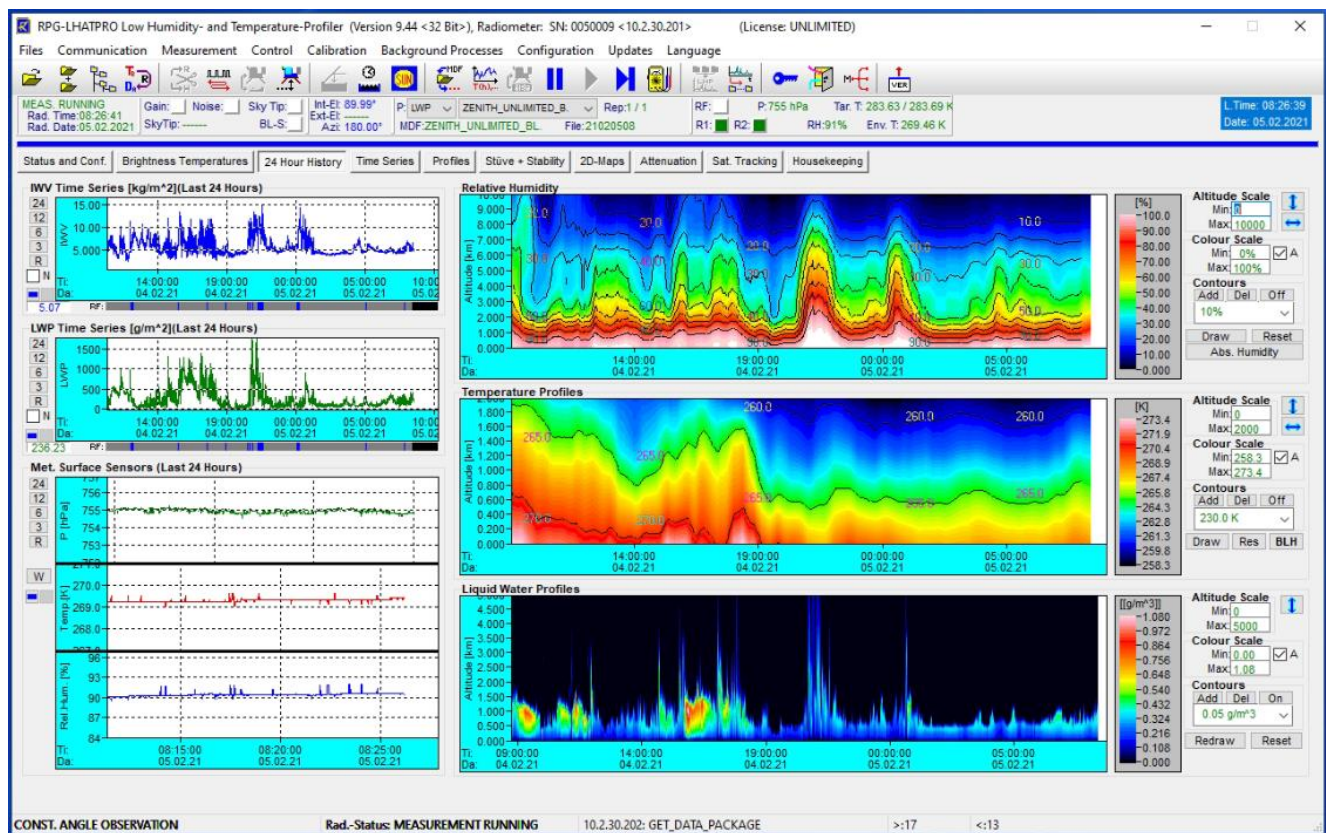


Figure 12.4. Example 24-hour history of the main types of measurements of the MWR on 5 February 2021 at 8:26 UTC at the Izaña Observatory.



Figure 12.5. MWR calibration with liquid nitrogen at IZO.

Figure 12.6 represents a comparison of the temperature profiles between the MWR and the radiosondes measurements on 19 May 2020 at 11 UTC and 23 UTC at the Izaña Observatory. These results demonstrate the close agreement of the profiles measured by these two different measurement techniques.

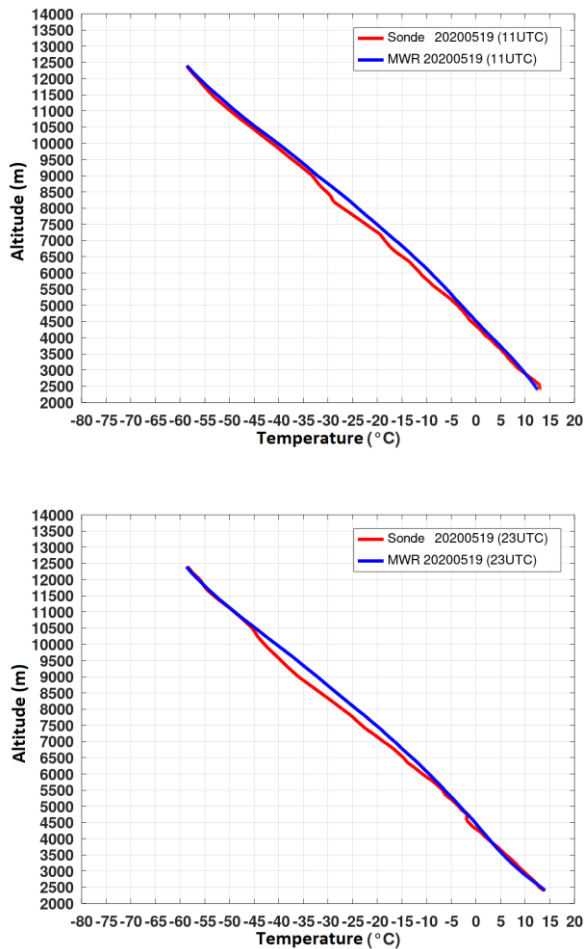


Figure 12.6. Temperature profiles from radiosondes (red) and MWR (blue) on 19 May 2020 at 11 UTC (upper panel) and 23 UTC (lower panel) at the Izaña Observatory.

12.3 Updating the PWV series: 2019-2020

Following a similar procedure to that of other authors (Botey et al., 2013); hourly, daily, monthly, annual and seasonal PWV averages are calculated when the data coverage is $\geq 60\%$.

12.3.1 Hourly variability of PWV from GNSS

Hourly variability of PWV is defined as the dispersion from the hourly mean value. From ultra rapid GNSS orbits, PWV values are calculated each 15 minutes. During an hour, a total of 5 values is obtained: 4 values + 1 additional one corresponding to the 59th minute. The hourly means have been calculated with a minimum of 3 hourly values (60%). The dispersion can be measured in several ways, by hourly standard deviations, hourly ranges or percentages of both (Table 12.1).

Table 12.1. Hourly PWV variability at SCO and IZO from GNSS (2008-2020).

Hourly PWV variability: 2008-2020		
	SCO	IZO
M(Hstd)	0.28 mm	0.17 mm
M(Hstdp)	1.49%	5.20%
M(Hran)	0.67 mm	0.40 mm
M(Hranp)	3.62%	12.44%

Hmean are the hourly means. Hstd are the hourly standard deviations from the hourly means. M(Hstd) is the mean value for the whole period 2008-2020 from the hourly standard deviations from the hourly means.

Hstdp = $Hstd/(Hmean) \cdot 100$ are the percentages of hourly standard deviations from the hourly means. M(Hstdp) is the mean value for the whole period 2008-2020 from the percentages of hourly standard deviations from the hourly means.

Hran are the hourly ranges estimated as $\max(\text{Hourly PWV}) - \min(\text{Hourly PWV})$. M(Hran) is the mean value for the whole period 2008-2020 from the hourly ranges.

Hranp = $Hran/Hmean \cdot 100$ are the percentages of hourly ranges from the hourly means. M(Hranp) is the mean value for the whole period 2008-2020 from the percentages of hourly ranges.

We apply the Tukey limits as criteria to test for possible outliers. In our Hmean series, we consider a value to be an outlier when the hourly mean value is outside of the interval:

$$[Q1 - 3 \cdot \text{irq}, Q3 + 3 \cdot \text{irq}],$$

where Q1 and Q3 are the 25th and 75th percentiles of the Hmean values, respectively, and irq is the interquartile range: $\text{irq} = Q3 - Q1$.

Applying these definitions to the PWV, the upper limit above which a PWV value is considered atypical (an outlier) in IZO is 20.8 mm, and we set the lower limit to 0 mm. There are some sporadic negative values in the PWV which are sometimes due to atypical values in the ZTDs, or to values atypical or insufficiently adequate of the pressures assigned to the sites. These are calculation limitations that can occur, especially in dry atmospheres like the IZO where we are very close to the GNSS detection limit.

Discarding all the records with atypical values, and considering hourly averages with $\geq 60\%$ data coverage, a total of 92,029 records corresponding to the entire 2008-2020 period have been analyzed at IZO.

In the case of SCO, the upper above which a value is considered atypical is 48.5 mm. As described for IZO, all

records that have not passed the quality filters have been discarded from the analysis. In total, 79,191 records corresponding to the entire period 2008-2020 have been analyzed at SCO. The dependency of the hourly standard deviation and hourly range with respect to the GNSS-PWV hourly mean at IZO and SCO during 2008-2020 is shown in Figure 12.7.

In summary, 1-hour is a reasonable time interval in which the PWV could be considered as a constant, both at the surface (SCO) and in the free troposphere (IZO) since most of its variation falls within the measurement error of $\pm 3.5\text{mm}$ (Schneider et al., 2010).

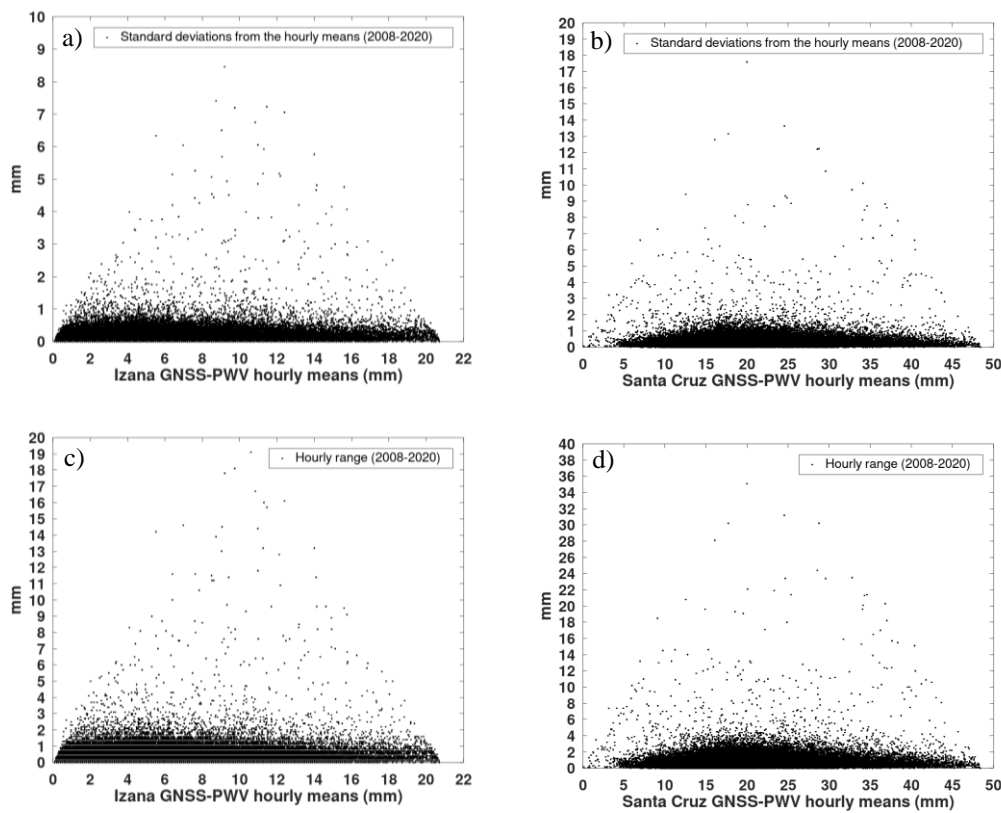


Figure 12.7. Hourly standard deviation with respect to the GNSS-PWV hourly means at a) IZO and b) SCO. Hourly range with respect to the GNSS-PWV hourly mean at c) IZO and d) SCO during 2008-2020.

12.3.2 Daily mean cycle of PWV from GNSS

The averaged daily cycles of PWV are shown for GNSS stations at SCO (2008-2020) and at IZO (2009-2020) (Fig. 12.8). Ultrafast orbits (those available) have been used for SCO, and precise orbits were used at IZO. The daily cycles have been calculated from averaged hourly anomalies. For these statistics, we have selected only those hourly average values with, at least 60% of high-quality intra-hours values, on days with at least 15 hourly means (60%). The daily time anomalies were obtained by subtracting the value of the corresponding daily average from the value of the hourly average: hourly mean - daily mean.

Then, for each hour, the averages for all of the available data anomalies within the time period of evaluation are calculated. A total of 4281 daily records for IZO and 3309 for SCO have been analyzed for the period 2008-2020.

The diurnal variations are quite similar at SCO and IZO, which suggests a synoptic cause (non-local), with a minimum observed around 6 UTC and 8 UTC at these stations, respectively, and a maximum around 15 UTC at both stations.

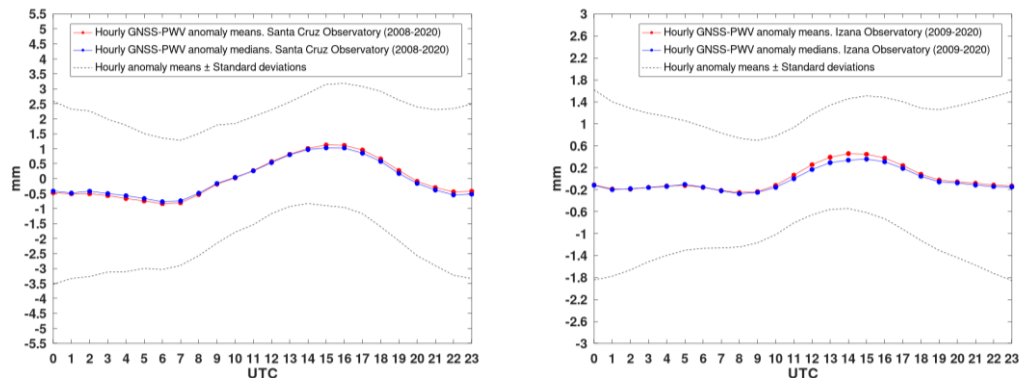


Figure 12.8. PWV daily mean cycle at SCO (left) and IZO (right) from GNSS.

12.3.3 Daily mean PWV data series from GNSS

The daily mean PWV data series are obtained from the hourly mean data calculated using the GNSS ZTD from ultra-fast orbits in SCO and from precise orbits in IZO, in days in which at least 15 (60%) of all possible daily hourly mean values are available

Fig. 12.9 shows these series for SCO and IZO for the period 2008-2020 and 2009-2020, respectively. Maximum values of PWV are observed in summer-autumn and minimum values are observed in winter.

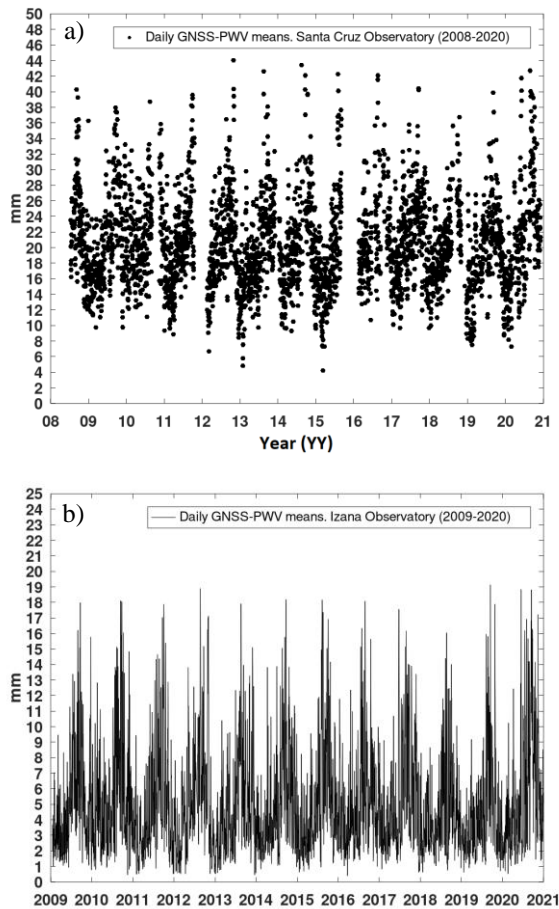


Figure 12.9. PWV daily data series at a) SCO for 2008-2020 and b) IZO for 2009-2020.

12.3.4 Monthly mean PWV data series from GNSS

Monthly PWV data series are shown for SCO and for IZO in Figure 12.10. However, the monthly series for SCO and IZO had some gaps. To fill these monthly gaps the following procedure is applied. Firstly, the monthly anomalies are calculated by subtracting the annual mean cycle from the monthly means (see Section 12.3.5). Then the gaps in the anomalies are linearly interpolated and finally, the annual mean cycle is added again. Applying the Wilcoxon-Mann-Whitney iterative test (Lanzante, 1996) as described in (Romero-Campos et al., 2011), using 99% confidence interval, no inhomogeneity was detected at SCO for either of the two series: original with gaps and filled without gaps.

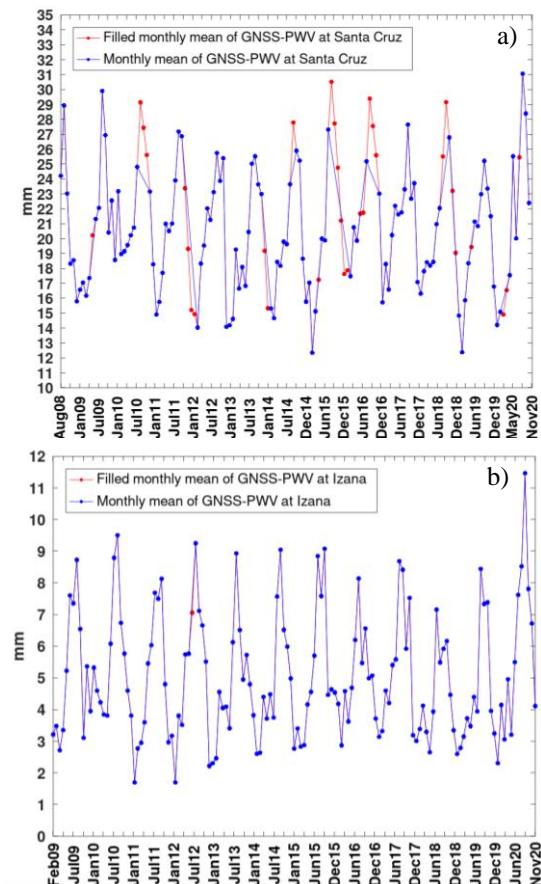


Figure 12.10. PWV monthly data series at a) SCO for 2008-2020 and b) IZO for 2009-2020.

12.3.5 Annual mean cycle of PWV from GNSS

The PWV annual mean cycles for SCO and IZO for the 2008-2020 and 2009-2020 period respectively are shown in Fig. 12.11 and Fig. 12.12. The seasonal maximum of PWV in Santa Cruz is observed at the end of the summer (September), which represents a one-month delay with respect to Izaña, where seasonal maximum is observed in August.

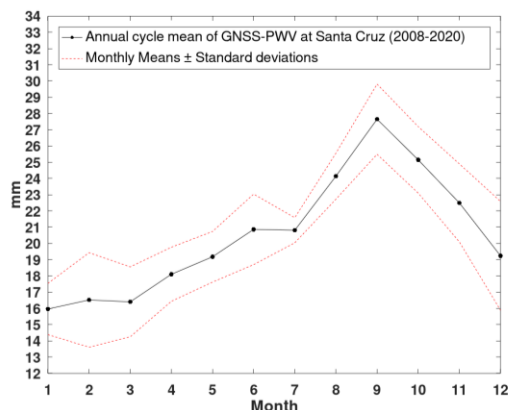


Figure 12.11. GNSS PWV annual mean cycle, SCO (2008-2020).

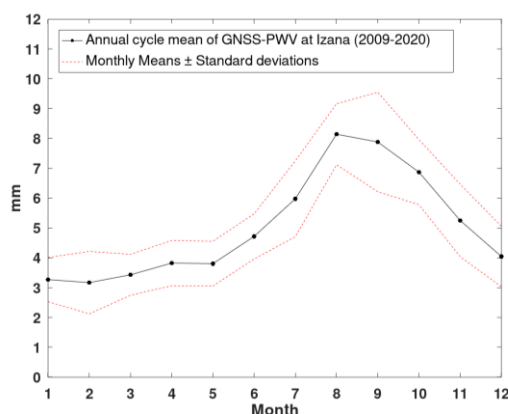


Figure 12.12. GNSS PWV annual mean cycle, IZO (2009-2020).

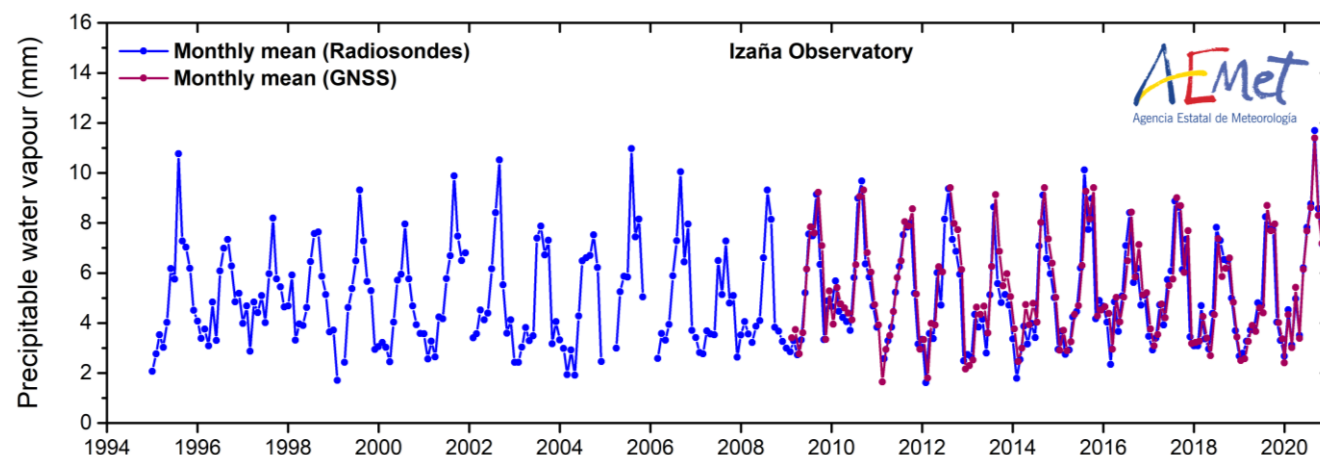


Figure 12.13 PWV monthly data series at IZO from radiosondes and GNSS for 1994-2020.

12.3.6 Monthly mean PWV from radiosondes at Tenerife

PWV monthly mean obtained from radiosondes at SCO and IZO are shown for the period 1995-2020 (Fig. 12.14). These are the values of PWV calculated over the duration of the radiosonde flight (about 2 hours or so) from the time of its release, and assuming that, during this period of time, the PWV remains constant. An annual cycle with peak in summer-autumn and minimum values in winter is seen in the data. Lower values of PWV are observed at IZO in comparison with SCO. The series was subjected to the corrections for different types of sondes described in (Romero Campos et al., 2011).

Using a 95% confidence level, inhomogeneity was found in the median of the monthly series of the PWV in SCO at 0 UTC in November 2011, but the signal-to-noise ratio at the point of change is weak ($0.043 < 0.05$). For the rest of the PWV monthly mean series, no lack of homogeneity was detected in the median at a confidence level $\geq 95\%$. There are no significant trends in any of the series.

Given that the presence of water vapor above 12,000 m is very small (90% of the water vapor is concentrated in the troposphere below 12,000 m), these values are comparable with those obtained with the GNSS technique. The agreement between the two techniques as depicted in Fig. 12.13 is very good; the small differences observed can be attributed to the fact that the GNSS measurements are zenith, while the radiosondes do not measure vertically, rather its profile moves horizontally, at a greater or lesser distance, depending on weather conditions on launch day.

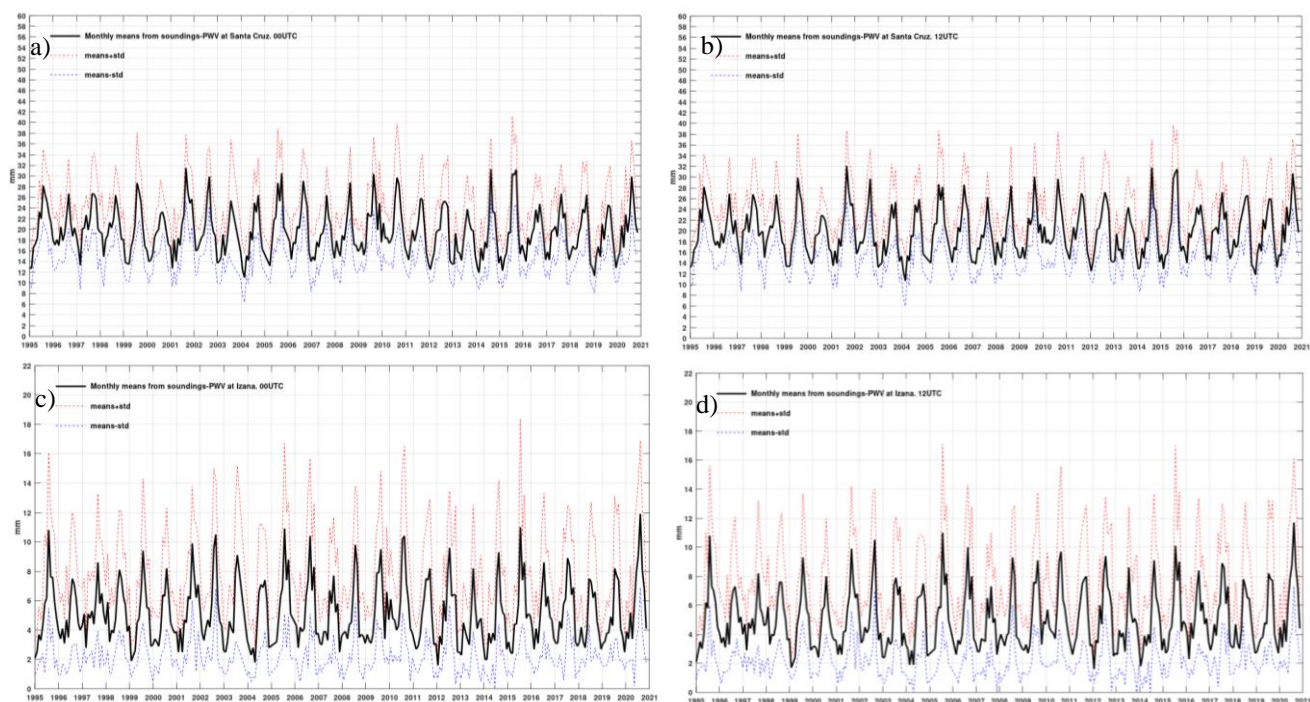


Figure 12.14. Monthly PWV means from Tenerife radiosondes for SCO a) 00UTC, b) 12UTC and IZO c) 00UTC and d) 12UTC (1995–2020).

12.3.7 PWV vertical stratification monthly statistics

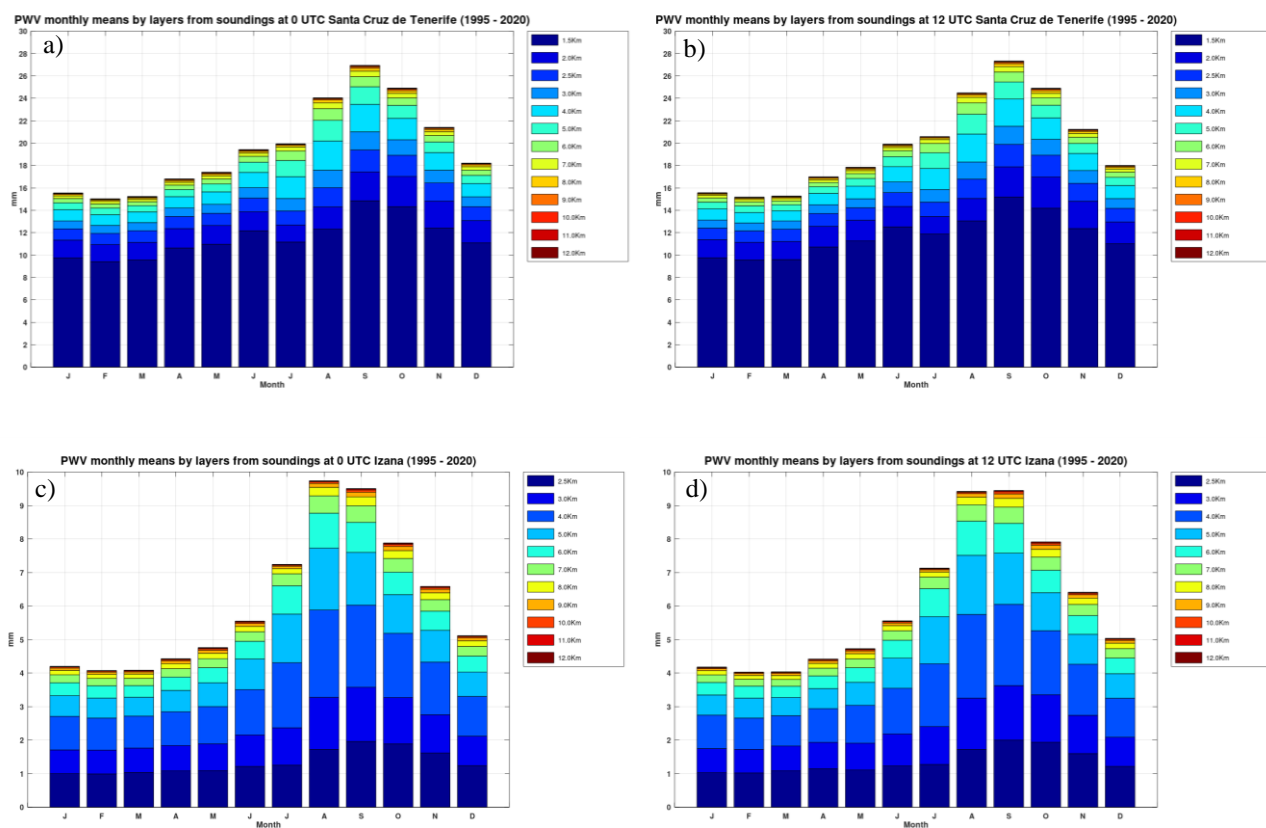


Figure 12.15. Monthly statistics of precipitable water vapour vertical distribution from Tenerife radiosondes for SCO a) 00UTC, b) 12UTC and IZO c) 00UTC and d) 12UTC (1995–2020).

The monthly average of PWV vertical distribution over Tenerife obtained from radiosondes data at 0 and 12UTC during the period 1995-2020, are depicted in Fig. 12.15 for SCO and IZO. The total height of each column corresponds to the total monthly averaged PWV at sea level. No significant differences are found between 00 and 12UTC.

Most of the PWV is concentrated within the first 1.5 km altitude. There is a “wet” season from August to October, with a maximum in September (~27 mm) in the case of Santa Cruz, and August-September (~ 9.5 mm) in the case of Izaña. Similarly, we observe a “dry” season corresponding to the months of January to April at both sites with minimums in February-March of about (~ 4 mm) in Izaña and (~ 15 mm) in Santa Cruz.

12.3.8 Evolution of annual and seasonal PWV from soundings at Tenerife

In the PWV seasonal averages (Fig. 12.16) winter and spring are seen as the driest seasons, and summer and autumn are the seasons with the highest PWV content. Regarding the evolution of seasonal anomalies, as of 2012, a predominance of negative anomalies is observed in winter, both in SCO and IZO. These anomalies are the difference between the annual seasonal means evaluated for each season and year and total seasonal means evaluated for each season in the whole period from 1995 to 2020.

The evolution of the annual means of the PWV (Fig. 12.17) reveals the existence of periods of different duration in which high and low values of the PWV alternate. There are “wet” and “dry” periods with PWV values above or below the mean for the entire period (1995-2020), respectively. The oscillation with the greatest amplitude corresponds to the year 2005 with a notable positive anomaly, both in SCO and in IZO, and for both 0 UTC and 12 UTC. Furthermore, it should be noted that, in Santa Cruz, the average for the entire period at 12 UTC is higher than the average at 0 UTC; however, in Izaña it is the opposite, although in both cases the values are very close to each other.

This observation can be explained by the greater presence of PWV in the lower troposphere fed by the evaporation of ocean water due to solar radiation and convection initiated from the lower layers. This convection is slowed in part because the quasi-permanent thermal inversion of the trade wind around 1000-1500 m, acts as a barrier. At Izaña, on the other hand, the atmosphere is quite dry, and the greater presence of water vapor during the night with respect to the day, could be mainly due to the advection of humid air masses from the northwest at high altitudes and the small contribution of the subsidence processes that occur more frequently at night.

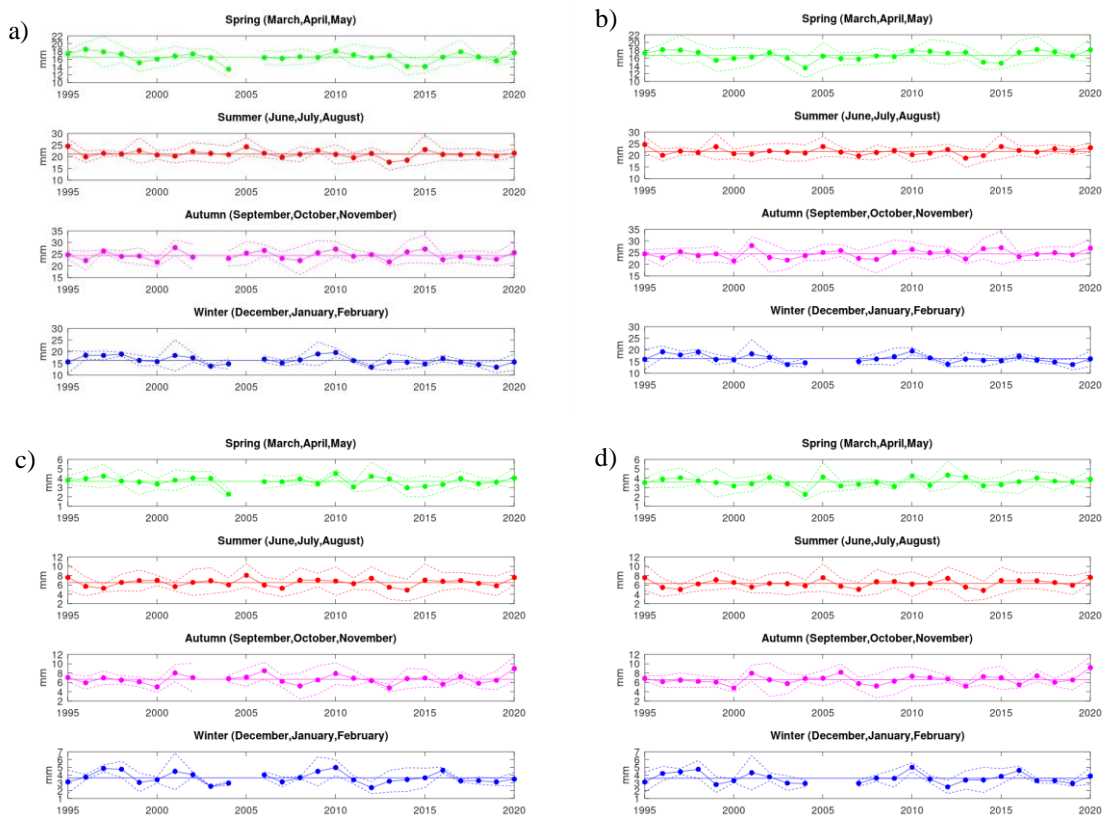


Figure 12.16. PWV seasonal means from Tenerife radiosondes, compared to 1995-2020 seasonal averages for SCO a) 00UTC, b) 12UTC and IZO c) 00UTC and d) 12UTC. Solid lines are Total Seasonal Means evaluated for each season in the whole period from 1995-2020. Solid-dotted lines are Annual Seasonal Means evaluated for each season and year. Dashed lines are the Annual Seasonal Means \pm Standard deviations.

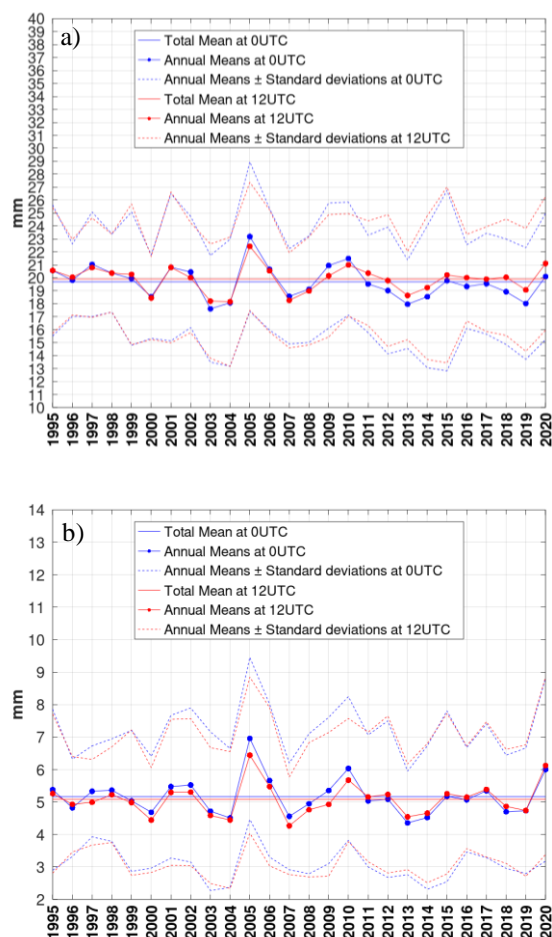


Figure 12.17. PWV annual means from Tenerife radiosondes, 1995-2020, compared to 1995-2020 average for a) SCO and b) IZO.

12.4 Summary of remarkable results during the period 2019-2020

12.4.1 Estimation of trends in tropospheric water vapor from radiosondes in Tenerife

Mixing ratio (MR) for water vapour is defined as the mass of water vapour contained in the total mass of the dry air. A study of trends in PWV and MR from Tenerife radiosondes from May 1994 to December 2019 has been carried out. The results that we present here are provisional. In the study, a previous analysis of the homogeneity at each level of the accumulated PWV and MR series is carried out, since, throughout the study period, changes have been introduced in the types of Vaisala sondes, at the site, launching methodology and system as well as monitoring and evaluation software. From the analysis, it is concluded that the accumulated PWV and MR series of the soundings can be considered reasonably homogeneous since 1995 from

2000 m altitude, in the case of 00 UTC, and 2500 m, in the case of 12 UTC.

To calculate the trends at each level, three different methods have been used based on the least squares adjustment of:

- 1) The series of annual averages.
- 2) The seasonally adjusted daily series.
- 3) The daily series filtered of high frequencies (annual and lower periods) by means of Fourier transforms.

The trends in MR obtained at each level by each of the three commented methods are shown in Fig. 12.18, and accumulated PWV is shown in Fig. 12.19.

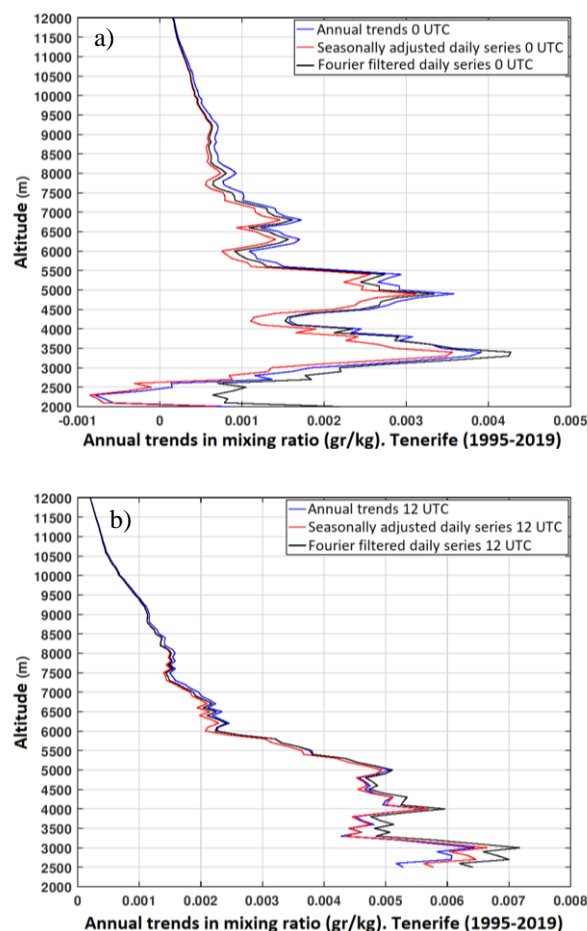


Figure 12.18. Water vapour mixing ratio trends at different altitude levels calculated by three different methods at a) 00 UTC and b) 12 UTC from radiosonde measurements in Tenerife (1995-2019).

Fourier transforms offers the highest levels of confidence in significant annual trends in relation to the standard error of the fit. This method produces confidence levels $\geq 95\%$ for

the vast majority of altitudes analyzed, both at 0 UTC and at 12 UTC.

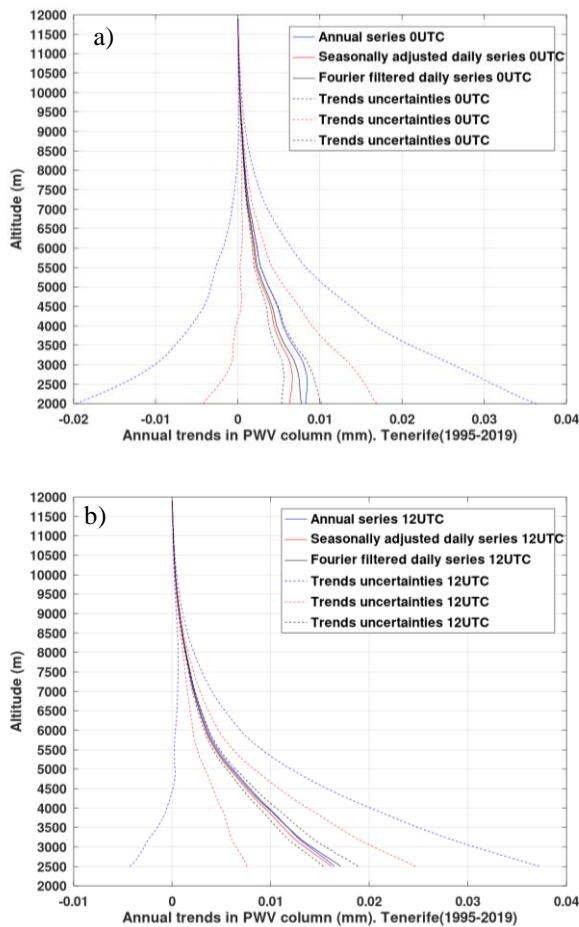


Figure 12.19. PWV trends at different altitude levels calculated by three different methods at a) 00 UTC and b) 12 UTC from radiosonde measurements in Tenerife (1995-2019).

Although the trends may have small uncertainties, they are not significant if the mean values of the PWV plus such trends are less than the sum of the mean values of the PWV plus the mean errors in the calculation of that variable.

From the previous graphs we can conclude that the trends obtained in the water vapor series in the free troposphere are small and positive; that is, a small increase in the amount of water vapor is detected at all levels above 2000 m, both at 0 UTC and at 12 UTC. The increase at 12 UTC in the accumulated precipitable water above 2500 m and up to 4000 m, while still small (Fig. 12.19b), is an order of magnitude higher than the increase at 0 UTC in the same range of altitudes (Fig. 12.19a). However, for all these trends to be significant (greater than the mean errors in the calculation of the respective variables), time periods of the order of one or several decades are needed, depending on the altitude and time.

12.5 References

- Botey, R., J. A. Guijarro y A. Jiménez. “Valores normales de precipitación mensual 1981 – 2010”. Agencia Estatal de Meteorología. NIPO: 281-13-007-X. 2013.
- Lanzante, J., *Resistant, Robust and Non-Parametric Techniques for the Analysis of Climate Data: Theory and Examples, including Applications to Historical Radiosonde Station Data.* International Journal of Climatology, Vol. 16, 1197-1226, CCC 0899-8418/9611197-30, by the Royal Meteorological Society, 1996.
- Romero Campos, P.M., Marrero, C., Alonso, S., Cuevas, E., Afonso, S., and Ortiz de Galisteo, J.P.: Una Climatología del Agua Precipitable en la Región Subtropical sobre la Isla de Tenerife basada en Datos de Radiosondeos. NTD n° 6 de AEMET. NIPO: 281-12-007-5. Centro de Investigación Atmosférica de Izaña. Agencia Estatal de Meteorología (España), 2011.
- Romero Campos, P.M., Cuevas, E., de Bustos, J.J.: Medida en tiempo cuasi-real y predicción a 24h del contenido atmosférico de agua precipitable a partir de una red de receptores GPS en la isla de Tenerife. NTD n° 20 de AEMET. NIPO: 281-16-002-6. Centro de Investigación Atmosférica de Izaña. Agencia Estatal de Meteorología (España), 2016.
- Schneider, M., Romero, P. M., Hase, F., Blumenstock, T., Cuevas, E., and Ramos, R.: Continuous quality assessment of atmospheric water vapour measurement techniques: FTIR, Cimel, MFRSR, GPS, and Vaisala RS92, Atmos. Meas. Tech., 3, 323-338, doi: 10.5194/amt-3-323-2010, 2010.

12.6 Staff

Pedro Miguel Romero Campos (AEMET; Head of programme)

Ramón Ramos (AEMET; Head of Infrastructure)

Dr África Barreto (AEMET; Research Scientist)

Sergio Afonso (AEMET; Ozone and meteorological soundings expert technician), retired in 2019

13 Meteorology

13.1 Izaña Observatory as a WMO Centennial Observing Station

Today, supercomputers and sophisticated models and satellites are important tools for climate scientists. However, long-term, high quality continuous observations from thermometers, rain gauges and other instruments remain essential. Without them, we could not be certain that the Earth has warmed by one degree centigrade over the past century. These long-term observations are vital to our scientific understanding of climate variability and change and essential for model and satellite validation activities.

To promote the recovery and continuation of these records, governments are nominating Centennial Observing Stations for formal recognition by WMO. Many Centennial Observation Stations are also of outstanding historical and cultural interest, recalling previous eras and the birth of modern meteorology. Taken together as a network, Centennial Observation Stations are uniquely able to tell the story of recent climate history.

Izaña Observatory was recognised as a Centennial Observation Station by the WMO in 2017. More information about the WMO Centennial Observing Stations can be found [here](#).

13.2 Main Scientific Goals

The main goals of the meteorology programme are:

- To provide diagnosis and operational weather forecasting to support routine operation activities at the IARC observatories and issue internal severe weather alerts and special forecasts for planned field campaigns, outdoor calibrations, repairs, etc.
- To configure and operate High Resolution Numerical Weather Prediction Models capable of capturing the complex meteorology of the mountain observatory, as an aid to improve the supporting forecasts.
- To operate back-trajectory models on a monthly basis to keep a database available for other scientific projects up-to-date.
- To investigate the use of machine learning strategies to improve the forecasting of meteorological and air quality parameters.
- To maintain meteorological parameter observations according to WMO specifications, and in the framework of AEMET's Synoptic and Climatological Observation Networks.
- To measure conventional meteorological parameters at different stations on the island of Tenerife, to support other observation programmes.



Figure 13.1. Izaña Observatory weather stations.

- To develop non-conventional meteorological parameters programmes.
- To provide meteorological analysis information and technical advice to interpret and support results from other observation programmes and scientific projects, designing and implementing specific algorithms and databases to reach these goals.

13.3 Measurement Programme

The Izaña Atmospheric Research Center directly manages six weather observation stations, located at IZO (3), SCO, BTO and TPO (see Section 3 for more details).

13.3.1 Izaña Observatory

IZO has three fully automatic weather stations, two of them are located in the weather garden (C430E/60010 and Meteo-STD), which includes a network of five cloud observation webcams, and the third station is on the instrument terrace of the observation tower (Meteo-Tower) at 30 m above ground level. Instrumentation for manual observations (staffed by personnel) with temperature, humidity, pressure and precipitation analog recorders (bands), is also maintained at IZO in order to preserve the historical series that started at Izaña Observatory in 1916.



Figure 13.2. Izaña Observatory, manual meteorological instrumentation.

13.3.2 Santa Cruz Observatory

SCO has a fully automatic weather station located on the instrument terrace.

13.3.3 Botanic Observatory

BTO has a fully automatic weather station installed at the ozonesounding station in the Botanic Garden in Puerto de la Cruz.

13.3.4 Teide Peak Observatory

TPO has an automatic very high-altitude weather station with temperature, humidity and pressure sensors, supplemented by data from a wind sensor installed at the Cable Car tower No.4, managed by the Cable car company.

The meteorology programme also has access to meteorological soundings data of pressure, temperature, humidity and wind from the Tenerife station (ID: WMO 60018) located in the town of Güimar. This station belongs to the AEMET upper-air observation network and is managed by the Meteorological Center of Santa Cruz de Tenerife (AEMET).

13.4 Meteorological Resources

To accomplish the objectives of the meteorology programme we have the following tools.

13.4.1 Man Computer Interactive Data Access System (McIDAS)

LINUX Workstations (Fedora Core) with the Man Computer Interactive Data Access System (McIDAS) provide access, exploitation and visualization of meteorological information from different geo-referenced observations, modelling and remote sensing (satellite, radar) platforms.

The application provides access to all data in real time in the AEMET National Prediction System, including the following data and products:

- Global synoptic surface observation and upper-air networks.

- Outputs of numerical prediction models from ECMWF Integrated Forecasting System (IFS) and AEMET (HIRLAM).
- METEOSAT satellite imagery.
- Images of the AEMET Weather Radar Network.
- Data from the AEMET Electrical Discharge Detection network.
- Products derived from SAF (Satellite Application Facilities) Nowcasting Meteosat Second Generation (MSG) images.

Utilising this application different automated processes for the exploitation of meteorological information have been developed, among which we can highlight:

1) Automatic generation of graphical products from specific model outputs and images from derived MSG products (RGB combinations), for consultation through an intranet website (Fig. 13.3).

2) Calculation of isentropic back trajectories of air masses from analysis outputs (4 cycles per day) and prediction (every 12 hours and range up to 132 hours) for Tenerife at nine different vertical levels (Fig. 13.4).

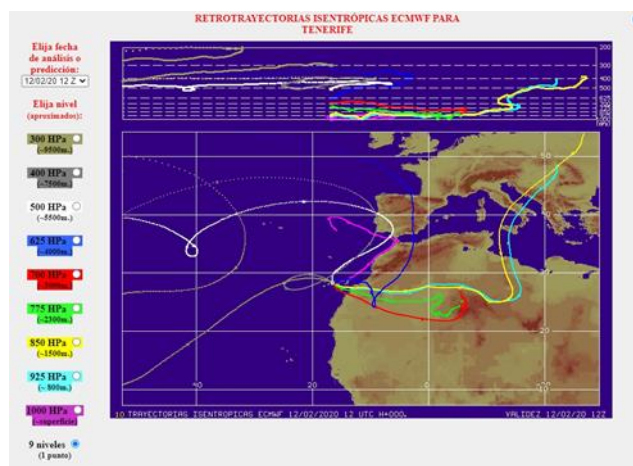


Figure 13.4. Screenshot of isentropic back-trajectories for Tenerife at nine levels on day 12/02/2020 12 UTC.

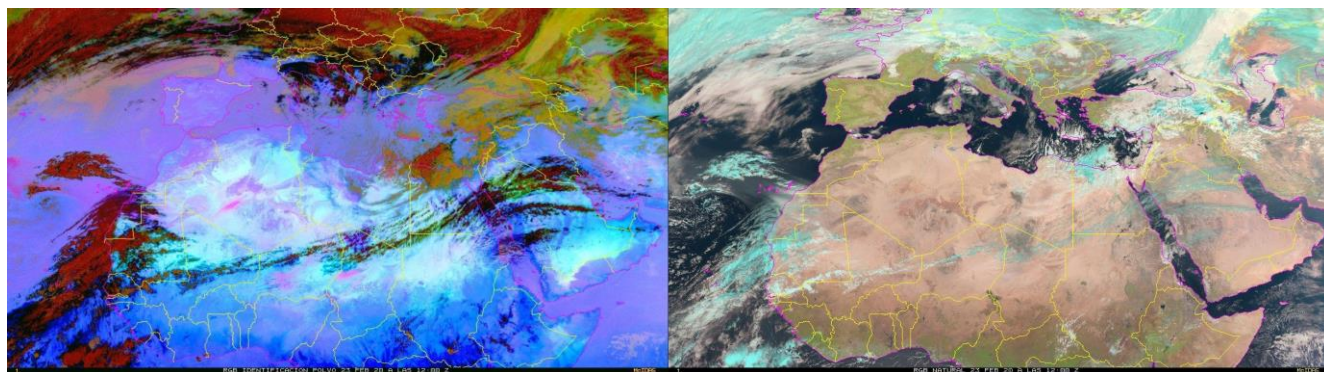


Figure 13.3. Two different RGB composite images from Meteosat-10 satellite for a dust event on 23/02/2020 12:00 UTC. Left panel: dust (channels 7, 9 and 10), right panel: natural (channels 1, 2 and 3).

3) Lightning strikes in situ detection and AEMET lightning detection network warning system, for taking preventive action to avoid damages in the facilities.

4) Automatic seven-day Meteogram generation of temperature, humidity, wind, pressure and clouds for Izaña Observatory using standard isobaric grid points interpolated to 2400 m a.s.l. The statistics have been weighted using the inverse distance to the validity forecast time taking into account the last five available model runs (Fig. 13.5).

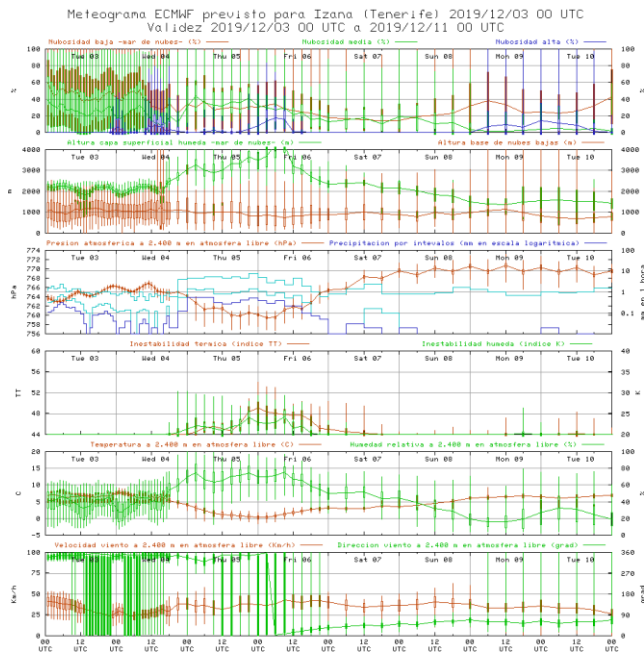


Figure 13.5. Ensemble week length meteogram forecast at IZO on 03/12/2019 at 00 UTC.

13.4.2 EUMETCast receiving system

The EUMETCast real-time receiving system for aerial imagery and meteorological satellite data distributed by EUMETSAT has its own internal web interface for displaying images received, and mass storage system for archiving images of compressed MSG segments in native format.

13.4.3 EUMETSAT Data Center

We have access to the EUMETSAT Data Center for retrieval of images and historical products of Meteosat satellites.

13.4.4 AEMET Server Meteorological Data System

We have access to numerical model databases, observations, bulletins, satellite and radar images available on the AEMET Server Meteorological Data System (SSDM).

13.4.5 ECMWF products and MARS archive

In addition, we have access to the European Centre for Medium-Range Weather Forecasts (ECMWF) computer systems and extractions of the Meteorological Archival and

Retrieval System (MARS), which is the archive of all operational products generated in ECMWF. From this system we have developed different exploitation processes such as:

- Routine extraction in two cycles per day of meteorological analysis and prediction fields of the ECMWF IFS model, which are decoded in a compatible format for exploitation from McIDAS and input of initial and boundary conditions for the integration of high-resolution models running locally on our computer systems.
- Monthly extraction of ERA-Interim reanalysis outputs for updating large data series for different projects.
- Extraction of previous analysis fields for computing back trajectories with FLEXTRA.
- Routine extraction in two cycles per day from Copernicus Atmosphere Monitoring Service (CAMS) system (Fig. 13.6).

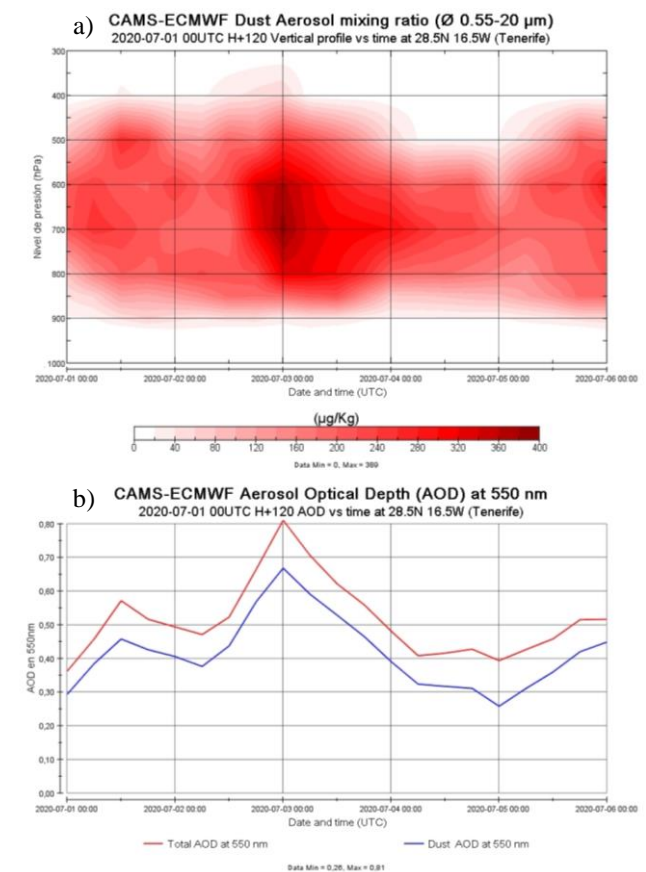


Figure 13.6. Examples of routine output cycles from CAMS. Forecast evolution of a) vertical profile of dust aerosol mixing ratio and b) Aerosol Optical Depth at 550 nm on 01/07/2020 00:00 UTC H+120 for 28.5N 16.5W (Tenerife).

13.4.6 AEMET National Climatological Data Base (BDCN)

We have access to the AEMET National Climatological Data Base (BDCN) for data extraction of observations from the AEMET principal and secondary climatological networks.

13.5 Numerical Models

13.5.1 Statistical forecasting model

A statistical forecasting model based on the analogous method shows the probability of occurrence of pollution events. In addition, meteorological values for a fixed point NE (29.25 °N 15.75 °W) of the Canary Islands, coloured depending on the quartile position relative to the historical values of the series, show at a glance the adverse meteorological conditions in a forecast range of 108 hours (Fig. 13.7) (for more details see Milford et al., 2008).

DATE	H	DIR	DIR	WS	EPI	BLH	B	ALT	T	ALT	B	TEM	T	TEM	MEDIAN	PER99	>=70	>=80
31-07-2020	00	042	NE	6.4	68	769	726	1240	14.7	25.0	*****	*****	**	**				
31-07-2020	06	023	NNE	5.5	61	792	726	1369	14.7	25.0	*****	*****	**	**				
31-07-2020	12	039	NE	5.5	51	712	814	1239	15.5	23.5	10.0	61.0	32	16				
31-07-2020	18	023	NNE	6.1	59	616	651	1245	17.6	23.8	*****	*****	**	**				
01-08-2020	24	045	NE	6.4	59	740	731	1246	16.9	24.4	*****	*****	**	**				
01-08-2020	30	029	NNE	6.1	73	533	511	1130	18.0	24.9	*****	*****	**	**				
01-08-2020	36	034	NE	6.9	72	530	512	1132	18.3	25.2	10.0	26.0	24	09				
01-08-2020	42	026	NNE	7.3	79	522	450	1023	19.2	25.5	*****	*****	**	**				
02-08-2020	48	030	NNE	8.0	78	529	513	1023	19.1	25.8	*****	*****	**	**				
02-08-2020	54	019	NNE	8.4	73	452	394	1024	19.6	25.7	*****	*****	**	**				
02-08-2020	60	020	NNE	10.8	82	488	395	922	20.2	25.9	13.0	70.0	36	20				
02-08-2020	66	025	NNE	10.8	84	495	342	1027	20.6	26.2	*****	*****	**	**				
03-08-2020	72	020	NNE	10.9	84	515	394	1026	19.8	25.9	*****	*****	**	**				
03-08-2020	78	019	NNE	10.2	87	487	393	921	18.9	26.4	*****	*****	**	**				
03-08-2020	84	022	NNE	10.8	85	538	450	1023	18.3	26.6	12.0	191.0	34	21				
03-08-2020	90	020	NNE	10.1	88	495	393	1024	19.0	26.8	*****	*****	**	**				
04-08-2020	96	020	NNE	10.5	72	515	393	1020	18.3	24.4	*****	*****	**	**				
04-08-2020	102	030	NNE	9.9	59	680	649	1012	16.6	22.4	*****	*****	**	**				
04-08-2020	108	027	NNE	8.7	54	721	386	1013	16.9	22.9	11.0	48.0	34	21				

Figure 13.7. Meteorological parameters summary table showing wind direction, wind velocity, Integrated Stability Parameter (EPI), boundary layer height (BLH), inversion layer height and temperature (base and top), median and 99 percentiles of the analogous selected, and probability of occurrences of exceedances over 80 and 70 percentiles of the historical series of SO₂ concentration.

13.5.2 The PSU/NCAR mesoscale model (MM5)

The meteorology programme has access to a clusters system in LINUX environment of parallel processors for the integration of a non-hydrostatic high resolution weather model (MM5) for the area of the Canary Islands. The initial and boundary conditions are from the ECMWF IFS model, and nested grids of 18, 6 and 2 km resolution are outputted with a forecasting range up to 144 hours.

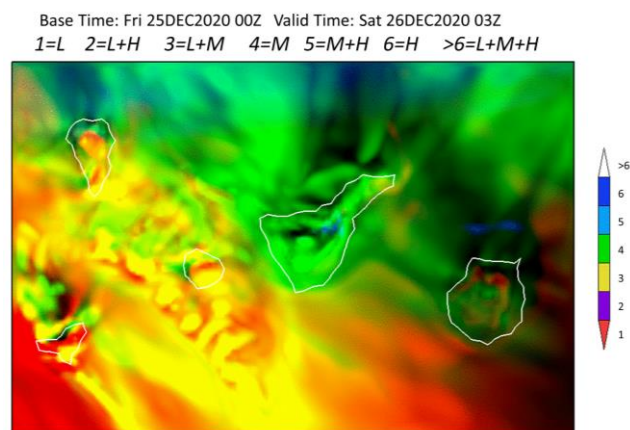


Figure 13.8. Example of graphical representation of total cloud fraction (low+medium+high) shaded in colours on 25 December 2020 at 03 UTC (output of MM5 model).

13.5.3 The Weather Research and Forecasting (WRF) model

A Super Workstation based on the Xeon Phi KNL processor, with 72 cores at 1.5 GHz and RAM 64 GiB, and a CentOS7.3 OS with the Fortran and C++ compiler Intel Parallel Studio XE, support the integration of the Weather Research and Forecasting - Advanced Research WRF (WRF-ARW) model at very high resolution. The initial and boundary conditions are also from the ECMWF IFS model, and nested grids of 6, 2 and 1 km resolution are outputted with a forecasting range up to 72 hours. A high-mountain gust parameterization was implemented in WRF which greatly improves the wind gust forecast at both the Izaña Observatory and the Teide Peak Observatory (Fig. 13.9 and 13.10).

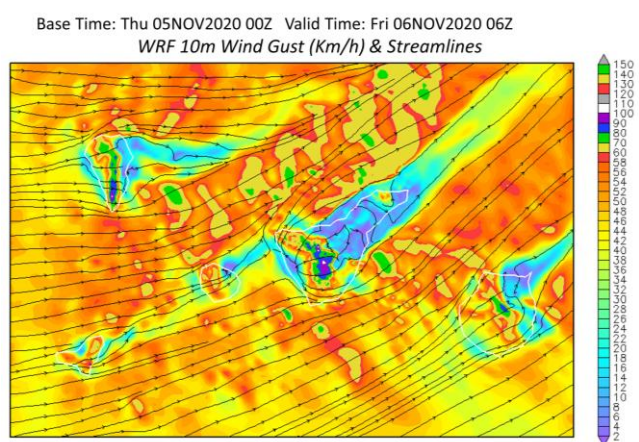


Figure 13.9. Example plot of forecasted wind gust velocity shaded in colours, overlapped with stream lines for a high wind speed episode on 5 November 2020 at 06 UTC.

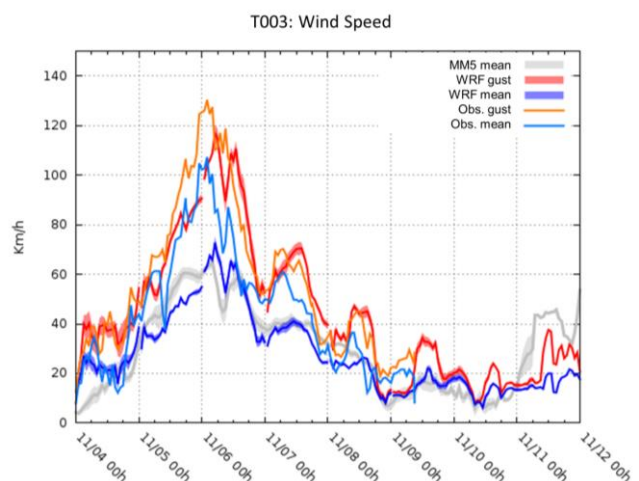


Figure 13.10. Example validation plot showing observed and forecasted wind and gust speeds from 4-11 November 2020. MM5 wind speed is also plotted.

13.5.4 Post-processed numerical results

The outputs of these models offer the added value of dynamic downscaling of the IFS model predictions for the complex topography of the Canary Islands. Various types of

post-processed numerical fields permit a better understanding of the atmospheric situations. In addition to these outputs an artificial neural network has been implemented that improves the prediction of local temperature and wind at the observatory, granting additional accuracy to the in situ forecast (Fig. 13.11). All these results are presented using a web server installed in the cluster.

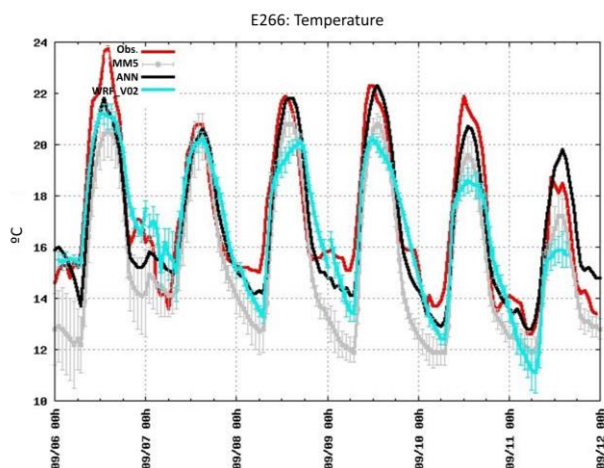


Figure 13.11. Example of the Artificial Neural Network (ANN) 2 m forecast temperature improvement from 6-11 September 2020. Black lines represent the ANN values, while red, grey and blue lines represent observations and direct MM5 and WRF output, respectively.

13.5.5 FLEXible TRAjectory (FLEXTRA) model

The FLEXible TRAjectory (FLEXTRA) model is installed in a dedicated server and simulates 10-day back-trajectories arriving at Izaña Observatory calculated at several levels. The back-trajectories provide relevant information on transport and source regions of air masses affecting the various components and parameters measured at IZO. The back-trajectories have been calculated, and archived, at six hourly intervals for the 1979-2020 period.

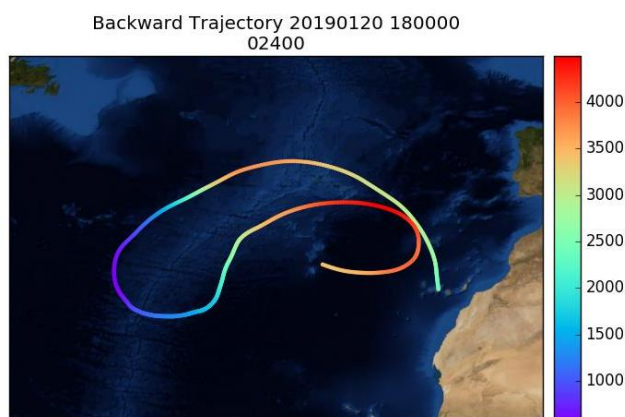


Figure 13.12. Image representing the track and height of a FLEXTRA back-trajectory with track ending on 20/01/2019 at 18 UTC.

Additional graphic information representing the track and its height is shown using a web server as a quick reference in order to select particular episodes (Figure 13.12). A later

more exact representation can be requested using a McIdas web based server (Fig. 13.13).

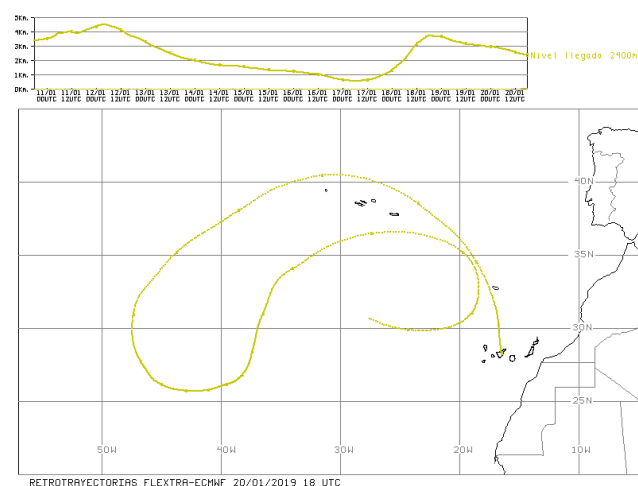


Figure 13.13. Detailed plot of a FLEXTRA back-trajectory with track ending on 20/01/2019 at 18 UTC.

13.5.6 HYbrid Single Particle Lagrangian Integrated Trajectory (HYSPLIT) model

The HYbrid Single Particle Lagrangian Integrated Trajectory (HYSPLIT) model has been installed on the same server as the FLEXTRA model in order to simulate 10-day back-trajectories using the National Centers for Environmental Prediction (NCEP) Global Forecast System (GFS) model as data input. The back-trajectories have been calculated, and archived, at six hourly intervals for the entire 1949-2020 period.

In addition, the HYSPLIT model was also installed in the cluster system using the MM5 output data and was run in dispersion mode using the parallel program settings to determine SO₂ concentrations in areas close to emission sources (Figure 13.14).

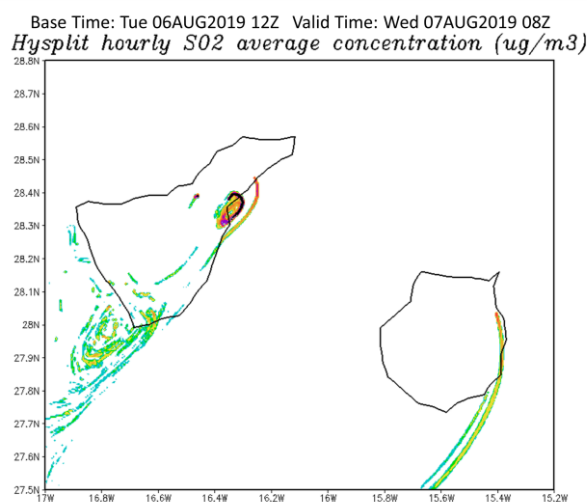


Figure 13.14. Average Hysplit SO₂ concentration forecasted on day 07/08/2019 at 08 UTC.

13.6 Summary of activities during the period 2019-2020

13.6.1 Meteorological long-term records

The series of average temperature, accumulated precipitation, sunshine duration, average relative humidity and average atmospheric pressure at Izaña Observatory have been updated for the years 2019 and 2020 (Fig. 13.15). This constitutes over a century of meteorological data and is the oldest uninterrupted climate series in the Canary Islands.

In the series of annual mean temperature at IZO (Fig. 13.15a), the rate of rise in temperature is maintained at 0.15°C per decade, consistent with the global warming trend. This series is especially relevant since the station is at altitude and is representative of conditions of quasi free troposphere. The annual mean temperature of 2019 and 2020 are situated in the 5th quintile of the 1961-90 reference series, with a classification of very warm, with data of 10.9 and 11.1 °C respectively.

Regarding total annual precipitation (Fig. 13.15b), both 2019 and 2020 have precipitation rates less than the 1961-90 median value. 2019 total annual precipitation is 265.1 mm and is classified as dry (in the 2nd quintile), while in 2020 the total annual precipitation is 217.1 mm and is classified as very dry (in the 1st quintile).

The total annual sunshine duration series also maintains a significant increasing trend of 39.2 h per decade trend (Fig. 13.15c). In 2019, total annual sunshine duration reached 4005.7 h, the maximum of the complete 105-year series since 1916. In 2020, the total annual sunshine duration was 3793.7 h, slightly below 3800 h (85% of the maximum possible number of hours).

The series of annual mean relative humidity (13.15d) continues the downward trend that began after the high values of the second half of the 20th century.

The evolution of the annual mean atmospheric pressure (13.15e) maintains the rate of rise of the last decade after the minimum of the 1950s-1960s, with the latest data for 2020 at 771.7 hPa being very close to the absolute maximum of the complete series.

An analysis was conducted to compare the meteorology of 2019 and 2020 at IZO to the long-term meteorological records. For example, 2020 broke the records for the highest

July and September monthly mean of daily maximum temperatures (Table 13.1).

Table 13.1. Meteorology of 2019 and 2020 at IZO in comparison with 1916-2020 meteorological records.

Extreme Event	Data	Date
Highest October daily maximum temperature	24.6 °C	1 Oct 2019
Maximum February daily wind path	2156 km	23 Feb 2020
Highest June maximum 10' mean wind velocity	105 km/h	17 Jun 2020
Maximum June precipitation intensity	6.0 mm/h	17 Jun 2020
Highest July monthly mean temperature	20.5 °C	Jul 2020
Highest July monthly mean of daily maximum temperatures	25.1 °C	Jul 2020
Highest August daily minimum soil temperature at 15 cm depth	26.8 °C	27 Aug 2020
Highest September daily minimum soil temperature at 15 cm depth	24.3 °C	6 Sep 2020
Highest September monthly mean of daily maximum temperatures	20.9 °C	Sep 2020

To ensure quality and continuity of observations within national and international meteorological and climatological observation networks in which IARC participates it is required to keep constant maintenance and vigilance of meteorological instrumentation and subsequent quality checking of meteorological data from IZO, SCO, BTO and TPO.

The networks in which IARC participates are the Synoptic Observation Network (WMO Region I, ID: 60010), included in the surface observation network of Global Climate Observing System, the AEMET Climatological Monitoring Network (ID C430E) and the Baseline Surface Radiation Network (BSRN; station # 61).

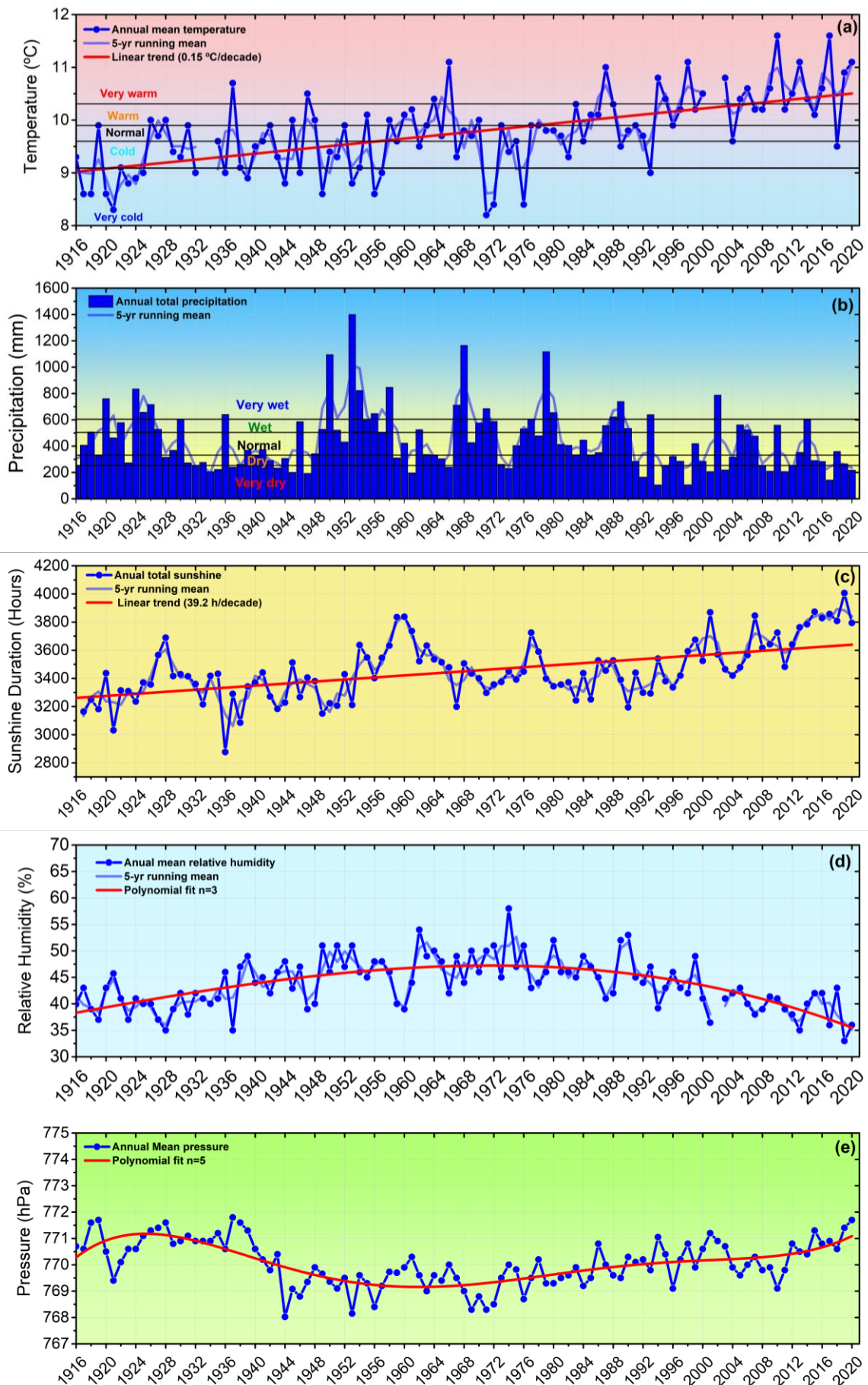


Figure 13.15. Time series (1916-2020) of a) annual mean temperature, b) total annual precipitation, c) annual sunshine duration, d) annual mean relative humidity and e) annual mean pressure at Izaña Observatory.

13.6.2 Prediction and analysis of severe weather events

Additional activities of the Meteorology programme include prediction and subsequent analysis of severe weather events that may affect operations of the various observation programmes at the four IARC observatories. We highlight some of the most important episodes during 2019-2020:

On 26 October 2019 there was an episode of intense rainfall with thunderstorms (Fig. 13.16) with an accumulation of rain of 43.6 mm, preceded by very strong winds from the SW on the 25 October, with a maximum gust of 113 km/h produced by a band of convergence in medium levels with humidity of tropical origin.



Figure 13.16. Photographic image of the storm on 26 October 2019, taken during the “Teide Clouds Laboratory” project from Izaña Observatory by Daniel López.

A storm on 5-6 December 2019 produced an accumulation of 93.4 mm total precipitation, a great part of which was snowfall, and in which wind gusts reached up to 118 km/h (Fig. 13.17).

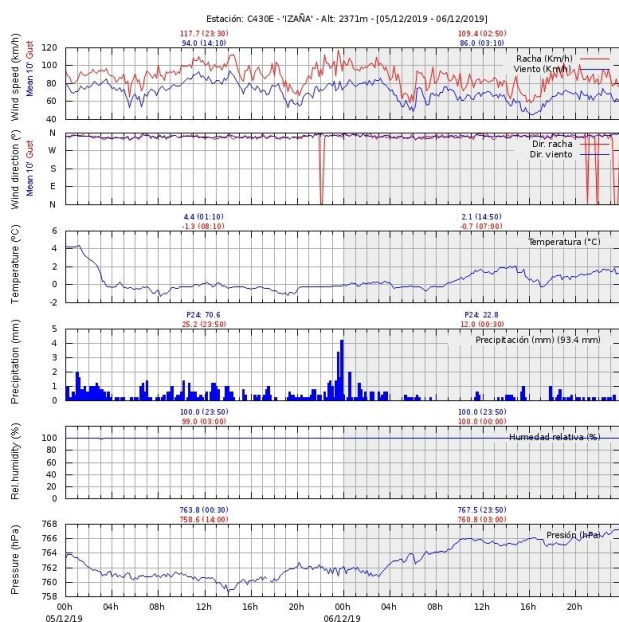


Figure 13.17. Meteorological data at Izaña Observatory recorded on 5 and 6 December 2019.

On 23 February 2020 there was a strong wind storm from the SE with gusts of hurricane wind speed up to 163 km/h, which resulted in an intense unprecedented desert dust outbreak in the Canary Islands (see Section 17).

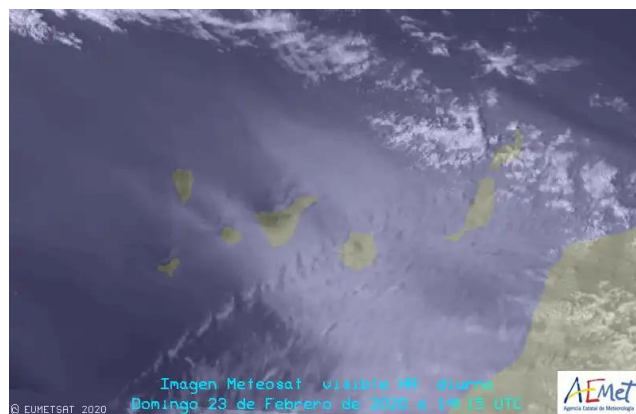


Figure 13.18. Meteosat image for 23 February 2020 at 14 UTC.

On 23 March 2020 there was a storm with a maximum recorded gust of 163 km/h and accumulated snow precipitation of 33.4 mm (Fig. 13.19).



Figure 13.19. Photograph of Izaña Observatory instrument terrace on 23 March 2020.

On 15 June 2020 there was an anomalous episode of strong wind with a maximum gust of 125 km/h and a maximum record for June wind speeds of sustained 10' mean wind velocity of 105 km/h.

On 20 October 2020 there was a storm with a maximum gust of 130 km/h.

A storm on 25-26 November 2020 produced an accumulation of 53.4 mm total precipitation (rain and snow) with maximum wind gusts of 149 km/h.

13.6.3 Project to improve the quality of forecasted PM₁₀ values during African desert dust outbreaks

We have participated in a project to improve the quality of forecasted PM₁₀ values during African desert dust outbreaks, utilising machine learning techniques, in conjunction with the Barcelona Supercomputer Centre (see Section 17 for more details).

13.6.4 Intercomparison of Boundary Layer Height from ECMWF IFS and radiosonde observations

In the context of research conducted to investigate the impact of desert dust outbreaks on air quality in urban areas (Milford et al., 2020), an intercomparison of Boundary Layer Height (BLH) was made for the period 2012–2017, using the ECMWF IFS numerical weather prediction model BLH output and the BLH calculated using the same ECMWF methodology from radiosonde observations at the AEMET Güimar Station. The histogram and correlation of the two datasets (observations and model) are shown in Figure 13.20a and b, demonstrating the good performance of the ECMWF IFS model in capturing the BLH distribution, with a correlation coefficient > 0.9.

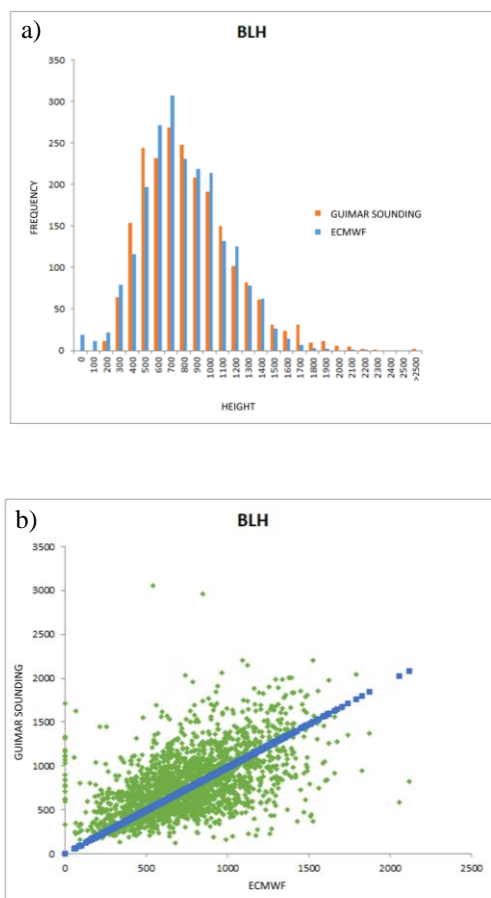


Figure 13.20. a) Histogram and b) correlation of daily values of Boundary Layer Height (BLH) from ECMWF IFS model and radiosonde observations for a six-year period (2012–2017).

13.6.5 Determination of temperature and humidity statistics at different levels using a sounding database

To study the vertical profile pattern related to the summer and winter seasons, for intense dust days and non-dust days, the temperature and the humidity have been grouped vertically in intervals of 50 m, and the median, the mean and the standard deviation calculated using six years of soundings at the Güimar station. The results are used as additional information included in Milford et al. (2020).

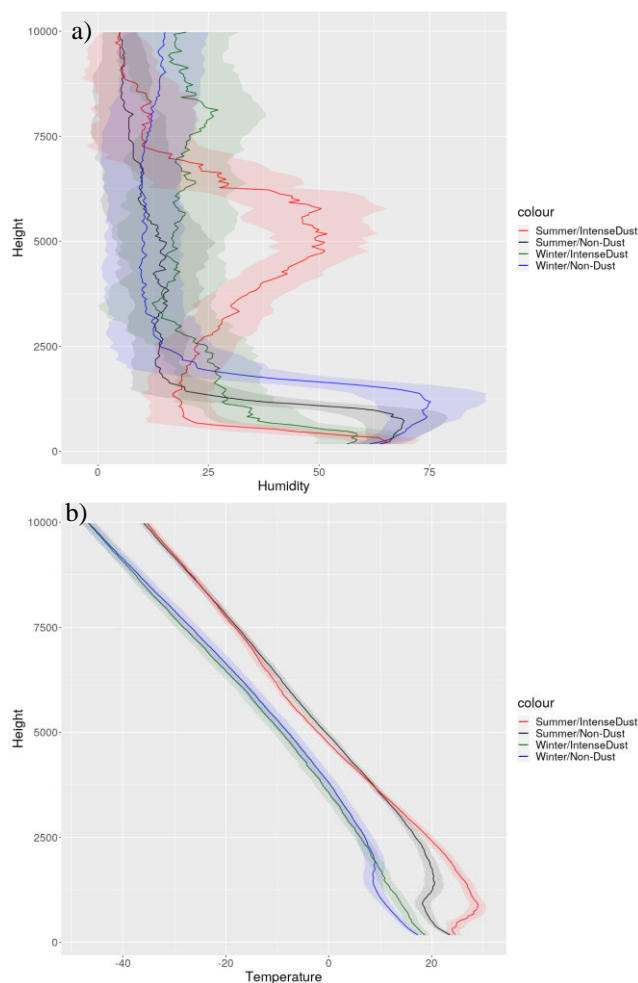
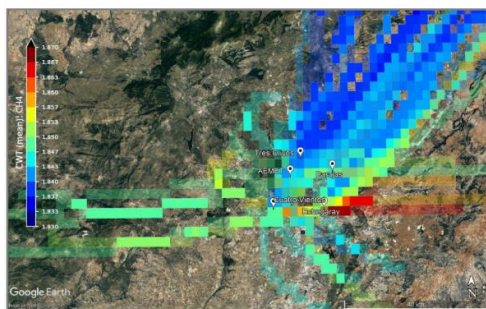


Figure 13.21. a) Median humidity and b) median temperature profiles for summer and winter, dust and non-dust classifications, shaded areas show the standard deviation.

13.6.6 Contributions to the campaign MEGEI-MAD

The project for the monitoring of urban greenhouse gases emission in Madrid (MEGEI-MAD) was conducted between 17 September – 9 October 2018, first results were shown in the NDACC/TCCON 2019 meeting (see Section 7.3.2 for more details). Specific high-resolution forecasts were made in order to plan the campaign. In addition, FLEXTRA back-trajectories were specifically calculated for the observation points at different vertical levels for every day of the campaign and used as inputs to the Concentration Weighted Trajectory (CWT) technique (Figure 13.22).

CH₄



CO₂

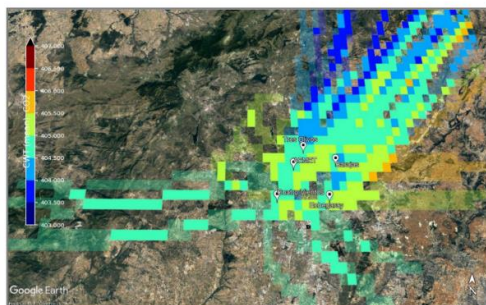


Figure 13.22. Image showing the concentrations of CH₄ and CO₂ and the back-trajectories using the Concentration Weighted Trajectories (CWT) technique (reprinted from García et al., 2019).

13.6.7 Contributions to the analysis of the Izaña and Santa Cruz temperature centennial series

We have participated in the study of the temperature centennial series at Izaña and Santa Cruz observatories, headed by Rosa García and Sara Izquierdo, in collaboration with the expert in Climatology, José A. Guijarro. Data have been analysed and processed in order to obtain a complete homogenised temperature series for both stations.

13.6.8 Back-trajectories for the Majadas flux-tower experimental site

A temporal series of daily FLEXTRA back-trajectories for 41 years (1979-2019) were calculated in order to evaluate the suitability of the Majadas de Tietar site (Extremadura, Spain) to install an experimental flux tower.

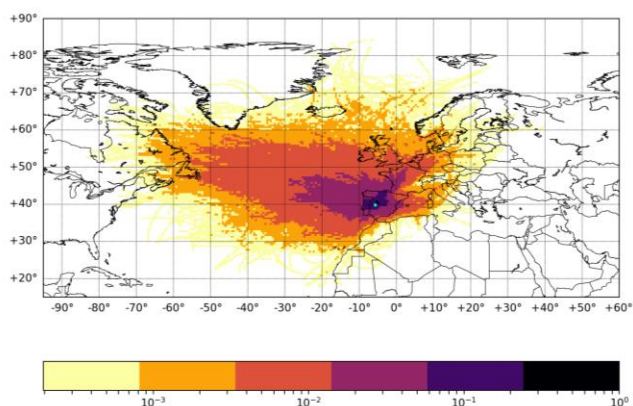


Figure 13.23. Multi annual footprint (1979-2019) obtained by Pedro Pablo Rivas, with monthly (January) relative frequencies of passing trajectories in every 0.5° x 0.5° grid cell.

13.6.9 Determination of the aerosol source contribution to the Payerne station in Switzerland

Back-trajectories have been calculated using both FLEXTRA and HYSPLIT models at different vertical levels from 2017 to 2019, as a contribution to a collaboration between AEMET and MeteoSwiss to investigate the location of the aerosol sources at the Payerne station in Switzerland. The main objective of this aerosol classification is to perform a complete statistical analysis of aerosol hygroscopic properties over Payerne. This information is the subject of a new scientific paper which is in preparation.

13.6.10 Vigilance and Equipment Checking

In order to maintain correct monitoring of the meteorological parameters to activate early warnings that prevent damage to specialized measurement equipment, a linux-based web logbook software has been installed and configured that is used by IARC staff to advise and record the malfunction of the equipment, granting the reliability of the observed data.

13.6.11 Contributions to the WMO GAW Report No. 259 WWRP 2021-1

A WMO GAW/WWRP report entitled: "Desert dust outbreak in the Canary Islands (February 2020): Assessment and impacts" (Cuevas et al., 2021) was prepared by a multidisciplinary group in order to document the intense unprecedented desert dust outbreak in the Canary Islands that occurred in 22-24 February 2020 and its associated impacts in different socio-economic sectors. A meteorological analysis was carried out to study the synoptic and mesoscale structures responsible for this event.

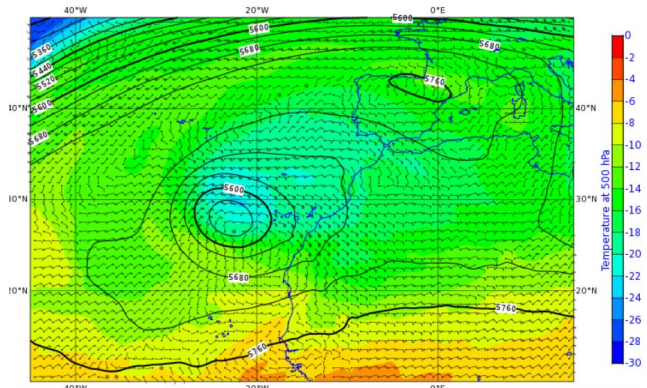


Figure 13.24. Analysis of the ECMWF IFS model on 23/2/2020 at 00 UTC of: geopotential height (black lines) and temperature (colour contouring) at 500 hPa and wind barbs at 850 hPa.

13.6.12 Study of PBL height with Vaisala CL51 ceilometer

An analysis of the PBL height (PBLH) was carried out in Santa Cruz de Tenerife (SCO) by Pedro Miguel Romero Campos using the backscatter profiles of the Vaisala CL51 ceilometer for the 2016-2019 period (see Section 9.2.2 for more details on the CL51 ceilometer). The analysis is based on the established definitions and techniques described in Moreira et al. (2020). Fig. 13.25 shows the evolution over time of the daily average of the PBLH, as well as the 30-day moving average and median. We see that the maximum PBLH is in summer and minimum is in winter.

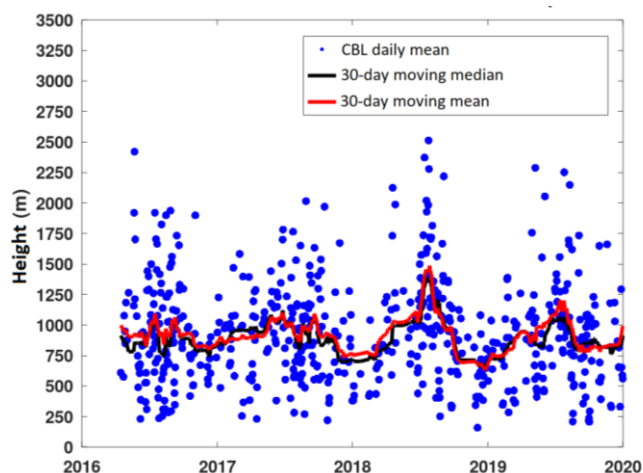


Figure 13.25. Evolution of the daily average of PBLH in Santa Cruz de Tenerife (2016-2019).

Fig. 13.26 shows the hourly averages of the PBLH averaged for each month in the 2016-2019 period. Maxima are seen in July around 1200-1300 UTC reaching ~ 1500 m altitude.

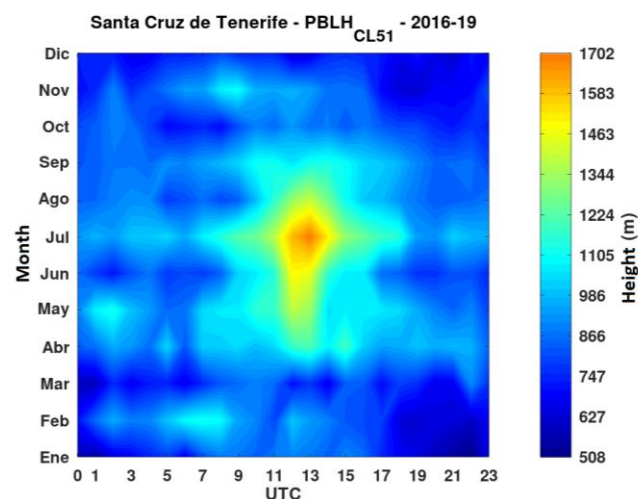


Figure 13.26. PBLH monthly hourly averages, Santa Cruz de Tenerife (2016-2019).

Box plots of the PBLH daily cycle for each season are shown in Fig. 13.27. These results demonstrate that the height of the PBL in Santa Cruz de Tenerife is, on average, ~ 1000 m during most of the year, except for the summer when it rises to approximately 1500 m.

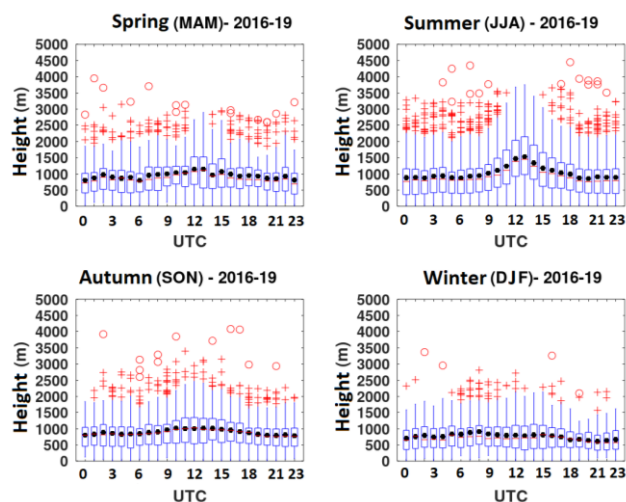


Figure 13.27. PBLH daily cycle for each season, Santa Cruz de Tenerife, 2016-2019. The red lines and the black points within the box represent the median and mean values, respectively, while the bottom and top of each box are the 25th and 75th percentiles. The outliers are indicated with crosses (1.5 to 3 x interquartile range) and with red circles (>3 x interquartile range).

13.6.13 Additional activities

We participated in the training course on "Advances in dust intrusion forecasts and their operational adaptation. Impact on aeronautical operations" organized by AEMET, held from 10 to 12 November 2020 (see Section 21.3 for more details). We presented results of the characterization of dust intrusions in the Canary Islands.

We participated as co-authors in Rodríguez et al. (2020) and in the Joint NDACC-IRWG and TCCON Meeting (20-24 May 2019), the XVIII Congreso de la Asociación Española de Teledetección (24-27 September 2019) and the 12th International Conference on Air Quality - Science and Application, 18-22 May 2020 with the following presentations:

- Monitoring of urban greenhouse gases emissions combining COCCON EM27 spectrometers and in-situ records (MEGEI-MAD) (García, et al., 2019a).
- Medida de las Concentraciones de Gases de Efecto Invernadero en Madrid (MEGEI-MAD) (García, et al., 2019b).
- Trends in air quality, Santa Cruz de Tenerife (Canary Islands) (Milford, et al., 2020).

13.7 References

Cuevas, E., Milford, C., Barreto, A., Bustos, J. J., García, R. D., Marrero, C. L., Prats, N., Bayo, C., Ramos, R., Terradellas, E., Suárez, D., Rodríguez, S., de la Rosa, J., Vilches, J., Basart, S., Werner, E., López-Villarrubia, E., Rodríguez-Mireles, S., Pita Toledo, M. L., González, O., Belmonte, J., Puigdemunt, R., Lorenzo, J.A., Oromí, P., and del Campo-Hernández, R.: Desert Dust Outbreak in the Canary Islands (February 2020): Assessment and Impacts. (Eds. Cuevas, E., Milford, C. and Basart, S.), State Meteorological Agency (AEMET), Madrid,

- Spain and World Meteorological Organization, Geneva, Switzerland, WMO Global Atmosphere Watch (GAW) Report No. 259, WWRP 2021-1, 2021.
- García, O., E. Sepúlveda, J.-A. Morgui, C. Estruch, R. Curcoll, M. Frey, C. Schneider, R. Ramos, C. Torres, S.F. León-Luis, F. Hase, A. Butz, C. Toledano, E. Cuevas, T. Blumenstock, C. Marrero, J.J. Bustos, J. López-Solano, V. Carreño, C. Pérez García-Pando, M. Guevara, O. Jorba, Monitoring of Urban Greenhouse Gases Emissions combining COCCON EM27 spectrometers and in-situ records (MEGEI-MAD), 2019 Joint NDACC-IRWG and TCCON Meeting, Wanaka, New Zealand, 20th-24th May, 2019a.
- García, O., Sepúlveda, E., Morgui, J.A., Frey, M., Schneider, C., Curcoll, R., Estruch, C., Ramos, R., Torres, C., León, S., Hase, F., Butz, A., Toledano, C., Cuevas, E., Blumenstock, T., Pérez, C., Guevara, M., Jorba, O., Marrero, C., Bustos, J.J., López-Solano, J., Romero-Campos, P.M., Medida de las Concentraciones de Gases de Efecto Invernadero en Madrid (MEGEI-MAD), XVIII Congreso de la Asociación Española de Teledetección, Valladolid (Spain), 24-27 September, 2019b.
- Milford, C., Cuevas, E., Marrero, C.L., Bustos, J., Gallo, V., Rodríguez, S., Romero-Campos, P.M., Torres, C. Impacts of Desert Dust Outbreaks on Air Quality in Urban Areas, *Atmosphere*, 11, 23, doi:10.3390/atmos11010023, 2020.
- Milford, C., Cuevas, E., Marrero, C., Bustos, J.J., Torres, C., Trends in air quality, Santa Cruz de Tenerife (Canary Islands), 12th International Conference on Air Quality - Science and Application, Online Conference, Hosted by Aristotle University, Thessaloniki, Greece, 18-22 May 2020.
- Milford, C., Marrero, C., Martin, C., Bustos, J. & Querol, X. Forecasting the air pollution episode potential in the Canary Islands. *Adv. Sci. Res.* 2, 21–26, 2008.
- Moreira, G. de A., Guerrero-Rascado, J.L., Bravo-Aranda, J.A., Foyo-Moreno, I., Cazorla, A., Alados, I., Lyamani, H., Landulfo, E., Alados-Arboledas, L., 2020. Study of the planetary boundary layer height in an urban environment using a combination of microwave radiometer and ceilometer. *Atmospheric Research* 240, 104932. <https://doi.org/10.1016/j.atmosres.2020.104932>
- Rodríguez, S., Calzolari, G., Chiari, M., Nava, S., García, M.I., López-Solano, J., Marrero, C., López-Darias, J., Cuevas, E., Alonso-Perez, S., Prats, N., Amato, F., Lucarelli, F., Querol, X.: Rapid changes of dust geochemistry in the Saharan Air Layer linked to sources and meteorology, *Atmospheric Environment*, 223, 117186 doi:10.1016/j.atmosenv.2019.117186, 2020.
- Cándida Hernández (AEMET; Meteorological Observer-GAW Technician)
- Dr Emilio Cuevas (AEMET; Research Scientist)
- Dr Rosa García (TRAGSATEC/UVA; Research Scientist)
- Pedro Miguel Romero Campos (AEMET; Research Scientist)

13.8 Staff

- Carlos Luis Marrero de la Santa Cruz (AEMET; Head of programme)
- Juan José Bustos (AEMET; Research Scientist)
- Ramón Ramos (AEMET; Head of Infrastructure, Responsible for Meteorological Observation Programme)
- Sergio Afonso (AEMET; Meteorological Observer-GAW Technician) retired in 2019
- Antonio Alcántara (AEMET; Meteorological Observer-GAW Technician)
- Concepción Bayo (AEMET; Meteorological Observer-GAW Technician)
- Virgilio Carreño (AEMET; Meteorological Observer-GAW Technician)

14 Aerobiology

The Aerobiology programme at the IARC is carried out jointly by IARC-AEMET and the Laboratori d'Anàlisis Palinològiques (LAP) of the Universidad Autònoma de Barcelona (UAB) with partial financing from Air Liquide España S.A through the Eolo-PAT project. This programme started in 2004 at SCO with the aim of improving the knowledge of the pollen and spore content in the air of Santa Cruz de Tenerife and its relation to the prevalence of respiratory allergy. A second aerobiological station was implemented at IZO thanks to the financial support of the Research and development (R+D) National Plan CGL-2005-07543 project ("Origin, transport and deposition of African atmospheric aerosol in the Canaries and the Iberian Peninsula based on its Chemical and Aerobiological Characterization"). These two projects also contribute to improvement of knowledge of the biological fraction of aerosols within the GAW program.

14.1 Main Scientific Goals

The main scientific goals of this programme are:

- To produce high quality standardized data on the biological component of the atmospheric aerosol.
- To establish the biodiversity and quantity of pollen and fungal spores registered in the air of Santa Cruz de Tenerife and Izaña.
- To establish the distribution pattern over the course of the year of the airborne pollen and fungal spores at Santa Cruz de Tenerife and Izaña, through the daily spectra.
- To put the Canary islands on the map of the global aerobiological panorama, along with the Spanish (REA; SEAIC) and European networks (EAN).
- To provide information useful for medical specialists and allergic patients.
- To set up the list of the allergenic pollen and spore taxa in the air of Santa Cruz de Tenerife and Izaña that will help doctors to diagnose the allergy aetiology and to rationalize the use of the medication.
- To produce weekly alerts on the allergenic pollen and spores for the days ahead to help doctors in the allergy detection and to help people suffering from allergies with a better planning of their activities and to improve the quality of their life.

A detailed description of this programme can be found in Belmonte et al. (2011).

14.2 Measurement Programme

The sampling instrument is a Hirst, 7-day recorder VPPS 2000 spore trap (Lanzoni S.r.l.) (Fig. 14.1) and the analysing instrument is a Light microscope, 600 X (Table 3.2). The pollen and spore analysis is conducted using palynological methods following the recommendations of the Spanish Aerobiology Network management and quality manual and the recommendations of the European Aerobiology Society (Galán et al. 2017). The sampling programme at SCO is continuous through the year, whereas samples are only collected at IZO from April-May to November because of adverse meteorological conditions during the rest of the year.

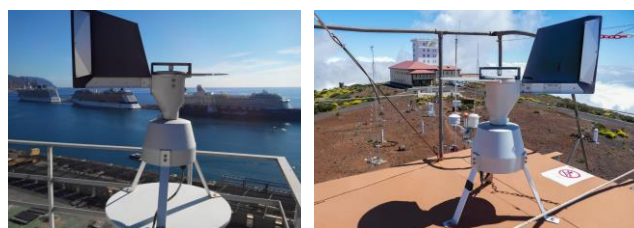


Figure 14.1. Hirst, 7-day recorder VPPS 2000 spore trap at SCO (left) and at IZO (right).

14.3 Summary of remarkable results during the period 2019-2020

The annual dynamics of the total pollen and total fungal spores taxa in Santa Cruz de Tenerife and Izaña are shown in Figs. 14.2 and 14.3. Data represent mean weekly concentrations of historical data and data from 2019.

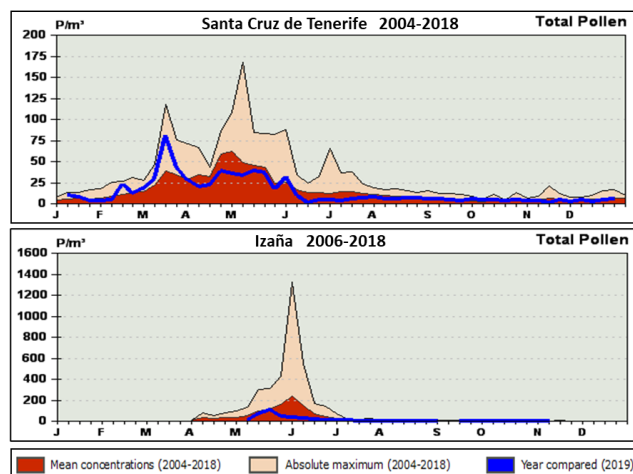


Figure 14.2. Dynamics of the mean weekly Total Pollen concentrations in Santa Cruz de Tenerife (upper) and Izaña (lower) during 2019 in comparison with 2004-2018 mean and maximum data.

Table 14.1. Airborne pollen and spore spectrum for SCO, year 2019.

SANTA CRUZ DE TENERIFE

1 January 2019 - 31 December 2019

	YEAR		WEEK		DAY	
	Integral P*day/m ³	Percentage %	Maximum P/m ³	Week nr. Nr.	Maximum P/m ³	Date of the Maximum dd/mm/yyyy
TOTAL POLLEN	4717	100	81.5	11	179.9	16/3/2019
POLLEN FROM TREES	1995	42.3	25.0	11	74.9	16/3/2019
<i>Acacia</i>	1	0.0	0.1	15	0.7	11/4/2019
<i>Ailanthus</i>	1	0.0	0.1	29	0.7	15/1/2019
<i>Alnus</i>	0	0.0	0.0		0.0	
<i>Castanea</i>	12	0.3	0.5	29	1.4	16/07/2019 ; 25/07/2019
<i>Casuarina</i>	27	0.6	0.9	49	4.9	4/12/2019
CUPRESSACEAE	118	2.5	2.0	7	7.0	31/3/2019
<i>Eucalyptus</i>	25	0.5	0.4	23	2.8	4/6/2019
<i>Ilex</i>	0	0.0	0.0		0.0	
MORACEAE	52	1.1	2.1	49	14.7	5/12/2019
<i>Myrica</i>	703	14.9	17.8	11	52.5	16/3/2019
OLEACEAE	171	3.6	7.5	22	39.2	27/5/2019
PALM TREES	341	7.2	8.4	7	47.6	14/2/2019
<i>Pinus</i>	140	3.0	4.3	16	23.1	16/4/2019
<i>Platanus</i>	8	0.2	0.7	11	1.4	11/03/2019 ; 12/03/2019 ; 16/03/2019
<i>Populus</i>	11	0.2	0.5	51	1.4	14/02/2019 ; 28/03/2019 ; 31/03/2019
<i>Quercus</i> total	161	3.4	8.6	13	46.9	27/3/2019
<i>Salix</i>	8	0.2	0.3	2	2.1	24/3/2019
<i>Schinus</i>	210	4.5	2.2	29	9.1	18/11/2019
<i>Tilia</i>	0	0.0	0.0		0.0	
<i>Ulmus</i>	3	0.1	0.3	36	2.1	8/9/2019
Other pollen from trees	5	0.1	-	-	-	-
POLLEN FROM SHRUBS	962	20.4	47.1	11	98.0	17/3/2019
CISTACEAE	1	0.0	0.1	6	0.7	43504
ERICACEAE	917	19.4	46.9	11	98.0	17/3/2019
<i>Ricinus</i>	32	0.7	0.6	20	2.1	16/12/2019
<i>Pistacia</i>	6	0.1	0.8	12	4.9	21/3/2019
Other pollen from shrubs	6	0.1	-	-	-	-
POLLEN FROM HERBS	1667	35.3	19.8	17	37.1	14/5/2019
COMPOSITAE total (incl. <i>Artemisia</i>)	621	13.2	13.6	17	25.9	3/4/2019
<i>Artemisia</i>	581	12.3	13.6	17	25.9	3/4/2019
BORAGINACEAE	32	0.7	1.6	8	10.5	24/2/2019
CYPERACEAE	20	0.4	0.7	22	2.1	14/05/2019 ; 27/05/19 ; 29/09/19
CRASSULACEAE	1	0.0	0.1	6	0.7	10/2/2019
CRUCIFERAE	34	0.7	1.3	12	4.9	18/3/2019
<i>Euphorbia</i>	2	0.0	0.2	22	0.7	29/05/2019 ; 02/06/2019 ; 28/07/2019
GRAMINEAE (Grasses)	333	7.1	5.4	21	15.4	26/5/2019
<i>Mercurialis</i>	46	1.0	0.9	11	4.9	12/3/2019
<i>Plantago</i>	57	1.2	1.1	11	3.5	22/3/2019
<i>Rumex</i>	160	3.4	2.1	7	9.1	14/2/2019
CHENOPODIACEAE/AMARANTHACEAE	125	2.6	1.8	7	6.3	14/2/2019
URTICACEAE	176	3.7	2.3	22	8.4	1/6/2019
Other pollen from herbs	60	1.2	-	-	-	-

	YEAR		WEEK		DAY	
	Integral S*day/m ³	Percentage %	Maximum S/m ³	Week nr. Nr.	Maximum S/m ³	Date of the Maximum dd/mm/yyyy
TOTAL SPORES	75387	100.0	592.4	43	1621.2	27/10/2019
<i>Alternaria</i>	1722	2.3	15.6	20	58.8	10/3/2019
Ascospores	25782	34.2	248.4	43	1156.4	27/10/2019
<i>Aspergillus/Penicillium</i>	1568	2.1	62	37	364.0	11/9/2019
<i>Cladosporium</i>	27350	36.3	203.2	20	694.4	30/4/2019
<i>Ustilago</i>	7036	9.3	101.6	20	380.8	26/5/2019
Other fungal spores	11928	15.8	-	-	-	-

Table 14.2. Airborne pollen and spore spectrum for IZO, year 2019.

IZAÑA

29 April 2019 - 04 November 2019

	YEAR		WEEK		DAY	
	Integral P*day/m ³	Percentage %	Maximum P/m ³	Week nr. Nr.	Maximum P/m ³	Date of the Maximum dd/mm/yyyy
TOTAL POLLEN	2488	100	106.2	20	203.0	16/5/2019
POLLEN FROM TREES	545	21.9	31.1	19	68.6	8/5/2019
<i>Acacia</i>	0	0.0	0.0		0.0	
<i>Ailanthus</i>	0	0.0	0.0		0.0	
<i>Alnus</i>	0	0.0	0.0		0.0	
<i>Castanea</i>	50	2.0	2.0	32	9.1	5/8/2019
<i>Casuarina</i>	2	0.1	0.2	39	0.7	24/09/2019 ; 25/09/2019 ; 09/10/2019
CUPRESSACEAE	22	0.9	2.4	23	16.1	7/7/2019
<i>Eucalyptus</i>	1	0.1	0.2	41	1.4	8/10/2019
<i>Ilex</i>	0	0.0	0.0		0.0	
MORACEAE	0	0.0	0.0		0.0	
<i>Myrica</i>	258	10.4	15.1	19	43.4	8/5/2019
OLEACEAE	11	0.4	0.6	22	2.8	2/7/2019
PALM TREES	1	0.1	0.1	23	0.7	07/07/2019 ; 25/10/2019
<i>Pinus</i>	195	7.8	15.9	19	27.3	11/5/2019
<i>Platanus</i>	0	0.0	0.0		0.0	
<i>Populus</i>	0	0.0	0.0		0.0	
<i>Quercus</i>	4	0.2	0.4	22	2.8	28/5/2019
<i>Salix</i>	1	0.0	0.1	34	0.7	24/8/2019
<i>Schinus</i>	1	0.0	0.1	39	0.7	25/9/2019
<i>Tilia</i>	0	0.0	0.0		0.0	
<i>Ulmus</i>	0	0.0	0.0		0.0	
Other pollen from trees	0	0.0	-	-	-	
POLLEN FROM SHRUBS	24	1.0	1.5	19	5.6	6/5/2019
CISTACEAE	0	0.0	0.0		0.0	
ERICACEAE	20	0.8	1.4	19	4.9	6/5/2019
<i>Ricinus</i>	3	0.1	0.2	21	0.7	06/05/2019 ; 21/05/2019 ; 26/05/2019
<i>Pistacia</i>	0	0.0	0.0		0.0	
Other pollen from shrubs	1	0.1	-	-	-	
POLLEN FROM HERBS	1795	72.1	96.0	20	189.7	16/5/2019
COMPOSITAE total (incl. <i>Artemisia</i>)	46	1.8	1.9	20	5.6	17/5/2019
<i>Artemisia</i>	45	1.8	1.9	20	5.6	17/5/2019
BORAGINACEAE	6	0.3	0.3	19	1.4	10/5/2019
CYPERACEAE	6	0.3	0.3	43	1.4	26/10/2019 ; 28/10/2019
CRASSULACEAE	0	0.0	0.0		0.0	
CRUCIFERAE	1383	55.6	78.6	20	182.7	16/5/2019
<i>Euphorbia</i>	0	0.0	0.0		0.0	
GRAMINEAE (Grasses)	85	3.4	4.0	20	14.7	18/5/2019
<i>Mercurialis</i>	0	0.0	0.0		0.0	
<i>Plantago</i>	7	0.3	0.3	20	1.4	13/05/2019 ; 28/05/2019 ; 20/06/2019
<i>Rumex</i>	56	2.3	3.2	20	10.5	13/5/2019
CHENOPODIACEAE/AMARANTHACEAE	31	1.2	0.8	41	2.8	12/10/2019
URTICACEAE	132	5.3	7.1	20	21.7	13/5/2019
Other pollen from herbs	43	1.7	-	-	-	-

	YEAR		WEEK		DAY	
	Integral S*day/m ³	Percentage %	Maximum S/m ³	Week nr. Nr.	Maximum S/m ³	Date of the Maximum dd/mm/yyyy
TOTAL SPORES	14218	100.0	263.6	25	1330.0	17/6/2019
<i>Alternaria</i>	574	4.0	9.6	43	25.2	25/10/2019
Ascospores	3030	21.3	28.9	37	89.6	15/9/2019
<i>Aspergillus/Penicillium</i>	81	0.6	4.0	22	28.0	28/5/2019
<i>Cladosporium</i>	6703	47.1	214.0	25	1285.2	17/6/2019
<i>Ustilago</i>	1893	13.3	32.4	22	106.4	28/5/2019
Other fungal spores	1937	13.6	-	-	-	-

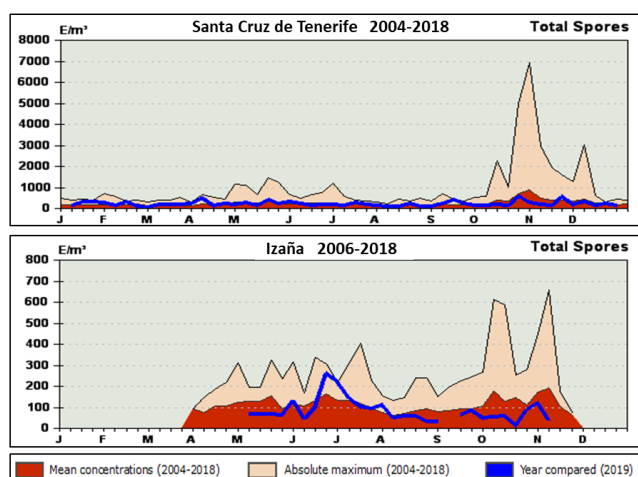


Figure 14.3. Dynamics of the mean weekly Total Fungal Spore concentrations in Santa Cruz de Tenerife (upper) and Izaña (lower) during 2019 in comparison with 2004-2018 mean and maximum data.

The plots show that the annual course of total concentration of pollen and fungal spores at SCO is very different from that observed at IZO. There is also a large interannual variability driven by weather conditions such as temperature and precipitation. While in SCO, concentration of pollen shows a broad maximum covering a spring season (March to late May), that in 2019 occurred mainly in March, in IZO higher pollen concentrations during the measurement period happen in two months (usually from May to late June) but centered in May in 2019. Usually, pollen concentration values are somewhat higher for IZO than for SCO (Fig. 14.2). Main pollen taxa in SCO were *Erica*, *Myrica*, *Artemisia*, palm trees and grasses, all of them are very important in the landscape, followed by *Schinus* and *Urticaceae* which are mainly urban taxa. In IZO, *Cruciferae* (or *Brassicaceae*) pollen is predominant, followed by *Myrica*, *Pinus*, *Urticaceae*, *Rumex* and grasses (Tables 14.1 and 14.2).

The total concentration of fungal spores shows a contrasting seasonal variation to that of total pollen. In 2019, in SCO the concentrations showed small peaks in September and in April that reached values slightly higher than the mean values. At IZO, in 2019, fungal spores concentrations exceeded the mean values by the end of June-early July. There is a big difference of the order of magnitude of the concentrations recorded in SCO and IZO (Fig. 14.3). Main fungal spore taxa are *Ascospores*, *Cladosporium* and *Ustilago*, followed by *Alternaria* and *Aspergillus/Penicillium* (Tables 14.1 and 14.2).

The results presented here are a summary of the detailed information generated. However individual taxa might have quite a different seasonal behaviour at each station (see Tables 14.1 and 14.2 and graphs that can be generated on the [webpage](#)).

A number of products, such as current levels and forecasts of the main allergenic pollens and fungal spores, historical

and current data and pollen calendar for SCO can be found at the Tenerife Aerobiology information (Proyecto EOLO-PAT) [web page](#).

14.4 Future Activities

- Continuation of pollens and fungal spores sampling, and aerobiological data analysis.
- Update of the airborne pollen and spores databases.
- Improvement of the information provided through the [webpage](#) and services to its users.
- Trend analysis.
- Internannual variability versus meteorology.

14.5 References

- Belmonte, J., Cuevas, E., Poza, P., González, R., Roure, J.M., Puigdemunt, R., Alonso-Pérez, S., Grau, F. Aerobiología y alergias respiratorias de Tenerife. Editor: Agencia Estatal de Meteorología/Ministerio de Medio Ambiente y Medio Rural y Marino, 2010. NIPO (versión electrónica): 784-10-006-2.
- Belmonte, J., C. De Linares, A. Fernández-Llamazares, C. Díaz de la Guardia, P. Cariñanos, S. Alonso-Pérez, E. Cuevas, J.M. Maya, S. Fernández, I. Silva, R. Tormo, Airborne Pinus pollen in Spain: pollination patterns and trends of the annual indexes and the peak dates, 5th European Symposium on Aerobiology, Krakow, Poland, 3 - 7 September, 2012.
- Belmonte, J., E. Cuevas: Proyecto EOLO-PAT. Estudio de alérgenos en Canarias. Resumen anual de datos 2012. Bellaterra: Proyecto EOLO-PAT, 2013.
- De Linares, C., Delgado, R., Aira, M.J., Alcázar, P., Alonso-Pérez, S., Boi, M., Cariñanos, P., Cuevas, E., Díaz de la Guardia, C., Elvira-Rendueles, B., Fernández-González, D., Galán, C., Gutiérrez-Bustillo, A.M., Pérez-Badia, R., Rodríguez-Rajo, F.J., Ruiz-Valenzuela, L., Tormo-Molina, R., Trigo, M.M., Valencia-Barrera, R.M., Valle, A., Belmonte, J. Changes in the Mediterranean pine forest: pollination patterns and annual trends of airborne pollen. *Aerobiologia*, 33: 375-391, 2017.
- Galán, C., Ariatti, A., Bonini, M., Clot, B., Crouzy, B., Dahl, A., Fernandez-González, D., Frenguelli, G., Gehrig, R., Isard, S., Levetin, E., Li, D.W., Mandrioli, P., Rogers, C.A., Thibaudon, M., Sauliene, I., Skjoth, C., Smith, M., Sofiev, M. Recommended terminology for aerobiological studies. *Aerobiologia*, 33: 293-295, 2017.

14.6 Staff

Dr Jordina Belmonte (UAB; Head of programme)

Dr Emilio Cuevas (AEMET; Co-PI)

Ramón Ramos (AEMET; Hirst sampler maintenance)

Virgilio Carreño (AEMET; Sampling)

Rut Puigdemunt (UAB; Technical Analyst)

David Navarro (UAB; Technical Analyst)

Dr Concepción De Linares (UAB; Research Scientist)

Cándida Hernández (AEMET; Meteorological Observer-GAW Technician)

Concepción Bayo (AEMET; Meteorological Observer-GAW Technician)

International Cooperation Programmes

15 ACTRIS

The Aerosol, Clouds and Trace Gases Research Infrastructure (ACTRIS) is the pan-European research infrastructure (RI) producing high-quality data and information on short-lived atmospheric constituents and on the processes leading to the variability of these constituents in natural and controlled atmospheres (simulation chambers).

ACTRIS enables access to high-quality long-term atmospheric data through a single-entry point. It offers access to world-class facilities providing researchers, from academia as well as from the private sector, with the best research environments and expertise promoting cutting-edge science and international collaboration.

ACTRIS is composed of nine connected elements: distributed National Facilities (Observational platforms and Exploratory platforms) both in Europe and globally, and eight Central Facilities (Head Office, Data Centre and six Topical Centres) (Fig. 15.1).

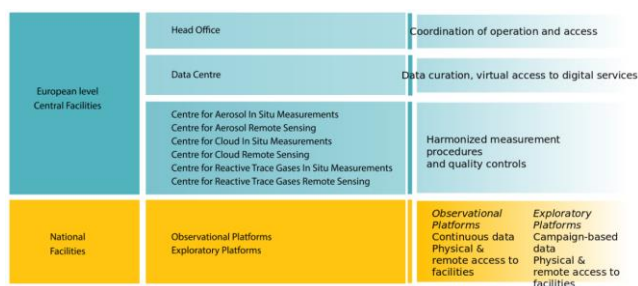


Figure 15.1. ACTRIS research infrastructure core components.

ACTRIS research infrastructure works towards:

- reducing uncertainties in quantification of emission sources, improved understanding of deposition processes that remove short-lived constituents from the atmosphere and quantification of their potential impacts on ecosystems.
- bringing essential information for understanding global biogeochemical interactions between the atmosphere and ecosystems, and how climate-ecosystem feedback loops may change atmospheric composition in the future.
- supporting the development of the required level of understanding of sources of the air pollutants that negatively affect human health.
- complementing Earth Observations from space with the necessary observations, providing unique ground-truthing of remote sensing information collected by current and future satellite missions.

15.1 ACTRIS-Implementation Phase Project

ACTRIS was included in the European Strategy Forum on Research Infrastructures (ESFRI) roadmap in 2016. After many years of community building, design phase, and three years of ACTRIS Preparatory Phase Project (ACTRIS PPP), ACTRIS is now immersed in a five-year implementation phase (2020-2024) dedicated to constructing and upgrading the National Facilities and Central Facilities, setting-up the user access and service provision, working on the governance and management tasks, increasing the connection with new users and member countries, further developing strategies within ACTRIS and for international collaboration and partnerships, and integrating ACTRIS at different strategic levels (national, European and internationally) (Fig. 15.2).

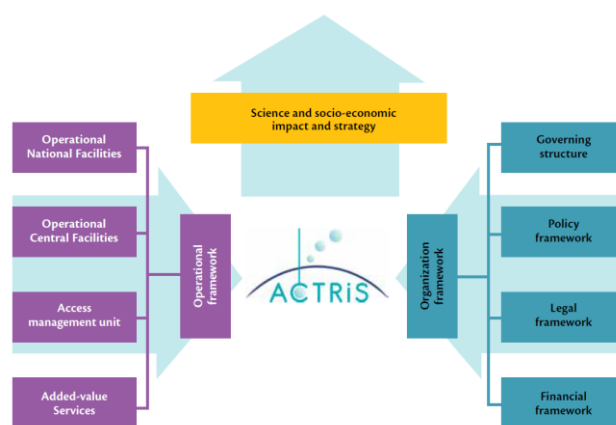


Figure 15.2. ACTRIS Work Breakdown Structure. Each box describes a key action/product. Reprinted from ACTRIS (2018).

The process is funded as ACTRIS Implementation Project (ACTRIS IMP), through the EU Horizon 2020 Coordination and Support Section (grant agreement No 871115) project. ACTRIS IMP started on 1 January 2020 for a period of five years.

The ACTRIS implementation project builds on the achievements of the successful ACTRIS PPP and on the scientific and technical deliveries of the ACTRIS-2 and EUROCHAMP-2020 projects. The ACTRIS IMP project objectives are based on the overall ACTRIS implementation phase objectives which are to coordinate and accomplish the actions required for implementing a globally recognised long-term sustainable research infrastructure with operational services by 2025 (see Fig. 15.3).

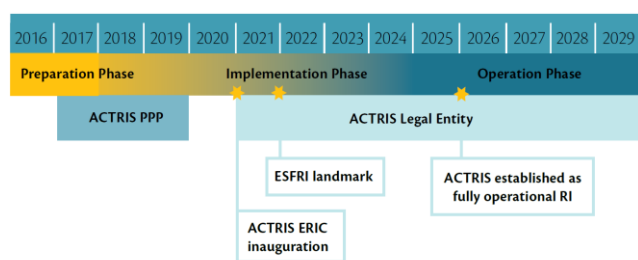


Figure 15.3. ACTRIS lifecycle phases from design to preparation, implementation and operation. The stars represent ACTRIS targets. Reprinted from ACTRIS (2018).

15.2 Centre for Aerosol Remote Sensing

The Centre for Aerosol Remote Sensing (CARS) is one of the six ACTRIS Topical Centres. The mission of CARS is to offer operation support to ACTRIS National Facilities operating aerosol remote sensing instrumentation: aerosol high-power lidars, automatic low power lidars and ceilometers, and automatic sun/sky/polarised/lunar photometers. Additionally, CARS offers specialised services for the above instruments and related ACTRIS variables, to ACTRIS users of various types: academia, business, industry and public services. CARS is composed by the following units, which are grouped in three clusters, one cluster for each measurement technique (see Fig. 15.4):

- 1) National Institute of Research and Development for Optoelectronics (INOE), Romania.
- 2) Meteorological Institute of the Ludwig-Maximilians-University (LMU-MIM), Germany.
- 3) Consiglio Nazionale delle Ricerche (CNR), Italy.
- 4) Hohenpeissenberg Meteorological Observatory, Deutscher Wetterdienst (DWD), Germany.
- 5) CNRS-Laboratoire d'Optique Atmosphérique, Lille University, France.
- 6) Atmospheric Optic Group, University of Valladolid (UVA), Spain.
- 7) Izaña Atmospheric Research Center (AEMET), Spain.

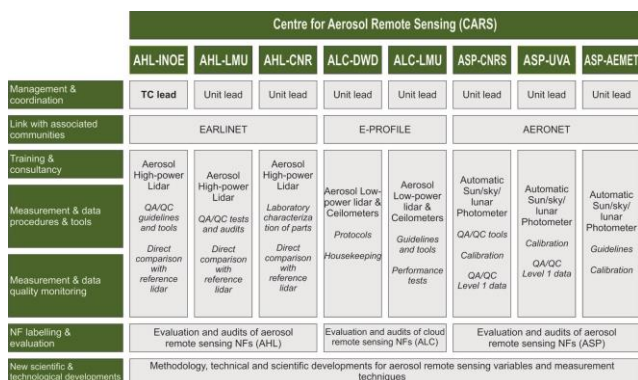


Figure 15.4. CARS organigram.

CARS offers operation support to ACTRIS National Facilities, as well as specialized services to ACTRIS users:

- Training and consultancy for setting up and running an aerosol remote sensing station.
- Measurement and data processing and tools for QA/QC of the lidar and photometer measurements.
- Measurement and data quality monitoring, including calibration of photometers, characterization of lidar optical blocks, direct comparison with reference systems, support for debugging, upgrading and optimizing the instruments.

The CARS activities related to the measurement technique Automatic Sun/sky/polarised/lunar Photometers (CARS-ASP) are provided by CNRS-LOA (Lille, France), UVA-GOA (Valladolid, Spain) and AEMET-Izaña (Izaña, Spain) (see Figs.15.4 and 15.5). Izaña Observatory provides a unique facility for absolute calibration of Master Cimel instruments (Fig. 15.6). For more details about the early AERONET-EUROPE Calibration Service, which is now incorporated into CARS-ASP, see previous IARC Activity Reports (e.g Cuevas et al., 2019).



Figure 15.5. Location of the three calibration facilities of CARS-ASP.

IZO continue to host a set of six reference instruments continuously in operation and available for the needs of the LOA and GOA facilities. AERONET-EUROPE master instruments from LOA and GOA are recalibrated every three months at IZO in order to assure measurement accuracy. Master instruments from other networks such as the China Aerosol Remote Sensing NETwork (CARSNET) are also recalibrated at IZO on a regular basis.

All users who operate either a standard or a polarized CIMEL sun/sky or triple (sun/sky/lunar) photometer located in Europe or outside Europe but run in the framework of international cooperation agreements can submit a proposal to ACTRIS CARS-ASP Calibration Service at any time. The instrument calibration and maintenance are performed

free of charge, and proposals are granted on the basis of a TransNational Access (TNA) selection panel review process. Instrument shipping expenses from and to the user site are not included and must be covered by the user institution.

Most of the accesses provided under ACTRIS CARS-ASP allow to assure quality of data on sites operating not only a sun or triple photometer but also multiple complementary in situ, remote sensing and radiation instruments. In the period 2019-2020 one TNA was granted to the company EKO Instruments Europe. An EKO MS-711 and a RSB grating spectroradiometer were installed in Izaña for intercomparison and evaluation of AOD and PWV as well as for improvement of the measurement accuracy of the stray light correction performed by these two instruments.

Quality-assured data from AERONET-EUROPE are widely used by modelling and satellite communities through several European programmes and initiatives (ESA, GMES, AEROCOM, etc). By the end of 2019, 31 AERONET sun-photometers were used for near-real-time validation of dust forecast models by the SDS-WAS Regional Center for North Africa, Middle East and Europe, most of them were calibrated by AERONET-EUROPE (Terradellas et al., 2020). CAMS also uses data of 67 AERONET sun-photometers in near real time for the specific model aerosol products verification performed in 2020 (Eskes et al., 2021).

15.3 References

ACTRIS Stakeholder Handbook 2018.

Cuevas, E., Milford, C., Bustos, J. J., R., García, O. E., García, R. D., Gómez-Peláez, A. J., Guirado-Fuentes, C., Marrero, C., Prats, N., Ramos, R., Redondas, A., Reyes, E., Rivas-Soriano, P. P., Rodríguez, S., Romero-Campos, P. M., Torres, C. J., Schneider, M., Yela, M., Belmonte, J., del Campo-Hernández, R., Almansa, F., Barreto, A., López-Solano, C., Basart, S., Terradellas, E., Werner, E., Afonso, S., Bayo, C., Berjón, A., Carreño, V., Castro, N. J., Chinea, N., Cruz, A. M., Damas, M., De Ory-Ajamil, F., García, M.I., Gómez-Trueba, V.,

Hernández, C., Hernández, Y., Hernández-Cruz, B., León-Luís, S. F., López-Fernández, R., López-Solano, J., Parra, F., Rodríguez, E., Rodríguez-Valido, M., Sálamo, C., Sanromá, E., Santana, D., Santo Tomás, F., Sepúlveda, E., and Sosa, E.: Izaña Atmospheric Research Center Activity Report 2017-2018. (Eds. Cuevas, E., Milford, C. and Tarasova, O.), State Meteorological Agency (AEMET), Madrid, Spain and World Meteorological Organization, Geneva, Switzerland, WMO/GAW Report No. 247, 2019.

Eskes, H.J., Basart, S., Benedictow, A., Bennouna, Y., Blechschmidt, A.-M., Chabrilat, S., Cuevas, E., Errera, Q., Flentje, H., Hansen, K. M., Kapsomenakis, J., Langerock, B., Ramonet, M., Richter, A., Schulz, M., Sudarchikova, N., Wagner, A., Warneke, T., Zerefos, C.: Observation characterisation and validation methods document, Copernicus Atmosphere Monitoring Service (CAMS) report, CAMS84_2018SC2_D6.1.1-2021_observations_v6.pdf, July 2021, doi:10.24380/3b4exb93.

Terradellas, E., Werner, E., Basart, S. and Benincasa, F.: Model inter-comparison and evaluation of dust forecasts, SDS-WAS Technical report SDS-WAS-2020-001, August 2020.

15.4 Staff

Dr Emilio Cuevas (PI of Izaña-AEMET facility until June 2020)

Dr África Barreto (PI of Izaña-AEMET facility since June 2020)

Dr Carmen Guirado Fuentes (UVA/AEMET; Research Scientist) left IARC in September 2019

Dr Philippe Goloub (PI of LOA-CNRS/University of Lille facility)

Dr Carlos Toledano (PI of GOA-University of Valladolid facility)

Dr Natalia Prats (Project Manager)



Figure 15.6. Cimel Masters at the Izaña Observatory Calibration facility.

16 Regional Brewer Calibration Center for Europe (RBCC-E)

16.1 Background

In November 2003 the WMO/GAW Regional Brewer Calibration Center for Europe (RA-VI region) (RBCC-E) was established at IZO. The RBCC-E reference is based on three double Mark-III Brewer spectrophotometers (the IZO triad): a Regional Primary Reference (Brewer 157), a Regional Secondary Reference (Brewer 183) and a Regional Travelling Reference (Brewer 185). As described in Section 3.1, IZO is located in a subtropical region (28°N) on a mountain plateau (2373 m a.s.l.) with pristine skies and low ozone variability. This location allows routine absolute calibrations of the references in similar conditions to the Mauna Loa Observatory (MLO), Hawaii, USA. The establishment of the RBCC-E Triad allows the implementation of a self-sufficient European Brewer calibration system that respects the world scale but works as an independent GAW infrastructure.

There are two European Calibration Centers for the two types of ozone spectrophotometers in use: Dobson and Brewer. The Regional Dobson Calibration Center for Europe (RDCC-E) is located at the Meteorological Observatory Hohenpeissenberg (Germany). Since 2009, the RBCC-E activities have largely been funded by the ESA project, “CEOS Intercalibration of Ground-Based Spectrometers and Lidars” which includes the participation of the two European Calibration Centers (RBCC-E and RDCC-E).

16.2 Objectives

The main objectives of this Cooperation programme are:

- To implement a system for routine absolute calibrations of the European Brewer regional reference instruments at IZO, fully compatible with absolute calibrations of the world reference triad at MLO.
- To perform periodical intercomparison campaigns using the Regional Primary Reference B157 (during intercomparisons held at IZO) and the Regional Travelling Reference B185 spectrophotometer (traceable to B157) in continental campaigns (Figs. 16.1 and 16.2).
- To perform regular comparisons of the Regional Brewer Primary Reference B157 with the Regional Dobson Reference D074 to monitor the relationship between both calibration scales in the RA-VI region.
- To study the sources of errors of the absolute calibrations and to determine the accuracy of total ozone measurement achievable by the Brewer spectrophotometer under different atmospheric conditions or instrumental characteristics.



Figure 16.1. Participants at the 14th RBCC-E Intercomparison campaign held at El Arenosillo in 2019.

16.3 Tasks

The main tasks of this Cooperation programme are:

- To develop quality control protocols and Standard Operating Procedures (SOPs) for establishment of traceability of measurements to the reference standards.
- To maintain laboratory and transfer standards that are traceable to the reference standards.
- To perform regular calibrations and audits at GAW sites.
- To provide, in cooperation with Quality Assurance/Science Activity Centres, training and technical assistance to stations.



Figure 16.2. The RBCC-E travelling reference Brewer #185 at the El Arenosillo 2019 campaign.

16.3.1 Main activities of the RBCC-E during the period 2019-2020

16.3.2 Absolute calibration transfer

The RBCC-E Brewer triad transfers the calibration from the world reference triad, located in Toronto (Canada) and managed by Environment and Climate Change Canada, Meteorological Service of Canada (ECCC-MSC). The RBCC-E travelling reference Brewer#185 ensures the world reference transference to the WMO-Region VI Brewer network. The link of the RBCC-E triad to the world reference has been performed in the past using the travelling standard Brewer#017 managed by the International Ozone Service (IOS). The WMO GAW Scientific Advisory Group on ozone and UV Radiation in 2011 authorized RBCC-E to conduct the transference of its own absolute calibration, based on Langley analysis at IZO. The link to the world reference in this case can be assured either by direct intercomparison with the world triad in Toronto or by common Langley campaigns at MLO or at IZO (Redondas 2014a).

At present, the RBCC-E maintains a triad of reference instruments (see section 16.1). Each spectrophotometer is calibrated independently with the standard Langley method at IZO and since 2011 transfer their own total ozone calibration at regular calibration campaigns and are regularly compared with the Toronto Triad. Redondas et al. (2018) and León-Luis et al. (2018) studied the stability of the RBCC-E triad during the period 2005-2015, using a mathematical method where the ozone values are fitted to a 2nd grade polynomial (Fioletov et al., 2005) or an extended 3rd grade polynomial (Stübi et al., 2017).

Redondas et al. (2018) and León-Luis et al. (2018) took into account two conditions: a) only days with at least 15 measurements distributed around the solar noon and with standard deviation < 0.5 were selected and b) measurements data from Brewer #185 during campaigns were removed. In addition to this study, the stability of the RBCC-E triad during the period 2005-2020 is presented in this report. The distribution of the difference between the ozone daily mean obtained by each Brewer with respect to the Triad mean O₃ value (O_{3_mean}) was calculated as follows:

$$O_{3_mean} = (O_{3_157} + O_{3_183} + O_{3_185})/3. \quad (1)$$

A good Gaussian profile can be observed in the distribution of the differences (Fig. 16.3) which confirms the stability of the IZO Brewer Triad during the period 2005-2020.

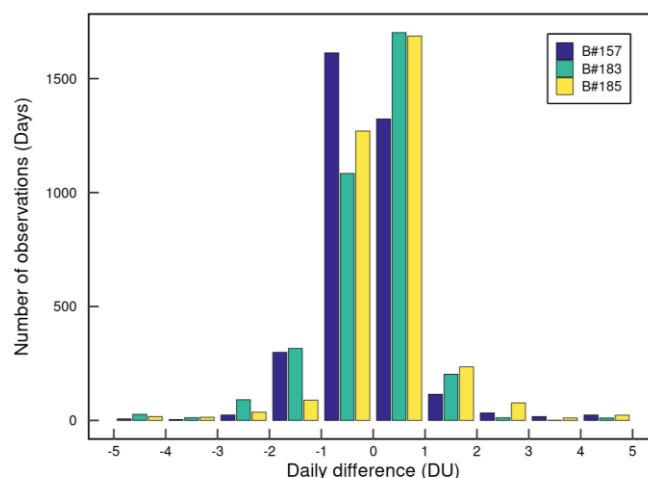


Figure 16.3. Distribution of the differences between the ozone daily mean obtained by each Brewer in the Triad with respect to the mean O₃ value of the RBCC-E Brewer Triad located at IZO for the period 2005-2020.



Figure 16.4. a) Monthly mean Total Ozone Column values measured at Izaña Observatory by the RBCC-E triad and b) Relative deviation of each Brewer from the monthly mean of the RBCC-E triad during the 2005-2020 period.

Figure 16.4 shows the relative deviations from the RBCC-E triad monthly mean TOC for each individual Brewer. This plot is used as a benchmark to identify if an instrument of the Triad needs to be recalibrated or for checking that a current calibration applied to a Brewer is good enough. The standard deviation of the relative deviations from the RBCC-E Triad monthly mean have values of 0.34%, 0.36% and 0.30% (B\#157, B\#183 and B\#185) for the period 2005-2020, 40% in 2005 and 38% in 2020 less than those reported for the MkII Canada Triad (Fioletov et al., 2005, Zhao et al., 2020), and 27% less than the MkIII Canada Triad (Zhao et al., 2020).

16.3.3 RBCC-E Intercomparison campaigns



Figure 16.5. The RBCC-E travelling reference Brewer #185 at the Arosa 2018 campaign (Photo: A. Redondas).

Brewer intercomparisons are held annually, alternating between Arosa in Switzerland and the El Arenosillo Sounding Station of INTA (Huelva, Spain). The aim is to collect simultaneous ozone data from a number of Brewers from invited organizations so that their calibration constants can be transferred from the reference instruments. The 14th RBCC-E intercomparison campaign was held at El Arenosillo from 17-28 June 2019, see Redondas et al. (2020). Due to the COVID-19 pandemic, no intercomparison campaign was carried out in 2020. The geographical origin of the Brewers calibrated by the RBCC-

E is shown in Fig. 16.6 and the number of calibrations performed by the RBCC-E every year is shown in Fig. 16.7. In 2019, 19 calibrations were performed. These routine intercomparison campaigns provide the Brewer community with the opportunity to assess the status of the European network instruments.

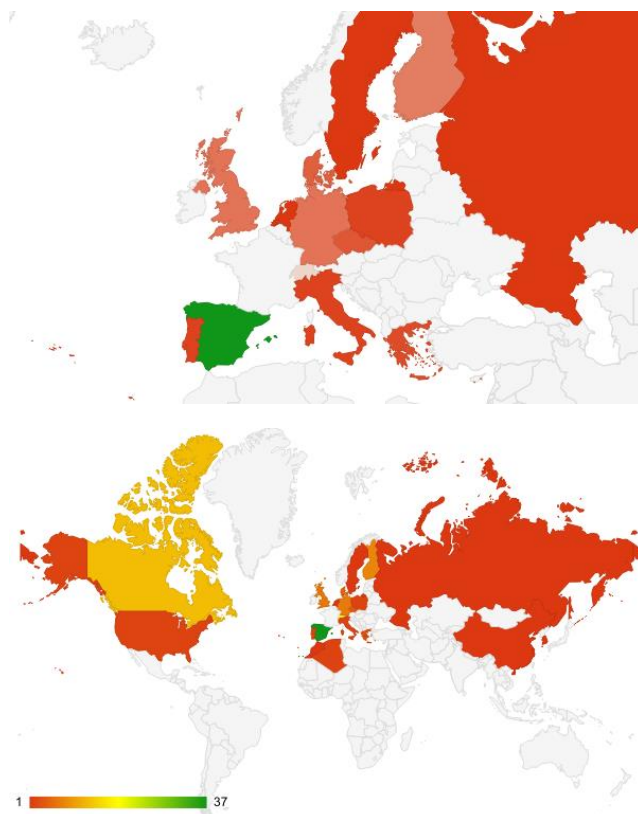


Figure 16.6. Geographical origin of the Brewers calibrated by the RBCC-E.

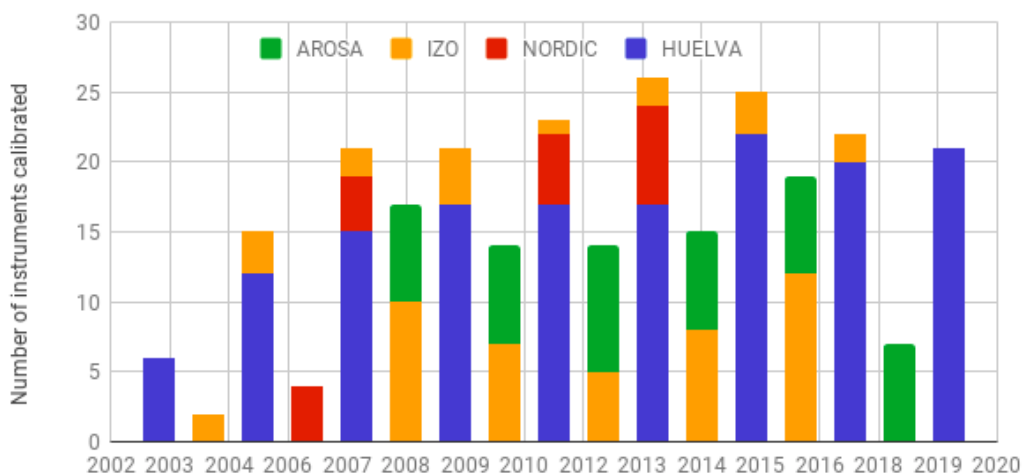


Figure 16.7. Calibrations performed by the RBCC-E per year.

Table 16.1. Participants at the 14th RBCC-E Intercomparison campaign held at El Arenosillo in 2019.

Institution	Participants	Instrument	Country
Arenosillo 2019 (Spain, 17–28 June) RBCC-E			
IARC-AEMET	Alberto Redondas Virgilio Carreño Sergio León Luis Alberto Berjón Javier López Solano	Brewer #185-MKIII	Spain
University of Thessaloniki	Alkis Bais Fani Gkertsí	Brewer #005-MKII	Greece
International Ozone Services (IOS)	Martin Stanek Volodya Savastiouk	Brewer #017-MKII	Canada
IARC-AEMET	J.M San Atanasio Juan R. Moreta Ana María Díaz Francisco García	Brewer #033-MKIV Brewer #070-MKIV Brewer #117-MKIV Brewer #151-MKIV Brewer #166-MKIII Brewer #186-MKIV	Spain
UK Meteorological Office (UKMO)	John Rimmer	Brewer #075-MKIV Brewer #126-MKII Brewer #172-MKIII	U.K.
Instituto Nacional de Técnica Aeroespacial (INTA)	Jose Manuel Vilaplana Margarita Yela Mónica Navarro	Brewer #150-MKIII	Spain
Kipp & Zonen (K&Z)	Pavel Babal	Brewer #158-MKIII	The Netherlands
World Radiation Center (WRC)	Luca Egli Gregor Huelsen	Brewer #163-MKIII	Switzerland
Japan Meteorological Agency	Hiroaki Fujiwara	Brewer #174-MKIII	Japan
Environment and Climate Change Canada	Michael Brohart	Brewer #190-MKIII	Canada
Office Nationale de la Météorologie	Sid Alamine Baika Abdessadek Saanouné	Brewer #201-MKIII	Algeria
Danmarks Meteorologiske Institut (DMI)	Niss Jepsen	Brewer #202-MKIII Brewer #228-MKIII	Denmark
Finnish Meteorological Institute (FMI)	Tomi Karpinen	Brewer #214-MKIII	Finland
York University	Tom McElroy		Canada



Figure 16.8. The 14th RBCC-E intercomparison campaign held at El Arenosillo, 17 – 28 June 2019.

Table 16.2. Participants at the Total Ozone Measurements Intercomparison campaign held at El Arenosillo in 2019.

Institution	Participants	Instrument	Country
Arenosillo 2019 (Spain, 17–28 June) RBCC-E			
IARC-AEMET	Alberto Redondas Virgilio Carreño Sergio León Luis Alberto Berjón Javier López Solano	Brewer #185-MKIII FTIR (EM27/SUN)	Spain
International Ozone Services (IOS)	Volodya Savastiouk	Brewer #017-MKII	Canada
World Radiation Center (WRC)	Luca Egli Gregor Huelsen	Brewer #163-MKIII QUASUME Koherento3	Switzerland
Japan Meteorological Agency	Hiroaki Fujiwara	Brewer #174-MKIII	Japan
Environment Canada	Michael Brohart	Brewer #190-MKIII	Canada
Instituto Nacional de Técnica Aeroespacial (INTA)	Jose Manuel Vilaplana Margarita Yela Mónica Navarro	Dobson	Spain
Universidad de Extremadura	Antonio Serrano Maria Cancillo	NILU #119 NILU #145	Spain
Agenzia Regionale per la Protezione dell'Ambiente della Valle D'Aosta	Illias Fountoulakis	Phaeton	Italy
Gigahertz-Optik GmbH	Ralf Zuber	BTS-Solar UV Spectroradiometer	Germany
Luftblick Earth Observing Technologies	Daniel Santana	Pandora	Austria
Laboratoire Atmosphères, Observations Spatiales	Andrea Pazzmino	Mini SAOZ	France

16.3.4 Intercomparison Results

In the 14th RBCC-E Intercomparison Campaign, the initial comparison (blind period), using the instruments' original calibration constants, showed that 74% of the operational Brewer instruments were in the $\pm 1.0\%$ range, while 31% of them (6 instruments) showed a perfect agreement within $\pm 0.5\%$ after two years calibration period (Figure 16.9).

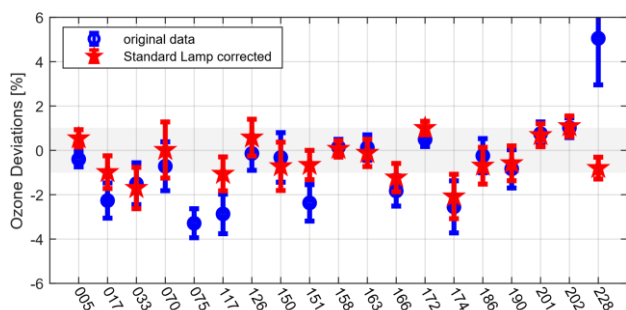


Figure 16.9. Initial period, percentage mean difference with the reference for the simultaneous direct sun measurements for all the participating instruments, with and without the standard lamp correction, in the stray-light free OSC region ($OSC < 900$).

It is worth noting that these results correspond to the stray-light free region, $OSC < 900$, but large errors (up to 4%) can be expected for single-monochromator Brewer instruments operating at $OSC > 1000$ DU. With the final calibration and including a correction for the stray light, all participating Brewer spectrophotometers were within the $\pm 0.5\%$ agreement range (Figure 16.10). See Redondas et al. (2020) for more details.

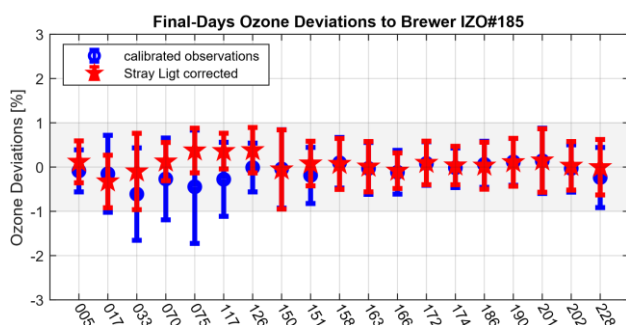


Figure 16.10. Final period, percentage mean difference with the reference for the simultaneous direct sun measurements for all the participating instruments. Blue symbols show results without the stray light correction and red symbols show results with the correction applied to single Brewer spectrophotometers.

16.3.5 Total Ozone Measurements Intercomparison at Huelva

In parallel to the 14th RBCC-E Brewer intercomparison campaign, a Total Ozone measurements intercomparison campaign was held at El Arenosillo Atmospheric Sounding Station INTA (Huelva, Spain) from 17-28 June 2019. The objective of this campaign was to compare TOC retrieved with different techniques. In total, 11 groups from eight

countries participated, with 15 instruments using 10 different techniques to measure Total Ozone Column (Table 16.2). The final report of the campaign is in preparation.

Preliminary results of the ozone comparison are shown in Fig. 16.11. The daily averages of the instruments present a standard deviation around 1.6% with respect to the average value, with differences between the maximum and the minimum around 16 DU (5%). These results have been obtained for different total column conditions, from 335 DU registered at the beginning of the campaign, to 307 DU at the end of the campaign.

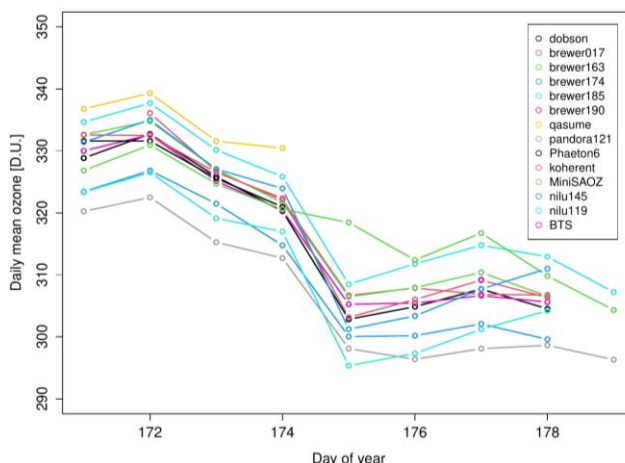


Figure 16.11. Preliminary comparison of the Total Ozone Column obtained during the campaign by the participating instruments.

It must be taken into account that the number of measurements that each instrument provided can be very different due to the difference in techniques used. In general, the different instruments generate between 50 and 100 daily Total Ozone Column measurements. For example, the Pandora generates about 800 daily measurements while the MiniSAOZ only measures twice a day, at dawn and sunset.

Differences in TOC provided by similar instruments are also analysed. Five Brewers and two NILU radiometers participated in the ozone intercomparison campaign. In the case of the Brewers, the daily averages of the instruments presented differences between the maximum and the minimum of around 3% with respect to the average value, that is around 10 DU. While the difference between the two NILU instruments was an average of 7 DU, which is approximately 2%.

16.3.6 Training activities

The RBCC-E, in conjunction with WMO/UNEP and EUBREWNET is involved in training and capacity building, by organizing operator courses and workshops which provide expert instruction and knowledge exchange using the considerable expertise available. We also actively support the monitoring programmes in developing countries.

Table 16.3. Participants at the Brewer course during the 14th RBCC-E Intercomparison campaign at El Arenosillo in 2019.

Institution	Participants	Country
Speakers		
IARC-AEMET	Alberto Redondas Virgilio Carreño Sergio León Luis Alberto Berjón Javier López Solano	Spain
International Ozone Services (IOS)	Volodya Savastiouk	Canada
Manchester University	John Rimmer	UK
Kipp & Zonen	Pavel Babal	The Netherlands
World Radiation Center	Luca Egli Gregor Huelsen	Switzerland
Environment Canada	Michael Brohart	Canada
Finnish Meteorological Institute	Tomi Karpinnen	Finland
York University	Tom McElroy	Canada
Agenzia Regionale per la Protezione dell'Ambiente della Valle D'Aosta	Henri Diémoz	Italy
Luftblick Earth Observing Technologies	Daniel Santana	Austria
Students		
Office Nationale de la Météorologie	Abdessadek Saanouné Sid Alamine Baïka	Algeria
Instituto Antártico Argentino	Héctor Adolfo Ochoa	Argentina
University of Tasmania	Kelvin Michael	Australia
Universidade Federal do Oeste do Pará	Lucas Vaz Peres	Brazil
University of Magallanes	Claudio Casiccia	Chile
National Institute of Meteorology and Hydrology	Cesar Tonato	Ecuador
Egyptian Meteorological Authority	Mohammed Hamdan Gadalla	Egypt
Hungarian Meteorological Service	Dénes Fekete	Hungary
India Meteorological Department	Siddhartha Singh	India
Malaysian Meteorological Department	Mohd Isa Bin Nasikin	Malaysia
Institute of Atmospheric Physics, Russian Academy of Sciences	Vladimir Savinykh	Russian Federation
Department of Atmospheric Sciences, Yonsei University	Dha Hyun Ahn	South Korea
Sakon Nakhon Rajabhat University	Oradee Pilahome Wilawan Kumharn	Thailand
Aero Meteorological Observatory, Vietnam Meteorological and Hydrological Administration	Thi Hoang Anh Nguyen	Vietnam

WMO-GAW Brewer course during 14th RBCC-E Campaign, El Arenosillo, 17-21 June 2019

This event (Fig. 16.12) was organized in collaboration with WMO-GAW and focused on the operational, scientific and technical issues of the Brewer instrument, with emphasis on the ozone, UV and AOD products available at EUBREWNET. In total, close to 20 students from countries all around the world took part in this course, see Table 16.3 for details. The course presentations are available [here](#).



Figure 16.12. Students at the Brewer Training Course during the 14th RBCC-E Intercomparison campaign at El Arenosillo in June 2019

16.4 References

- Fioletev, V.E., Kerr J.B., McElroy C.T., Wardle D.I., Savastiouk V., Granjkar T.S., The brewer reference triad, *Geophys. Res. Lett.*, 32 L208805. 2005.
- León-Luis, S. F., Redondas, A., Carreño, V., López-Solano, J., Berjón, A., Hernández-Cruz, B., and Santana-Díaz, D., Internal consistency of the Regional Brewer Calibration Centre for Europe triad during the period 2005–2016. *Atmos. Meas. Tech.*, 11, 4059–4072, 2018.
- Redondas, A., Carreño, V., León-Luis, S. F., Hernández-Cruz, B., López-Solano, J., Rodriguez-Franco, J. J., Vilaplana, J. M., Gröbner, J., Rimmer, J., Bais, A. F., Savastiouk, V., Moreta, J. R., Boulkelia, L., Jepsen, N., Wilson, K. M., Shirovov, V. and Karppinen, T.: EUBREWNET RBCC-E Huelva 2015 Ozone Brewer Intercomparison, *Atmospheric Chemistry and Physics*, 18(13), 9441–9455, doi:<https://doi.org/10.5194/acp-18-9441-2018>, 2018.
- Stübi, R., Schill, H., Klausen, J., Vuilleumier, L. and Ruffieux, D.: Reproducibility of total ozone column monitoring by the Arosa Brewer spectrophotometer triad, *Journal of Geophysical Research: Atmospheres*, 122(8), 4735–4745, doi:[10.1002/2016JD025735](https://doi.org/10.1002/2016JD025735), 2017.
- Redondas, A., Berjón, A., López-Solano, J., Carreño, V., León-Luis, S.F., Santana, D.: Fourteenth Intercomparison Campaign of the Regional Brewer Calibration Centre Europe. El Arenosillo Atmospheric Sounding Station, Huelva, Spain, 17–28 June 2019. Vol. WMO/GAW Report No. 257. Joint publication of State Meteorological Agency (AEMET), Madrid, Spain and World Meteorological Organization (WMO), 550 p., 2020. Available from: https://library.wmo.int/doc_num.php?explnum_id=10640

Redondas, A., Rodríguez-Franco J.J., Carreño, V., and Sierra, M., "Ten years of the Regional Brewer Calibration Center- Europe" COST ACTION ES1207 EUBREWNET OPEN CONGRESS /14th WMO-GAW BREWER USERS GROUP MEETING EUBREWNET & WMO GAW, Tenerife, 24–28 March 2014, 2014.

Redondas, A., S.F. León-Luis, V. Carreño, B. Hernández, J. López-Solano, A. Berjón, D. Santana-Díaz, and M. Rodríguez, Stability of the RBCCE triad during the period 2005–2015, Quadrennial Ozone Symposium 2016, Edinburgh, 4–10 September 2016.

16.5 Staff

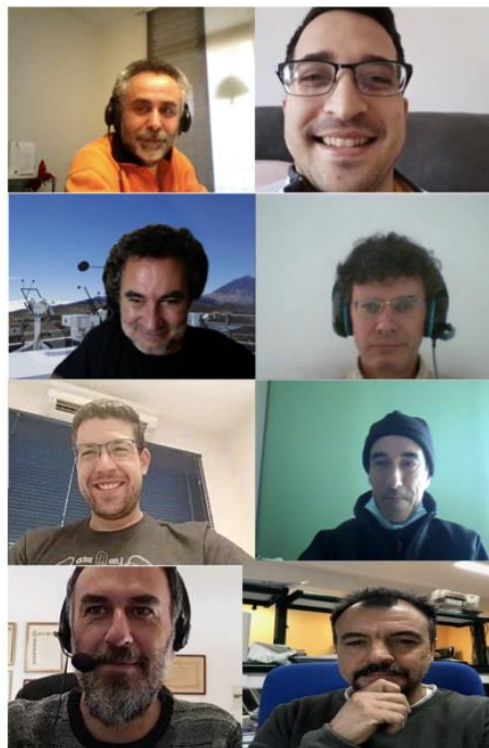


Figure 16.13. Members of the RBCC-E team. Left to right, top to bottom: A. Berjón, D. Santana, A. Redondas, J. López-Solano, S. León Luis, V. Carreño, F. Parra-Rojas and M. Rodríguez Valido.

- Alberto Redondas Marrero (AEMET; PI in charge of RBCC-E)
- Virgilio Carreño (AEMET; Meteorological Observer-GAW Technician)
- Dr Sergio Fabián León Luis (TRAGSATEC; Research Scientist)
- Daniel Santana (Sieltec/LuftBlick; Research Scientist)
- Dr Francisco Parra Rojas (AEMET; Research Scientist)
- Dr Alberto Berjón (TRAGSATEC; Research Scientist)
- Dr Javier López Solano (TRAGSATEC; Research Scientist)
- Dr Manuel Rodríguez Valido (ULL, Research Scientist)

17 Sand and Dust Storm Centres

The Sand and Dust Storm Warning Advisory and Assessment System (SDS-WAS) aims to establish a coordinated global network of SDS research and forecasting centers to enhance operational SDS forecasts through technology transfer from research. SDS-WAS partners with Global Atmosphere Watch (WMO, 2019, 2020).

The Izaña Atmospheric Research Center participates actively in the management, operation, and research and development activities of the two SDS Regional Centres described below: 1) the WMO Sand and Dust Storm Warning Advisory and Assessment System Regional Center for Northern Africa, Middle East and Europe (SDS-WAS-NA-ME-E), and 2) the Barcelona Dust Forecast Centre (BDFC).

17.1 WMO Sand and Dust Storm Warning Advisory and Assessment System (SDS-WAS) Regional Center

The Sand and Dust Storm Warning Advisory and Assessment System is a programme of the World Meteorological Organization with the mission to enhance the ability of countries to deliver timely and qualitative information related to sand and dust storm forecasts and observations to end users and improve the knowledge of this phenomena.

The Regional Centre for Northern Africa, Middle East and Europe (NA-ME-E) was established in 2007 to coordinate SDS-WAS activities within this region. The Centre, as a consortium of AEMET and the Barcelona Supercomputing Centre – National Supercomputing Centre (BSC-CNS), soon evolved into a structure that hosted international and interdisciplinary research cooperation between numerous organizations in the region and beyond, including national meteorological services, environmental agencies, research groups and international organizations.

The Center's [website](#) (Fig. 17.1) is a place where visitors can find the latest dust-related observations and the most up-to-date experimental dust forecasts. The activities carried out by the SDS-WAS Regional Centre have been broadly disseminated at international workshops and conferences (Basart et al., 2018a; Cuevas et al., 2017a, 2017b). A detailed description of the main activities of the SDS-WAS regional Centre can be found in Terradellas et al. (2016).

A global observational network is crucial to any forecast and early warning system for real-time monitoring, validation and evaluation of forecast products, as well as for data assimilation. The main data sources are in-situ aerosol measurements performed at air quality monitoring stations, indirect observations (visibility and present weather) from meteorological stations, sun photometric measurements

(e.g. AERONET network), lidar, ceilometers and satellite products.

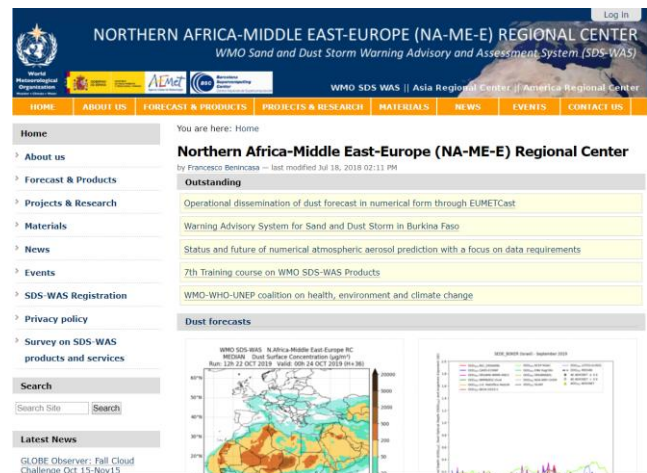


Figure 17.1. SDS-WAS Regional Center Web portal.

The exchange of forecast products is a core part of the WMO SDS-WAS programme and the basis for the joint visualization and evaluation initiative. The web portal offers side-by-side dust forecasts (dust surface concentration and dust optical depth at 550 nm) generated by 12 modelling systems as well as the multi-model median. The models are BSC-DREAM8b_v2, CAMS-ECMWF, DREAM8-NMME-MACC, NMMB/BSC-Dust, NASA GEOS-5, NCEP-NGAC, EMA RegCM4, UK Met Office, DREAM ABOL, NOAA-WRF-CHEM, SILAM and LOTOS-EUROS.

An important element of any forecasting system is the evaluation of the products. The main goal of this process is to assess whether the modelling systems successfully simulate the evolution of dust-related parameters. In addition, the evaluation improves the understanding of the model capabilities, limitations, and appropriateness for the purpose for which they were designed. The evaluation is performed by comparing the model forecasts with observational data. The individual models and multi-model median forecasts of the dust optical depth (DOD) at 550 nm are compared with AERONET observations of aerosol optical depth (AOD) for 40 selected dust-prone stations. In addition to this near-real-time evaluation, a system to assess quantitatively the performance of the different models has been implemented. It yields evaluation scores computed from the comparison of the simulated DOD with the AERONET retrievals of AOD.

The SDS-WAS Regional Centre works toward strengthening the capacity of countries to use the observational and forecast products distributed in the framework of the WMO SDS-WAS programme in partnership with National Meteorological and Hydrological Services (NMHSs) in the region and other relevant organizations.

17.2 The Barcelona Dust Forecast Centre

In May 2013, in view of the demand of many national meteorological services and the good results obtained by the SDS-WAS related to operationalization, the 65th Session of the WMO Executive Council designated the consortium formed by AEMET and the BSC-CNS as the first Regional Specialized Meteorological Centre with activity specialization on Atmospheric Sand and Dust Forecast (RSMC-ASDF). The Centre operationally generates and distributes predictions for Northern Africa (north of equator), Middle East and Europe.



The Barcelona Dust Forecast Centre prepares regional forecast fields using the NMMB/BSC-Dust model continuously throughout the year on a daily basis (Terradellas et al., 2015). The model consists of a numerical weather prediction model incorporating on-line parameterizations of all the major phases of the atmospheric dust cycle. It is run at a horizontal resolution of 0.1 degrees longitude per 0.1 degrees latitude for a domain covering Northern Africa, Middle East and Europe (25°W-65°E, 0°-65°N). This domain covers the main dust source areas in Northern Africa and Middle East, as well as the main transport routes and deposition zones from the equator to the Scandinavian Peninsula.

Following its efforts to make the predictions reach all potential users and, in particular, the national meteorological and hydrological services, the BDFC started to broadcast dust forecast through the EUMETCast service in November 2015.

17.3 Activities performed for the SDS Centres in 2019-2020

IARC is actively involved in the strategic planning and supervision of main activities of the two SDS Regional Centers activities (AEMET Commission to BSC-CNS); scientific contributions on aerosol dust; contribution to international aerosol dust-related infrastructures and networks; and workshops and capacity building activities.

17.3.1 AEMET Commission to BSC-CNS for the development and improvement of products and services supplied by the WMO Regional Centers for Atmospheric Sand and Dust Forecast: 2018-2021

The director of IARC is the manager, on behalf of AEMET, of the AEMET Commission to BSC-CNS for the development and improvement of products and services supplied by the WMO Regional Centers for Atmospheric

Sand and Dust Forecast. The present Commission began on 10 September 2018 and ends on 9 September 2021.

The AEMET Commission to the BSC-CNS addresses new developments and improvements of products and services of the two regional centers and includes the following activities:

- 1) Redesign of the information portals of the Regional Centers, as well as the system for disseminating available information adapted to the needs and capacities of the countries that are within the territorial scope of the Regional Center. All the information is unified in a single portal for the two Regional Centers.
- 2) Improvement of the daily forecast of mineral dust in the geographic domain of the RSMC-ASDF.
- 3) Development of a regional dust reanalysis for the entire region based on the operational model and the observations available with the data assimilation system.

The activities of Item 2 (Improvement of the daily forecast of mineral dust) were motivated by technical needs identified, to a large extent, from the experience gained in the systematic evaluation of the CAMS dust model, carried out in the framework of the CAMS-84 service and previously from the MACC project (Monitoring Atmospheric Composition and Climate). The different evaluation reports in which Sara Basart and Emilio Cuevas participated are accessible [here](#).

The activities identified as essential to improve operational dust forecasts were the following:

- Improvement of the emission schemes of the NMMB-MONARCH model.
- Development of an operational data assimilation system.

The upgraded version of the MONARCH model was operational from 17 December 2020 (see Basart et al., 2020 for more details).

In relation to the development of a regional dust reanalysis, the experience in the evaluation of the MACC reanalysis was used (see Cuevas et al., 2015), as well as that of CAMS, within the framework of CAMS-84 in which Sara Basart and Emilio Cuevas participated. The CAMS report covering the global Reanalysis of aerosols and reactive gases for 2003-2017 (Bennouna et al., 2020) is available [here](#).

The advanced reanalysis of the regional dust model for North Africa, the Middle East and Europe (SDS-WA NAMEE Regional Centre), covering 10 years (2007-2016) based on the MONARCH atmospheric model and the new dust data assimilation system was completed and made available on 14 December 2020. The announcement of the completion of the reanalysis was made through the European Research Area for Climate Services (ERA4CS) newsletter. Access to this dust reanalysis is, for the time

being, restricted to members of the DustClim consortium (see below) of which AEMET is a member.

New features of the reanalysis include a high spatial resolution (10 km x 10 km), the assimilation of satellite products over dust source regions, and a comprehensive evaluation using a wide variety of observations and data from experimental ground-based campaigns and satellite products. This reanalysis is being used for the development of dust services specifically designed for air quality, aviation, and solar energy, such as those developed under the DustClim project.

17.4 Scientific contributions on aerosol dust

17.4.1 Impacts of Desert Dust outbreaks on Air Quality in Urban Areas

The influence of desert dust outbreaks on air quality in Santa Cruz de Tenerife was investigated using air-quality observations and data on the vertical structure of the atmosphere for a six-year period (2012–2017). It was found that desert dust outbreaks reduced the height of the marine boundary layer in the study area (Canary Islands region) by > 45%, on average, in summer and by ~ 25%, on average, in winter (Milford et al., 2020). This thinning of the marine boundary layer was associated with an increase of local anthropogenic pollution during dust outbreaks. NO₂ and NO mean concentrations more than doubled and even larger relative increases in black carbon were observed during the more intense summer dust outbreaks (Fig. 17.2); increases also occurred during the winter outbreaks but were less than in summer. This has public health implications; local anthropogenic emissions need to be reduced even further in

areas that are impacted by desert dust outbreaks to reduce adverse health effects.

17.4.2 Rapid changes of dust geochemistry in the Saharan Air Layer linked to sources and meteorology

A study of rapid changes of dust geochemistry in the Saharan Air Layer linked to sources and meteorology (Rodríguez et al., 2020) was performed by a team of scientists from IARC, CSIC, the Italian National Institute of Nuclear Physics, the University of La Laguna and the European University of the Canaries (see Section 8.3.1 for more details).

17.4.3 Desert Dust Outbreak in the Canary Islands (February 2020): Assessment and Impacts

In this report a comprehensive study of the exceptionally severe dust outbreak that affected the Canary archipelago between 22–24 February 2020, is presented. It was a unique episode due to its unprecedented intensity and its associated impacts on different socio-economic sectors.

The 22–24 February 2020 dust outbreak was reported extensively in local, national and international media, especially because of the closure of airports and the enormous problems caused to tens of thousands of tourists who suffered the cancellation of their flights. The long-term aerosol observations (PM₁₀, AOD measured from ground-based and satellite instruments, and horizontal visibility as a proxy of suspended dust) confirmed that the dust outbreak that occurred between 22–24 February 2020 was the most intense dust episode so far recorded in the Canary Islands.

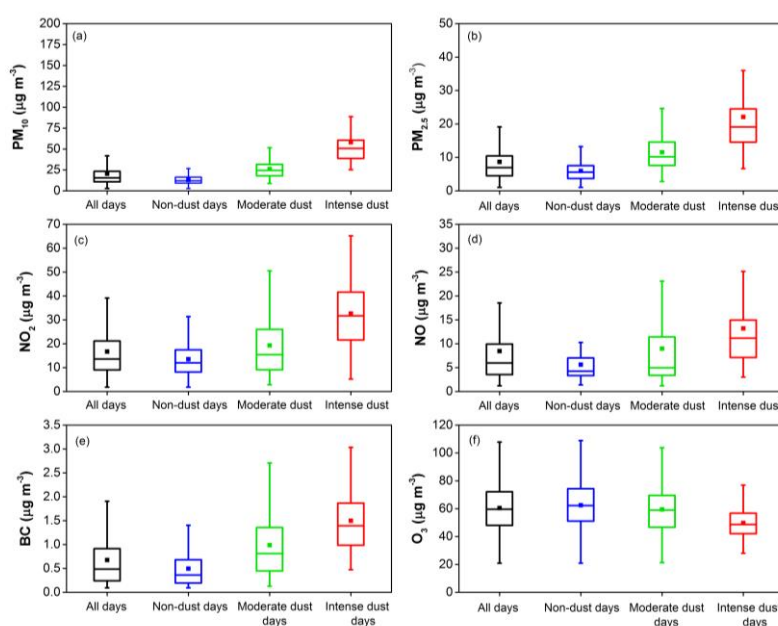


Figure 17.2. Mean (24-h) concentrations of (a) PM₁₀; (b) PM_{2.5}; (c) NO₂; (d) NO; (e) Black Carbon (BC) ≤ 10 μm, and (f) O₃ calculated for all days, non-dust outbreak days, and different intensities of dust outbreaks during summer (July–August). The horizontal lines and the squares within the box represent the median and mean values, respectively, while the bottom and top of each box are the 25th and 75th percentiles. The whiskers are the 5th and 95th percentiles. All data are for the 2012 to 2017 period except for black carbon data, which are for 2014–2017. Reprinted from Milford et al. (2020).

This dust outbreak, like most outbreaks affecting the Canary Islands that take place in winter, was caused by a very deep cut-off low that became detached from the mid-latitudes circulation and was located in the vicinity of the Canary Islands archipelago, causing very intense winds (around 90 km h⁻¹ at 1500 m a.s.l.) over the western Sahara that transported mineral dust to the Canary archipelago within a relatively short distance.

The air quality stations of the Canary Islands recorded three peaks of PM₁₀ and PM_{2.5} concentrations on 22, 23 and 24 February 2020, with extremely high PM₁₀ and PM_{2.5} hourly concentrations, which exceeded 3000 and 1000 µg m⁻³, respectively, during the largest peak recorded on 23 February 2020 (Fig. 17.3).

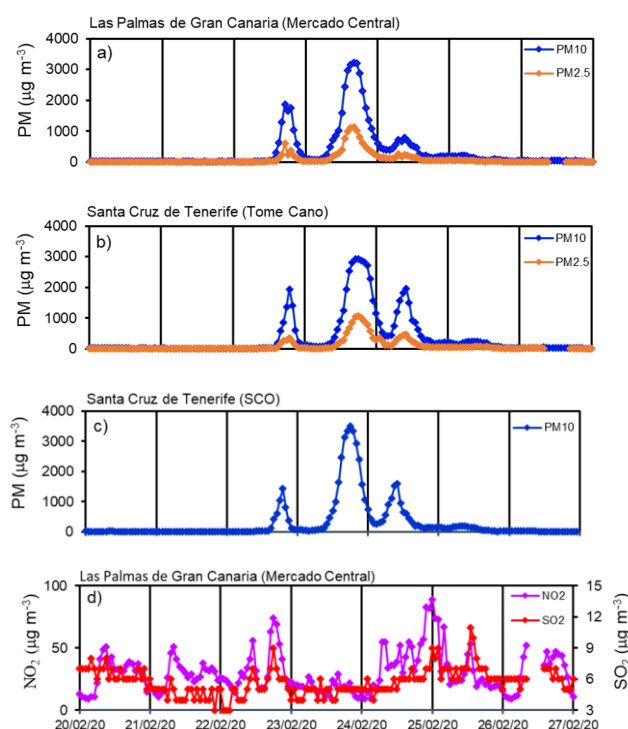


Figure 17.3. PM₁₀ and PM_{2.5} mean hourly concentrations for 20–27 February 2020 in: (a) Las Palmas de Gran Canaria (Mercado Central) and (b) Santa Cruz de Tenerife (Tomé Cano), (c) PM₁₀ mean hourly concentrations in Santa Cruz de Tenerife (SCO) and (d) NO₂ and SO₂ mean hourly concentrations in Las Palmas de Gran Canaria (Mercado Central). Data from the Canary Islands Government Air Quality Network (Mercado Central and Tomé Cano) and from IARC-AEMET (SCO). Reprinted from Cuevas et al. (2021).

Analysis of the chemical composition of aerosols measured during the dust outbreak shows that from 22 to 25 February 2020 most of the aerosol consisted of mineral dust (> 95%). Different optical properties of the dust were characterized. The AOD at 500 nm reached values of 3.11 at sea level, and 0.84 at 2400 m altitude (23 February 2020). The AE values were very low (< 0.4), and close to zero during 23 February, indicating that the dust particles were of a considerable size (up to 6 µm) due to the geographical proximity of their sources located in the western Sahara. The Micro Pulse Lidar recorded an abnormally high Saharan Air Layer (~ 5

km) for this type of winter dust outbreak whose vertical extension does not usually exceed 2.5 km.

The desert dust outbreak was well predicted (the spread but also the vertical distribution) by the BDFC MONARCH model (Fig. 17.4), especially for the easternmost islands, with a delay in the forecast of the arrival of the dust intrusion to Tenerife and forecasting a lower intensity on this island than observed. It was also well predicted by probabilistic prediction of dust outbreaks for the Canary Islands (based on the SDS-WAS multi-model ensemble) which included Ensemble Prediction System (EPS) Meteograms of PM₁₀ for the Canary Islands air quality stations.

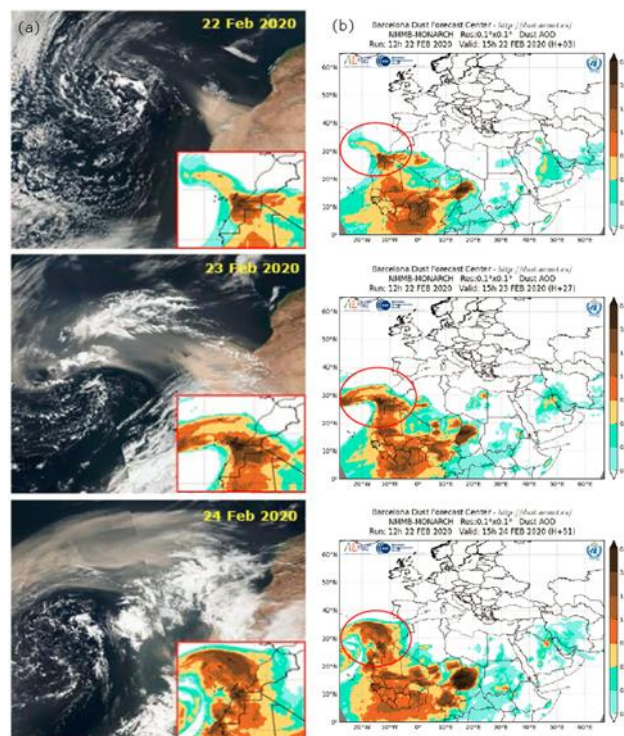


Figure 17.4. (a) Images for 22–24 February 2020 obtained by the VIIRS sensor aboard the NASA Suomi polar satellite. The images are daily and were taken between 13 and 14 UTC, (b) Dust AOD forecast for 22, 23 and 24 February 2020 at 15 UTC. Reprinted from Cuevas et al. (2021).

Studies carried out in the two main cities of the Canary Islands, Las Palmas de Gran Canaria and Santa Cruz de Tenerife, indicated that there were hospital admissions attributable to this episode, despite the effectiveness of weather alerts and early warning systems, which prevented part of the population from being exposed to exceptional PM₁₀ levels during the Saharan dust episode. Around 70% of the excess hospital admissions recorded during the first trimester of 2020, attributable to dust, corresponded only to this episode.

Another important impact of this intrusion was on the air operations of airports, due to the unprecedented reduction in visibility recorded in all eight Canary Islands airports, with a minimum visibility of 400 m being recorded at Gran Canaria Airport. For the first time in history, all airports in

the archipelago, and their airspace, were closed for a few hours. This resulted in the cancellation of ~1000 flights throughout the Canary Islands, which involved an estimated cost of at least 17,650,000 euros, and a major disruption for tens of thousands of passengers who were trapped on the islands for at least two days.

The solar photovoltaic energy production sector was also negatively affected by this severe dust event. On 23 February 2020, production was reduced by 52% and on 24 February by 72% compared to normal production. However, this was not the only impact of dust intrusion. Due to the intense dust deposition on the photovoltaic modules, the performance of the installation decreased from 96% under pre-dust intrusion conditions, to 75% after the dust intrusion. This situation continued for almost a month until precipitation cleaned the modules. It is estimated that this dust event caused an economic cost in the Canary Islands solar photovoltaic energy production system of one million euros.

There were also ecological impacts on flora and fauna. Most of the analyses that appear in this report were carried out in 2020, although the report was published in 2021 (Cuevas et al., 2021).

17.5 Contribution of SDS Regional Centres to international aerosol dust-related infrastructures and networks

17.5.1 WMO SDS-WAS

WMO released the third and fourth issues of “Airborne Dust Bulletin” on May 2019 and 2020, respectively (Fig. 17.5).

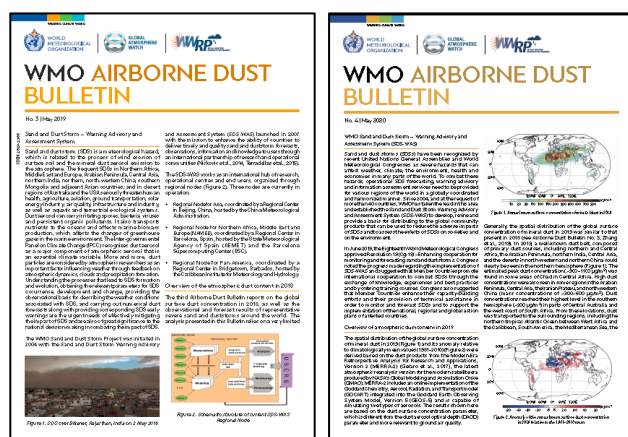


Figure 17.5. WMO Airborne Dust Bulletins, No. 3 (2019) and No. 4 (2020).

In WMO Airborne Dust Bulletin No. 3, the Warning Advisory System for Sand and Dust Storm in Burkina Faso, developed by AEMET and BC-CNS, was described. This issue also included the short article entitled “Challenges in Dust Observation in Remote Desert Regions”, a contribution in which new developments performed at IARC were cited (Almansa et al., 2017). In WMO Airborne

Dust Bulletin No. 4, the section entitled “New Instrumental Developments to measure atmospheric dust” was dedicated to the description of characteristics of the new radiometer ZEN-R52 (Almansa et al., 2020) and its differences from its predecessor prototype, the ZEN-R41 (Almansa et al., 2017).

17.5.2 InDust

The International Network to Encourage the Use of Monitoring and Forecasting Dust Products (InDust) is a European COST Action (CA16202). InDust started in November 2017 and is funded for a 4-year period. Its overall objective is to establish a network involving research institutions, service providers and potential end users of information on airborne dust. Because airborne dust transport has multi- and trans-disciplinary effects at local, regional and global scales; InDust involves a multidisciplinary group of international experts on aerosol measurements, regional aerosol modelling, stakeholders and social scientists. InDust also searches to coordinate and harmonise the process of transferring dust observation and prediction data to users as well as to assist the diverse socio-economic sectors affected by the presence of high concentrations of airborne mineral dust.

17.5.3 DustClim

DustClim (Dust Storm Assessment for the development of user-oriented Climate services in Northern Africa, the Middle East and Europe) is a project of several European groups that contribute to the SDS-WAS NAMEE Regional Center node financed by European Research Area for Climate Services. Several European institutions participate in the project and contribute in the following areas: Observations (CNR-DTA/IMAA of Italy, and CNRS- LISA of France), modelling (BSC, and CNR-DTA/ISAC of Italy) and products and services (AEMET, IMF of Finland, and CNR-DTA/ISAC of Italy).

DustClim has five work packages with the following objectives:

- WP1 Review, compilation and treatment of dust observations,
- WP2 Generation of high-resolution dust reanalysis,
- WP3 Development of products and services from the reanalysis model: aviation, solar energy and air quality, together with a visualization tool for the products,
- WP4 Dissemination of products and services,
- WP5 Project Management.

EAMET is responsible for work package 4.

DustClim has a duration of three years, ending in June 2021. The reanalysis, available from 14 Dec 2020, is being used and verified by the groups participating in DustClim.

17.5.4 Development of a dust storm warning system for West Africa: MAC-CLIMA and CREWS

In 2018, a warning advisory system for sand and dust storm was launched for the 13 administrative regions into which the territory of Burkina Faso is divided (Terradellas et al., 2018). This system has been designed and is operated by the AEMET and BSC in collaboration with the Burkina Faso National Meteorological Agency. Daily dust warnings are released through the WMO SDS WAS Regional Centre. This was a pilot project funded by the CREWS initiative.

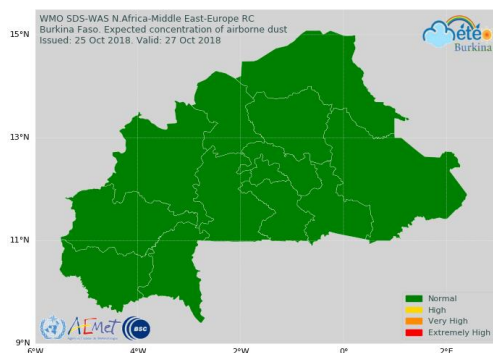


Figure 17.6. Example plot of SDS-WAS Burkina Faso forecasted alert level for 27 October 2018.

Inspired by the Burkina Faso pilot project, the SDS-WAS Regional Center has participated in two projects, MAC-CLIMA and CREWS with complementary strategies, and with a common goal: to implement dust prediction in Western African countries and evaluate them by means of a network of low-cost sensors that measure in-situ (PM_{10}) and column (AOD) aerosols, to be deployed in the region by IARC-AEMET.

The region to be covered in the future by synergies of MAC-CLIMA and CREWS (West Africa) is very large, and includes the following countries: Benin, Burkina Faso, Cape Verde, Gambia, Ghana, Guinea, Guinea-Bissau, Ivory Coast, Liberia, Mali, Mauritania, Niger, Nigeria, Senegal, Sierra Leone and Togo, and in the future, also Chad, Cameroon and Central African Republic (Fig. 17.7).



Figure 17.7. Map of West Africa.

The **MAC-CLIMA** project aims to generate a meteorological and ocean observation system and using these observations to promote resilience and adaptation to climate change. The objectives of MAC-CLIMA are to promote the progressive creation of an institutional, scientific and social network among the countries of the cooperation area to work, in a coordinated manner, for the adaptation to and mitigation of climate change. The cooperation area is made up of the outermost regions of Madeira, Azores and the Canary Islands and the three geographically close countries that have accepted to participate in the programme: Cape Verde, Senegal and Mauritania.

The **CREWS** (Climate Risk and Early Warning Systems) West Africa project, financed by the CREWS Trust Fund managed by WMO, has a main goal to improve short- to medium-range forecast capabilities focusing on severe weather, based on a seamless operational forecast systems and offering technical assistance for capacity building in West Africa.

The collaboration in these two projects, currently covers the following countries: Senegal, Mauritania, Cabo Verde, Mali, Niger and Chad.

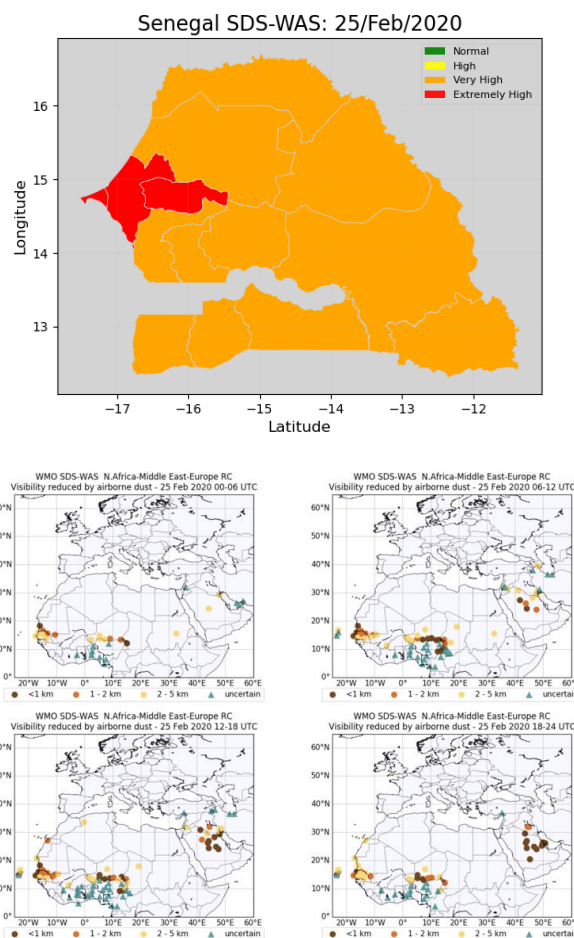


Figure 17.8. Comparison between a) warning map for Senegal (25 February 2020) and b) visibility reduction reported in the country.

As an example, the forecast of dust storms is shown for the different provinces of Senegal with a 4-color code map, equivalent to that developed for Burkina Faso, for 25 February 2020 (Figure 17.8a). A qualitative comparison with mineral dust visibility reduction maps obtained from visibility data from airports in West Africa including Senegal, for the same day, is presented in Figure 17.8b.

Tested Particulate Matter – Low-Cost Sensors (PM-LCS) are provided to key stations of this regions in order to perform quantitative evaluation of surface dust concentration forecast in a region with a lack of in-situ measurements. Online workshops on installation, management and operation of instrumentation, as well as on interpretation of the Warning Advisory System (WAS) and its implementation in the daily work routine have been organized.

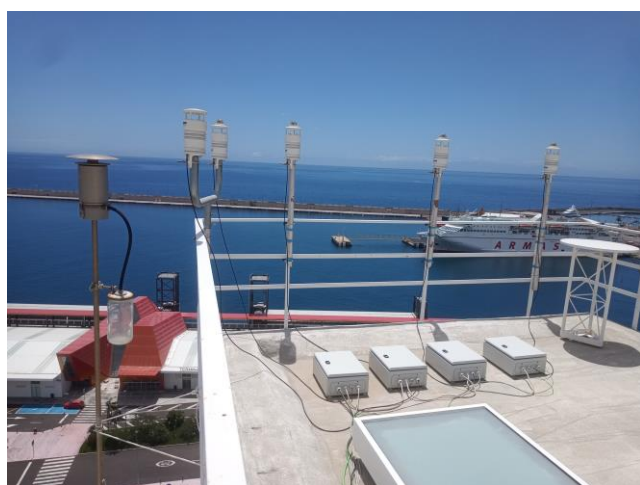


Figure 17.9. Comparison campaign of PM-LCS (five sensors) with a PM-BETA automatic-system at Santa Cruz de Tenerife.

Several PM-LCS were tested at SCO observatory during 2019 and 2020 by comparing them with an automatic PM BETA analyser (Fig. 17.9).

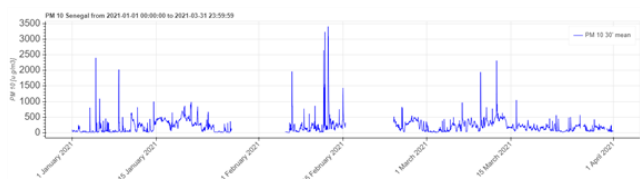


Figure 17.10. PM₁₀ data/PM-LCS installation at ANACIM building in Dakar, Senegal (upper panel). First measurements (lower panel).

In December 2020, the first PM-LCS at the ANACIM (Agence Nationale de l'Aviation Civile et de la Météorologie, National Agency of Civil Aviation and Meteorology) office in Dakar, Senegal, started data submission (Fig. 17.10).

17.5.5 Development of a surface dust concentration warning system for the Canary Islands

In 2018, a two-year pilot project was initiated to implement a surface dust concentration alert system for the Canary Islands based on the outputs of a dust multi-model ensemble of the SDS-WAS Regional Center. It includes a filtering of the models adjusted for the archipelago using surface PM data from the Canary Islands Air Quality network (Fig.17.11), and the design of surface dust concentration exceedance probability maps and ENSgrams.



Figure 17.11. Stations of the Canary Islands Government Air Quality Network used for dust forecasts evaluation.

17.5.6 SDS-WAS and Copernicus CAMS-84 Service

The Copernicus programme consists of a complex set of systems, which collect data from multiple sources: earth observation satellites and in situ sensors such as ground stations, airborne and sea-borne sensors. It processes these data and provides users with reliable and up-to-date information through a set of services related to environmental and security issues.



The Copernicus Atmosphere Monitoring Service (CAMS) has been developed to address environmental concerns, providing data and processed information, aiming at supporting policymakers, business and citizens with enhanced atmospheric environmental information.

CAMS-84 is a global and regional a posteriori validation activity, with focus on the Arctic and Mediterranean areas. The SDS-WAS Regional Centre, through BSC-CNS as the

main partner and AEMET as a third-party, participates in CAMS-84 providing validation and evaluation of dust and aerosols products. Mineral dust validation activities were carried out as CAMS-84 services and published as Quarterly Reports. The SDS-WAS Regional Centre participated in the preparation of 13 reports during the period 2019-20 (Basart et al., 2019; Bennouna et al., 2019, 2020; Christophe et al. 2019a, 2019b, 2020; Eskes et al., 2019, 2020; Ramonet et al. 2019, 2020; Schulz et al., 2019, 2020; and Sudarchikova et al., 2021).

17.6 References

- Almansa, A. F., Cuevas, E., Torres, B., Barreto, Á., García, R. D., Cachorro, V. E., de Frutos, Á. M., López, C., and Ramos, R.: A new zenith-looking narrow-band radiometer-based system (ZEN) for dust aerosol optical depth monitoring, *Atmos. Meas. Tech.*, 10, 565-579, doi:10.5194/amt-10-565-2017, 2017.
- Almansa, A.F.; Cuevas, E.; Barreto, Á.; Torres, B.; García, O.E.; Delia García, R.; Velasco-Merino, C.; Cachorro, V.E.; Berjón, A.; Mallorquín, M.; López, C.; Ramos, R.; Guirado-Fuentes, C.; Negrillo, R.; de Frutos, Á.M: Column Integrated Water Vapor and Aerosol Load Characterization with the New ZEN-R52 Radiometer, *Remote Sens.* 2020, 12, 1424, 2020.
- Basart, S., García-Castrillo, G., Cuevas, E., Goloub, P., Cazorla, A., Alastuey, A., Mortier, A., Benedetti, A. and Terradellas, E. Towards continuous evaluation of dust profiles in the WMO SDS-WAS. 9th International Workshop on Sand/Dust storms and Associated Dustfall, La Laguna, Tenerife, Spain, 22-24 May 2018.
- Basart, S., A. Benedictow, Y. Bennouna, A.-M. Blechschmidt, S. Chabrillat, Y. Christophe, E. Cuevas, H. J. Eskes, K. M. Hansen, O. Jorba, J. Kapsomenakis, B. Langerock, T. Pay, A. Richter, N. Sudarchikova, M. Schulz, A. Wagner, C. Zerefos, Upgrade verification note for the CAMS real-time global atmospheric composition service: Evaluation of the esuite for the CAMS upgrade of July 2019, Copernicus Atmosphere Monitoring Service (CAMS) report, CAMS84_2018SC1_D3.2.1-201907_esuite_v1.pdf, July 2019, doi:10.24380/fcwq-yp50, 2019.
- Basart, S., Pérez, C., Jorba, O., Benincasa, F., Olid, M., Serradell, K., Montanyé, G., Werner, E. Upgrading the MONARCH operational forecast: Deployment protocol and dust emission upgrades over NAMEE. Technical Report BDRC-2020-001, 38 pp, available at <https://dust02.bsc.es/resources/barcelona-dust-regional-center-technical-report-2020>, 30 November 2020.
- Bennouna, Y., M. Schulz, Y. Christophe, H.J. Eskes, S. Basart, A. Benedictow, A.-M. Blechschmidt, S. Chabrillat, H. Clark, E. Cuevas, H. Flentje, K.M. Hansen, U. Im, J. Kapsomenakis, B. Langerock, K. Petersen, A. Richter, N. Sudarchikova, V. Thouret, A. Wagner, Y. Wang, C. Zerefos, Validation report of the CAMS global Reanalysis of aerosols and reactive gases, years 2003-2017, Copernicus Atmosphere Monitoring Service (CAMS) report, CAMS84_2018SC1_D5.1.1-2017_v1.pdf, February 2019, doi:10.24380/xjkh-zt69, 2019.
- Bennouna, Y., Christophe, Schulz, M., Y. Christophe, H.J. Eskes, S. Basart, A. Benedictow, A.-M. Blechschmidt, S. Chabrillat, H. Clark, E. Cuevas, H. Flentje, K.M. Hansen, U. Im, J. Kapsomenakis, B. Langerock, K. Petersen, A. Richter, N. Sudarchikova, V. Thouret, A. Wagner, Y. Wang, T. Warneke, C. Zerefos, Validation report of the CAMS global Reanalysis of aerosols and reactive gases, years 2003-2019, Copernicus Atmosphere Monitoring Service (CAMS) report, CAMS84_2018SC2_D5.1.1-2019.pdf, April 2020, doi:10.24380/2v3p-ab79, 2020.
- Christophe, Y., M. Ramonet, A. Wagner, M. Schulz, H. J. Eskes, S. Basart, A. Benedictow, Y. Bennouna, A.-M. Blechschmidt, S. Chabrillat, E. Cuevas, A. ElYazidi, H. Flentje, K.M. Hansen, U. Im, J. Kapsomenakis, B. Langerock, A. Richter, N. Sudarchikova, V. Thouret, T. Warneke, C. Zerefos, Validation report of the CAMS near-real-time global atmospheric composition service: Period March - May 2019, Copernicus Atmosphere Monitoring Service (CAMS) report, CAMS84_2018SC1_D1.1.1_MAM2019_v1.pdf, September 2019, doi:10.24380/1t4q-1h53, 2019a.
- Christophe, Y., Schulz, M., Y. Bennouna, H.J. Eskes, S. Basart, A. Benedictow, A.-M. Blechschmidt, S. Chabrillat, H. Clark, E. Cuevas, H. Flentje, K.M. Hansen, U. Im, J. Kapsomenakis, B. Langerock, K. Petersen, A. Richter, N. Sudarchikova, V. Thouret, A. Wagner, Y. Wang, T. Warneke, C. Zerefos, Validation report of the CAMS global Reanalysis of aerosols and reactive gases, years 2003-2018, Copernicus Atmosphere Monitoring Service (CAMS) report, CAMS84_2018SC1_D5.1.1-2018_v1.pdf, May 2019, doi:10.24380/dqws-kg08, 2019b.
- Christophe, Y., M. Ramonet, A. Wagner, M. Schulz, H. J. Eskes, S. Basart, A. Benedictow, Y. Bennouna, A.-M. Blechschmidt, S. Chabrillat, E. Cuevas, A. ElYazidi, H. Flentje, P. Fritzsche, K.M. Hansen, U. Im, J. Kapsomenakis, B. Langerock, A. Richter, N. Sudarchikova, V. Thouret, T. Warneke, C. Zerefos, Validation report of the CAMS near-real-time global atmospheric composition service: Period March - May 2020, Copernicus Atmosphere Monitoring Service (CAMS) report, CAMS84_2018SC2_D1.1.1_MAM2020.pdf, September 2020, doi:10.24381/7q7w-h823, 2020.
- Cuevas, E., Camino, C., Benedetti, A., Basart, S., Terradellas, E., Baldasano, J. M., Morcrette, J. J., Marticorena, B., Goloub, P., Mortier, A., Berjón, A., Hernández, Y., Gil-Ojeda, M., and Schulz, M.: The MACC-II 2007-2008 reanalysis: atmospheric dust evaluation and characterization over northern Africa and the Middle East, *Atmos. Chem. Phys.*, 15, 3991-4024, doi:10.5194/acp-15-3991-2015, 2015.
- Cuevas, E., Ground Observation, SDS-WAS: Dust observation Side Event, GAW Symposium, WMO headquarters, Geneva, Switzerland, 10-13 April 2017a.
- Cuevas, E., E. Terradellas, and S. Nickovic, Sand and Dust Storm Advisory, 10th Session WWRP Scientific Steering Committee (WWRP SSC10), Geneva, WMO Headquarters, 25-26 October 2017b.
- Cuevas, E., Milford, C., Barreto, A., Bustos, J. J., García, R. D., Marrero, C. L., Prats, N., Bayo, C., Ramos, R., Terradellas, E., Suárez, D., Rodríguez, S., de la Rosa, J., Vilches, J., Basart, S., Werner, E., López-Villarrubia, E., Rodríguez-Mireles, S., Pita Toledo, M. L., González, O., Belmonte, J., Puigdemunt, R., Lorenzo, J.A., Oromí, P., and del Campo-Hernández, R.: Desert Dust Outbreak in the Canary Islands (February 2020): Assessment and Impacts. (Eds. Cuevas, E., Milford, C. and Basart, S.), State Meteorological Agency (AEMET), Madrid, Spain and World Meteorological Organization, Geneva, Switzerland, WMO Global Atmosphere Watch (GAW) Report No. 259, WWRP 2021-1, 2021.
- Eskes, H.J., S. Basart, A. Benedictow, Y. Bennouna, A.-M. Blechschmidt, S. Chabrillat, Y. Christophe, E. Cuevas, H. Flentje, K. M. Hansen, J. Kapsomenakis, B. Langerock, M. Ramonet, A. Richter, M. Schulz, N. Sudarchikova, A. Wagner, T. Warneke, C. Zerefos, Observation characterisation and validation methods document, Copernicus Atmosphere

- Monitoring Service (CAM5) report, December 2019, doi: 10.24380/Onsdwb26, 2019.
- Eskes, H. J., S. Basart, A. Benedictow, Y. Bennouna, A.-M. Blechschmidt, S. Chabrillat, Y. Christophe, K. M. Hansen, J. Kapsomenakis, B. Langerock, M. Pitkanen, M. Ramonet, A. Richter, N. Sudarchikova, M. Schulz, A. Wagner, T. Warneke (UBC), C. Zerefos, Upgrade verification note for the CAM5 near-real time global atmospheric composition service: Evaluation of the e-suite for the CAM5 47R1 upgrade of October 2020, Copernicus Atmosphere Monitoring Service (CAM5) report, CAMS84_2018SC2_D3.2.1-202009_esuite.pdf, 2 October 2020, doi:10.24380/fzdx-j890 2020.
- García-Cabrera, R. D., Cuevas-Agulló, E., Barreto, Á., Cachorro, V. E., Pó, M., Ramos, R., and Hoogendijk, K.: Aerosol retrievals from the EKO MS-711 spectral direct irradiance measurements and corrections of the circumsolar radiation, *Atmos. Meas. Tech.*, 13, 2601–2621, <https://doi.org/10.5194/amt-13-2601-2020>, 2020.
- Milford, C.; Cuevas, E.; Marrero, C.L.; Bustos, J.; Gallo, V.; Rodríguez, S.; Romero-Campos, P.M.; Torres, C. Impacts of Desert Dust Outbreaks on Air Quality in Urban Areas. *Atmosphere* 2020, 11, 23. <https://doi.org/10.3390/atmos11010023>, 2020.
- Ramonet, M., A. Wagner, M. Schulz, Y. Christophe, H. J. Eskes, S. Basart, A. Benedictow, Y. Bennouna, A.-M. Blechschmidt, S. Chabrillat, E. Cuevas, A. ElYazidi, H. Flentje, K.M. Hansen, U. Im, J. Kapsomenakis, B. Langerock, A. Richter, N. Sudarchikova, V. Thouret, T. Warneke, C. Zerefos, Validation report of the CAM5 near-real-time global atmospheric composition service: Period June - August 2019, Copernicus Atmosphere Monitoring Service (CAM5) report, CAMS84_2018SC1_D1.1.1_JJA2019_v1.pdf, November 2019, doi:10.24380/def9-na43, 2019.
- Ramonet, M., A. Wagner, M. Schulz, Q. Errera, H. J. Eskes, S. Basart, A. Benedictow, Y. Bennouna, A.-M. Blechschmidt, S. Chabrillat, Christophe, Y., E. Cuevas, A. El-Yazidi, H. Flentje, P. Fritzsche, K.M. Hansen, U. Im, J. Kapsomenakis, B. Langerock, A. Richter, N. Sudarchikova, V. Thouret, T. Warneke, C. Zerefos, Validation report of the CAM5 near-real-time global atmospheric composition service: Period June - August 2020, Copernicus Atmosphere Monitoring Service (CAM5) report, CAMS84_2018SC2_D1.1.1_JJA2020.pdf, January 2021, doi:10.24381/8pxnq362, 2020.
- Rodríguez, S., Calzolari, G., Chiari, M., Nava, S., García, M.I., Lopez-Solano, J., Marrero, C., Lopez-Darias, J., Cuevas, E., Alonso-Perez, S., Prats, N., Amato, F., Lucarelli, F., Querol, X., Rapid changes of dust geochemistry in the Saharan Air Layer linked to sources and meteorology. *Atmospheric Environment* 2020, Volume 223, 15 February 2020, 117186 <https://doi.org/10.1016/j.atmosenv.2019.117186>, 2020.
- Schulz, M., Y. Christophe, M. Ramonet, Wagner, A., H.J. Eskes, S. Basart, A. Benedictow, Y. Bennouna, A.-M. Blechschmidt, S. Chabrillat, E. Cuevas, A. ElYazidi, H. Flentje, K.M. Hansen, U. Im, J. Kapsomenakis, B. Langerock, A. Richter, N. Sudarchikova, V. Thouret, T. Warneke, C. Zerefos, Validation report of the CAM5 near-real-time global atmospheric composition service: Period December 2018 -February 2019, Copernicus Atmosphere Monitoring Service (CAM5) report, CAMS84_2018SC1_D1.1.1_DJF2019_v1.pdf, June 2019, doi:10.24380/7th6-tk72, 2019.
- Schulz, M., Y. Christophe, M. Ramonet, Wagner, A., H. J. Eskes, S. Basart, A. Benedictow, Y. Bennouna, A.-M. Blechschmidt, S. Chabrillat, E. Cuevas, A. ElYazidi, H. Flentje, P. Fritzsche, K.M. Hansen, U. Im, J. Kapsomenakis, B. Langerock, A. Richter, N. Sudarchikova, V. Thouret, T. Warneke, C. Zerefos, Validation report of the CAM5 near-real-time global atmospheric composition service: Period December 2019 – February 2020, Copernicus Atmosphere Monitoring Service (CAM5) report, CAMS84_2018SC2_D1.1.1_DJF2020.pdf, June 2020, doi:10.24380/322n-jn39, 2020.
- Sudarchikova, N., M. Schulz, Q. Errera, M. Ramonet, H. J. Eskes, S. Basart, A. Benedictow, Y. Bennouna, A.-M. Blechschmidt, S. Chabrillat, Christophe, Y., E. Cuevas, A. El-Yazidi, H. Flentje, P. Fritzsche, K.M. Hansen, U. Im, J. Kapsomenakis, B. Langerock, A. Richter, V. Thouret, A. Wagner, T. Warneke, C. Zerefos, Validation report of the CAM5 near-real-time global atmospheric composition service: Period September - November 2020, Copernicus Atmosphere Monitoring Service (CAM5) report, CAMS84_2018SC3_D1.1.1_SON2020.pdf, March 2021, doi: 10.24380/rysv-7371, 2021.
- Terradellas, E., S. Basart, and E. Cuevas: 2013-2015 Activity Report of the SDS-WAS Regional Center for Northern Africa, Middle East and Europe, Joint publication of AEMET and WMO; NIPO: 281-16-007-3; WMO / GAW Report No. 230; WMO / WWRP No. 2016-2, 2016.
- Terradellas, E., Werner, E., Basart, S. and F. Benincasa 2018: Warning Advisory System for Sand and Dust Storm in Burkina Faso, WMO SDS-WAS, Barcelona, 9 pp. SDS-WAS-2018-001, 2018.
- Wagner, A., M. Schulz, Y. Christophe, M. Ramonet, H. J. Eskes, S. Basart, A. Benedictow, Y. Bennouna, A.-M. Blechschmidt, S. Chabrillat, E. Cuevas, A. ElYazidi, H. Flentje, K.M. Hansen, U. Im, J. Kapsomenakis, B. Langerock, A. Richter, N. Sudarchikova, V. Thouret, T. Warneke, C. Zerefos, Validation report of the CAM5 near-real-time global atmospheric composition service: Period September - November 2019, Copernicus Atmosphere Monitoring Service (CAM5) report, CAMS84_2018SC2_D1.1.1_SON2019_v1.pdf, February 2020, doi:10.24380/xzkk-bz05, 2019.
- WMO, WMO Airborne Dust Bulletin: Sand and Dust Storm Warning Advisory and Assessment System, No. 3 - May 2019, 2019.
- WMO, WMO Airborne Dust Bulletin: Sand and Dust Storm Warning Advisory and Assessment System, No. 4 - May 2020 2020.

17.7 Staff

- Dr Emilio Cuevas (AEMET; SDS-WAS Regional Centre NA-ME-E Scientific Advisor)
- Ernest Werner (AEMET, Technical Director of the SDS WAS Regional Centre NA-ME-E, and the BDFC)
- Dr Sara Basart (BSC; Research Scientist)
- Dr Sergio Rodríguez (CSIC-IPNA, Scientific advisor)
- Dr Natalia Prats (AEMET; Research Scientist)
- Dr Celia Milford (IARC-AEMET; Scientific collaborator)
- Francesco Benincasa (BSC-AEMET; Technical support)
- Kim Serradell (BSC; Technical support)

18 GAW Tamanrasset twinning programme

In 2006, the “GAW-Twinning” between IZO and Tamanrasset GAW stations was initiated with the Saharan Air Layer Air Mass characterization (SALAM) project. This was part of a cooperation programme between the l’Office Nationale de la Météorologie (ONM, Algeria) and AEMET. In September 2006, the AERONET Tamanrasset-AEMET Cimel station was installed (Fig. 18.1). The instruments of the GAW Tamanrasset twinning programme are located on the roof of the Regional Meteorological Center (southern regional meteorological department, ONM, Algeria) in Tamanrasset (92,635 inhabitants). This area, free of industrial activities, is in the highlands of the Algerian Sahara. Tamanrasset-Assekrem is a WMO Global Atmosphere Watch station.



Figure 18.1. The AERONET Cimel (upper image) at Tamanrasset on the terrace of the Regional Meteorological Centre (lower image).

This station now has a relatively long time series of AERONET data, covering the period 2006-2020 (Fig. 18.2), despite the enormous environmental and logistical difficulties to keep it in operation, in large part thanks to the effort and great collaboration of the human team in charge of the GAW Tamanrasset-Assekrem facilities.

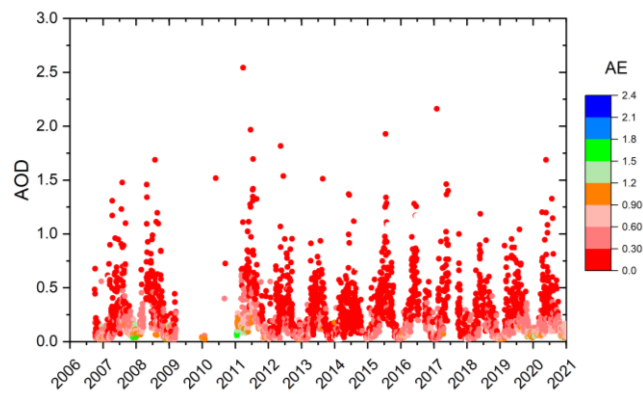


Figure 18.2. The Tamanrasset AERONET AOD data series (2006-2020).

The GAW station Tamanrasset is in the south of Algeria, in the heart of the Sahara, and provides unique and precious data in an extensive region near important dust sources. Tamanrasset station is the only permanent AERONET observation site in the heart of the Sahara region (Fig. 18.3a). This station is strategic not only for the characterization of atmospheric composition over the Sahara Desert in the frame of the GAW Programme, but also to evaluate atmospheric models and validate satellite data. The Tamanrasset station has been regularly used to evaluate satellite-derived products, such as the IASI aerosols product including desert mineral dust (e.g. Callewaert et al., 2019). In fact, it is a key station to assess the performance of mineral dust prediction models in a challenging region where there are numerous nearby dust sources.

Tamanrasset is a singular station of special attention for the Sand and Dust Storm Warning Advisory and Assessment System Regional Center (e.g. Terradellas et al., 2016) (see Section 17 for more details). This AERONET photometer is calibrated by the IARC on an approximately annual basis. Further details of this programme are provided in Guirado et al. (2014).

An automatic comparison of 12 model forecasts of Dust Optical Depth (DOD) at 550 nm versus AERONET AOD data for the month of February 2019 at Tamanrasset is shown in Fig. 18.3b. This comparison is available at the SDS-WAS [website](#).

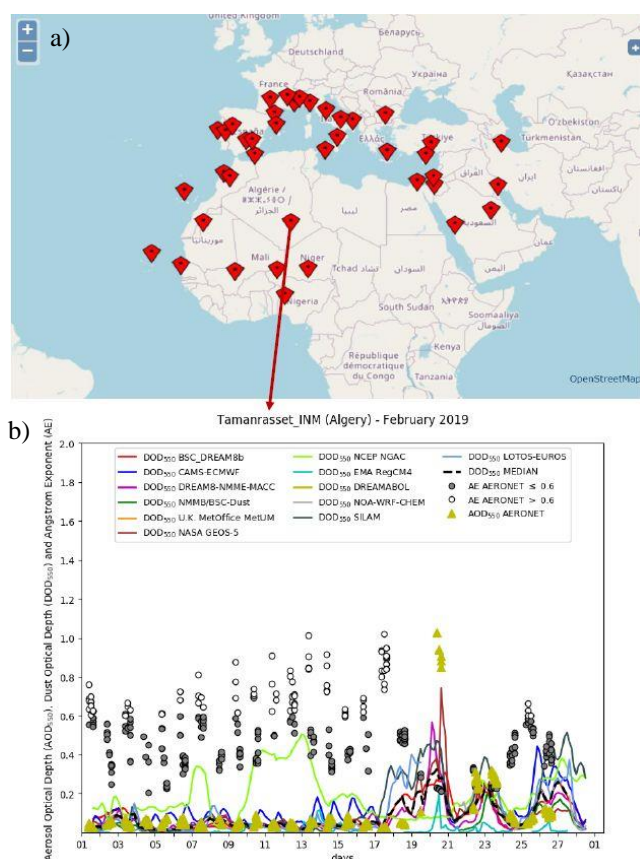


Figure 18.3. a) Map of the AERONET stations in Northern Africa used by the Sand and Dust Storm Warning Advisory and Assessment System Regional Centre and b) AERONET dust AOD comparison with 12 dust models, dust optical depth (DOD) and median of the models at Tamanrasset in February 2019.

Tamanrasset is also a key station for evaluating global operational forecast services, such as CAMS-Copernicus, under conditions of almost pure dust. An automatic comparison of CAMS-Copernicus outputs for several aerosol types with the Tamanrasset AERONET level 1.5 AOD data for the month of July 2020 is shown in Fig. 18.4 and can be found [here](#), where it is possible to select other intercomparison time periods.

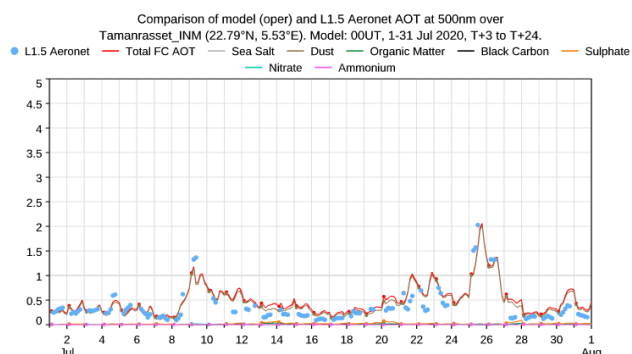


Figure 18.4. Comparison of COPERNICUS CAMS operational aerosols product and AERONET level 1.5 AOD at Tamanrasset site during July 2020.

The twinning was completed with the installation at Tamanrasset of a double Brewer Spectrophotometer #201 (MARK-III) in October 2011 (Fig. 18.5), thanks to the project entitled “Global Atmosphere Watch in the Maghreb-Sahara Region” (GAW-Sahara) financed by the Spanish Agency for International Development Cooperation (AECID).



Figure 18.5. Brewer#201 at Tamanrasset on the terrace of the Regional Meteorological Centre. On the left, the AERONET Cimel photometer.

An operational Dobson (#11; WMO station code 002) spectrophotometer has been operated at Tamanrasset since April 1994. This station is now one of the few sites in the world where permanent and long-term intercomparison between the Dobson, the Brewer and the present and future satellite-based sensors could be performed on a routine basis. This initiative has been strongly recommended by the WMO Ozone Scientific Advisory Group and represents a unique contribution to the total ozone global network Quality Assurance. In addition, the Brewer instrument provides spectral ultraviolet radiation data.

Tamanrasset, with the Brewer Spectrophotometer #201, plays an important role in the context of other global observation networks, e.g. in the EUBREWNET network (Fig. 18.6) (see Section 6.3.1 for more details) providing near-real-time data of column ozone, spectral radiation and AOD in the UV range (see López-Solano et al., 2018).

As an example, Figure 18.6 shows two of the many products that EUBREWNET provides. The total ozone data on 16 April 2019 is shown in Fig. 18.6b. During this day there were clear conditions that allowed more than 100 direct sun measurements, with a very low ozone content of 271 DU and quite stable values (standard deviation of 1.3), making it a day that can be used for Langley calibration. In Fig. 18.6c, the diurnal variation of the UV-index at Tamanrasset on 1 March 2019 is shown.

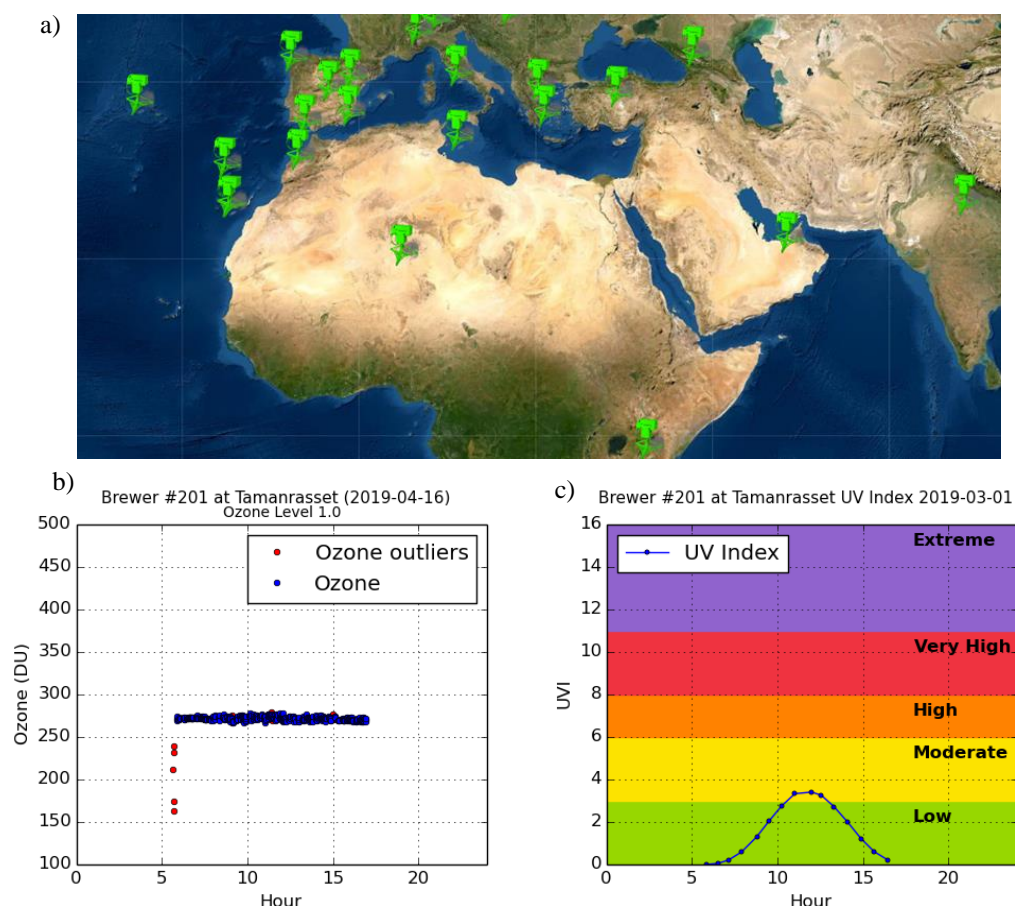


Figure 18.6. a) The Brewer spectrophotometer of Tamanrasset as part of the EUBREWNET network, b) example of total ozone data display on 16 April 2019, c) example of UV index diurnal variation at Tamanrasset on 1 March 2019.

The Brewer #201 is periodically calibrated by the Regional Brewer Calibration Center for Europe hosted by the IARC taking advantage of the biannual intercomparisons that are held at the INTA station at El Arenosillo-Huelva (Southern Spain). In fact, this instrument was repaired and participated in the 14th RBCC-E intercomparison campaign which was held at El Arenosillo from 17-28 June 2019, see Redondas et al. (2020), with the participation of Sidi Alamine Baika and Abdessadek Saanounne, members of the l'ONM staff at the Tamanrasset station (Fig. 18.7).



Figure 18.7. Abdessadek Saanounne (1st from the right) and Sidi Alamine Baika (2nd from the right) (l'ONM Tamanrasset station staff) along with participants of a workshop held during the 14th Brewer intercomparison campaign organized by the RBCC-E at El Arenosillo (Spain) in June 2019.

Since March 2017, a Calitoo hand-held sun photometer has been operating at Tamanrasset. During this time, the performance of the Calitoo under the challenging conditions in a desert area have been tested with very good results (see Fig. 18.8).

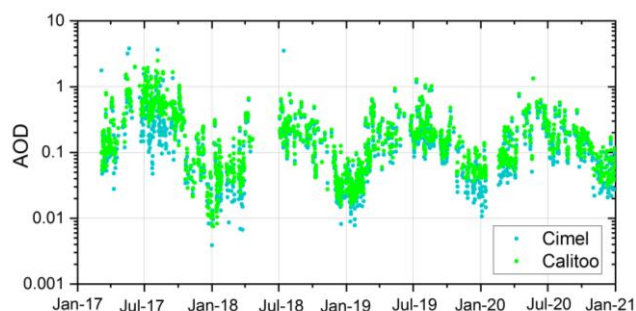


Figure 18.8. AERONET AOD computed at 500 nm from Cimel sun-photometer versus AOD computed at 540 nm from CALITOO hand-held sun-photometer at Tamanrasset (2017-2020). The gap in data in 2018 is due to the replacement of the Calitoo for a newly calibrated one.

18.1 References

- Callewaert, S., Vandenbussche, S., Kumps, N., Kylling, A., Shang, X., Komppula, M., Goloub, P., and De Mazière, M.: The Mineral Aerosol Profiling from Infrared Radiances (MAPIR) algorithm: version 4.1 description and evaluation, *Atmos. Meas. Tech.*, 12, 3673–3698, <https://doi.org/10.5194/amt-12-3673-2019>, 2019.
- Guirado, C., Cuevas, E., Cachorro, V. E., Toledano, C., Alonso-Pérez, S., Bustos, J. J., Basart, S., Romero, P. M., Camino, C., Mimouni, M., Zeudmi, L., Goloub, P., Baldasano, J. M., and de Frutos, A. M.: Aerosol characterization at the Saharan AERONET site Tamanrasset, *Atmos. Chem. Phys.*, 14, 11753–11773, [doi:10.5194/acp-14-11753-2014](https://doi.org/10.5194/acp-14-11753-2014), 2014.
- López-Solano, J., Redondas, A., Carlund, T., Rodríguez-Franco, J. J., Diémoz, H., León-Luis, S. F., Hernández-Cruz, B., Guirado-Fuentes, C., Kouremeti, N., Gröbner, J., Kazadzis, S., Carreño, V., Berjón, A., Santana-Díaz, D., Rodríguez-Valido, M., De Bock, V., Moreta, J. R., Rimmer, J., Smedley, A.R.D., Boulkelia, L., Jepsen, N., Eriksen, P., Bais, A. F., Shirov, V., Vilaplana, J. M., Wilson, K. M., and Karppinen, T. Aerosol optical depth in the European Brewer Network, *Atmos. Chem. Phys.*, <https://doi.org/10.5194/acp-18-3885-2018>, 18, 3885–3902, 2018.
- Redondas, A., Berjón, A., López-Solano, J., Carreño, V., León-Luis, S.F., Santana, D.: Fourteenth Intercomparison Campaign of the Regional Brewer Calibration Centre Europe. El Arenosillo Atmospheric Sounding Station, Huelva, Spain, 17–28 June 2019. Vol. WMO/GAW Report No. 257. Joint publication of State Meteorological Agency (AEMET), Madrid, Spain and World Meteorological Organization (WMO), 550 p., 2020. Available from: https://library.wmo.int/doc_num.php?explnum_id=10640
- Terradellas, E., S. Basart, and E. Cuevas: 2013-2015 Activity Report of the SDS-WAS Regional Center for Northern Africa, Middle East and Europe, Joint publication of AEMET and WMO; NIPO: 281-16-007-3; WMO / GAW Report No. 230; WMO / WWRP No. 2016-2, 2016.

18.2 Staff

Dr Emilio Cuevas (AEMET, PI of the Tamanrasset-Izaña twinning)

Alberto Redondas (AEMET, PI of the Ozone and UV Programme)

Ramón Ramos (AEMET, logistics and instrumentation)

Dr Carmen Guirado Fuentes (UVA/AEMET) left IARC in September 2019

Virgilio Carreño (AEMET; Meteorological Observer-GAW Technician)

Local contributors:

Mr Sidi Baika (Tamanrasset-Assekrem GAW station, Head)

Mr Abdessadek Saanouni, Mr L. Zeudmi-Sahraoui and Mr M. Zoukani (Technical staff).

19 WMO Testbed for Aerosols and Water Vapour Remote Sensing Instruments

The mission of the Commission for Instruments and Methods of Observations (CIMO) was to promote and facilitate international standardisation and compatibility of instruments and methods of observations used by Members, in particular within the WMO Global Observing System, to improve quality of products and services delivered to/by Members and to meet their requirements (see [Report](#) from the President to Cg-XV (2007), [Report](#) from the President to Cg-XVI (2011) and [Report](#) from the President to Cg-XVII (2015). Following approval of the WMO Reform package by the Eighteenth World Meteorological Congress in June 2019, a Joint Session of the new Technical Commissions and Research Board agreed on working structures in May 2020. As a result of the WMO reform of the constituent bodies, CIMO was dissolved and its activities were included in the activities of the Commission for Observation, Infrastructure and Information Systems (INFCOM).

CIMO XVI nominated Izaña Observatory as WMO-CIMO Testbed for Aerosols and Water Vapour Remote Sensing Instruments. The CIMO aim to promote the advancement of observing systems of WMO member countries through its WMO Integrated Global Observing System (WIGOS). It is also expected that Testbeds centres can play a decisive role in the effort of WMO to reduce the differences between countries, favouring the completion of training and capacity building through specific collaborations with stations and observatories in developing countries. The General Terms of Reference for the CIMO Testbeds for Ground based Remote-sensing and In-situ Observations (CIMO TB) can be found at the [Terms of Reference of CIMO Testbeds](#).

19.1 Main objectives and activities of the Izaña Testbed

The main ongoing activities of the Izaña Observatory Testbed are related to instrument validation, development of new methodologies and devices for aerosol observations.

19.2 EKO Campaign: Aerosol and water vapour retrievals from the EKO MS-711 spectral direct irradiance measurements

An EKO MS-711 and RSB grating spectroradiometer have been tested in the CIMO Testbed programme since March 2019 at IZO. Within these activities aerosol and water vapour retrievals have been obtained from EKO spectral direct irradiance measurements.

From this campaign two articles have been published (García et al., 2020 and García et al., 2021) which are described in the following subsections.

19.2.1 Aerosol retrievals from the EKO MS-711 spectral direct irradiance measurements and corrections of the circumsolar radiation

Between April and September 2019, AOD at several wavelengths (340, 380, 440, 500, 675, and 870 nm) was determined from spectral direct UV–visible normal solar irradiance (DNI) performed with an EKO MS-711 grating spectroradiometer and compared with synchronous AOD measurements from a reference AERONET sun photometer (García et al., 2020).

The EKO MS-711 was calibrated at the Izaña Observatory by using the Langley plot method during the study period. Although this instrument has been designed for spectral solar DNI measurements, and therefore has a field of view (FOV) of 5° that is twice the recommended amount in solar photometry for AOD determination, the AOD differences compared to the AERONET–Cimel reference instrument (FOV ~ 1.2°) are fairly small. A comparison of the results from the Cimel AOD and EKO MS-711 AOD presents a root mean square (RMSE) of 0.013 (24.6 %) at 340 and 380 nm, and 0.029 (19.5 %) for longer wavelengths (440, 500, 675, and 870 nm). However, under relatively high AOD, near-forward aerosol scattering might be significant because of the relatively large circumsolar radiation (CSR) due to the large EKO MS-711 FOV, which results in a small but significant AOD underestimation in the UV range.

The AOD differences decrease considerably when CSR corrections, estimated from LibRadtran radiative transfer model simulations, are performed. This leads to reduction of RMSE to 0.006 (14.9 %) at 340 and 380 nm, and 0.005 (11.1 %) for longer wavelengths. The EKO AOD–Cimel AOD differences within the WMO traceability limits were > 95% at 500, 675, and 870 nm with no CSR corrections (Fig. 19.1). After applying the CSR corrections, the percentage of AOD differences within the WMO traceability limits increased for all wavelengths (see Fig. 19.1) and were > 95% for 380, 440, 500, 675, and 870 nm.

The EKO MS-711 has proven to be an instrument which, despite having been designed for solar radiation measurements, can provide high-quality AOD measurements in the VIS and near-IR ranges, with excellent results when compared to the AERONET–Cimel reference radiometer.

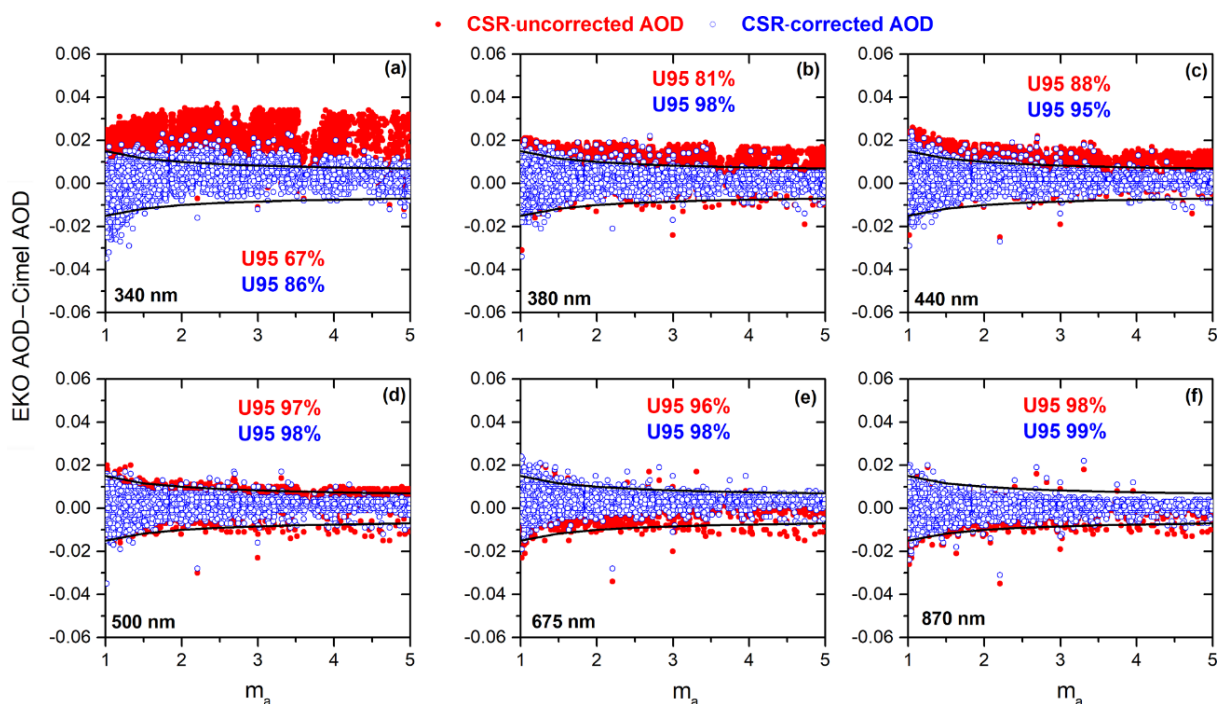


Figure 19.1. AOD differences (EKO AOD–Cimel AOD) versus the optical air mass (m_a). Black lines represent the U_{95} uncertainty limits. Reprinted from García et al. (2020).

19.2.2 Water Vapor Retrievals from Spectral Direct Irradiance Measured with an EKO MS-711 Spectroradiometer - Intercomparison with Other Techniques

Precipitable water vapor retrievals are of major importance for assessing and understanding atmospheric radiative balance and solar radiation resources. On that basis, this study presents the first PWV values measured with a EKO MS-711 grating spectroradiometer (Fig. 19.2) from direct normal irradiance in the spectral range between 930 and 960 nm at the Izaña Observatory between April and December 2019. These results were published by García et al. (2021).

The expanded uncertainty of PWV (UPWV) was theoretically evaluated using the Monte-Carlo method to be 0.37 ± 0.11 mm. The estimated uncertainty depends on PWV. For $PWV \leq 5$ mm (62% of the data), the mean UPWV is 0.31 ± 0.07 mm, while for $PWV > 5$ mm (38% of the data) it is 0.47 ± 0.08 mm.

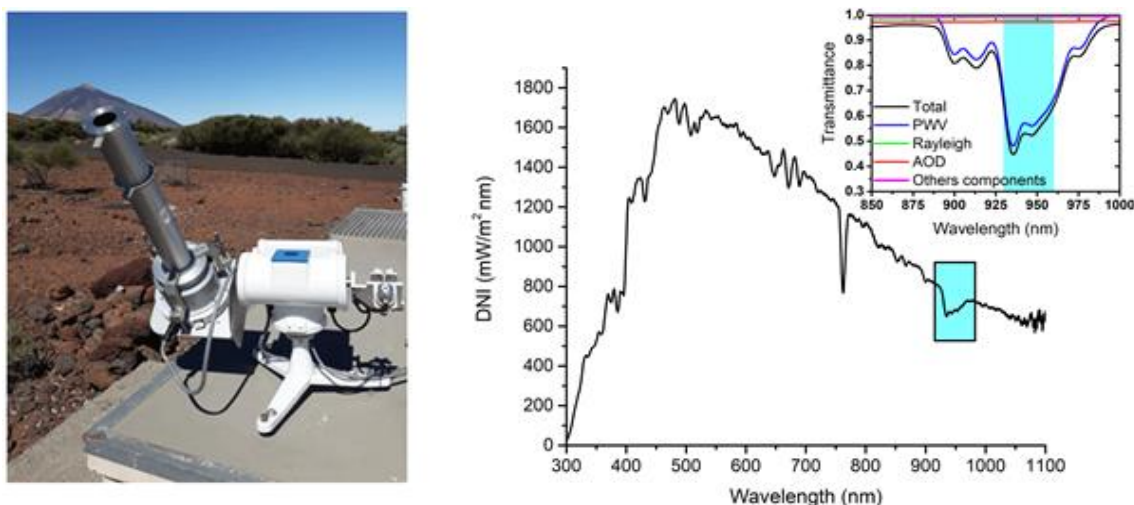


Figure 19.2 EKO MS-711 spectroradiometer installed at Izaña Observatory. Direct normal irradiance, measured with the EKO MS-711 spectroradiometer on 20 May 2019 (13:00 UTC) at IZO. The blue box indicates the water vapor absorption band selected in this work for the PWV retrievals (930–960 nm). The zoomed graphic shows the direct transmittance simulated with MODTRAN model between 850 and 1000 nm on 20 May 2019 (13:00 UTC). Reprinted from García et al. (2021).

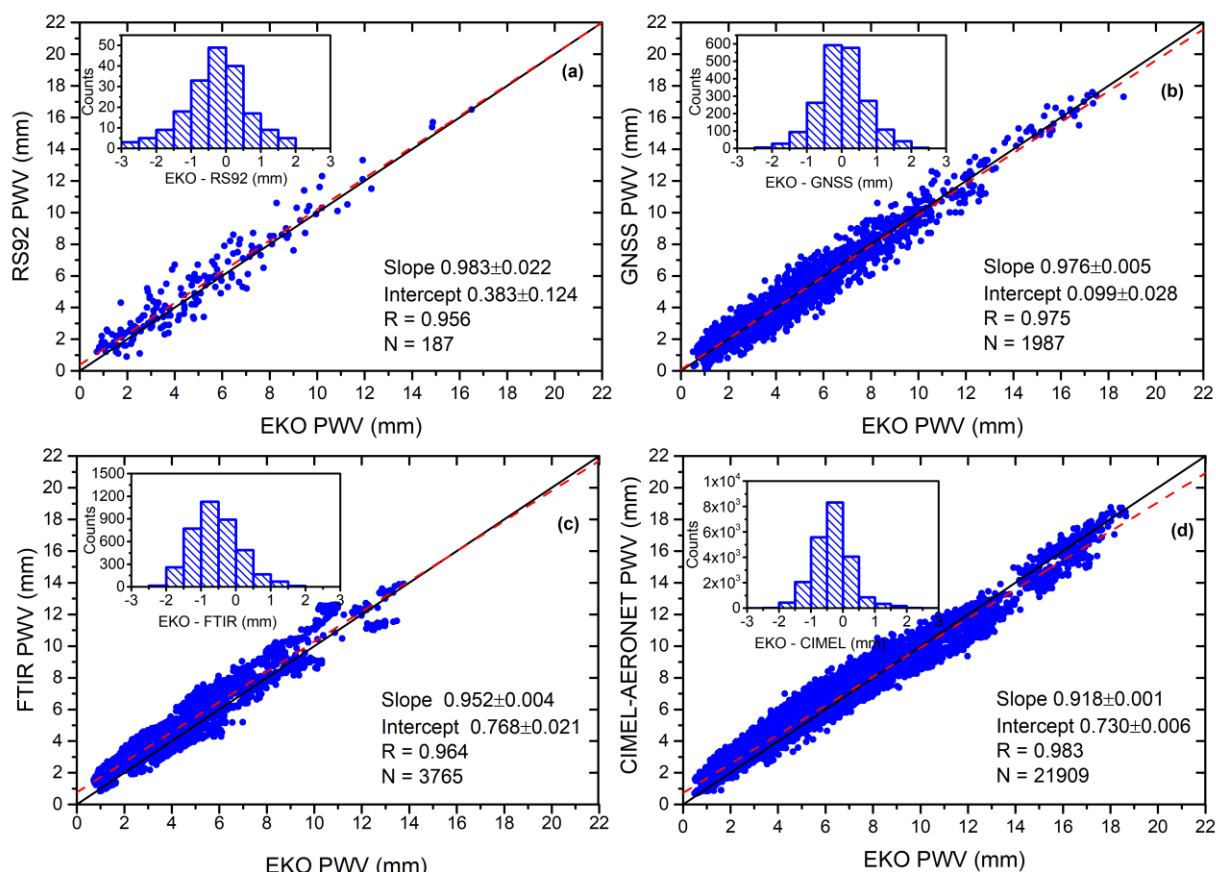


Figure 19.3. Scatterplot of EKO PWV (mm) versus (a) RS92 PWV, (b) GNSS PWV, (c) FTIR PWV, and (d) CIMEL-AERONET PWV between April and December 2019 at IZO. The dotted lines are the least-squares fits and the black solid lines are the diagonals ($x = y$). The least-squares fit parameters are shown in the legend (slope, intercept and Pearson correlation coefficient R). N is the amount of data. The small figures represent the occurrence distributions of the mean bias in mm. Reprinted from García et al. (2021).

In addition, the EKO PWV retrievals were comprehensively compared against the PWV measurements from several reference techniques available at IZO, including meteorological radiosondes, Global Navigation Satellite System, CIMEL-AERONET sun photometer and Fourier Transform Infrared spectrometry (Fig. 19.3). The EKO PWV values closely align with the above-mentioned different techniques, providing a mean bias and standard deviation of -0.30 ± 0.89 mm, 0.02 ± 0.68 mm, -0.57 ± 0.68 mm and 0.33 ± 0.59 mm, with respect to the RS92, GNSS, FTIR and CIMEL-AERONET measurements. According to the theoretical analysis, Mean Bias decreases when comparing values for $PWV > 5$ mm, leading to a PWV MB between -0.45 mm (EKO vs. FTIR), and 0.11 mm (EKO vs. CIMEL-AERONET).

These results confirm that the EKO MS-711 spectroradiometer is precise enough to provide reliable PWV data on a routine basis and as a result, can complement existing ground-based PWV observations. The implementation of PWV measurements in a spectroradiometer increases the capabilities of these types of instruments to simultaneously obtain key parameters used in certain applications such as monitoring solar power plants performance.

19.3 Column Integrated Water Vapour and Aerosol Load Characterization with the New ZEN-R52 Radiometer

Following the ZEN system design published by Almansa et al. (2017), conceived for dust aerosol optical depth monitoring, the capacity of the new ZEN-R52 radiometer to measure both column-integrated precipitable water vapor and AOD is presented in Almansa et al. (2020). This study presented PWV retrieved by the ZEN-R52 radiometer in IZO over a 10-month period (August 2017 to June 2018).

The ZEN-R52 has recent improvements in comparison with the old ZEN-R4: such as a smaller field of view; an increased signal-to-noise ratio; better stray light rejection and an additional channel at 940 nm for PWV retrieval. PWV and AOD are retrieved by using Zenith Sky Radiance (ZSR) measurements along with a lookup table (LUT) methodology. A comprehensive validation of ZEN PWV and AOD was performed using AERONET and FTIR spectrometer measurements as reference (Fig. 19.4). The ZEN-R52 AOD uncertainty was calculated as 0.01 ± 0.13 AOD.

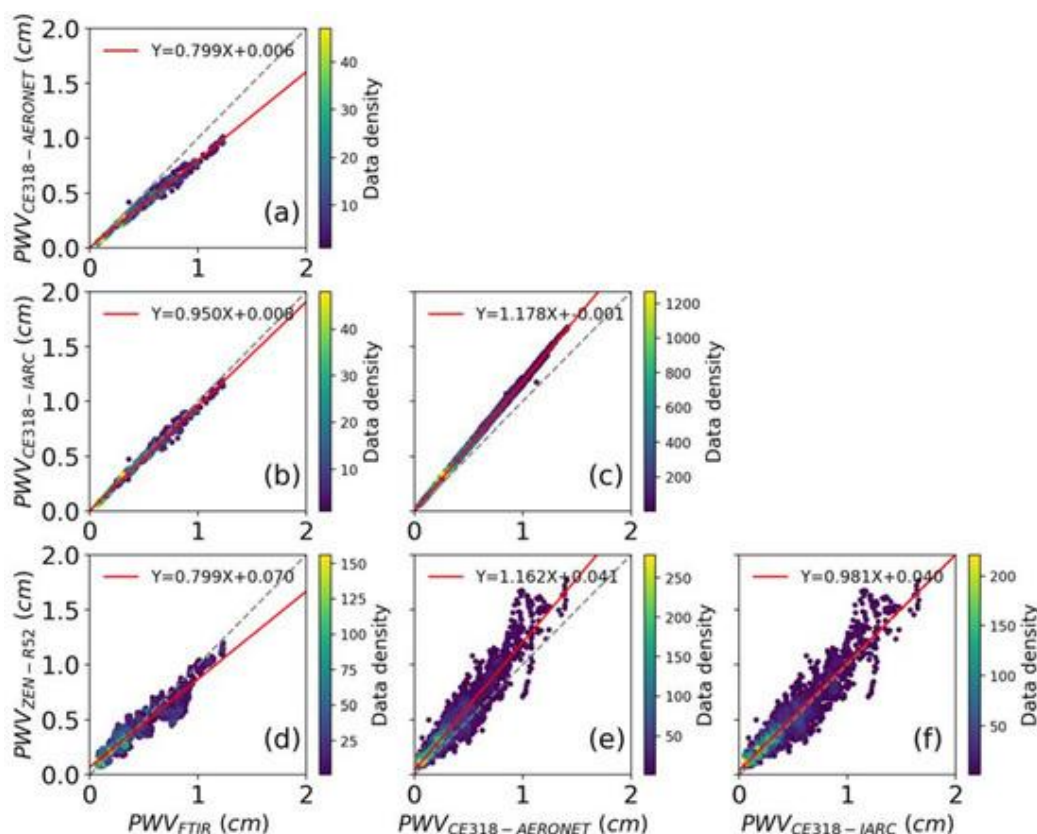


Figure 19.4. PWV scatterplots between ZEN-R52, CE318-AERONET, CE318-IARC and FTIR at Izaña over a 10-month period (August 2017 to June 2018 a–f). The red line shows the linear fit equation, the broken grey line shows the diagonal and the colour bar indicates the density of data. Reprinted from Almansa et al. (2020).

Regarding the PWV analysis, a good agreement was found between the ZEN, AERONET and FTIR. The ZEN-R52 PWV uncertainty was calculated as ± 0.089 cm or $\pm 0.036 + 0.061$ PWV for $\text{PWV} < 1$ cm.

The results published in this study confirm the suitability of the ZEN system to monitor aerosols and water vapour in remote regions. This new system can play an important role in increasing representativeness of ground based observing network which can be critical for constraining global and relatively coarse-resolution models and also for improving satellite validation and aerosol model evaluation and assimilation in remote regions.

19.4 Evaluation of night-time aerosol measurements and lunar irradiance models in the frame of the first multi-instrument nocturnal intercomparison campaign

Photometric measurements have been used during decades to provide reliable and valuable information to compile long-term global AOD and other aerosol properties records in order to increase our knowledge on the role of aerosols in the Earth's radiative balance. However, AOD data provided

by sun photometers is severely restricted since it is limited to daytime, which seriously constrain the study of atmospheric processes in which day-to-night variations play an important role, such as in the case of polar regions, aerosol nucleation during the daytime, convective processes or other processes with a well-defined time pattern (traffic, domestic heating among others).

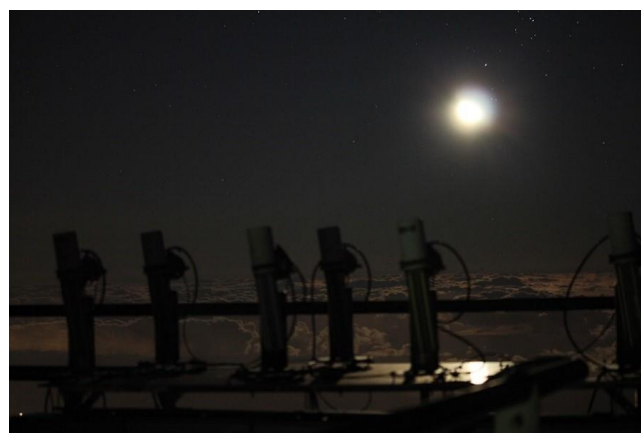


Figure 19.5. Cimel CE318-T photometers operating in Izaña during the field campaign.

The first multi-instrumental comparison campaign of nocturnal measurements held at Izaña Observatory in 2017

was the first time that nocturnal measurements were performed coincidentally with different photometers (Fig. 19.5). Three different instruments were involved in this field campaign: two different lunar photometers (LunarPFR, from PMOD /WRC, and Cimel CE318-T) and one stellar photometer. The stellar photometer that participated in this campaign is a non-commercial instrument which measures direct star irradiance and it belongs to University of Granada. The review of the different calibration techniques for lunar photometry as well as the uncertainty estimation of the nocturnal AOD are an important outcome of the work recently published by Barreto et al. (2019). In addition, the new free and open-access ROLO Implementation for Moon-photometry Observation (RIMO) model has been released which will allow the scientific community to obtain reliable lunar exo-atmospheric irradiance values for the analysis of photometric data.

The result of this field campaign suggest that lunar photometry is a reliable technique, especially for low aerosol loading conditions (see Fig. 19.6). Small instrumental differences between the two lunar photometers were observed during the field campaign. These discrepancies were only appreciated under pristine sky conditions and are hypothesized to be caused by the different pointing process or dark current correction performed by the two lunar photometers.

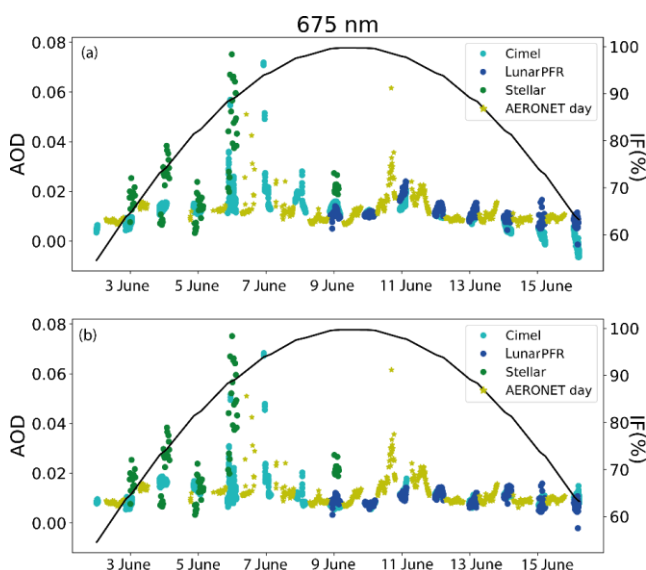


Figure 19.6. AOD time series from the two lunar photometers involved in the field campaign (at 674.8 nm), LunarPFR (at 675.6 nm) and the stellar photometer (at 670.0 nm), including daytime AERONET (at 675.7 nm) in the period 2-17 June 2017. AOD from lunar photometers have been extracted by means of (a) Lunar-Langley calibration with the RIMO model, and (b) Langley-plot calibration with V_{0c} values. The black line and right y axis correspond to the evolution of the Moon's illumination factor (IF, in %) in this period. Reprinted from Barreto et al. (2019).

19.5 Correction of a lunar-irradiance model for aerosol optical depth retrieval and comparison with a star photometer

New technological advances permit lunar-irradiance to be measured with classical photometers. Lunar photometry has appeared as a suitable technique to retrieve aerosol information in nocturnal period, increasing the potential to derive AOD at night-time. However, the fast change in illumination throughout the Moon's cycle implies that an accurate and time-dependent knowledge of the extraterrestrial lunar irradiance is mandatory in lunar photometry.

The RIMO model (an implementation of the ROLO – Robotic Lunar Observatory – model) has been considered a useful tool to estimate the AOD at night-time (Barreto et al., 2019). However, important uncertainties and biases have been reported to affect both ROLO and RIMO models (e.g. Viticchie et al., 2013; Lacherade et al., 2014; Barreto et al., 2017, 2019).

A new empirical correction factor to the RIMO model (RCF or RIMO Correction Factor) has been implemented in Roman et al. (2020) by means of Cimel CE318-T Sun-sky-Moon photometer for 98 pristine nights with low and stable AOD conditions at the Izaña Observatory. The expected day-to-night coherence allowed the authors to estimate the inaccuracies inherent to the RIMO model and provides a RIMO corrected lunar irradiance model. The RCF correction applied to the RIMO model varies both with the Moon Phase Angle (MPA) and with wavelength, ranging from 1.01 to 1.14.

These results revealed an expected overall underestimation of the RIMO model. The AOD derived by this corrected method is compared with the independent and co-located two-year AOD dataset made by a star photometer at Granada (Spain) (Fig. 19.7). Average differences between -0.015 and -0.005 were found, and standard deviations are between 0.03 and 0.04 for 440, 500, 675, and 870 nm. Differences were higher for the 380 nm spectral band. No significant dependences on the Moon-star AOD differences as a function of MPA were found (Roman et al., 2020).

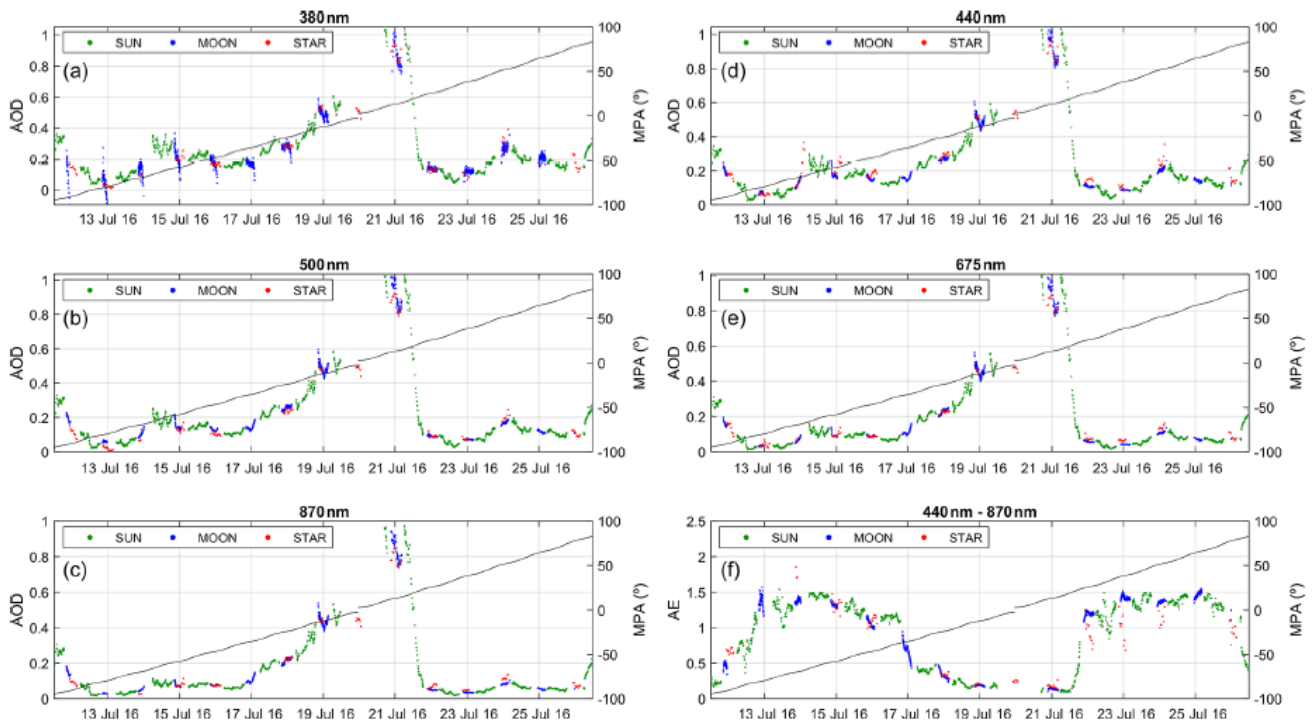


Figure 19.7. AOD values from the Sun, Moon, and star photometer at Granada (Spain) from the first to third Moon quarters in July 2016. Panel (f) shows the Ångström Exponent calculated with the wavelengths of 440, 500, 675 and 870 nm (436, 500, 670, and 880 nm for the star photometer). Moon phase angle is represented with a black line in each panel. Reprinted from Román et al. (2020).

19.6 ESA projects

19.6.1 Lunar spectral irradiance measurement and modelling for absolute calibration of EO optical sensors (2017-2019)

This project, launched in 2017, was assigned to a consortium of three members: University of Valladolid/Izaña Atmospheric Research Center, National Physical Laboratory (NPL, London) and Flemish Institute for Technological Research (Vlaamse Instelling voor Technologisch Onderzoek, Belgium). The main goal of the project is to use ground-based lunar measurements performed with a CE318-TP9 photometer to improve the modelling of the lunar disk irradiance variations through its cycles with a threshold of 2% in the final model uncertainty.

The main outcome of this project is the new lunar irradiance model LIME (Lunar Irradiance Model ESA). LIME is an improved lunar irradiance model with < 2% absolute radiometric uncertainty (SI traceable), derived from 150 nights of lunar observations at IZO and TPO stations and an uncertainty analysis based on a Monte Carlo Evaluation (Fig. 19.8). These results improve considerably the absolute radiometric uncertainty involved in the previous lunar models (~ 5-10 %).

This new model is expected to play an important role in EO radiometric calibration, which can be validated using radiometrically stable natural targets, like the lunar disk irradiance. With this information, EO measurements can be radiometrically linked to all past, present and future sensors having performed similar measurements.

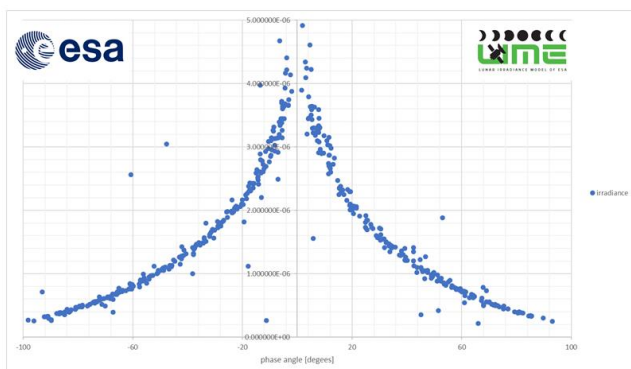


Figure 19.8. LIME lunar irradiance model at 440 nm for the lunar phase angle range between -100 and 100 degrees.

19.6.2 Maintenance of lunar photometer and lunar irradiance model (2020-2023)

The previous ESA project has been extended for four more years, and the ESA photometer is still in operation in IARC-AEMET stations (IZO and TPO) (Fig. 19.9). The main objective of this extension is to update and refine the LIME model on a yearly basis based on an extended set of measurements.



Figure 19.9. Cimel CE318-TP9 in operation in Teide Peak Observatory.

19.7 Field test of the Mars 2020 Rover Mission in terrain analogous to Mars in Teide Peak

NASA's Mars 2020 mission began in July 2020 with the launch from Cape Canaveral (Florida) of the Atlas V rocket. On-board, the Mars 2020/Perseverance rover is equipped with seven different instruments specially designed to conduct unprecedented scientific experiments on the Red Planet to seek signs of ancient life and gather rocks and soil samples for a possible return to Earth. In particular, the Mars Environmental Dynamics Analyzer (MEDA) instrument was designed to perform weather measurements including radiation, wind speed and direction, temperature and humidity, and also to measure the amount and size of dust particles in the Martian atmosphere. MEDA is an environmental suite of sensors developed by some research centers and led by the Spanish Centro de Astrobiología (CSIC-INTA) in Madrid.

As a twin experience in a terrestrial analogy of Mars, the MEDA instrument was tested and verified in the Teide Peak. This experience began in September 2020 with the deployment of the MEDA sensor in the Fortaleza area, in the Teide Peak (see Section 22.7), carried out by scientists from CSIC-INTA, Universidad de Alcalá (UAH), Instituto Geográfico Nacional and AEMET, and the technical support of the National Park and Volcano Teide. The MEDA instrument logged the environmental parameters, which will be compared to routine measurements taken from AEMET's nearby stations such as direct normal irradiance, global radiation, diffuse radiation, aerosol optical depth, Angström exponent for aerosols and meteorological parameters. These measurements provided helpful information to the NASA 2020 mission to verify and understand the atmospheric dynamics and relevant information registered by MEDA on the Red Planet's surface.

19.8 Color Sky Quality Meter

Four novel multispectral Color Sky Quality Meter (CoSQM) photometers were installed in April 2019 in four different locations in Tenerife differently affected by their proximity to the lighting sources and elevation: SCO, IZO (Fig. 19.10), IAC Observatory and TPO. This deployment is considered a first step toward a worldwide CoSQM network, with Tenerife as an important site for atmospheric sensing science thanks to the IARC-AEMET facilities which can be considered reference in terms of aerosol detection and cross calibration capabilities. This cheap and open-source instrument is able to sample the multispectral properties of the artificial light scattered by the atmosphere. These night sky brightness measurements will be used to partly fill the gaps in the spatio-temporal AOD dataset.



Figure 19.10. CoSQM instrument deployed at Izaña Observatory. Photo Credit: Martin Aube.

A new methodology will be developed in an ongoing publication that links together the zenith artificial night sky brightness and the AOD. Such method is especially suitable to be applied to moonless nights and to light polluted sites.

19.9 Prede/PFR/Cimel/Brewer/FTIR/EKO/ Pandora intercomparison project

In November 2019, an intercomparison campaign and a scientific workshop took place at Izaña Observatory involving different types of photometric observations utilising different techniques. The comparison project consisted in a 1-yr field campaign at the Izaña Observatory involving Brewer, EKO, PFR and Cimel operational photometric measurements as well as AOD measurements performed by means of FTIR (not operational and product under validation). Izaña provided also in situ aerosol measurements, lidar and meteorological measurements as ancillary data. This comparison project is within the WMO strategies, which follows a multi-platform approach with the goal of ensuring a global homogenization of the current photometric observing networks, important for satellite calibration/validation and model assimilation/validation.

This campaign is also within the future scope of the EMPIR and ACTRIS/CARS projects.

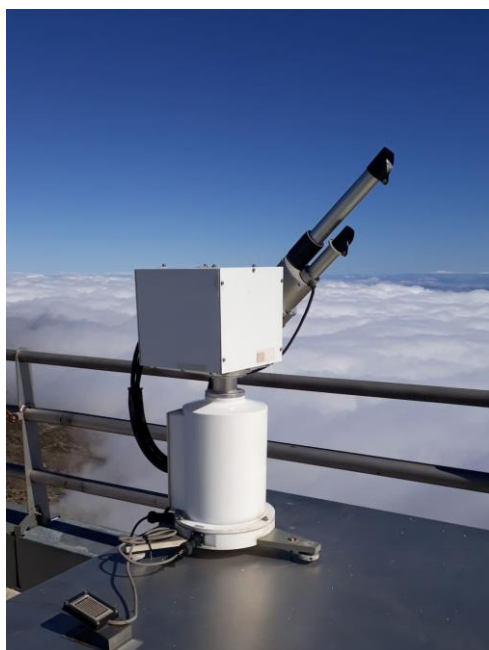


Figure 19.11 PREDE instrument deployed in Izaña Observatory for the intercomparison project.

A Prede sun photometer, the reference instrument in the **SKYNET** network, was installed at IZO as a collaboration between IARC/AEMET, the Italian National Research Council and the University of Valencia (Spain). Private companies such as Cimel Electronique also collaborated in this project from a scientific point of view. The University of Valladolid provided **Caelis** as a common platform for this multi-instrument comparison.

19.10 References

- Almansa, A. F., Cuevas, E., Torres, B., Barreto, Á., García, R. D., Cachorro, V. E., de Frutos, Á. M., López, C., and Ramos, R.: A new zenith-looking narrow-band radiometer-based system (ZEN) for dust aerosol optical depth monitoring, *Atmos. Meas. Tech.*, 10, 565–579, doi:10.5194/amt-10-565-2017, 2017.
- Almansa, A.F.; Cuevas, E.; Barreto, Á.; Torres, B.; García, O.E.; Delia García, R.; Velasco-Merino, C.; Cachorro, V.E.; Berjón, A.; Mallorquín, M.; López, C.; Ramos, R.; Guirado-Fuentes, C.; Negrillo, R.; de Frutos, Á.M. Column Integrated Water Vapor and Aerosol Load Characterization with the New ZEN-R52 Radiometer. *Remote Sens.* 2020, 12, 1424. Accessible at <https://www.mdpi.com/705210>.
- Barreto, Á., Cuevas, E., Granados-Muñoz, M. J., Alados-Arboledas, L., Romero, P. M., Gröbner, J., Kouremeti, N., Almansa, A. F., Stone, T., Toledano, C., Román, R., Sorokin, M., Holben, B., Canini, M., and Yela, M.: The new sun-sky-lunar Cimel CE318-T multiband photometer – a comprehensive performance evaluation, *Atmos. Meas. Tech.*, 9, 631–654, <https://doi.org/10.5194/amt-9-631-2016>, 2016.
- Barreto, Á., Román, R., Cuevas, E., Berjón, A. J., Almansa, A. F., Toledano, C., González, R., Hernández, Y., Blarel, L., Goloub, P., Guirado, C., and Yela, M.: Assessment of nocturnal aerosol optical depth from lunar photometry at the Izaña high mountain

observatory, *Atmos. Meas. Tech.*, 10, 3007–3019, <https://doi.org/10.5194/amt-10-3007-2017>, 2017.

Barreto, A., R. Román, E. Cuevas, D. Pérez-Ramírez, A.J. Berjón, N. Kouremeti, S. Kazadzis, J. Gröbner, M. Mazzola, C. Toledano, J.A. Benavent-Oltra, L. Doppler, J. Juryšek, A.F. Almansa, S. Victori, F. Maupin, C. Guirado-Fuentes, R. González, V. Vitale, P. Goloub, L. Blarel, L. Alados-Arboledas, E. Woolliams, S. Taylor, J.C. Antuña, M. Yela: Evaluation of night-time aerosols measurements and lunar irradiance models in the frame of the first multi-instrument nocturnal intercomparison campaign, *Atmospheric Environment*, Volume 202, 2019, Pages 190–211, ISSN 1352-2310, <https://doi.org/10.1016/j.atmosenv.2019.01.006>.

García, R. D., Cuevas-Agulló, E., Barreto, Á., Cachorro, V. E., Pó, M., Ramos, R., and Hoogendijk, K.: Aerosol retrievals from the EKO MS-711 spectral direct irradiance measurements and corrections of the circumsolar radiation, *Atmos. Meas. Tech.*, 13, 2601–2621, <https://doi.org/10.5194/amt-13-2601-2020>, 2020.

García, R.D.; Cuevas, E.; Cachorro, V.E.; García, O.E.; Barreto, Á.; Almansa, A.F.; Romero-Campos, P.M.; Ramos, R.; Pó, M.; Hoogendijk, K.; Gross, J. Water Vapor Retrievals from Spectral Direct Irradiance Measured with an EKO MS-711 Spectroradiometer—Intercomparison with Other Techniques. *Remote Sens.* 2021, 13, 350. <https://doi.org/10.3390/rs13030350>.

Lacherade, S., Aznay, O., Fougny, B., and Lebègue, L.: POLO: a unique dataset to derive the phase angle dependence of the Moon irradiance, in: *Sensors, Systems, and Next-Generation Satellites XVIII*, vol. 9241, p. 924112, International Society for Optics and Photonics, 2014.

Román, R., González, R., Toledano, C., Barreto, Á., Pérez-Ramírez, D., Benavent-Oltra, J. A., Olmo, F. J., Cachorro, V. E., Alados-Arboledas, L., and de Frutos, Á. M.: Correction of a lunar-irradiance model for aerosol optical depth retrieval and comparison with a star photometer., *Atmos. Meas. Tech.*, 13, 6293–6310, <https://doi.org/10.5194/amt-13-6293-2020>, 2020.

Viticchie, B., Wagner, S., Hewison, T., Stone, T., Nain, J., Gutierrez, R., Muller, J., and Hanson, C.: Lunar calibration of MSG/SEVIRI solar channels, in: *Proceedings of the EUMETSAT Meteorological Satellite Conference*, Vienna, Austria, 16–20 September 2013, 16–20, 2013.

19.11 Staff

- Dr Emilio Cuevas (AEMET; PI of Testbed)
- Dr Africa Barreto (AEMET; Research Scientist)
- Ramón Ramos (AEMET; Head of Infrastructure)
- Pedro Miguel Romero Campos (AEMET; Research Scientist)
- Dr Rosa García (TRAGSATEC/UVA; Research Scientist)
- Dr Antonio Fernando Almansa (CIMEL/AEMET; Research Scientist)
- Dr Carmen Guirado Fuentes (UVA/AEMET; Research Scientist) left IARC in September 2019
- Dr Yenny González (CIMEL; Research Scientist)
- César López Solano (SIELTEC)
- Dr Omaira García (AEMET; Research Scientist)
- Dr Victoria Cachorro (University of Valladolid; Head of Atmospheric Optics Group)

20 Activities in collaboration with IAC

IARC-AEMET, within the framework of the Specific Collaboration Agreement between AEMET and the Instituto de Astrofísica de Canarias (IAC) (Institute of Astrophysics of the Canary Islands), provide information and data to IAC. In particular, IARC provides data that allows IAC to characterize and monitor parameters that determine the astronomical quality of their observatories in the Canary Islands: 1) Teide Observatory (OT), in Tenerife, approximately 1km away from the Izaña Observatory (IZO) of IARC-AEMET and 2) Roque de los Muchachos Observatory (RMO) on the island of La Palma.

IARC provides measurements of aerosol optical depth in different channels, aerosol optical properties and water vapour in the atmospheric column, to IAC, both for OT and RMO, from measurements obtained by sunphotometers enrolled in AERONET installed at IZO and RMO, respectively (Fig. 20.1).



Figure 20.1. The AERONET sunphotometer at Roque de los Muchachos Observatory (RMO), La Palma.

Near-real-time information on column water vapour (precipitable water) is provided from a high-precision GNSS receiver installed at IZO. Real-time PM₁₀ particulate matter data is provided from the PM TEOM analyzer installed at IZO, for operational purposes (Fig. 20.2). This information allows decisions to be made about the operability of the telescopes based on aerosols surface concentration; as above a relatively low threshold, aerosols, and specifically mineral dust, can cause damage to the optics and other mechanical elements of the telescopes.

Airborne Particulate Matter at Izaña

Atmospheric particulate matter 10 micrometers or less in diameter (PM₁₀, $\mu\text{g}/\text{m}^3$) at Izaña.

Average of the hour before. Sensitivity of 2 $\mu\text{g}/\text{m}^3$ (1.9 means PM₁₀×2).

Data obtained and released by the Izaña Atmospheric Research Center (CIAI-AEMet) at the Izaña Atmospheric Observatory (IZO).

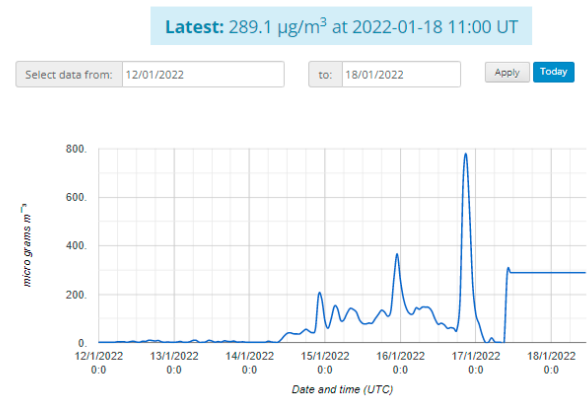


Figure 20.2. IAC Internal web page with PM₁₀ real-time information from the TEOM analyzer at IZO (IARC-AEMET).

In addition, data from the radiosondes launched daily at 00 and 12 UTC from the AEMET Güímar (Tenerife) automatic radiosonde station (WMO GRUAN station, #60018) (Fig. 20.3) are provided to the IAC for both operational and scientific purposes.



Figure 20.3. Image of the AEMET GRUAN automatic radiosonde station in Güímar (Tenerife).

IAC also has real-time access to the images obtained with the all-sky and regular cameras installed at IZO, which show the state of the sky every five minutes. Meteorological information from the automatic meteorological stations installed at IZO and RMO is also provided.

In addition to meteorological and atmospheric observations, AEMET provides specific meteorological forecasts at the two sites (OT and RMO), of geopotential height, temperature, relative humidity, wind, precipitation, cloud cover and mineral dust from the Sahara, which allows IAC to carry out a flexible scheduling of telescope operation. Much of this information is very useful for short- and medium-term planning of observations.

21 Capacity Building Activities

During 2019-2020 IARC participated in various capacity building activities, some of which are described here. For further details of these activities, see individual sections or the IARC [webpage](#).

21.1 8th Training Workshop on Sand and Dust Storms in West and Northern Africa: Dakar, Senegal, 9-11 December 2019

AEMET organised the 8th Training Workshop on Sand and Dust Storms in West and Northern Africa, which was held in Dakar, Senegal on 9-11 December 2019 in collaboration with WMO, BSC-CNS, EUMETSAT and CSIC. The objectives of the workshop were:

- To enhance the understanding of the physical processes involved in the dust cycle
- To examine the impacts of airborne dust on air quality, health, aviation and other socio-economic sectors
- To enhance the technical capacities of operational meteorologists from West and Northern Africa on the analysis and prediction of sand and dust storms, including the use of ground and satellite observations, as well as available dust predictions.

The workshop was attended by 24 participants from 23 northern and western African countries, most of them weather forecasters and climatologists from National Meteorological Services, and with local lecturers' presentations from Burkina Faso, Guinea Bissau, Niger, Nigeria, Senegal and Sudan.



Figure 21.1. Participants of the 8th training workshop on Sand and Dust Storms in West Africa, held in Dakar, Senegal, 9-11 December 2019.

21.2 “Modeling of the chemical composition of the atmosphere”, On-Line AEMET Course, 19-23 October 2020

Dr Natalia Prats (IARC-AEMET) participated in a training course, organized and coordinated by Isabel Martínez Marco, Head of Applications Area (Dept. Development and Applications) in AEMET, entitled: “Modeling of the chemical composition of the atmosphere” held On-Line, during 19-23 October 2020.

During the last decades, authorities related to the environment and health, together with the media and the general public, have shown a growing interest in atmospheric pollution produced by anthropogenic activities and its consequences for the health of people and ecosystems. Air quality predictions have been developed in recent years in an attempt to address those concerns. The meteorological services, among other institutions, have assumed the role of supplier of this information, using air quality or chemical transport models (CTM) as a tool. This course presented the chemical composition of the atmosphere and the models used by AEMET to study its evolution in the short and medium term, as well as the products developed to prepare an air quality prediction.

21.3 “Advances in dust intrusion forecasts and their operational adaptation. Impact on aeronautical operations”, On-Line AEMET Course, 10-12 November 2020

Carlos Marrero and Dr Natalia Prats (IARC-AEMET) participated in a training course, organized and coordinated by David Suárez (AEMET), entitled: “Advances in dust intrusion forecasts and their operational adaptation. Impact on aeronautical operations” held On-Line, during 10-12 November 2020.

The Canary Islands (and the Iberian Peninsula to a lesser extent), due to its geographical location, are affected on numerous occasions throughout the year by dust intrusions. Such events have a great impact on aeronautical operations as well as on airfields. Therefore, predicting these episodes with certainty is essential to minimize their impact. This training course aimed to train staff (mainly focused on predictors) in the prediction of airborne dust events. For this, the dust prediction models and new developments focused on dust prediction, observation and verification tools, etc. were presented. In addition, the results obtained in the characterization of dust intrusions in the Canary Islands were presented.

22 Scientific Communication

The main tool of scientific communication of the IARC is, undoubtedly, its webpage (<http://izana.aemet.es>). Scientific information and articles are regularly posted there. Also, there is a Wikipedia [page](#). In this section, we give details of some of the science communication activities during the 2019-2020 period.

22.1 International Day of Women and Girls in Science: 11 February 2019

At a time when most of the challenges we face (health crisis, energy crisis, environmental crisis, food crisis) depend on Science and Technology, we cannot afford to do without the talent of half the population (<https://11defebrero.org/>). For this reason, the Izaña Atmospheric Research Center joined several activities on 11th and 12th of February 2019 to celebrate the “International Day of Women and Girls in Science”. Researchers from IARC gave several talks explaining the role of women in science and the scientific activities carried out by IARC, bringing our work closer to the young.



Figure 22.1 Dr Natalia Prats, presenting the scientific activities carried out by IARC at the Onésimo Redondo primary school (Santa Cruz de Tenerife), 11 Feb 2019.



Figure 22.2 Dr Omaira García, giving a talk about “Women and Science: What do we do at the Izaña Atmospheric Research Center?” at the Adamancacis primary school (El Paso, La Palma), 11 Feb 2019.

22.2 IV Jornadas de Investigación en Ingeniería Industrial, Informática y Medioambiental (I3MA): 5 April 2019

Dr Omaira García (IARC-AEMET) participated in the “IV Jornadas de Investigación en Ingeniería Industrial, Informática y Medioambiental (I3MA),” (IV Research Meeting on Industrial, Informatic and Environmental Engineering) at the University of La Laguna (Tenerife) on 5 April 2019, giving a talk about the monitoring of atmospheric composition using Fourier Transform Infrared Spectrometry.

22.3 Presentation of results from the MEGEI-MAD project: 9 May 2019

Dr Omaira García (IARC-AEMET) presented the preliminary results from the MEGEI-MAD project during a seminar in Madrid Council facilities on 9 May 2019. For more details of the MEGEI-MAD project see Section 7.3.2.

22.4 Science Week: November 2019

Dr Omaira García (IARC-AEMET) gave a talk about the role of Women in Science at the Montessori primary school, Santa Cruz de Tenerife, November 2019.

22.5 ICOS within COP25 Climate change conference: December 2019

Carmen Rus (AEMET) together with Dr Emilio Cuevas (IARC-AEMET) and Melchor González (Institute of Oceanography and Global Change (IOCAG) of Las Palmas de Gran Canaria University) announced that Spain will join the European Research Infrastructure Integrated Carbon Observation System (ICOS) during its parallel event at the UN Climate change conference COP25, which took place in Madrid in December 2019.



Figure 22.3. Announcement of Spain joining ICOS during its parallel event at COP25, Madrid, December 2019. Left to right: Melchor González (IOCAG), Carmen Rus (AEMET), Werner Kutsch (ICOS) and Emilio Cuevas (IARC-AEMET).

22.6 Teidelab images: 2019-2020

Teidelab is an initiative created between the Teide Cable Car Company and various other institutions, including IARC to produce high quality content that advances and disseminates knowledge about the natural, scientific, cultural and recreational values of Teide National Park. It seeks to facilitate collaboration between different institutions, both those with a direct presence in Teide National Park, as well as those that are particularly relevant to the interests of the Park.

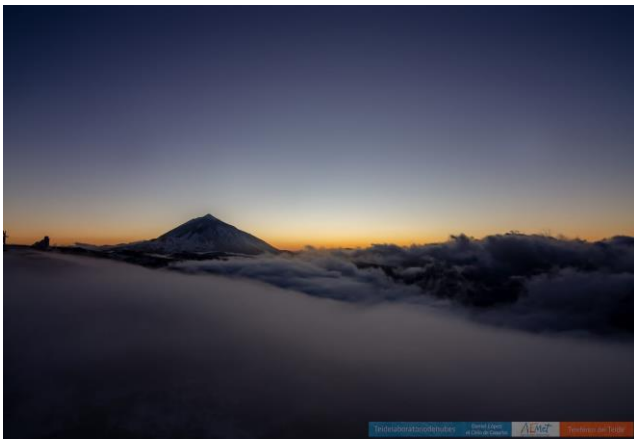


Figure 22.4. Photographic images taken during the “Teide Clouds Laboratory” project from Izaña Observatory by Daniel López.

The “Teide Clouds Laboratory” project, which started in December 2015, is one of four projects within Teidelab. The project is the result of a collaboration between the IARC,

the Teide Cable Car Company, and the renowned Astrophotographer Daniel López, with the main aim of registering meteorological phenomena in Teide National Park using high quality photographic images and high temporal resolution “time-lapse” videos. Cameras have been placed within the main Izaña Observatory technical tower and in a “Cloud Tower” outside the observatory to allow diurnal and nocturnal photographic images to be captured remotely (e.g. Fig. 22.4). A video presentation of the “Teide Clouds Laboratory” project can be found [here](#).

22.7 Field test of the Mars 2020 Rover Mission in terrain analogous to Mars in Teide Peak: September 2020

NASA’s Mars 2020 mission began in July 2020 with the launch from Cape Canaveral (Florida) of the Atlas V rocket with the Perseverance rover in it. The key objectives of this mission are to seek signs of ancient life and gather rocks and soil samples for a possible return to Earth. (It finally landed on Mars in February 2021). On-board, the Mars 2020/Perseverance rover is equipped with seven different instruments specially designed to conduct unprecedented scientific experiments on the Red Planet. In particular, the Mars Environmental Dynamics Analyzer (MEDA) instrument was designed to perform weather measurements including radiation, wind speed and direction, temperature and humidity, and also to measure the amount and size of dust particles in the Martian atmosphere. MEDA is an environmental suite of sensors developed by some research centers and led by the Spanish Centro de Astrobiología (CSIC-INTA) in Madrid.

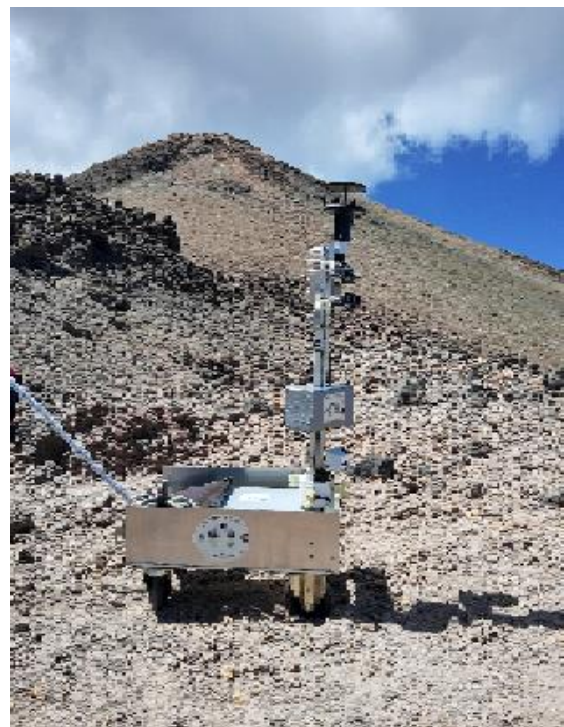


Figure 22.5. MEDA instrument deployed in Fortaleza area (Teide Peak) September 2020.

As a twin experience in a terrestrial analogy of Mars, the MEDA instrument is being tested and verified in the Teide Peak. This experiment began in September 2020 with the deployment of the MEDA sensor in the Fortaleza area, in the Teide Peak (Fig. 22.5), carried out by scientists from the Centro de Astrobiología (CSIC-INTA), Universidad de Alcalá (UAH), Instituto Geográfico Nacional (IGN) and Agencia Española de Meteorología (AEMET), and the technical support of the National Park and Volcano Teide. The MEDA instrument will log the environmental magnitudes at this site until November 2020, which will be compared to routine measurements taken from AEMET's nearby stations such as direct normal irradiance, global radiation, diffuse radiation, aerosol optical depth, Angström exponent for aerosols and meteorological parameters. These measurements will be helpful to verify and understand the atmospheric dynamics and relevant information registered by MEDA on the Red Planet's surface:

23 Publications

23.1 List of peer-reviewed papers

2020

- Almansa, A.F.; Cuevas, E.; Barreto, Á.; Torres, B.; García, O.E.; Delia García, R.; Velasco-Merino, C.; Cachorro, V.E.; Berjón, A.; Mallorquín, M.; López, C.; Ramos, R.; Guirado-Fuentes, C.; Negrillo, R.; de Frutos, Á.M: Column Integrated Water Vapor and Aerosol Load Characterization with the New ZEN-R52 Radiometer, *Remote Sens.* 2020, 12, 1424.
- Barreto, Á.; García, O.E.; Schneider, M.; García, R.D.; Hase, F.; Sepúlveda, E.; Almansa, A.F.; Cuevas, E.; Blumenstock, T. Spectral Aerosol Optical Depth Retrievals by Ground-Based Fourier Transform Infrared Spectrometry. *Remote Sens.* 2020, 12, 3148
- Blumenstock, T., Hase, F., Keens, A., Czurlak, D., Colebatch, O., Garcia, O., Griffith, D. W. T., Grutter, M., Hannigan, J. W., Heikkinen, P., Jeseck, P., Jones, N., Kivi, R., Lutsch, E., Makarova, M., Imhasin, H. Kh., Mellqvist, J., Morino, I., Nagahama, T., Notholt, J., Ortega, I., Palm, M., Raffalski, U., Rettinger, M., Robinson, J., Schneider, M., Servais, C., Smale, D., Stremme, W., Strong, K., Sussmann, R., Té, Y., and Velazco, V. A.: Characterisation and potential for reducing optical resonances in FTIR spectrometers of the Network for the Detection of Atmospheric Composition Change (NDACC), *Atmos. Meas. Tech. Discuss.*, <https://doi.org/10.5194/amt-2020-316>, in review, 2020.
- Collaud Coen, M., Andrews, E., Alastuey, A., Arsov, T. P., Backman, J., Brem, B. T., Bukowiecki, N., Couret, C., Eleftheriadis, K., Flentje, H., Fiebig, M., Gysel-Beer, M., Hand, J. L., Hoffer, A., Hooda, R., Hueglin, C., Joubert, W., Keywood, M., Kim, J. E., Kim, S.-W., Labuschagne, C., Lin, N.-H., Lin, Y., Lund Myhre, C., Luoma, K., Lyamani, H., Marinoni, A., Mayol-Bracero, O. L., Mihalopoulos, N., Pandolfi, M., Prats, N., Prenni, A. J., Putaud, J.-P., Ries, L., Reisen, F., Sellegri, K., Sharma, S., Sheridan, P., Sherman, J. P., Sun, J., Titos, G., Torres, E., Tuch, T., Weller, R., Wiedensohler, A., Zieger, P., and Laj, P.: Multidecadal trend analysis of in situ aerosol radiative properties around the world, *Atmos. Chem. Phys.*, 20, 8867–8908, <https://doi.org/10.5194/acp-20-8867-2020>, 2020..
- Cooper, O.R, Schultz, MG, Schröder, S, Chang, K-L, Gaudel, A, Benítez, GC, Cuevas, E, Fröhlich, M, Galbally, IE, Molloy, S, Kubistin, D, Lu, X, McClure-Begley, A, Nédélec, P, O'Brien, J, Oltmans, SJ, Petropavlovskikh, I, Ries, L, Senik, I, Sjöberg, K, Solberg, S, Spain, GT, Spangl, W, Steinbacher, M, Tarasick, D, Thouret, V and Xu, X. : Multi-decadal surface ozone trends at globally distributed remote locations., *Elem Sci Anth* 2020, 8: 23. DOI: <https://doi.org/10.1525/elementa.420>.
- Dogniaux, M., Crevoisier, C., Armante, R., Capelle, V., Delahaye, T., Cassé, V., De Mazière, M., Deutscher, N. M., Feist, D. G., Garcia, O. E., Griffith, D. W. T., Hase, F., Iraci, L. T., Kivi, R., Morino, I., Notholt, J., Pollard, D. F., Roehl, C. M., Shiomi, K., Strong, K., Té, Y., Velazco, V. A., and Warneke, T.: The Adaptable 4A Inversion (5AI): Description and first XCO₂ retrievals from OCO-2 observations, *Atmos. Meas. Tech. Discuss.*, <https://doi.org/10.5194/amt-2020-403>, in review, 2020.
- Dominguez-Rodriguez, A.; Baez-Ferrer, N.; Rodríguez, S.; Avanzas, P.; Abreu-Gonzalez, P.; Terradellas, E.; Cuevas, E.; Basart, S.; Werner, E. Saharan Dust Events in the Dust Belt - Canary Islands- and the Observed Association with in-Hospital Mortality of Patients with Heart Failure. *J. Clin. Med.* 2020, 9, 376.
- García-Cabrera, R. D., Cuevas-Agulló, E., Barreto, Á., Cachorro, V. E., Pó, M., Ramos, R., and Hoogendijk, K.: Aerosol retrievals from the EKO MS-711 spectral direct irradiance measurements and corrections of the circumsolar radiation, *Atmos. Meas. Tech.*, 13, 2601–2621, <https://doi.org/10.5194/amt-13-2601-2020>, 2020.
- García, O., Schneider, M., Ertl, B., Sepúlveda, E., Borger, C., Diekmann, C., Hase, F., Krosraw, F., Cansado, A., and Allué, M.: Monitoring of atmospheric methane and nitrous oxide concentrations from Metop/IASI. *Revista de Teledetección*, [S.l.], n. 57, p. 1-11, ISSN 1988-8740, [doi:https://doi.org/10.4995/raet.2020.13290](https://doi.org/10.4995/raet.2020.13290), 2020.
- González, R., Toledano, C., Román, R., Fuertes, D., Berjón, A., Mateos, D., Guirado-Fuentes, C., Velasco-Merino, C., Antuña-Sánchez, J. C., Calle, A., Cachorro, V. E., and de Frutos, Á. M.: Daytime and nighttime aerosol optical depth implementation in CÆLIS, *Geosci. Instrum. Method. Data Syst.*, 9, 417–433, <https://doi.org/10.5194/gi-9-417-2020>, 2020.
- Laj, P., Bigi, A., Rose, C., Andrews, E., Lund Myhre, C., Collaud Coen, M., Lin, Y., Wiedensohler, A., Schulz, M., Ogren, J. A., Fiebig, M., Gliß, J., Mortier, A., Pandolfi, M., Petäjä, T., Kim, S.-W., Aas, W., Putaud, J.-P., Mayol-Bracero, O., Keywood, M., Labrador, L., Aalto, P., Ahlberg, E., Alados Arboledas, L., Alastuey, A., Andrade, M., Artíñano, B., Ausmeel, S., Arsov, T., Asmi, E., Backman, J., Baltensperger, U., Bastian, S., Bath, O., Beukes, J. P., Brem, B. T., Bukowiecki, N., Conil, S., Couret, C., Day, D., Dayanitolis, W., Degorska, A., Eleftheriadis, K., Fetzatzis, P., Favez, O., Flentje, H., Gini, M. I., Gregorić, A., Gysel-Beer, M., Hallar, A. G., Hand, J., Hoffer, A., Hueglin, C., Hooda, R. K., Hyvärinen, A., Kalapov, I., Kalivitis, N., Kasper-Giebl, A., Kim, J. E., Kouvarakis, G., Kranjc, I., Krejci, R., Kulmala, M., Labuschagne, C., Lee, H.-J., Lihavainen, H., Lin, N.-H., Löschau, G., Luoma, K., Marinoni, A., Martins Dos Santos, S., Meinhardt, F., Merkel, M., Metzger, J.-M., Mihalopoulos, N., Nguyen, N. A., Ondracek, J., Pérez, N., Perrone, M. R., Petit, J.-E., Picard, D., Pichon, J.-M., Pont, V., Prats, N., Prenni, A., Reisen, F., Romano, S., Sellegri, K., Sharma, S., Schauer, G., Sheridan, P., Sherman, J. P., Schütze, M., Schwerin, A., Sohmer, R., Sorribas, M., Steinbacher, M., Sun, J., Titos, G., Toczko, B., Tuch, T., Tulet, P., Tunved, P., Vakkari, V., Velarde, F., Velazquez, P., Villani, P., Vratolis, S., Wang, S.-H., Weinhold, K., Weller, R., Yela, M., Yus-Diez, J., Zdimal, V., Zieger, P., and Zikova, N.: A global analysis of climate-relevant aerosol properties retrieved from the network of Global Atmosphere Watch (GAW) near-surface observatories, *Atmos. Meas. Tech.*, 13, 4353–4392, <https://doi.org/10.5194/amt-13-4353-2020>, 2020.
- Lakkala, K., Kujanpää, J., Brogniez, C., Henriot, N., Arola, A., Aun, M., Auriol, F., Bais, A. F., Bernhard, G., De Bock, V., Catalfamo, M., Deroo, C., Diémoz, H., Egli, L., Forestier, J.-B., Fountoulakis, I., Garane, K., Garcia, R. D., Gröbner, J., Hassinen, S., Heikkilä, A., Henderson, S., Hülsen, G., Johnsen, B., Kalakoski, N., Karanikolas, A., Karppinen, T., Lamy, K., León-Luis, S. F., Lindfors, A. V., Metzger, J.-M., Minvielle, F., Muskatel, H. B., Portafaix, T., Redondas, A., Sanchez, R., Siani, A. M., Svendby, T., and Tamminen, J.: Validation of the TROPospheric Monitoring Instrument (TROPOMI) surface UV radiation product, *Atmos. Meas. Tech.*, 13, 6999–7024, <https://doi.org/10.5194/amt-13-6999-2020>, 2020.
- Marquis, J. W., Oyola, M.I, Campbell, J.R., Ruston, B.C., Córdoba-Jabonero, C., Cuevas, E., ; Lewis, J.R., Toth, T.D., Zhang, J.: Conceptualizing the Impact of Dust Contaminated

- Infrared Radiances on Data Assimilation for Numerical Weather Prediction, *J. Atmos. Oceanic Technol.*, doi: <https://doi.org/10.1175/JTECH-D-19-0125.1>, 2020.
- Milford, C.; Cuevas, E.; Marrero, C.L.; Bustos, J.; Gallo, V.; Rodríguez, S.; Romero-Campos, P.M.; Torres, C.: Impacts of Desert Dust Outbreaks on Air Quality in Urban Areas, *Atmosphere* 2020, 11, 23. <https://doi.org/10.3390/atmos11010023>.
- Prados-Roman, C., Fernández, M., Gómez-Martín, L., Cuevas, E., Gil-Ojeda, M., Maruszczak, N., Puente-dura, O., Sonke, J.E., Saiz-Lopez, A.: Atmospheric formaldehyde at El Teide and Pic du Midi remote high-altitude sites, *Atmospheric Environment*, doi: <https://doi.org/10.1016/j.atmosenv.2020.117618>, 2020.
- Ramonet, M., P. Ciais, F. Apadula, J. Bartyzel, A. Bastos, P. Bergamaschi, P. E. Blanc, D. Brunner, L. Caracciolo di Torchiolo, F. Calzolari, H. Chen, L. Chmura, A. Colomb, S. Conil, P. Cristofanelli, E. Cuevas, R. Curcoll, M. Delmotte, A. di Sarra, L. Emmenegger, G. Forster, A. Frumau, C. Gerbig, F. Gheusi, S. Hammer, L. Haszpra, J. Hatakka, L. Hazan, M. Heliasz, S. Henne, A. Hensen, O. Hermansen, P. Keronen, R. Kivi, K. Komínková, D. Kubistin, O. Laurent, T. Laurila, J. V. Lavric, I. Lehner, K. E. J. Lehtinen, A. Leskinen, M. Leuenberger, I. Levin, M. Lindauer, M. Lopez, C. Lund Myhre, I. Mammarella, G. Manca, A. Manning, M. V. Marek, P. Marklund, D. Martin, F. Meinhardt, N. Mihalopoulos, M. Mölder, J. A. Morgui, J. Necki, S. O'Doherty, C. O'Dowd, M. Ottosson, C. Philippon, S. Piacentino, J. M. Pichon, C. Plass-Duelmer, A. Resovsky, L. Rivier, X. Rodó, M. K. Sha, H. A. Scheeren, D. Sferlazzo, T. G. Spain, K. M. Stanley, M. Steinbacher, P. Trisolino, A. Vermeulen, G. Vítková, D. Weyrauch, I. Xueref-Remy, K. Yala, and C. Yver Kwok: The fingerprint of the summer 2018 drought in Europe on ground-based atmospheric CO₂ measurements, *Philosophical Transactions of the Royal Society B: Biological Sciences*, Royal Society, The, 375 (1810), pp.20190513. [ff10.1098/rstb.2019.0513](https://doi.org/10.1098/rstb.2019.0513), [ff10.1098/rstb.2019.0513](https://doi.org/10.1098/rstb.2019.0513), [ff10.1098/rstb.2019.0513](https://doi.org/10.1098/rstb.2019.0513), 2020.
- Rodríguez, S., Calzolari, G., Chiari, M., Nava, S., García, M.I., Lopez-Solano, J., Marrero, C., Lopez-Darias, J., Cuevas, E., Alonso-Perez, S., Prats, N., Amato, F., Lucarelli, F., Querol, X.: Rapid changes of dust geochemistry in the Saharan Air Layer linked to sources and meteorology, *Atmospheric Environment*, 223, 2020, <https://doi.org/10.1016/j.atmosenv.2019.117186>.
- Rodríguez, S., Prospero, J.M., López-Darias, J., García-Alvarez, M. I., Zuidema, P., Nava, S., Lucarelli, F., Gaston, C.J., Galindo, L., Sosa, E.: Tracking the changes of iron solubility and air pollutants traces as African dust transits the Atlantic in the Saharan dust outbreaks, *Atmospheric Environment*, 118092, ISSN 1352-2310, <https://doi.org/10.1016/j.atmosenv.2020.118092>, 2020.
- Román, R., González, R., Toledano, C., Barreto, Á., Pérez-Ramírez, D., Benavent-Oltra, J. A., Olmo, F. J., Cachorro, V. E., Alados-Arboledas, L., and de Frutos, Á. M.: Correction of a lunar-irradiance model for aerosol optical depth retrieval and comparison with a star photometer, *Atmos. Meas. Tech.*, 13, 6293–6310, <https://doi.org/10.5194/amt-13-6293-2020>, 2020.
- Steinbrecht, W., Kubistin, D., Plass-Dulmer, C., Tarasick, D.W., Davies, J., Gathen, P.V., Deckelmann, H., Jepsen, N., Kivi, R., Lyall, N., Palm, M., Notholt, J., Kois, B., Oelsner, P., Allaart, M., Piter, A., Gill, M., Malderen, R.V., Delcloo, A.W., Sussmann, R., Mahieu, E., Servais, C., Romanens, G., Stubi, R., Ancellet, G., Godin-Beekmann, S., Yamanouchi, S., Strong, K., Johnson, B., Cullis, P., Petropavlovskikh, I., Hannigan, J., Hernandez, J.L., Rodriguez, A.D., Nakano, T., Chouza, F., Leblanc, T., Torres, C., Garcia, O., Rohling, A., Schneider, M., Blumenstock, T., Tully, M., Jones, N., Querel, R., Strahan, S., Inness, A., Engelen, R., Chan, K.L., Cooper, O.R., Stauffer, R.M., Thompson, A.M., Did the COVID-19 Crisis Reduce Free Tropospheric Ozone across the Northern Hemisphere?, *Earth and Space Science Open Archive*, 20, doi:10.1002/essoar.10505226.1, <https://doi.org/10.1002/essoar.10505226.1>, 2020.

2019

- Adame J.A., Cupeiro M., Yela M., Cuevas E., Carbajal G.: Ozone and carbon monoxide at the Ushuaia GAW-WMO global station, *Atmospheric Research*, 217, 1-9, 2019.
- Baez-Ferrer, N., Dominguez Rodriguez, A., Hernandez-Vaquero, D., Rodriguez, S., Avanzas, P., Abreu-Gonzalez, P., and Cuevas, E.: P3420 Is there an association between Saharan dust events and acute coronary syndrome incidence?, *European Heart Journal*, 40(Supplement_1), ehz745-0294, 2019.
- Barreto, A., R. Román, E. Cuevas, D. Pérez-Ramírez, A.J. Berjón, N. Kouremeti, S. Kazadzis, J. Gröbner, M. Mazzola, C. Toledano, J.A. Benavent-Oltra, L. Doppler, J. Juryšek, A.F. Almansa, S. Victori, F. Maupin, C. Guirado-Fuentes, R. González, V. Vitale, P. Goloub, L. Blarel, L. Alados-Arboledas, E. Woolliams, S. Taylor, J.C. Antuña, M. Yela: Evaluation of night-time aerosols measurements and lunar irradiance models in the frame of the first multi-instrument nocturnal intercomparison campaign, *Atmospheric Environment*, Volume 202, 2019, Pages 190-211, ISSN 1352-2310, <https://doi.org/10.1016/j.atmosenv.2019.01.006>
- Benavent-Oltra, J. A., Román, R., Casquero-Vera, J. A., Pérez-Ramírez, D., Lyamani, H., Ortiz-Amezcu, P., Bedoya-Velásquez, A. E., de Arruda Moreira, G., Barreto, Á., Lopatin, A., Fuertes, D., Herrera, M., Torres, B., Dubovik, O., Guerrero-Rascado, J. L., Goloub, P., Olmo-Reyes, F. J., and Alados-Arboledas, L.: Different strategies to retrieve aerosol properties at night-time with the GRASP algorithm, *Atmos. Chem. Phys.*, 19, 14149–14171, <https://doi.org/10.5194/acp-19-14149-2019>, 2019
- Berjón, A., Barreto, A., Hernández, Y., Yela, M., Toledano, C., and Cuevas, E.: A 10-year characterization of the Saharan Air Layer lidar ratio in the subtropical North Atlantic, *Atmos. Chem. Phys.*, 19, 6331-6349, <https://doi.org/10.5194/acp-19-6331-2019>, 2019.
- Che, H., Xia, X., Zhao, H., Dubovik, O., Holben, B. N., Goloub, P., Cuevas-Agulló, E., Estelles, V., Wang, Y., Zhu, J., Qi, B., Gong, W., Yang, H., Zhang, R., Yang, L., Chen, J., Wang, H., Zheng, Y., Gui, K., Zhang, X., and Zhang, X.: Spatial distribution of aerosol microphysical and optical properties and direct radiative effect from the China Aerosol Remote Sensing Network, *Atmos. Chem. Phys. Discuss.*, <https://doi.org/10.5194/acp-2019-405>, in review, 2019.
- Che, H., Gui, K., Xia, X., Wang, Y., Holben, B. N., Goloub, P., Cuevas-Agulló, E., Wang, H., Zheng, Y., Zhao, H., and Zhang, X.: Large contribution of meteorological factors to inter-decadal changes in regional aerosol optical depth, *Atmos. Chem. Phys.*, 19, 10497–10523, <https://doi.org/10.5194/acp-19-10497-2019>, 2019.
- Cuevas, E., Romero-Campos, P. M., Kouremeti, N., Kazadzis, S., Räisänen, P., García, R. D., Barreto, A., Guirado-Fuentes, C., Ramos, R., Toledano, C., Almansa, F., and Gröbner, J.: Aerosol optical depth comparison between GAW-PFR and AERONET-Cimel radiometers from long-term (2005–2015) 1 min synchronous measurements, *Atmos. Meas. Tech.*, 12, 4309–4337, <https://doi.org/10.5194/amt-12-4309-2019>, 2019.

- Domínguez Rodríguez, A., Baez-Ferrer, N., Rodríguez, S., Abreu-González, P., González-Colaço Harmand, M., Amarnani-Amarnani, V., Cuevas, E., Consuegra-Sánchez, L., Alonso-Pérez, S., Avanzas, P., Burillo Putze, G.: Impacto de la exposición a la calima del polvo del Sáhara en los pacientes con insuficiencia cardíaca aguda atendidos en un servicio de urgencias, *Emergencias*, 31, 161-166, 2019.
- Frey, M., Sha, M. K., Hase, F., Kiel, M., Blumenstock, T., Harig, R., Surawicz, G., Deutscher, N. M., Shiomi, K., Franklin, J. E., Bösch, H., Chen, J., Grutter, M., Ohyama, H., Sun, Y., Butz, A., Mengistu Tsidu, G., Ene, D., Wunch, D., Cao, Z., García, O., Ramonet, M., Vogel, F., and Orphal, J.: Building the Collaborative Carbon Column Observing Network (COCCON): long-term stability and ensemble performance of the EM27/SUN Fourier transform spectrometer, *Atmos. Meas. Tech.*, 12, 1513-1530, <https://doi.org/10.5194/amt-12-1513-2019>.
- Garane, K., Koukoulis, M.-E., Verhoelst, T., Lerot, C., Heue, K.-P., Fioletov, V., Bais, A., Balis, D., Bazureau, A., Dehn, A., Goutail, F., Granville, J., Griffin, D., Hubert, D., Keppens, A., Lambert, J.-C., Loyola, D., Mclinden, C., Pazmino, A., Pommereau, J.-P., Redondas, A., Romahn, F., Valks, P., Roozendaal, M.V., Xu, J., Zehner, C., Zerefos, C., Zimmer, W.: TROPOMI/S5P total ozone column data: global ground-based validation and consistency with other satellite missions. *Atmospheric Measurement Techniques*, 12(10) 5263-5287, DOI: 10.5194/amt-12-5263-2019, 2019.
- García-Cabrera, R. D., Cuevas-Agulló, E., Barreto, Á., Cachorro, V. E., Pó, M., Ramos, R., and Hoogendijk, K.: Characterization of an EKO MS-711 spectroradiometer: aerosol retrieval from spectral direct irradiance measurements and corrections of the circumsolar radiation, *Atmos. Meas. Tech. Discuss.*, <https://doi.org/10.5194/amt-2019-467>, 2019.
- García, R. D., Cuevas, E., Ramos, R., Cachorro, V. E., Redondas, A., and Moreno-Ruiz, J. A.: Description of the Baseline Surface Radiation Network (BSRN) station at the Izaña Observatory (2009–2017): measurements and quality control/assurance procedures, *Geosci. Instrum. Method. Data Syst.*, 8, 77-96, <https://doi.org/10.5194/gi-8-77-2019>, 2019.
- Gomez-Pelaez, A. J., Ramos, R., Cuevas, E., Gomez-Trueba, V., and Reyes, E.: Atmospheric CO₂, CH₄, and CO with the CRDS technique at the Izaña Global GAW station: instrumental tests, developments, and first measurement results, *Atmos. Meas. Tech.*, 12, 2043-2066, <https://doi.org/10.5194/amt-12-2043-2019>, 2019.
- Kulawik, S. S., Crowell, S., Baker, D., Liu, J., McKain, K., Sweeney, C., Biraud, S. C., Wofsy, S., O'Dell, C. W., Wennberg, P. O., Wunch, D., Roehl, C. M., Deutscher, N. M., Kiel, M., Griffith, D. W. T., Velasco, V. A., Notholt, J., Warneke, T., Petri, C., De Mazière, M., Sha, M. K., Sussmann, R., Rettinger, M., Pollard, D. F., Morino, I., Uchino, O., Hase, F., Feist, D. G., Roche, S., Strong, K., Kivi, R., Iraci, L., Shiomi, K., Dubey, M. K., Sepulveda, E., Rodriguez, O. E. G., Té, Y., Jeseck, P., Heikkinen, P., Dlugokencky, E. J., Gunson, M. R., Eldering, A., Crisp, D., Fisher, B., and Osterman, G. B.: Characterization of OCO-2 and ACOS-GOSAT biases and errors for CO₂ flux estimates, *Atmos. Meas. Tech. Discuss.*, <https://doi.org/10.5194/amt-2019-257>, in review, 2019.
- Tarasick, D., Galbally, I.E., Cooper, O.R., Schultz, M.G., Ancellet, G., Leblanc, T., Wallington, T.J., Ziemke, J., Liu, X., Steinbacher, M., Staehelin, J., Vigouroux, C., Hannigan, J.W., García, O., Foret, G., Zanis, P., Weatherhead, E., Petropavlovskikh, I., Worden, H., Osman, M., Liu, J., Chang, K.-L., Gaudel, A., Lin, M., Granados-Muñoz, M., Thompson, A.M., Oltmans, S.J., Cuesta, J., Dufour, G., Thouret, V., Hassler, B., Trickl, T. and Neu, J.L., 2019. Tropospheric Ozone Assessment Report: Tropospheric ozone from 1877 to 2016, observed levels, trends and uncertainties. *Elem Sci Anth*, 7(1), p.39. DOI: <http://doi.org/10.1525/elementa.376>, 2019.
- Tsuruta, A., Aalto, T., Backman, L., Krol, M.C., Peters, W., Lienert, S., Joos, F., Miller, P.A. Zhang, W., Laurila, T., Hatakka, J., Leskinen, A., Lehtinen, K.E.J., Peltola, O., Vesala, T., Levula, J., Dlugokencky, E., Heimann, M., Kozlova, E., Aurela, M., Lohila, A., Kauhaniemi, M., and Gomez-Pelaez, A.J.: Methane budget estimates in Finland from the CarbonTracker Europe-CH4 data assimilation system, *Tellus B: Chemical and Physical Meteorology*, DOI: 10.1080/16000889.2018.1565030, 2019.
- Wei, Z., X. Lee, F. Aemisegger, M. Benetti, M. Berkelhammer, M. Casado, K. Caylor, E. Christner, C. Dyroff, O. García, Y. González, T. Griffis, N. Kurita, J. Liang, M.-C. Liang, G. Lin, D. Noone, K. Gribanov, N. C. Munksgaard, M. Schneider, F. Ritter, H. C. Steen-Larsen, C. Vallet-Coulomb, X. Wen, J. S. Wright, W. Xiao, and K. Yoshimura: A global database of water vapor isotopes measured with high temporal resolution infrared laser spectroscopy, *Scientific Data* volume6, Article number: 180302, doi.org/10.1038/sdata.2018.302, 2019.
- Zhou, M., Langerock, B., Vigouroux, C., Sha, M. K., Hermans, C., Metzger, J.-M., Chen, H., Ramonet, M., Kivi, R., Heikkinen, P., Smale, D., Pollard, D. F., Jones, N., Velasco, V. A., García, O. E., Schneider, M., Palm, M., Warneke, T., and De Mazière, M.: TCCON and NDACC XCO measurements: difference, discussion and application, *Atmos. Meas. Tech.*, 12, 5979–5995, <https://doi.org/10.5194/amt-12-5979-2019>, 2019.

23.2 List of peer-reviewed papers that use IARC data

The following references are studies that use IARC data but do not include IARC-AEMET in the co-authorship.

2020

- Feng, C., Zhang, X., Wei, Y., Zhang, W., Hou, N., Xu, J., Kun, J., Yunjun, Y., Xianhong, X. Bo J., Jie C. and Zhao, X. Estimating surface downward longwave radiation using machine learning methods. *Atmosphere*, 11(11), 1147, <https://doi.org/10.3390/atmos11111147>, 2020.
- Fernández-Peruchena, C.M., Polo, J., Martín, L., Mazorra, L. Site-Adaptation of Modeled Solar Radiation Data: The SiteAdapt Procedure. *Remote Sens.*, 12, 2127. <https://doi.org/10.3390/rs12132127>, 2020.
- Franco, B., Clarisse, L., Stavrou, T., Müller, J.-F., Taraborrelli, D., Hadji-Lazaro, J., Hannigan, J.W., Hase, F., Hurtmans, D., Jones, N., Lutsch, E., Mahieu, E., Ortega, I., Schneider, M., Strong, K., Vigouroux, C., Clerbaux, C., and Coheur, P.-F., Spaceborne measurements of formic and acetic acids: A global view of the regional sources. *Geophysical Research Letters*, 47, e2019GL086239. <https://doi.org/10.1029/2019GL086239>, 2020.
- Massie, S. T., Cronk, H., Merrelli, A., O'Dell, C., Schmidt, K. S., Chen, H., and Baker, D.: Analysis of 3D cloud effects in OCO-2 XCO₂ retrievals, *Atmos. Meas. Tech. Discuss.*, <https://doi.org/10.5194/amt-2020-366>, 2020.
- Nalli, N.R.; Tan, C.; Warner, J.; Divakarla, M.; Gambacorta, A.; Wilson, M.; Zhu, T.; Wang, T.; Wei, Z.; Pryor, K.; Kalluri, S.; Zhou, L.; Sweeney, C.; Baier, B.C.; McKain, K.; Wunch, D.; Deutscher, N.M.; Hase, F.; Iraci, L.T.; Kivi, R.; Morino, I.; Notholt, J.; Ohyama, H.; Pollard, D.F.; Té, Y.; Velasco, V.A.;

- Warneke, T.; Sussmann, R.; Rettinger, M. Validation of Carbon Trace Gas Profile Retrievals from the NOAA-Unique Combined Atmospheric Processing System for the Cross-Track Infrared Sounder. *Remote Sens.*, **12**, 3245. <https://doi.org/10.3390/rs12193245>, 2020.
- Oshio, H.; Yoshida, Y.; Matsunaga, T.; Deutscher, N.M.; Dubey, M.; Griffith, D.W.T.; Hase, F.; Iraci, L.T.; Kivi, R.; Liu, C.; Morino, I.; Notholt, J.; Oh, Y.-S.; Ohyama, H.; Petri, C.; Pollard, D.F.; Roehl, C.; Shiomi, K.; Sussmann, R.; Té, Y.; Velazco, V.A.; Warneke, T.; Wunch, D. Bias Correction of the Ratio of Total Column CH₄ to CO₂ Retrieved from GOSAT Spectra. *Remote Sens.*, **12**, 3155. <https://doi.org/10.3390/rs12193155>, 2020.
- Pinardi, G., Van Roozendaal, M., Hendrick, F., Theys, N., Abuhassan, N., Bais, A., Boersma, F., Cede, A., Chong, J., Donner, S., Drosoglou, T., Dzhola, A., Eskes, H., Frieß, U., Granville, J., Herman, J. R., Holla, R., Hovila, J., Irie, H., Kanaya, Y., Karagkiozidis, D., Kouremeti, N., Lambert, J.-C., Ma, J., Peters, E., Pithers, A., Postlyakov, O., Richter, A., Remmers, J., Takashima, H., Tiefengraber, M., Valks, P., Vlemmix, T., Wagner, T., and Wittrock, F.: Validation of tropospheric NO₂ column measurements of GOME-2A and OMI using MAX-DOAS and direct sun network observations, *Atmos. Meas. Tech.*, **13**, 6141–6174, <https://doi.org/10.5194/amt-13-6141-2020>, 2020.
- Schneider, A., Borsdorff, T., van de Brugh, J., Aemisegger, F., Feist, D. G., Kivi, R., Hase, F., Schneider, M., and Landgraf, J.: First data set of H₂O/HDO columns from the Tropospheric Monitoring Instrument (TROPOMI), *Atmos. Meas. Tech.*, **13**, 85–100, <https://doi.org/10.5194/amt-13-85-2020>, 2020.
- Strahan, S. E., Smale, D., Douglass, A. R., Blumenstock, T., Hannigan, J. W., Hase, F., Jones, N., Mahieu, E., Notholt, J., Oman, L.D., Ortega, I., Palm, M., Prignon, M., Robinson, J., Schneider, M., Sussmann, R. and Velazco, V.A. Observed hemispheric asymmetry in stratospheric transport trends from 1994 to 2018. *Geophysical Research Letters*, **47**, <https://doi.org/10.1029/2020GL088567>, 2020.
- Vigouroux, C., Langerock, B., Bauer Aquino, C. A., Blumenstock, T., Cheng, Z., De Mazière, M., De Smedt, I., Grutter, M., Hannigan, J. W., Jones, N., Kivi, R., Loyola, D., Lutsch, E., Mahieu, E., Makarova, M., Metzger, J.-M., Morino, I., Murata, I., Nagahama, T., Notholt, J., Ortega, I., Palm, M., Pinardi, G., Röhl, A., Smale, D., Stremme, W., Strong, K., Sussmann, R., Té, Y., van Roozendaal, M., Wang, P., and Winkler, H.: TROPOMI–Sentinel-5 Precursor formaldehyde validation using an extensive network of ground-based Fourier-transform infrared stations, *Atmos. Meas. Tech.*, **13**, 3751–3767, <https://doi.org/10.5194/amt-13-3751-2020>, 2020.
- Zhang, Y., Jacob, D. J., Lu, X., Maasakkers, J. D., Scarpelli, T. R., Sheng, J.-X., Shen, L., Qu, Z., Sulprizio, M. P., Chang, J., Bloom, A. A., Ma, S., Worden, J., Parker, R. J., and Boesch, H.: Attribution of the accelerating increase in atmospheric methane during 2010–2018 by inverse analysis of GOSAT observations, *Atmos. Chem. Phys. Discuss.*, <https://doi.org/10.5194/acp-2020-964>, 2020.
- 2019**
- Gröbner, J. and Kouremeti, N.: The Precision Solar Spectroradiometer (PSR) for direct solar irradiance measurements, *Solar Energy*, **185**, 199–210, <https://doi.org/10.1016/j.solener.2019.04.060>, 2019.
- Hedelius, J. K., He, T.-L., Jones, D. B. A., Baier, B. C., Buchholz, R. R., De Mazière, M., Deutscher, N. M., Dubey, M. K., Feist, D. G., Griffith, D. W. T., Hase, F., Iraci, L. T., Jeseck, P., Kiel, M., Kivi, R., Liu, C., Morino, I., Notholt, J., Oh, Y.-S., Ohyama, H., Pollard, D. F., Rettinger, M., Roche, S., Roehl, C. M., Schneider, M., Shiomi, K., Strong, K., Sussmann, R., Sweeney, C., Té, Y., Uchino, O., Velazco, V. A., Wang, W., Warneke, T., Wennberg, P. O., Worden, H. M., and Wunch, D.: Evaluation of MOPITT Version 7 joint TIR–NIR XCO retrievals with TCCON, *Atmos. Meas. Tech.*, **12**, 5547–5572, <https://doi.org/10.5194/amt-12-5547-2019>, 2019.
- Kivimäki, E.; Lindqvist, H.; Hakkarainen, J.; Laine, M.; Sussmann, R.; Tsuruta, A.; Detmers, R.; Deutscher, N.M.; Dlugokencky, E.J.; Hase, F.; Hasekamp, O.; Kivi, R.; Morino, I.; Notholt, J.; Pollard, D.F.; Roehl, C.; Schneider, M.; Sha, M.K.; Velazco, V.A.; Warneke, T.; Wunch, D.; Yoshida, Y.; Tamminen, J. Evaluation and Analysis of the Seasonal Cycle and Variability of the Trend from GOSAT Methane Retrievals. *Remote Sens.* **11**, 882. <https://doi.org/10.3390/rs11070882>, 2019.
- Renner, M., Wild, M., Schwarz, M., and Kleidon, A. Estimating Shortwave Clear-Sky Fluxes From Hourly Global Radiation Records by Quantile Regression. *Earth and Space Science*, **6**, 1532–1546. <https://doi.org/10.1029/2019EA000686>, 2019.
- Tang, W., Yang, K., Qin, J., Li, X., and Niu, X. A 16-year dataset (2000–2015) of high-resolution (3 h, 10 km) global surface solar radiation, *Earth Syst. Sci. Data*, **11**, 1905–1915, <https://doi.org/10.5194/essd-11-1905-2019>, 2019.
- Zhang, T., Stackhouse, P. W., Cox, S. J., Mikovitz, J. C., and Long, C. N. Clear-Sky Shortwave Downward Flux at the Earth's Surface: Ground-Based Data vs. Satellite-Based Data. *Journal of quantitative spectroscopy & radiative transfer*, **224**, 247–260. <https://doi.org/10.1016/j.jqsrt.2018.11.015>, 2019.
- Zhou, M., Langerock, B., Wells, K. C., Millet, D. B., Vigouroux, C., Sha, M. K., Hermans, C., Metzger, J.-M., Kivi, R., Heikkinen, P., Smale, D., Pollard, D. F., Jones, N., Deutscher, N. M., Blumenstock, T., Schneider, M., Palm, M., Notholt, J., Hannigan, J. W., and De Mazière, M.: An intercomparison of total column-averaged nitrous oxide between ground-based FTIR TCCON and NDACC measurements at seven sites and comparisons with the GEOS-Chem model, *Atmos. Meas. Tech.*, **12**, 1393–1408, <https://doi.org/10.5194/amt-12-1393-2019>, 2019.

23.3 Conference Presentations/Posters

2020

- Barreto, A., Román, R., Prats, N., Lopatin, A., Fuertes, D., Berjón, A. J., Almansa, F., Cuevas, E., Yela, M. Aerosol Profiles From MPL-Lidar And Photometric Measurements Using GRASP In A Subtropical North Atlantic Site. Evaluation with In-Situ Data, European Lidar Conference (online), 18-20 November 2020.
- Barreto, A. Cimels developments in the Arctic, 4th Lunar workshop, Ny-Alesund (Svalbard), February 2020.
- Garane, K., Koukouli, M.-E., Verhoelst, T., Lerot, C., Heue, K.-P., Balis, D., Redondas, A., Pazmino, A., Bazureau, A., Romahn, F., Zimmer, W., Xu, J., Lambert, J.-C., Loyola, D., Van Roozendaal, M., Goutail, F., Pommereau, J.-P.: 2.5 years of TROPOMI SSP total ozone column data: geophysical global ground-based validation and inter-comparison with other satellite missions. EGU General Assembly Conference Abstracts, 8109, 2020.
- García, O., E. Sepúlveda, M. Schneider, F. Hase, T. Blumenstock, Groß, J., Röhl, A., León-Luis, S.F., Carreño, V., Izaña site

- report, 2020 Joint NDACC-IRWG and TCCON Meeting, online meeting, 12-14 May 2020.
- Milford, C., Cuevas, E., Marrero, C., Bustos, J.J., Torres, C., Trends in air quality, Santa Cruz de Tenerife (Canary Islands), 12th International Conference on Air Quality – Science and Application, Online Conference, Hosted by Aristotle University, Thessaloniki, Greece, 18-22 May 2020.
- Schneider, M., Diekmann, C., Ertl, B., Khosrawi, F., Röhling A., Hase, F., García, O.E., Sepúlveda, E., Landgraf, J., Meinhardt, F., Steinbacher, M., Synergetic use TROPOMI and IASI for generating a tropospheric CH₄ product, 16th international workshop on greenhouse gas measurements from space, online meeting, 2-5 June 2020.
- Sha, M.K., Bavo Langerock, M. De Mazière, Minqiang Zhou, Yang Yang, D. G. Feist, R. Sussmann, F. Hase, M. Schneider, T. Blumenstock, J. Notholt, T. Warneke, C. Petri, R. Kivi, Y. Té, P. O. Wennberg, D. Wunch, L. Iraci, K. Strong, D. W. T. Griffith, N.M. Deutscher, V. Velazco, I. Morino, H. Ohyama, O. Uchino, K. Shiomi, T. Y. Goo, D. F. Pollard, Pucui Wang, T. Borsdorff, H. Hu, O. Hasekamp, J. Landgraf, C. Roehl, M. Kiel, G. Toon, TCCON team & NDACC-IRWG team, Validation results of S-5P methane and carbon monoxide products using TCCON and NDACC-IRWG data, 2020 Joint NDACC-IRWG and TCCON Meeting, online meeting, 12-14 May 2020.
- Sha, M.K., Bavo Langerock, Martine De Mazière, Dietrich G. Feist, Ralf Sussmann, Frank Hase, Matthias Schneider, Thomas Blumenstock, Justus Notholt, Thorsten Warneke, Rigel Kivi, Yao Té, Paul O. Wennberg, Debra Wunch, Laura Iraci, Kimberly Strong, David W. T. Griffith, Nicholas M. Deutscher, Voltaire Velazco, Isamu Morino, Hirofumi Ohyama, Osamu Uchino, Kei Shiomi, Tae-Young Goo, David F. Pollard, Minqiang Zhou, Yang Yang, Pucui Wang, Alba Lorente, Haili Hu, Tobias Borsdorff, Otto Hasekamp, Jochen Landgraf, Coleen Roehl, Matthäus Kiel, Geoffrey Toon and TCCON and NDACC-IRWG team, Lessons learned from 2.5 years of Sentinel-5P methane validation using global TCCON and NDACC-IRWG data, 16th international workshop on greenhouse gas measurements from space, online meeting, 2-5 June 2020.
- Taylor, S., Adriaensen, S., Toledano, C., Berjón, A., Barreto, A., Woolliams, E., Garcia-Miranda, M., Bouvet, M. LIME: Lunar Irradiance Model of ESA, 3rd Joint GSICS/IVOS Lunar Calibration Workshop, Darmstadt (Germany), 16-19 November 2020.
- ## 2019
- Adriaensen, S., Bouvet, M., Woolliams, E., Greenwell, C., Garcia-Miranda, M., Toledano, C., Berjón, A., Barreto, A. Lunar irradiance measurement and modelling for absolute radiometric calibration of EO sensors, GSICS Annual Meeting 2019, Frascati (Italy), 4-8 March 2019.
- Barreto, A., Toledano, C., Berjón, A. J., Adriaensen, S., Wooloams, E., Greenwell, C., García-Miranda, M., Bouvet, M. Lunar spectral irradiance measurements and modelling for absolute radiometric calibration of EO sensors, 3rd Lunar workshop, Connecticut (USA), 14-17 May 2019.
- Barreto, A., E. Cuevas, J. Carrillo, A. Berjón, C. Guirado-Fuentes, Y. Hernández, J. C. Guerra, M. Yela, N. Prats, Vertical characterization of the Saharan Air Layer using MPL and radiosondes at a subtropical site, Geophysical Research Abstracts Vol. 21, EGU2019-16592, EGU General Assembly, Vienna (Austria), 7-12 April 2019.
- Cuevas, E., Barreto, A., Carrillo, J., Berjón, A., Guirado-Fuentes, C., Hernández, Y., Guerra, J. C., Yela, M. Vertical characterization of the Saharan Air Layer using MPL and radiosondes at a subtropical site, EGU General Assembly, Vienna (Austria), 7-12 April 2019.
- Darko Dubravica, Matthias Frey, Frank Hase, Thomas Blumenstock, Johannes Orphal, and the COCCON team, The Collaborative Carbon Column Observing Network (COCCON): Current status, Geophysical Research Abstracts Vol. 21, EGU2019-9754, EGU General Assembly, Vienna (Austria), 7-12 April, 2019.
- Frey, M., Hase, F., Blumenstock, T., Orphal, J., Vogel, F., Staufer, J., Broquet, G., Ciaia, P., Xueref-Remy, I., Chelin, P., Te, Y., García, O., Sepúlveda, E., Ramos, R., Torres, C., Leon, S., Cuevas, E., Butz, A., Schneider, C., and the COCCON Paris team, The COCCON city campaigns: Monitoring greenhouse gas emissions of Paris and Madrid, Geophysical Research Abstracts Vol. 21, EGU2019-5197, EGU General Assembly, Vienna (Austria), 7-12 April 2019.
- Frey, M., Hase, F., Darko Dubravica, Thomas Blumenstock, Mahesh K. Sha, Matthäus Kiel, Roland Harig, Gregor Surawicz, Nicholas M. Deutscher, Kei Shiomi, Jonathan E. Franklin, Hartmut Bösch, Jia Chen, Michel Grutter, Hirofumi Ohyama, Youwen Sun, Zhensong Cao, Andre Butz, Gizaw Mengistu Tsidu, Dragos Ene, Debra Wunch, Omaira Garcia, Michel Ramonet, Felix Vogel and Johannes Orphal, The Collaborative Carbon Column Observing Network (COCCON): overview and current status, 15th International Workshop on Greenhouse Gas Measurements from Space (IWGGMS-15), Sapporo (Japan), 3-5 June 2019.
- García-Cabrera, R.D., Cuevas, E., Barreto, A., Ramos, R., Bayo, C., Arbelo, M., Cachorro, V., López, C., Yela, M., Atenuación de la irradiancia directa espectral debida a la presencia de cirros en el Observatorio de Izaña, XVIII Congreso de la Asociación Española de Teledetección, Valladolid (Spain), 24-27 September 2019.
- García, O., J.-A. Morgui, R. Curcoll, C. Estruch, E. Sepúlveda, R. Ramos, E. Cuevas, Characterizing methane emissions in Madrid City within the MEGE-MAD project: the temporal and spatial ground-based mobile approach, 8th International Symposium on Non-CO₂ Greenhouse Gases (NCGG8), Amsterdam (The Netherlands), June 12-14 2019.
- García, O., Schneider, M., Ertl, B., Sepúlveda, E., Borger, C., Diekmann, C., Wiegeler, A., Hase, F., Barthlott, S., Blumenstock, T., Raffalski, U., Gómez-Peláez, A., Steinbacher, M., Ries, L., Monitorización Global de los Gases de Efecto Invernadero Metano y Óxido Nitroso a partir del Metop/IASI, XVIII Congreso de la Asociación Española de Teledetección, Valladolid (Spain), 24-27 September 2019.
- García, O., M. Schneider, E. Sepúlveda, F. Hase, T. Blumenstock, E. Cuevas, A.J. Gómez-Peláez, R.D. García, E. Reyes, R. Ramos, A. Redondas, V. Carreño, S.F. León-Luis, P.M. Romero-Campos, M. Navarro, M. Yela, 20 years of Fourier Transform Spectrometry at the Izaña Atmospheric Observatory, 2019 Joint NDACC-IRWG and TCCON Meeting, Wanaka, New Zealand, 20-24 May 2019.
- García, O., E. Sepúlveda, J.-A. Morgui, C. Estruch, R. Curcoll, M. Frey, C. Schneider, R. Ramos, C. Torres, S.F. León-Luis, F. Hase, A. Butz, C. Toledano, E. Cuevas, T. Blumenstock, C. Marrero, J.J. Bustos, J. López-Solano, V. Carreño, C. Pérez García-Pando, M. Guevara, O. Jorba, Monitoring of Urban Greenhouse Gases Emissions combining COCCON EM27 spectrometers and in-situ records (MEGEI-MAD), 2019 Joint

- NDACC-IRWG and TCCON Meeting, Wanaka, New Zealand, 20th-24th May 2019.
- García, O., Sepúlveda, E., Morgui, J.A., Frey, M., Schneider, C., Curcoll, R., Estruch, C., Ramos, R., Torres, C., León, S., Hase, F., Butz, A., Toledano, C., Cuevas, E., Blumenstock, T., Pérez, C., Guevara, M., Jorba, O., Marrero, C., Bustos, J.J., López-Solano, J., Romero-Campos, P.M., Medida de las Concentraciones de Gases de Efecto Invernadero en Madrid (MEGEI-MAD), XVIII Congreso de la Asociación Española de Teledetección, Valladolid (Spain), 24-27 September 2019.
- García, O., E. Sepúlveda, M. Schneider, F. Hase, T. Blumenstock, Izaña site report, 2019 Joint NDACC-IRWG and TCCON Meeting, Wanaka, New Zealand, 20th-24th May 2019.
- Hase, F., Carlos Alberti, Dimitrios Balis, Caroline Bes, Thomas Blumenstock, Hartmut Boesch, André Butz, Zhensong Cao, Paolo Castracane, Jia Chen, Alexandru Dandoci, Nicholas M. Deutscher, Angelika Dehn, Florian Dietrich, Manvendra Krishna Dubey, Darko Dubravica, Dragos Ene, Matthias Frey, Jonathan Franklin, Omaira Garcia, David W. T. Griffith, Michel Grutter, Pauli Heikkinen, Sander Houweling, Niki Jacobs, Ralph Kleinscheck, Marvin Knapp, Matthäus Kiel, Morgan Lopez, Rigel Kivi, Maria Makarova, Gizaw Mengistu Tsidu, Marios Mermigkas, Isamu Morino, Nicholas Jones, Hirofumi Ohyama, Paul Palmer, Dave Pollard, Uwe Raffalski, Michel Ramonet, E. Sepulveda, Mahesh Kumar Sha, Kei Shiomi, William R. Simpson, Wolfgang Stremme, Youwen Sun, Yao Té, Qiansi Tu, Johannes Orphal, Felix Vogel, Thorsten Warneke, Steven C. Wofsy, Debra Wunch, Vyacheslav Zakharov, The Collaborative Carbon Column Observing Network (COCCON): status and perspective, ESA S5P Validation Team Meeting, Frascati (Italy), 12 November 2019.
- Kulawik, S.S., Sean Crowell, David Baker, Junjie Liu, Kathryn McKain, Colm Sweeney, Sebastien C. Biraud, Steve Wofsy, Christopher W. O'Dell, Gregory B. Osterman, Paul O. Wennberg, Debra Wunch, Coleen M. Roehl, Nicholas M. Deutscher, Matthäus Kiel, David W.T. Griffith, Voltaire A. Velasco, Justus Notholt, Thorsten Warneke, Christof Petril, Martine De Maziere, Mahesh K. Sha, Ralf Sussmann, Markus Rettinger, Dave Pollard, Isamu Morino, Osamu Uchino, Frank Hase, Dietrich G. Feist, Kimberly Strong, Rigel Kivi, Laura Iraci, Kawakami Shuji, Manvendra K. Dubey, Eliezer Sepulveda, Omaira Elena Garcia Rodriguez, Yao Te, Pascal Jeseck, Pauli Heikkinen, Edward J. Dlugokencky, Michael R. Gunson, Annmarie Eldering, David Crisp, Brendan Fisher, Characterization of OCO-2 and ACOS-GOSAT biases and errors for flux estimates, 15th International Workshop on Greenhouse Gas Measurements from Space (IWGGMS-15), Sapporo (Japan), 3-5 June 2019.
- Ninja Röhlings, A., Hase, F., Raffalski, U., Garcia, O.E., Sepúlveda, E. and Blumenstock, T., Evaluation of Trace Gases Using Time Series of Ground-Based FTIR Observations for the Validation of Tropomi/Sentinel-5 Precursor Satellite Data, Living Planeta Symposium, ESA, Milan (Italy), 13-17 May 2019.
- Ninja Röhlings, A., Thomas Blumenstock, Ugur Cayoglu, Omaíra E. Garcia, Frank Hase, Tobias Kerzenmacher, Uwe Raffalski, and Eliezer Sepúlveda, Validation of Tropomi/Sentinel-5 Precursor Satellite Data Using Time Series of Ground-Based FTIR Sites at Different Latitudes, ESA S5P Validation Team Meeting, Frascati (Italy), 12 November 2019.
- Román, R., Barreto, A., Pérez-Ramírez, D., González, R., Benavent-Oltra, J. A., Toledano, C., Herreras, M., Antuña, J. C., Velasco-Merino, C., Mateos, D., Cachorro, V. E., Olmo, F. J., Cuevas, E., Alados-Arboledas, L., and de Frutos, A. M. Improvements on lunar photometry: comparison with star photometer measurements, 7^a Reunión Ibérica de Ciencia y Tecnología de Aerosoles (RICTA), Lisboa (Portugal), 9-11 July 2019.
- Taylor, S., Toledano, C., Berjón, A., Barreto, A., Adriaensen, S., Greenwell, C., Woolliams, E., Bouvet, M. Deriving an improved lunar spectral irradiance model from lunar photometer measurements, Living Planet Symposium, Milan (Italy), 13-17 May 2019.

23.4 Non-peer reviewed papers and reports

2020

- Bennouna, Y., Christophe, Schulz, M., Y. Christophe, H.J. Eskes, S. Basart, A. Benedictow, A.-M. Blechschmidt, S. Chabrillat, H. Clark, E. Cuevas, H. Flentje, K.M. Hansen, U. Im, J. Kapsomenakis, B. Langerock, K. Petersen, A. Richter, N. Sudarchikova, V. Thouret, A. Wagner, Y. Wang, T. Warneke, C. Zerefos, Validation report of the CAMS global Reanalysis of aerosols and reactive gases, years 2003-2019, Copernicus Atmosphere Monitoring Service (CAMS) report, CAMS84_2018SC2_D5.1.1-2019.pdf, April 2020, doi:10.24380/2v3p-ab79, 2020.
- Christophe, Y., M. Ramonet, A. Wagner, M. Schulz, H. J. Eskes, S. Basart, A. Benedictow, Y. Bennouna, A.-M. Blechschmidt, S. Chabrillat, E. Cuevas, A. ElYazidi, H. Flentje, P. Fritzsche, K.M. Hansen, U. Im, J. Kapsomenakis, B. Langerock, A. Richter, N. Sudarchikova, V. Thouret, T. Warneke, C. Zerefos, Validation report of the CAMS near-real-time global atmospheric composition service: Period March – May 2020, Copernicus Atmosphere Monitoring Service (CAMS) report, CAMS84_2018SC2_D1.1.1_MAM2020.pdf, September 2020, doi:10.24381/7q7w-h823, 2020a.
- Eskes, H. J., S. Basart, A. Benedictow, Y. Bennouna, A.-M. Blechschmidt, S. Chabrillat, Y. Christophe, K. M. Hansen, J. Kapsomenakis, B. Langerock, M. Pitkanen, M. Ramonet, A. Richter, N. Sudarchikova, M. Schulz, A. Wagner, T. Warneke (UBC), C. Zerefos, Upgrade verification note for the CAMS near-real time global atmospheric composition service: Evaluation of the e-suite for the CAMS 47R1 upgrade of October 2020, Copernicus Atmosphere Monitoring Service (CAMS) report, CAMS84_2018SC2_D3.2.1-202009_esuite.pdf, 2 October 2020, doi:10.24380/fzdx-j890 2020.
- Matthews, B., O. E. García, E. Cuevas, W. Spangl, and P. Castro: Report on how EIONET and EEA can contribute to the urban in situ requirements of a future Copernicus anthropogenic CO₂ observing system, European Environment Agency (EEA) – Negotiated procedure No EEA/IDM/R0/17/008, 2020.
- Ramonet, M., A. Wagner, M. Schulz, Q. Errera, H. J. Eskes, S. Basart, A. Benedictow, Y. Bennouna, A.-M. Blechschmidt, S. Chabrillat, Christophe, Y., E. Cuevas, A. El-Yazidi, H. Flentje, P. Fritzsche, K.M. Hansen, U. Im, J. Kapsomenakis, B. Langerock, A. Richter, N. Sudarchikova, V. Thouret, T. Warneke, C. Zerefos, Validation report of the CAMS near-real-time global atmospheric composition service: Period June – August 2020, Copernicus Atmosphere Monitoring Service (CAMS) report, CAMS84_2018SC2_D1.1.1_JJA2020.pdf, January 2021, doi:10.24381/8pxnq362, 2020.
- Redondas, A., Berjón, A., López-Solano, J., Carreño, V., León-Luis, S.F., Santana, D.: “El Arenosillo” 2019 Campaign Report. Joint publication of State Meteorological Agency (AEMET), Madrid, Spain and World Meteorological Organization

- (WMO), Geneva, Switzerland, WMO/GAW Report No. 257, 2020.
- Redondas, A., León-Luis, S.F., Berjón, A., López-Solano, J., Carreño, V.: Decimotercera campaña de intercomparación del Centro Regional de Calibración Brewer para Europa. Observatorio Atmosférico de Arosa (Suiza) 30 de julio a 10 de agosto de 2018. State Meteorological Agency (AEMET), Madrid, Spain and World Meteorological Organization (WMO) (WMO/GAW Reports), 2020.
- Redondas, A., León-Luis, S.F., López-Solano, J., Berjón, A., Parra Rojas, F.C., Carreño Corbella, V.: Decimosegunda campaña de intercomparación del Centro Regional de Calibración Brewer para Europa: Estación de Sondeos Atmosféricos de El Arenosillo, Huelva (España), 29 de mayo a 9 de junio de 2017. 2020.
- Schulz, M., Y. Christophe, M. Ramonet, Wagner, A., H. J. Eskes, S. Basart, A. Benedictow, Y. Bennouna, A.-M. Blechschmidt, S. Chabrilat, E. Cuevas, A. ElYazidi, H. Flentje, P. Fritzsche, K.M. Hansen, U. Im, J. Kapsomenakis, B. Langerock, A. Richter, N. Sudarchikova, V. Thouret, T. Warneke, C. Zerefos, Validation report of the CAMS near-real-time global atmospheric composition service: Period December 2019 – February 2020, Copernicus Atmosphere Monitoring Service (CAMS) report, CAMS84_2018SC1_D1.1.1_DJF2020.pdf, June 2020, doi:10.24380/322n-jn39, 2020.
- WMO, WMO Airborne Dust Bulletin: Sand and Dust Storm Warning Advisory and Assessment System, No. 4 – May 2020, 2020.
- ## 2019
- Basart, S., A. Benedictow, Y. Bennouna, A.-M. Blechschmidt, S. Chabrilat, Y. Christophe, E. Cuevas, H. J. Eskes, K. M. Hansen, O. Jorba, J. Kapsomenakis, B. Langerock, T. Pay, A. Richter, N. Sudarchikova, M. Schulz, A. Wagner, C. Zerefos, Upgrade verification note for the CAMS real-time global atmospheric composition service: Evaluation of the esuite for the CAMS upgrade of July 2019, Copernicus Atmosphere Monitoring Service (CAMS) report, CAMS84_2018SC1_D3.2.1-201907_esuite_v1.pdf, July 2019, doi:10.24380/fcwq-yp50, 2019.
- Bennouna, Y., M. Schulz, Y. Christophe, H.J. Eskes, S. Basart, A. Benedictow, A.-M. Blechschmidt, S. Chabrilat, H. Clark, E. Cuevas, H. Flentje, K.M. Hansen, U. Im, J. Kapsomenakis, B. Langerock, K. Petersen, A. Richter, N. Sudarchikova, V. Thouret, A. Wagner, Y. Wang, C. Zerefos, Validation report of the CAMS global Reanalysis of aerosols and reactive gases, years 2003-2017, Copernicus Atmosphere Monitoring Service (CAMS) report, CAMS84_2018SC1_D5.1.1-2017_v1.pdf, February 2019, doi:10.24380/xjhc-zt69, 2019.
- Christophe, Y., M. Ramonet, A. Wagner, M. Schulz, H. J. Eskes, S. Basart, A. Benedictow, Y. Bennouna, A.-M. Blechschmidt, S. Chabrilat, E. Cuevas, A. ElYazidi, H. Flentje, K.M. Hansen, U. Im, J. Kapsomenakis, B. Langerock, A. Richter, N. Sudarchikova, V. Thouret, T. Warneke, C. Zerefos, Validation report of the CAMS near-real-time global atmospheric composition service: Period March – May 2019, Copernicus Atmosphere Monitoring Service (CAMS) report, CAMS84_2018SC1_D1.1.1_MAM2019_v1.pdf, September 2019, doi:10.24380/1t4q-1h53, 2019a.
- Christophe, Y., Schulz, M., Y. Bennouna, H.J. Eskes, S. Basart, A. Benedictow, A.-M. Blechschmidt, S. Chabrilat, H. Clark, E. Cuevas, H. Flentje, K.M. Hansen, U. Im, J. Kapsomenakis, B. Langerock, K. Petersen, A. Richter, N. Sudarchikova, V. Thouret, A. Wagner, Y. Wang, T. Warneke, C. Zerefos, Validation report of the CAMS global Reanalysis of aerosols and reactive gases, years 2003-2018, Copernicus Atmosphere Monitoring Service (CAMS) report, CAMS84_2018SC1_D5.1.1-2018_v1.pdf, May 2019, doi:10.24380/dqws-kg08, 2019b.
- Cuevas, E., Milford, C., Bustos, J. J., R., García, O. E., García, R. D., Gómez-Peláez, A. J., Guirado-Fuentes, C., Marrero, C., Prats, N., Ramos, R., Redondas, A., Reyes, E., Rivas-Soriano, P. P., Rodríguez, S., Romero-Campos, P. M., Torres, C. J., Schneider, M., Yela, M., Belmonte, J., del Campo-Hernández, R., Almansa, F., Barreto, A., López-Solano, C., Basart, S., Terradellas, E., Werner, E., Afonso, S., Bayo, C., Berjón, A., Carreño, V., Castro, N. J., Chinea, N., Cruz, A. M., Damas, M., De Ory-Ajamil, F., García, M.I., Gómez-Trueba, V., Hernández, C., Hernández, Y., Hernández-Cruz, B., León-Luís, S. F., López-Fernández, R., López-Solano, J., Parra, F., Rodríguez, E., Rodríguez-Valido, M., Sálamo, C., Sanromá, E., Santana, D., Santo Tomás, F., Sepúlveda, E., and Sosa, E.: Izaña Atmospheric Research Center Activity Report 2017-2018. (Eds. Cuevas, E., Milford, C. and Tarasova, O.), State Meteorological Agency (AEMET), Madrid, Spain and World Meteorological Organization, Geneva, Switzerland, WMO/GAW Report No. 247, 2019.
- Eskes, H.J., S. Basart, A. Benedictow, Y. Bennouna, A.-M. Blechschmidt, S. Chabrilat, Y. Christophe, E. Cuevas, H. Flentje, K. M. Hansen, J. Kapsomenakis, B. Langerock, M. Ramonet, A. Richter, M. Schulz, N. Sudarchikova, A. Wagner, T. Warneke, C. Zerefos, Observation characterisation and validation methods document, Copernicus Atmosphere Monitoring Service (CAMS) report, December 2019, doi: 10.24380/0nsdwb26, 2019.
- Ramonet, M., A. Wagner, M. Schulz, Y. Christophe, H. J. Eskes, S. Basart, A. Benedictow, Y. Bennouna, A.-M. Blechschmidt, S. Chabrilat, E. Cuevas, A. ElYazidi, H. Flentje, K.M. Hansen, U. Im, J. Kapsomenakis, B. Langerock, A. Richter, N. Sudarchikova, V. Thouret, T. Warneke, C. Zerefos, Validation report of the CAMS near-real-time global atmospheric composition service: Period June – August 2019, Copernicus Atmosphere Monitoring Service (CAMS) report, CAMS84_2018SC1_D1.1.1_JJA2019_v1.pdf, November 2019, doi:10.24380/def9-na43, 2019.
- Redondas, A., León-Luis, S.F., Berjón, A., López-Solano, J., Carreño, V. : Thirteenth Intercomparison Campaign of the Regional Brewer Calibration Center Europe – Lichtklimatisches Observatorium, Arosa, Switzerland 30 July– 10 August 2018, State Meteorological Agency (AEMET), Madrid, Spain and World Meteorological Organization. 2019.
- Redondas, A., León-Luis, S. F., Berjón, A., López-Solano, J., Parra-Rojas, F. C., Carreño-Corbella, V.(2019). Twelfth Intercomparison Campaign of the Regional Brewer Calibration Center Europe – El Arenosillo Atmospheric Sounding Station, Huelva, Spain 29 May to 9 June 2017. State Meteorological Agency (AEMET), Madrid, Spain and World Meteorological Organization (WMO). 2019.
- Schulz, M., Y. Christophe, M. Ramonet, Wagner, A., H.J. Eskes, S. Basart, A. Benedictow, Y. Bennouna, A.-M. Blechschmidt, S. Chabrilat, E. Cuevas, A. ElYazidi, H. Flentje, K.M. Hansen, U. Im, J. Kapsomenakis, B. Langerock, A. Richter, N. Sudarchikova, V. Thouret, T. Warneke, C. Zerefos, Validation report of the CAMS near-real-time global atmospheric composition service: Period December 2018 -February 2019, Copernicus Atmosphere Monitoring Service (CAMS) report, CAMS84_2018SC1_D1.1.1_DJF2019_v1.pdf, June 2019, doi:10.24380/7th6-tk72, 2019.

Wagner, A., M. Schulz, Y. Christophe, M. Ramonet, H. J. Eskes, S. Basart, A. Benedictow, Y. Bennouna, A.-M. Blechschmidt, S. Chabrillat, E. Cuevas, A. ElYazidi, H. Flentje, K.M. Hansen, U. Im, J. Kapsomenakis, B. Langerock, A. Richter, N. Sudarchikova, V. Thouret, T. Warneke, C. Zerefos, Validation report of the CAMS near-real-time global atmospheric composition service: Period September – November 2019, Copernicus Atmosphere Monitoring Service (CAMS) report, CAMS84_2018SC2_D1.1.1_SON2019_v1.pdf, February 2020, doi:10.24380/xzkk-bz05, 2019.

WMO, WMO Airborne Dust Bulletin: Sand and Dust Storm Warning Advisory and Assessment System, No. 3 – May 2019, 2019.

24 List of scientific projects

Table 24.1. List of scientific projects at IARC during 2019-2020.

Project Title	Duration	Funding Agency	Project Website	Principal Investigator/ Contact
Solutions for Sustainable Access to Atmospheric Research Facilities (ATMO-ACCESS)	2021-2025	H2020-INFRAIA-2018-2020 (H2020)	https://izana.aemet.es/atmo-access-isaf/#home	PI (CNRS): Prof Paolo Laj PI (IARC-AEMET): Dr Natalia Prats
Metrology for aerosol optical properties (MAPP)	2020-2023	EURAMET: European Association of National Metrology Institutes	https://www.pmodwrc.ch/en/MAPP/	PI (SFI Davos): Dr Julian Gröbner PI (IARC-AEMET): Dr África Barreto
Brewer Error Budget in Eubrewnet (BREWEB)	2020-2022	European Space Agency (ESA) 4000117151/16/I-LG KNMI-2020/658	http://www.tropomi.eu/data-products/mission-performance-centre	PI (ESA): Dr Angelika Dehn PI (IARC-AEMET): Alberto Redondas
S5P Nitrogen Dioxide and Formaldehyde Validation using NDACC and complementary FTIR and UV-Vis DOAS ground-based remote sensing data (NIDFORVal)	2016-2023	European Space Agency (ESA) ID28607		PI (BIRA-IASB): Dr Corinne Vigouroux Dr Gai Pinardi PI (IARC-AEMET): Dr Omaira García
Validation of S5P Methane and Carbon Monoxide with TCCON Data (TCCON4S5P)	2016-2023	European Space Agency (ESA)		PI (BIRA-IASB): Dr Filip Desmet PI (IARC-AEMET): Dr Omaira García
Medida de Gases de Efecto Invernadero en Ambientes Urbanos (MEGEI)	2018-ongoing	Meteorological State Agency (AEMET)	https://izana.aemet.es/projects/#megei	PI (IARC-AEMET): Dr Omaira García
EIONET Group of Copernicus In Situ Data Experts	2018-2020	European Environmental Agency Negotiated procedure No EEA/IDM/R0/17/008		PI (IGN): Nuria Valcárcel PI (IARC-AEMET): Dr Emilio Cuevas
MOisture Transport and Isotopologues of water Vapour (MOTIV)	2017-2020	Deutsche Forschungsgemeinschaft SCHN 1126/2-1		PI (KIT): Dr Matthias Schneider PI (IARC-AEMET): Dr Omaira García
IASI para sondear el Metano y Óxido de Nitroso en la Troposfera (INMENSE)	2017-2020	Spanish Ministry of Economy, Industry and Competitiveness CGL2016-80688-P	https://izana.aemet.es/inmense	PI (IARC-AEMET): Dr Omaira Gracia

Equipment for the monitoring and research of atmospheric parameters and components that modulate climate change, at the Izaña Global GAW station (MICA)	2018-2019	Spanish Ministry of Economy, Industry and Competitiveness		PI (IARC-AEMET): Dr Emilio Cuevas
ACTRIS PPP - Aerosols, Clouds and Trace gases Preparatory Phase Project	2017-2019	H2020-INFRADEV-2016-2017 (H2020)	https://www.actris.eu/Projects/ACTRISPPP(2017-2019).aspx	PI (FMI): Dr Sanna Sorvari PI (IARC-AEMET): Dr África Barreto
Multidecadal variability and trends of aerosol properties in the North Atlantic (AEROATLAN)	2016-2018 (extension 2019)	Spanish Ministry of Economy and Competitiveness	http://aeroatlan.aemet.es/	PI (IARC-AEMET): Dr Sergio Rodríguez/ Dr Natalia Prats from 2019 onwards
Aerosols, Clouds, and Trace gases Research InfraStructure (ACTRIS-2)	2015-2019	H2020-INFRAIA-2014-2015 (H2020)	http://www.actris.eu/	PI (CNR-IMAA): Dr Gelsomina Pappalardo PI (IARC-AEMET): Dr Emilio Cuevas
SDS-Africa	2007-ongoing	Spanish Agency for International Development Cooperation	—	PI (IARC-AEMET): Dr Emilio Cuevas
GAW-Sahara	2007-ongoing	Spanish Agency for International Development Cooperation	—	PI (IARC-AEMET): Alberto Redondas

For a definition of the acronyms used in the above table, see Section 28.

25 List of major national and international networks, programmes and initiatives

The Izaña Atmospheric Research Center participates in the following national and international networks, programmes and initiatives:

ACTRIS	Aerosols, Clouds, and Trace gases Research InfraStructure Network
AERONET	AErosol RObotic NETwork
ALC	Automatic Ceilometer and Lidars Network
BSRN	Baseline Surface Radiation Network
CarbonTracker	CO ₂ measurement and modeling system developed by NOAA to keep track of sources and sinks of carbon dioxide around the world
CarbonTracker Europe	
COCCON	Collaborative Carbon Column Observing Network
EAN	European Aeroallergen Network
EARLINET	European Aerosol Research Lidar Network
E-GVAP	EUMETNET GPS water vapour Programme
EPN	EUREF Permanent Network
EUBREWNET	European Brewer Network
GAW	WMO Global Atmosphere Watch Programme
GCOS	Global Climate Observing System
GEOMON	Global Earth Observation and Monitoring of the Atmosphere
GLOBALVIEW-CO₂	
GLOBALVIEW-CH₄	
GLOBALVIEW-CO	
GLOBALVIEW-CO₂C₁₃	
GURME	WMO GAW Urban Research Meteorology and Environment project
ICOS	Integrated Carbon Observation System
LOTUS	Long-term Ozone Trends and Uncertainties in the Stratosphere
MACC	Monitoring Atmospheric Composition and Climate
MPLNet	Micro-Pulse Lidar NETwork
NDACC	Network for the Detection of Atmospheric Composition Change
NOAA/ESRL/GMD CCGG Cooperative Air Sampling Network	
Pandonia Global Network	
PHOTONS	PHOtométrie pour le Traitement Opérationnel de Normalisation Satellitaire
RBCC-E	Regional Brewer Calibration Center for Europe
REA	Red Española de Aerobiología
REDMAAS	Red Española de DMAs Ambientales

SDS-WAS	WMO Sand and Dust Storm Warning, Advisory and Assessment System
SPALINET	Spanish and Portuguese Aerosol Lidar Network
SPARC	Stratosphere-troposphere Processes And their Role in Climate
TCCON	Total Carbon Column Observing Network
TOAR	Tropospheric Ozone Assessment Report
WCCAP	World Calibration Centre for Aerosol Physics
WDCGG	WMO GAW World Data Centre for Greenhouse Gases
WDCRG	WMO GAW World Data Center for Reactive Gases
WOUDC	World Ozone and Ultraviolet Data Center
WRC-WORCC	World Radiation Centre-World Optical Depth Research and Calibration Centre
WRC-WCC-UV	World Radiation Centre-World Calibration Center-Ultraviolet Section
WRDC	WMO World Radiation Data Centre

26 Staff

Research Staff			
Name	Position	Email	Personal Web Page
Dr Emilio Cuevas-Agulló	Izaña Atmospheric Research Center: Director	ecuevasa@Taemet.es	ResearchGate Google Scholar
Óscar Alvarez Losada ^b	Column Aerosols Programme	proyecto_empir@Taemet.es	
Dr África Barreto	Column Aerosols Programme: Head	abarretov@Taemet.es	ResearchGate
Juan J. de Bustos-Seguela	Meteorology Programme McIdas and Eumetcast Manager	jbustoss@Taemet.es	ResearchGate
Dr Omaira E. García-Rodríguez	FTIR Programme: Head	ogarcia@Taemet.es	ResearchGate Google Scholar
Carlos L. Marrero de la Santa Cruz	Meteorology Programme: Head	cmarrerod@Taemet.es	
Dr Francisco Parra Rojas	Ozone and UV Programme	proyecto_brewb_ciai@Taemet.es	
Pedro Pablo Rivas Soriano	Greenhouse Gases and Carbon Cycle Programme: Head	privass@Taemet.es	
Dr Natalia Prats Porta	In situ Aerosols Programme: Head	npratasp@Taemet.es	ResearchGate
Alberto Redondas-Marrero	Ozone and UV Programme: Head	aredondasm@Taemet.es	ResearchGate Google Scholar
Pedro M. Romero-Campos	Radiation and Water Vapour Programme: Head	promeroc@Taemet.es	
Dr Eliezer Sepúlveda ^a	FTIR Programme	esepulvedah@Taemet.es	ResearchGate
Carlos J. Torres García	Reactive Gases and Ozone sondes Programme: Head	ctorresg@Taemet.es	

^aLeft IARC in 2019-2020, ^bJoined IARC in 2021

Research Staff from other Institutions				
Name	Affiliation	Programme	Email	Personal Web Page
Dr Antonio F. Almansa-Rodríguez	CIMEL	UV-Vis Photodiode Array Spectrometer development	FernandoATsietec.es	
Dr Alberto Berjón	TRAGSA TEC	Ozone and UV Programme	aberjonATtragsa.es	ResearchGate Google Scholar
Nayra Chinaea	SIELTEC/ TRAGSA TEC	Reactive Gases and Ozonesondes Programme	nayra.chineaATsietec.es	
Dr Rosa D. García-Cabrera	TRAGSA TEC/UVA	Radiation Programme	rgarci47ATtragsa.es	ResearchGate Google Scholar
Dr Yenny González	CIMEL	Column Aerosols Programme	y-gonzalezATcimel.fr	ResearchGate
Dr Carmen Guirado-Fuentes ^a	UVA	ACTRIS Project	carmenfATgoa.uva.es	
Dr Sergio León-Luís	TRAGSA TEC	ICOS	sleon2ATtragsa.es	ResearchGate
Dr Javier López-Solano	TRAGSA TEC	Ozone and UV Programme/CIMO Testbed	jlopez15ATtragsa.es	ResearchGate
Dr Celia Milford		In situ Aerosols Programme	cmilford2ATgmail.com	ResearchGate
Daniel Santana	SIELTEC/ LuftBlick	Ozone and UV Programme	daniel.santanaATluftblick.at	

^aLeft IARC in 2019-2020

Technical Staff			
Name	Position	Email	Web Page
Sergio Afonso-Gómez ^a	Meteorological Observer /GAW technician	safonsogATAemet.es	
Antonio Alcántara ^b	Meteorological Observer /GAW technician	aalcantararATAemet.es	
Concepción Bayo-Pérez	Meteorological Observer /GAW technician	cbayopATAemet.es	
Virgilio Carreño-Corbella	Meteorological Observer /GAW technician	vcarrenocATAemet.es	
Néstor J. Castro-Quintero	IT specialist	ncastroqATAemet.es	
Antonio M. Cruz-Martín	IT specialist	acruzmaATAemet.es	
Cándida Hernández-Hernández	Meteorological Observer /GAW technician	chernandezhATAemet.es	
Rocío López-Fernández	IT specialist	rlopezfATAemet.es	
Julián Pérez de la Puerta ^a	Meteorological Observer /GAW technician	jperezdaATAemet.es	
Ramón Ramos-López	Scientific instrumentation and infrastructures: Head	rramoslATAemet.es	
Enrique Reyes-Sánchez	Scientific instrumentation and infrastructures	ereyessATAemet.es	
Antonio Serrano ^b	Scientific instrumentation and infrastructures	aserranotATAemet.es	

^aRetired in 2019-2020, ^bJoined IARC in 2021

Administration Staff			
Name	Position	Email	Personal Web Page
Dr Emilio Cuevas-Agulló	Izaña Atmospheric Research Center: Director	ecuevasaATaemet.es	ResearchGate Google Scholar
Marcos Damas-García	Driver	mdamasgATaemet.es	
Dr Natalia Prats Porta	Project Manager	nprataspATaemet.es	
Concepción Sálamo-Hernández ^a	Secretary	csalamohATaemet.es	
J. Félix Santo Tomás-Castro	Accounting officer	jsantotomascATaemet.es	

^aRetired in 2019

27 List of Acronyms

ACE-FTS - Atmospheric Chemistry Experiment - Fourier Transform Spectrometry

ACMAD - African Centre of Meteorological Application for Development

ACSO - Absorption Cross Sections of Ozone

ACTRIS - Aerosol, Clouds and Trace Gases Research Infrastructure

ADF - aerosol radiative forcing

AE - Angstrom Exponent

AECID - Spanish Agency for International Development Cooperation

AEMET - State Meteorological Agency

AEROCOM - Aerosol Comparisons between Observations and Models

AERONET - AErosol RObotic NETwork

AF - Radiative Forcing

ALC - Automatic Ceilometer and Lidars Network

AMISOC - Atmospheric MINorSpecies relevant to the OzoneChemistry at both sides of the Subtropical jet

ANACIM - Agence Nationale de l'Aviation Civile et de la Météorologie

ANN - Artificial Neuronal Networks

AOD - Aerosol Optical Depth

APS - Aerosol Polarimetry Sensor

ARTI - African Residence Time Index

ATC - Atmospheric Thematic Center

ATMOZ - Traceability for atmospheric total column ozone

AQG - Air Quality Guideline

BBCH - Biologische Bundesanstalt, Bundessortenamt und Chemische Industrie

BC - Black Carbon

BDCN - National Climatological Data Base

BDFC - Barcelona Dust Forecast Centre

BIRA-IASB - Royal Belgian Institute for Space Aeronomy

BSC-CNS - Barcelona Supercomputing Centre – National Supercomputing Centre

BSRN - Baseline Surface Radiation Network

BTO - Botanic Observatory

CALIMA - Cloud, Aerosols and Ice Measurements in the Saharan Air Layer

CAMS - Copernicus Atmosphere Monitoring Service

CARS - Centre for Aerosol Remote Sensing

CARSNET - China Aerosol Remote Sensing NETwork

CBL - Convective Boundary Layer

CCD - Charge-coupled device

CCGG - Carbon Cycle Greenhouse Gases group

CCI - Climate Change Initiative

CCLs - Central Calibration Laboratories

CEILAP - Laser and Applications Research Center

CEIP - Colegio de Educación Infantil y Primaria

CEO - Centro de Educación Obligatoria

CEOS - Committee on Earth Observation Satellites

CICERO - Center for International Climate and Environmental Research

CIEMAT - Center for Energy, Environmental and Technological Research

CIMO - Commission for Instruments and Methods of Observations

CINDI - Cabauw Intercomparison campaign Nitrogen Dioxide measuring Instrument

CMA - China Meteorological Administration

CNR - National Research Council of Italy

CNRS - Centre National de la Recherche Scientifique

COST - European Cooperation in Science and Technology

CPCs - Condensation Particle Counter

CPT - Cold Point Tropopause

CRDS - Cavity Ring-Down Spectroscopy

CREWS - Climate Risk and Early Warning System

CRR - Convective Rainfall Rate

CSIC - Consejo Superior de Investigaciones Científicas

CWT - Concentration Weighted Trajectory

DBM - Daumont, Brion & Malicet

DMN - Direction de la Météorologie Nationale

DNI - Direct Normal Irradiance

DOAS - Differential Optical Absorption Spectroscopy

DOD - Dust Optical Depth

DREAM - Dust REgional Atmospheric Model

DS - Direct Sun

DSCR - Digital Sky Colour Radiometer

DU - Dobson Unit

DVB - Digital Video Broadcast

DWD - German Meteorological Service

EAN - European Aeroallergen Network

ECC - Electrochemical concentration cell

ECMWF - European Centre for Medium-Range Weather Forecasts

ECMWF-IFS - European Centre for Medium-Range Weather Forecasts - Integrated Forecasting System

ECN - Energy research Centre of the Netherlands

ECV - Essential Climate Variable

EGVAP - EUMETNET GPS Water Vapour Programme

EMA - Egyptian Meteorological Authority

EMPA - Eidgenössische Materialprüfungs- und Forschungsanstalt

EMRP - European Metrology Research Programme

Eolo-PAT EOLO-Predicción Aerobiológica para Tenerife

EPA - Environmental Protection Agency

EPS - Ensemble Prediction System

ERA4CS - European Research Area for Climate Services

ERA-Interim – ECMWF global atmospheric reanalysis from 1979

ERDF - European Regional Development Fund	GOA-UVA - University of Valladolid Atmospheric Optics Group
ERIC - European Research Infrastructure Consortium	GOME - Global Ozone Monitoring Experiment
ESA - European Space Agency	GPS - Global Positioning System
ESA-CALVAL – European Space Agency Calibration and Validation project	GRASP - Generalized Retrieval of Aerosol and Surface Properties
ESFRI - European Strategy Forum on Research Infrastructures	GRUAN - Global Climate Observing System Reference Upper-Air Network
ESRL - Earth System Research Laboratory	GSR - Global Solar Radiation
ET-ACMQ - Expert Team -Atmospheric Composition Measurement Quality	H2020 - Horizon 2020
ETC - Extraterrestrial constant	HIRLAM - High Resolution Limited Area Model
EU COST - European Cooperation in Science and Technology	HYSPLIT - Hybrid Single Particle Lagrangian Integrated Trajectory Model
EUDAT - European Data Infrastructure	IAC - Instituto de Astrofísica de Canarias
EUMETSAT - European Organisation for the Exploitation of Meteorological Satellites	IAEA - International Atomic Energy Agency
EURAMET - European Association of National Metrology Institutes	IARC - Izaña Atmospheric Research Center
FCS - Fraction Clear Sky	IASI -Infrared Atmospheric Sounding Interferometer
FLEXTRA - FLEXible TRAjectories	ICIA - Instituto Canario de Investigaciones Agrarias
FMI - Finnish Meteorological Institute	ICOS - Integrated Carbon Observation System
FNL - Final Analysis Data	ICP-AES - Inductively Coupled Plasma Atomic Emission Spectroscopy
FOV - Field Of View	ICP-MS - Inductively Coupled Plasma Mass Spectroscopy
FP7 - European Community’s Seventh Framework Programme	IDAEA - Institute of Environmental Assessment and Water Research
FRM - Fiducial Reference Measurements	IEO - Spanish Institute of Oceanography
FRM4DOAS - FRM for DOAS	IES - Instituto de Educación Secundaria
FT - Free Troposphere	IGAC - International Global Atmospheric Chemistry Project
FTIR - Fourier transform infrared spectroscopy	IGACO - Integrated Global Atmospheric Observations
FTS - Fourier Transform Spectrometry	IGN - Spanish National Geographic Institute
FW2 - Fitting Window 2	ILAS - Improved Limb Atmospheric Spectrometer
FW5 - Fitting Window 5	IMAA - Institute of Methodologies for Environmental Analysis
FWHM - Full Width at Half Maximum	IMK-ASF - Institut für Meteorologie und Klimaforschung - Atmosphärische Spurengase und Fernerkundung
GAW - Global Atmosphere Watch	INM - Institut National de la Météorologie
GAW-PFR - Global Atmosphere Watch - Precision Filter Radiometer	INSTAAR - Institute of Arctic and Alpine Research
GAWSIS - GAW Station Information System	INTA - Instituto Nacional de Técnica Aeroespacial
GCOS - Global Climate Observing System	IO3C - International Ozone Commission
GC-RGD - Gas Chromatography Reduction Gas Analyser	IPMA - Instituto Português do Mar e da Atmosfera
GDAS - Global Data Assimilation System	IR – Infrared
GEO – Geostationary Orbit	ISAF - Izaña Subtropical Access Facility
GEOS-5 -Goddard Earth Observing System model	IUP - Institut für Umweltphysik / Institute of Environmental Physics
GFS - Global Forecast System	IZO - Izaña Observatory
GHG - Greenhouse Gas	JRC - Joint Research Centre
GLOBE - Global Learning and Observations to Benefit the Environment	KIT - Karlsruhe Institute of Technology
GLONASS - Global Navigation Satellite System	LAP - Laboratori d’Anàlisis Palinològiques
GMD - Global Monitoring Division	LEO - Low Earth Orbit
GMES - Global Monitoring for Environment and Security	LIDAR - Laser Imaging Detection and Ranging
GNSS - Global Navigation Satellite System	LIME - Lunar Irradiance Model ESA
GOA - Atmospheric Optics Group	

LOA - Laboratoire d'Optique Atmosphérique	NIST - National Institute for Standards and Technology
LR - Lidar Ratio	NMHSS - National Meteorological and Hydrological Services
LUT – Look Up Table	NMMB - Nonhydrostatic Multiscale Model on the B-grid
MAAP - Multi Angle Absorption Photometer	NMME - North American Multi-Model Ensemble
MARS - Meteorological Archival and Retrieval System	NOA - National Observatory of Athens
MAXDOAS - Multi Axis Differential Optical Absorption Spectroscopy	NOAA - National Oceanic and Atmospheric Administration
MBL - Marine Boundary Layer	NORS - Demonstration Network Of ground-based Remote Sensing Observations in support of the Copernicus Atmospheric Service
McIDAS - Man Computer Interactive Data Access System	NPF - New Particle Formation
MEDA - Mars Environmental Dynamics Analyzer	NRT - Near Real Time
MetUN - Met Office Unified Model	ODSs - Ozone Depleting Substances
MEE - Mass Extinction Efficiency	OMI - Ozone Monitoring Instrument
MFRSR - Multi Filter Rotating Shadow-Band Radiometer	ONM - Office National de la Météorologie
MGA - Modified Geometrical Approach	OLI - Operational Land Imager
MIPAS - Michelson Interferometer for Passive Atmospheric Sounding	OSC - ozone slant column
MIR - Middle Infrared	OT - Ozone Tropopause
MISR - Multi-angle Imaging SpectroRadiometer	PAR - Photosynthetic Active Radiation
MLO - Mauna Loa Observatory	PFR - Precision Filter Radiometer
MM5 - Mesoscale Model	PI - Principal Investigator
MOCAGE - Modèle de Chimie Atmosphérique de Grande Echelle	PIXE - Particle-Induced X ray Emission
MODIS - Moderate Resolution Imaging Spectroradiometer	PLASMA - Photomètre Léger Aéroporté pour la Surveillance des Masses d’Air
MOL-RAO - Meteorologisches Observatorium Lindenberg - Richard Aßmann-Observatorium	PM - Particle Matter
MOSAIC - Multidisciplinary drifting Observatory for the Study of Arctic Climate	PM-LCS - Particle Matter – Low Cost Sensors
MPA - Moon phase angle	PMOD - Physikalisch-Meteorologisches Observatorium Davos
MPL - Micro Pulse Lidar	PSR - Precision Solar Spectroradiometer
MSG - Meteosat Second Generation	PTB - Physikalisch-Technische Bundesanstalt
MUSICA - MUlti-platform remote Sensing of Isotopologues for investigating the Cycle of Atmospheric water	PV - Potential Vorticity
NAFDI - North African Dipole Intensity	PWV - Precipitable Water Vapour
NA-ME-E - The Regional Centre for Northern Africa, Middle East and Europe	QA - Quality Assurance
NAO - North Atlantic Oscillation	QASUME - Quality Assurance of Spectral Ultraviolet Measurements
NAS - Network-Attached Storage	QA4EO - Quality Assured Data for Earth Observation communities
NASA - National Aeronautics and Space Administration	QC - Quality Control
NASA MPLNET - The NASA Micro Pulse Lidar Network	RA - Row Anomaly
NCDB National Climatological Data Base (AEMET)	R&D - Research and Development
NCEP - National Centers for Environmental Prediction	RBCC-E - Regional Brewer Calibration Center for Europe
NDIR - Non Dispersive	RCF - RIMO Correction Factor
NEMS - NOAA Environmental Modeling System	REA - Red Española de Aerobiología
NGAC - NEMS GFS Aerosol Component	REDMAAS - Red Española de DMAs Ambientales
NIDFORVal - Nitrogen Dioxide and FORMALdehyde Validation	RGB - composite - Red Green Blue composite
NIES - National Institute for Environmental Studies	RH - Relative Humidity
NILU - Norwegian Institute for Air Research	RIMO - ROLO Implementation for Moon-photometry Observation
NIPR - National Institute of Polar Research of Japan	RMSE - Root Mean Square Error
NIR - Near Infrared	ROLO - RObotic Lunar Observatory model

RSMC-ASDF - Regional Specialized Meteorological Centre with activity specialization on Atmospheric Sand and Dust Forecast	TSP - Total Suspended Particles
RTM - Radiative Transfer Model	TT - Thermal Tropopause
SAF - Satellite Application Facilities	UAB - Universidad Aut3noma de Barcelona
SAG - Scientific Advisory Group	UFPs - Ultrafine Particles
SAL - Saharan Air Layer	ULL - University of La Laguna
SALAM - Air Layer Air Mass characterization	UNEP - United Nations Environment Programme
SAO - Smithsonian Astrophysical Observatory	UPC - Universitat Polit3cnica de Catalunya
SAUNA - Sodankylä Total Column Ozone Intercomparison	UPS - Uninterruptible Power Supply
SCIAMACHY - Scanning Imaging Absorption Spectrometer for Atmospheric Chartography	UT – Upper Troposphere
SCILLA - Summer Campaign for Intercomparison of Lunar measurements of Lindenberg’s Aerosol	UTC - Coordinated Universal Time
SC-MINT - Standing Committee on Measurement, Instrumentation and Traceability	UTLS - Upper Troposphere Lower Stratosphere
SCO - Santa Cruz Observatory	UV - Ultraviolet
SD - Sunshine Duration	UVA - University of Valladolid
SDM - Standard Delivery Mode	VIS - Visible
SDR - Shortwave downward radiation	VMR - Volume Mixing Ratio
SDS - Sand and Dust Storm	WCC - World Calibration Center
SDS-WAS - Sand and Dust Storm Warning Advisory and Assessment System	WCCAP - World Calibration Centre for Aerosols Physics
SEAIC - Sociedad Española de Aerobiología e Inmunología Clínica	WCRP - World Climate Research Programme
SeaWIFS - Sea-Viewing Wide Field-of-View Sensor	WDCA - World Data Centre for Aerosols
SEM - Standard Error of the Mean	WDCGG - World Data Centre for Greenhouse Gases
SHL - Saharan Heat Low	WDCRG - World Data Center for Reactive Gases
SIOS - Svalbard Integrated Arctic Earth Observing System	WIGOS – WMO Integrated Global Observing System
SMN - Argentinian Meteorological Service	WMO - World Meteorological Organization
SMPS - Scanning Mobility Particle Sizer	WORCC - World Optical Depth Research and Calibration Center
SOC - Stratospheric Ozone Column	WOUDC - World Ozone and Ultraviolet Data Center
SOL - Significant Obstructive Lesions	WRC - World Radiation Center
SONA - Sistema de Observación de Nubes Automático	WS-CRDS - Wavelength-Scanned Cavity Ring-Down Spectroscopy
SOP - Standard Operating Procedure	WWRP - World Weather Research Programme
SPARC - Stratosphere-troposphere Processes And their Role in Climate	XS - Cross Section
SPC - Science Pump Corporation	ZHD - Zenith Hydrostatic Delay
SSDM - Server Meteorological Data System	ZSR - Zenith Sky Radiance
STJ - Subtropical Jet Stream	ZTD - Zenith Total Delay
STS - Sky Temperature Sensor	
STT - Stratosphere-to-troposphere	
SWIR - short-wave infrared	
SWVID - Stable Water Vapor Isotope Database	
SYNOP - Surface Synoptic Observation	
SZA - Solar Zenith Angle	
TNA - Trans National Access	
TOB - Tropospheric Ozone Burden	
TOC - Total Ozone Column	
TPO - Teide Peak Observatory	

28 Acknowledgements

A dedicated, enthusiastic and motivated team formed by scientific, technical and administrative staff is the key factor to run a centre like IARC. This report summarizes the activities carried out by IARC in 2019-2020 and is an expression of recognition of work done by each and every one of the people working in IARC and in all the institutions which collaborate with IARC. The year 2020 was a particularly challenging year due to the global crisis associated with COVID-19 and we thank all the personnel who showed an exceptional dedication to maintaining the measurement programmes at all the IARC facilities through this difficult period.

We would also like to express our sincere gratitude for the extraordinary effort carried out by IARC and AEMET personnel to assist in the deployment and collaborative effort among many organisations, as part of the emergency response to the volcanic eruption that occurred in La Palma from 19 September-13 December 2021. This period is not included in the 2019-2020 activity report, however, the dedication of time and resources from September 2021 onwards was a key example of the collaborative expertise of the scientific community providing a service to society.

We are grateful for the strong support to IARC from the former Director of Planning, Strategy and Business Development (DPEDC-AEMET), Julio González-Breña, who has always shown a high level of interest and enthusiasm for all the IARC activities. We also thank Ms Ana Melgar (DPEDC-secretary) for assisting us in many ways.

The World Meteorological Organization Global Atmosphere Watch Programme has been an excellent framework within which to develop our activities, where we have always found great assistance and support. IARC has been contributing to the GAW Programme since it was established in 1989 and we thank the WMO and its associated bodies for their work in coordinating and developing the GAW Programme and for its continuing support to all the IARC activities.

We thank Miguel Ángel García-Couto, Head of AEMET Documentation Service, for his support in the final publication of this report and other technical publications. We also thank the AEMET central library team, headed by Elena Morato who have always provided invaluable help.

We express our sincere gratitude to all those institutions, included in this report, which work closely with IARC and collaborate on both national and international projects. These collaborations are crucial to the activities at all the IARC facilities and provide an enriching and synergistic research environment.

Back cover photograph: Izaña Observatory (Photo: Fernando Rey Daluz)



For more information, please contact:
Izaña Atmospheric Research Center
Calle La Marina, 20, Planta 6
Santa Cruz de Tenerife
Tenerife, 38001, Spain
<http://izana.aemet.es>